Vol. 64 February, 1960 No. 2

THE JOURNAL OF PHYSICAL CHEMISTRY

(Registered in U. S. Patent Office)

CONTENTS

NOTES

THE JOURNAL OF PHYSICAL CHEMISTRY

(Registered in U. S. Patent Office)

W. Albert Noyes, Jr., Editor

Allen D. Bliss — Assistant Editors — A. B. F. Duncan

Editorial Board

A. O. Allen
C. E. H. Bawn
John D. Ferry
S. C. Lind
R. G. W. Norrish
R. E. Rundle
W. H. Stockmayer
G. B. B. M. Sutherland
A. R. Ubbelohde
E. R. Van Artsdalen
Edgar F. Westrum, Jr.

Published monthly by the American Chemical Society at 20th and Northampton Sts., Easton, Pa.

Second-class mail privileges authorized at Easton, Pa. This publication is authorized to be mailed at the special rates of postage prescribed by Section 131.122.

The *Journal of Physical Chemistry* is devoted to the publication of selected symposia in the broad field of physical chemistry and to other contributed papers.

Manuscripts originating in the British Isles, Europe and Africa should be sent to F. C. Tompkins, The Faraday Society, 6 Gray's Inn Square, London W. C. 1, England.

Manuscripts originating elsewhere should be sent to W. Albert Noyes, Jr., Department of Chemistry, University of Rochester, Rochester 20, N. Y.

Correspondence regarding accepted papers, proofs and reprints should be directed to Assistant Editor, Allen D. Bliss, Department of Chemistry, Simmons College, 300 The Fenway, Boston 15, Mass.

Business Office: Alden H. Emery, Executive Secretary, American Chemical Society, 1155 Sixteenth St., N. W., Washington 6, D. C.

Advertising Office: Reinhold Publishing Corporation, 430 Park Avenue, New York 22, N. Y.

Articles must be submitted in duplicate, typed and double spaced. They should have at the beginning a brief Abstract, in no case exceeding 300 words. Original drawings should accompany the manuscript. Lettering at the sides of graphs (black on white or blue) may be pencilled in and will be typeset. Figures and tables should be held to a minimum consistent with adequate presentation of information. Photographs will not be printed on glossy paper except by special arrangement. All footnotes and references to the literature should be numbered consecutively and placed in the manuscript at the proper places. Initials of authors referred to in citations should be given. Nomenclature should conform to that used in *Chemical Abstracts*, mathematical characters be marked for italic, Greek letters carefully made or annotated, and subscripts and superscripts clearly shown. Articles should be written as briefly as possible consistent with clarity and should avoid historical background unnecessary for specialists.

Notes describe fragmentary or incomplete studies but do not otherwise differ fundamentally from articles and are subjected to the same editorial appraisal as are articles. In their preparation particular attention should be paid to brevity and conciseness. Material included in Notes must be definitive and may not be republished subsequently.

Communications to the Editor are designed to afford prompt preliminary publication of observations or discoveries whose value to science is so great that immediate publication is imperative. The appearance of related work from other laboratories is in itself not considered sufficient justification for the publication of a Communication, which must in addition meet special requirements of timeliness and significance. Their total length may in no case exceed 500 words or their equivalent. They differ from Articles and Notes in that their subject matter may be republished.

Symposium papers should be sent in all cases to Secretaries of Divisions sponsoring the symposium, who will be responsible for their transmittal to the Editor. The Secretary of the Division by agreement with the Editor will specify a time after which symposium papers cannot be accepted. The Editor reserves the right to refuse to publish symposium articles, for valid scientific reasons. Each symposium paper may not exceed four printed pages (about sixteen double spaced typewritten pages) in length except by prior arrangement with the Editor.

Remittances and orders for subscriptions and for single copies, notices of changes of address and new professional connections, and claims for missing numbers should be sent to the American Chemical Society, 1155 Sixteenth St., N. W., Washington 6, D. C. Changes of address for the *Journal of Physical Chemistry* must be received on or before the 30th of the preceding month.

Claims for missing numbers will not be allowed (1) if received more than sixty days from date of issue (because of delivery hazards, no claims can be honored from subscribers in Central Europe, Asia, or Pacific Islands other than Hawaii), (2) if loss was due to failure of notice of change of address to be received before the date specified in the preceding paragraph, or (3) if the reason for the claim is "missing from files."

Subscription Rates (1960): members of American Chemical Society, $12.00 for 1 year; to non-members, $24.00 for 1 year. Postage to countries in the Pan-American Union $0.80; Canada, $0.40; all other countries, $1.20. Single copies, current volume, $2.50; postage, $0.10. Back volumes (Vol. 56–59) $25.00 per volume; (starting with Vol. 60) $30.00 per volume; foreign postage per volume $1.20, Canadian, $0.15; Pan-American Union, $0.25. Single copies: back issues, $3.00; for current year, $2.50; postage, single copies: foreign, $0.15; Canadian, $0.05; Pan American Union, $0.05.

The American Chemical Society and the Editors of the *Journal of Physical Chemistry* assume no responsibility for the statements and opinions advanced by contributors to This Journal.

The American Chemical Society also publishes *Journal of the American Chemical Society*, *Chemical Abstracts*, *Industrial and Engineering Chemistry*, International Editon of *Industrial and Engineering Chemistry*, *Chemical and Engineering News*, *Analytical Chemistry*, *Journal of Agricultural and Food Chemistry*, *Journal of Organic Chemistry*, *Journal of Chemical and Engineering Data* and *Chemical Reviews*. Rates on request.

-4 W.A. 2503

THE JOURNAL OF PHYSICAL CHEMISTRY

(Registered in U. S. Patent Office) (© Copyright, 1960, by the American Chemical Society)

VOLUME 64 FEBRUARY 24, 1960 NUMBER 2

KINETICS OF OXIDATION-REDUCTION REACTIONS OF PLUTONIUM. THE REACTION BETWEEN PLUTONIUM(IV) AND TITANIUM(III) IN PERCHLORATE SOLUTION[1]

BY S. W. RABIDEAU AND R. J. KLINE

Contribution from the University of California, Los Alamos Scientific Laboratory, Los Alamos, New Mexico

Received February 20, 1959

The kinetics of the reaction between Pu(IV) and Ti(III) has been studied by following the rate of disappearance of Pu(IV) spectrophotometrically at 4695 Å. The rate law for the reaction can be written: $-d[Pu(IV)]/dt = -d[Ti(III)]/dt = k_1[Pu^{+4}][Ti^{+3}][H^+]^{-1}$. From a study of the temperature coefficient of the reaction rate in molar perchloric acid solutions of ionic strength 1.02, the thermodynamic quantities associated with the activation process have been calculated in terms of the principal species. At 25° they have been calculated to be: $\Delta F^{\ddagger} = 15.0 \pm 0.1$ kcal./mole, $\Delta H^{\ddagger} = 16.7 \pm 0.72$ kcal./mole and $\Delta S^{\ddagger} = 5.9 \pm 2$ e.u. The reaction between Ti(III) and perchlorate ion has been considered and the effect of chloride ion on the rate of reaction between Pu(IV) and Ti(III) has been found to be negligible.

Introduction

This study of the reaction between Pu(IV) and Ti(III) in aqueous perchlorate solutions continues a kinetic survey of reactions of plutonium in various oxidation states with inorganic oxidation–reduction reagents. It is hoped that the addition of the thermodynamic description of the kinetics of this reaction to already existent data will aid in the understanding of the kinetic behavior of plutonium specifically, and inorganic reaction kinetics in general.

Good precision can be obtained in kinetic studies in which Pu(IV) is involved as one of the reactants with the use of the absorption peak at 4695 Å. This peak has been shown to obey Beer's law and the molar absorptivity at this wave length is *ca.* 55 M^{-1} cm.$^{-1}$ in strongly acid solutions at 25°. Consequently, to achieve the required degree of precision in the measurements of the optical densities, it is necessary to use solutions approximating concentrations of $10^{-3}M$. In the present study, the observed specific rate constants are of magnitudes which permit measurements to be obtained at room temperature and below.

Experimental

Spectrophotometric measurements were made with the Cary Model 14 recording instrument. The progress of the reaction was followed by means of measurements of the optical densities at 4695 Å. At this wave length, Pu^{+4} and $PuOH^{+3}$ are the major absorbing species with a relatively minor contribution to the observed optical densities made by Ti(III), Ti(IV) and Pu(III). The solutions of Pu(IV) and Ti(III) were contained in separate legs of a double chambered 10 cm. spectrophotometer cell which had been flushed with nitrogen. The cell was immersed in a water-bath held at constant temperature within ± 0.1°. At time zero, the solutions were mixed and placed in the thermostated cell compartment of the spectrophotometer. The first measurements of the optical densities were made within 30 seconds of the time of mixing.

Plutonium(III) solutions of desired acidity were freshly made for each experiment by the dissolution of weighed quantities of oxide-free, high-purity plutonium metal in the requisite amount of standardized 71% perchloric acid. Oxidation of weight aliquots of this diluted acid solution of Pu(III) was accomplished in the spectrophotometer cell by the addition of known weights of 0.1 *N* standardized potassium dichromate solution. The quantity of dichromate solution used was always less than the amount required for the complete conversion of Pu(III) to Pu(IV) to avoid the complications introduced by the presence of $Cr_2O_7^{=}$ in the rate experiments. Since the potassium dichromate solution was prepared in water without added sodium perchlorate or perchloric acid, it was necessary to add an equal volume of an acid–salt solution with a concentration of twice the final desired value to maintain the acidity and ionic strength at the desired levels. The oxidation of Pu(III) to Pu(IV) by dichromate is known to proceed rapidly.[2]

A titanium(III) chloride stock solution was prepared in 6 *N* hydrochloric acid by dissolving titanium hydride manu-

(1) This work was done under the auspices of the U. S. Atomic Energy Commission.

(2) R. E. Connick, W. H. McVey and G. E. Sheline, Report CN-1360, Feb. 10, 1944, p. 3; Paper 3.12 of "The Transuranium Elements," National Nuclear Energy Series, Div. IV, 14B, McGraw-Hill Book Co., Inc., New York, N. Y., 1949.

factured by Metal Hydrides, Inc., Beverly, Mass. This solution was filtered and stored under an atmosphere of helium. Dilutions were made by the addition of 2 ml. of stock to 98 ml. of helium-saturated perchloric acid or perchloric acid–sodium perchlorate mixtures of the acidity and ionic strength to be used in the kinetic study. The concentration of Cl^- present in this reagent was reduced further by an approximate sevenfold dilution which occurred on mixing the reactants. The final concentration of hydrochloric acid was 0.02*M* during the rate runs.

Perchloric acid solutions were made from Baker and Adamson reagent grade 71% acid which had been boiled to remove organic matter, filtered through a sintered glass funnel and standardized on a weight basis against Baker analyzed grade mercuric oxide.

Sodium perchlorate was prepared by the neutralization of C.P. grade sodium carbonate with perchloric acid and then by double recrystallization from distilled water. The salt was dried thoroughly at 110° before use.

Sodium chloride was purified by precipitation of the C.P. material from aqueous solution with concentrated hydrochloric acid. The product was filtered and ignited at 600° overnight in a muffle-type furnace.

Distilled water which had been redistilled in an all-Pyrex apparatus from alkaline permanganate solution was used in the preparation of all solutions.

Ti(III) Analysis.—It was necessary to determine the Ti(III) concentration as function of time because of the side reaction between Ti(III) and perchlorate. The kinetics of the reduction of perchlorate by this reagent has been studied.[3] The concentration of Ti(III) at the time of mixing of the reactant solutions was determined from an analysis prior to mixing together with an experimentally measured rate of change of the Ti(III) concentration under the conditions of temperature, acidity and ionic strength as used in the kinetic study.

In order to determine the rate of change of Ti(III), 5-ml. aliquots of the titanium solution were quenched in solutions containing 5 ml. of 0.01 *N* ceric sulfate in 40 ml. of 1 *N* sulfuric acid just prior to, during and after each rate run. The concentration of the remaining Ce(IV) was determined spectrophotometrically at 4390 Å. Cerium(IV) controls containing 5 ml. of perchlorate solution were measured in the same way and the Ti(III) concentration was calculated from the amount of Ce(IV) that disappeared. Pseudo first-order plots of log [Ti(III)] *versus* time gave straight lines from which the Ti(III) concentration could be found at any time.[4]

The molar absorptivity of Ce(IV) in 1 *N* sulfuric acid at 25° and 4390 Å. was found to be 191.1 ± 0.03 M^{-1} cm.$^{-1}$. For this determination, cerium(IV) sulfate solutions were standardized against U. S. Bureau of Standards As_2O_3, sample 83a.

Calculations.—At 4695 Å., Pu(IV) has an absorption peak with experimentally determined molar absorptivities in 1 *M* perchloric acid of 59.6 M^{-1} cm.$^{-1}$ at 2.5° and 55.6 M^{-1} cm.$^{-1}$ at 25°. Under the same conditions, the molar absorptivities of Pu(III) are 3.87 and 3.48 M^{-1} cm.$^{-1}$, respectively. Corrections to the observed optical densities were made for the contributions of Cr(III) formed in the reduction of $Cr_2O_7^=$ with Sn(II), Fe(II), Ti(III) and HCOOH. Its value, 4.14 ± 0.01 M^{-1} cm.$^{-1}$, has been found to be temperature independent between 2.4 and 25.0°. Neither Ti(III) nor Ti(IV) absorb appreciably at this wave length.

From the change of optical density with time, the concentration of Pu(IV) at any time *t* was found. Correction of the optical density for the contribution of Pu(III) was made by successive approximations, the total Pu(III) concentration at any time being equal to the initial Pu(III) concentration plus the amount of Pu(IV) reduced at that time.

A correction for the disproportionation of Pu(IV) was found not to be required. At 25° in molar perchloric acid, for example, only *ca.* 6×10^{-8} mole/l. decrease in the concentration of Pu(IV) could have occurred in the time required to prepare the solutions for the kinetic experiments. The disproportionation reaction, of course, is even slower at lower temperatures.

Observed rate constants were calculated from slopes of plots of log $\{[Pu(IV)]_0/[Ti(III)]_0([Ti(III)]_0 - x)/([Pu(IV)]_0 - x)\}$ *versus* time. The zero subscripts refer to initial concentrations. Excellent linearity of these plots was observed even to 95% completion of the reaction.

The rate constant data were treated statistically by the method of least squares to yield the value for the activation energy. The uncertainties correspond to the standard deviations.

Results

Stoichiometry.—In aqueous acid solution, reduction of Pu(IV) produces Pu(III). Visual observation confirmed the formation of Pu(III) in the reduction of Pu(IV) with Ti(III); the characteristic blue color of Pu(III) intensified as the reaction proceeded. The oxidation of Ti(III) to Ti(IV) was confirmed by consideration of rate runs in which the zero-time concentrations of Pu(IV) were greater than those of Ti(III). The final optical densities measured at a time corresponding to the essential completion of the reaction compared favorably with calculated values in which a one-electron change was assumed for the oxidation of titanium.

Rate Expressions.—The rate law for the reaction between Pu(IV) and Ti(III) in perchloric acid solution can be written

$$-\mathrm{d[Pu(IV)]}/\mathrm{d}t = k_1[Pu^{+4}][Ti^{+3}][H^+]^{-1} \quad (1)$$

where the Roman numerals refer to total metal ion concentrations. With the formation constant for the hydrolysis of Pu^{+4} given by the relation

$$K = [PuOH^{+3}][H^+]/[Pu^{+4}] \quad (2)$$

it can be shown that

$$[Pu^{+4}] = [Pu(IV)][H^+]/([H^+] + K) \quad (3)$$

With the substitution of the expression for Pu^{+4} given by equation 3 into equation 1, it follows that

$$-\mathrm{d[Pu(IV)]}/\mathrm{d}t = k_1[Pu(IV)][Ti^{+3}]/([H^+] + K) \quad (4)$$

$$= k_{obsd}[Pu(IV)][Ti^{+3}] \quad (5)$$

where $k_1 = k_{obsd}([H^+] + K)$. In equation 5, k_{obsd} corresponds to the experimentally observed specific rate constant and as shown in equation 1, k_1 is the specific rate constant for the reaction in which the rate law is written in terms of the principal species.

Effect of Hydrogen Ion on Rate.—The hydrogen ion concentration dependence of the reaction between Pu(IV) and Ti(III) was studied in a series of experiments at 2.4° in perchloric acid solutions of ionic strength 2.02. Sodium perchlorate was used to maintain the ionic strength at a constant value. The results are given in Table I. A value of 0.019 was calculated for the formation constant for the hydrolysis of Pu(IV) in per-

(3) F. R. Duke and P. R. Quinney, *J. Am. Chem. Soc.*, **76**, 3800 (1954).

(4) Rate constants for the reaction between Ti(III) and ClO_4^- have been obtained in 0.024 *M* Cl^- at various temperatures and hydrogen ion concentrations at an ionic strength of 1.02. Values of an apparent rate constant have been calculated. Extrapolation of these values to zero hydrogen ion concentration have given a specific rate constant for the hydrogen ion independent path. Analysis of these values in the usual way resulted in the calculation of a heat of activation of 27.5 ± 4 kcal./mole. At 40° the value of the specific rate constant for the hydrogen ion independent path was found to be 7.49 × 10^{-2} M^{-1} min.$^{-1}$ (*cf.* ref. 3).

Only a 15% variation in the apparent rate constants was found as the hydrogen ion concentration was changed from 0.27 to 1.02 *M* at 40°. Thus, it is not possible to ascribe this variation uniquely to a hydrogen ion dependent path because of possible medium effects.

With Duke's value[3] for the formation constant for $TiCl^{+2}$ it has been calculated that the Ti(III) is complexed to the extent of *ca.* 5% in solutions containing chloride ion concentrations as were used in the present work.

TABLE I

HYDROGEN ION CONCENTRATION DEPENDENCE OF THE RATE CONSTANT FOR THE Pu(IV)-Ti(III) REACTION IN PERCHLORATE SOLUTIONS AT $\mu = 2.02$ AT 2.4°

$[H^+]$, M	k_{obsd}, M^{-1} sec.$^{-1}$	k_1, sec.$^{-1}$
2.02	5.63	11.5
	5.53	11.3
	5.77	11.8
1.02	12.5	13.0
	12.0	12.5
	11.3	11.7
0.52	24.8	13.4
	26.7	14.4
0.27	46.9	13.6
	47.1	13.6
	Mean	12.7 ± 0.3

chlorate media of ionic strength two at 2.4 from previously determined thermodynamic data.[5] With the assumption that the hydrolysis quotient for Ti(III) is of the same order of magnitude as that found for Fe(III) in solutions of ionic strength two, namely, 1.5×10^{-3},[6] a correction of the rate constants for the hydrolysis of Ti(III) would be insignificant.

One possible mechanism which is in accord with the second-order nature of the reaction and with the observed hydrogen ion concentration dependence is

$$Pu^{+4} + H_2O = PuOH^{+3} + H^+ \text{ (rapid)} \quad (6)$$

$$PuOH^{+3} + Ti^{+3} = Pu^{+3} + TiO^{+2} + H^+ \text{ (rate determining)} \quad (7)$$

A kinetically equivalent mechanism in which $TiOH^{+2}$ and Pu^{+4} are involved in the rate determining step is also in accord with the data. There appears to be no hydrogen ion independent path; instead, the reaction is favored by the prior loss of hydrogen ion and the consequent charge decrease.

Temperature Coefficient of Reaction Rate.—The effect of the variation of temperature upon the rate of reaction has been studied in molar perchloric acid solutions of ionic strength 1.02 between 2.4 and 25.0°. The results are given in Table II.

It was necessary to use solutions with concentrations of approximately 1 to 5×10^{-3} M in Pu(IV) and Ti(III) to obtain optimum changes in optical density. Thus, with an average observed rate constant of 65.5 M^{-1} sec.$^{-1}$ at 25.0°, a considerable portion of the reaction was over before the first optical densities were recorded. This is believed to account for the lower precision observed in the values of the specific rate constants at the higher temperatures. For the calculation of the hydrolysis quotient K as a function of temperature in solutions of ionic strength 1.02, the temperature coefficient found previously[5] for this quotient in perchlorate solutions of ionic strength 2.0 was used. From a linear plot of $\log k_1$ *versus* $1/T$, a least squares slope of 3778 ± 157 is calculated which corresponds to an experimental activation energy of 17.3 ± 0.72 kcal./mole. From expressions of the transition state theory,[7] values of the heat, free energy and entropy of activation were calculated in terms of the principal species, *i.e.*, $Pu^{+4} + Ti^{+3} + H_2O = (Pu{\cdot}Ti{\cdot}OH)^{+6} + H^+$. These quantities are: $\Delta F^{\ddagger} = 15.0 \pm 0.1$ kcal./mole, $\Delta H^{\ddagger} = 16.7 \pm 0.72$ kcal./mole and $\Delta S^{\ddagger} = 5.9 \pm 2$ e.u. For this calculation, a rate constant of 69.0 sec.$^{-1}$ at 25.0° was used. With the use of individual ionic entropies ($H^+ = 0$), the entropy of the activated complex is calculated to be − 125 e.u. This is in good agreement with the values found for other activated complexes with a charge of +6.[8]

TABLE II

TEMPERATURE DEPENDENCE OF THE RATE CONSTANT FOR THE Pu(IV)-Ti(III) REACTION IN MOLAR PERCHLORIC ACID SOLUTIONS OF IONIC STRENGTH 1.02

Temp., °C.	$k_{obsd.}$, M^{-1} sec.$^{-1}$	k_1, sec.$^{-1}$
25.0	58.4	61.4
	75.2	79.0
	61.3	64.4
	78.9	82.9
	54.3	57.1
15.2	18.0	18.7
	22.1	23.0
	23.2	24.1
9.4	11.7	12.1
	11.9	12.3
	14.8	15.3
2.4	6.05	6.24
	5.78	5.96
	5.69	5.87
	6.10	6.29
	5.65	5.83

Effect of Ionic Strength.—The effect of ionic strength upon the rate of the reaction has been examined. The results of this study are given in Table III. An increase in the values of the specific rate constants by a factor of about two is observed at each acidity as the ionic strength is changed from 1.02 to 2.02.

TABLE III

INFLUENCE OF IONIC STRENGTH ON THE REACTION RATE IN PERCHLORATE SOLUTIONS AT 2.4°

$[H^+]$, M	μ	$k_{obsd.}$ M^{-1} sec.$^{-1}$
1.02	1.02	6.05, 5.78, 5.69, 5.65, 6.10
0.52	1.02	15.1, 15.8, 14.1
0.27	1.02	24.3, 24.7
1.02	2.02	12.5, 12.0, 11.3
0.52	2.02	24.8, 26.7
0.27	2.02	46.9, 47.1

TABLE IV

EFFECT OF CHLORIDE ION ON Pu(IV)-Ti(III) REACTION RATE IN MOLAR PERCHLORIC ACID SOLUTION AT 2.4°

$[Cl^-]$, M	μ	[Ti(III)], M	[Pu(IV)], M	$k_{obsd.}$ M^{-1} sec.$^{-1}$
0.020	1.02	.....	.....	5.85[a]
.031	1.03	2.396×10^{-3}	1.442×10^{-3}	5.69
.050	1.05	2.245×10^{-3}	1.506×10^{-3}	6.24

[a] Average value at 2.4° from Table II.

(5) S. W. Rabideau, *J. Am. Chem. Soc.*, **79**, 3675 (1957).
(6) R. Milburn and W. Vosburgh, *ibid.*, **77**, 1352 (1955).
(7) S. Glasstone, K. Laidler and H. Eyring, "The Theory of Rate Processes," McGraw-Hill Book Co., Inc., New York, N. Y., 1941, p. 417.
(8) T. W. Newton and S. W. Rabideau, THIS JOURNAL, **63**, 365 (1959).

Influence of Chloride Ion.—The presence of Cl^- could not be avoided in perchlorate solutions to which Ti(III) had been added. Therefore it was necessary to determine the effect of Cl^- on the rate of the Pu(IV)-Ti(III) reaction. The results are given in Table IV.

A comparison of the values of the observed rate constants in Table IV reveals that small additions of Cl^- did not significantly alter the rate of the reaction. It should be noted that a small difference of ionic strength existed among the experiments which may account for the small spread in the specific rate constant values.

Acknowledgment.—The authors wish to express their appreciation to Dr. J. F. Lemons for valuable discussions and interest shown in this work.

AN ELECTROKINETIC APPROACH TO THE ENERGETICS OF THE QUARTZELECTROLYTE SOLUTION INTERFACE[1]

BY RAYMOND R. MYERS AND ARMAND F. LEWIS

Lehigh University, Bethlehem, Penna.

Received March 26, 1959

Streaming potentials generated by the passage of electrolyte solutions over quartz wool were measured at temperatures ranging from 25 to 65°. The parameter $\Delta P/E$ (applied pressure/streaming potential) was used in the analysis of the data, and was given the symbol ρ to represent the charge density of the electrokinetically active portion of the double layer. Isothermal plots of ρ *versus* ionic strength μ at four temperatures permitted the calculation of the heat of streaming at constant ρ. This heat term was called the isocoulombic heat. The calculation gave heats that ranged from 1.3 to 4.4 kcal./mole, depending on the electrolyte and also on temperature. This order of magnitude indicates that the generation of a streaming potential involves a physical process. The response of the isocoulombic heats to temperature paralleled the trend in sediment values of quartz powder in the same electrolytes, thereby suggesting an application of electrokinetics to the problem of stability.

Certain surface chemistry measurements (heats of immersion and contact angles for example) are adaptable to the evaluation of the total energy change at a surface in the process of being wetted; however, they do not characterize the double layer which is formed at the interface. The purpose of this paper is to develop a better understanding of the electrokinetic properties of a solid–liquid interface and of the double layer which gives rise to this electrical effect. Electrokinetics offers one of the few approaches for critically studying the already wetted surface, as distinguished from the process of wetting.

One of the least developed areas in electrokinetics is the temperature coefficient of streaming potential generation. Several important variables were studied in connection with this present work with the objective of creating a new tool for the study of the energetics of wetted surfaces. In this paper, the temperature coefficient of a particular streaming potential parameter is used to characterize the electrical double layer. Quartz was chosen for this work because of its frequent use in electrokinetic studies[2-4] and because of its consistent composition and structure.

The evaluation of a streaming potential involves the measurement of the e.m.f. E generated across a diaphragm per unit pressure gradient ΔP. In a given solid–liquid system at interfacial equilibrium, the ratio of E to ΔP is a constant. An analysis of the parameter $\Delta P/E$ reveals that it has the dimensions of e.s.u./cm.^{3}, which is essentially a space charge density term. Henceforth $\Delta P/E$ is called the *electrokinetic charge density* and is assigned the symbol ρ. From an experimental analysis of this parameter, a new treatment of streaming potential has evolved which is independent of the classical zeta potential concept of Helmholtz and Smoluchowski.[5]

Experimental

Materials.—Streaming plugs 4.0 cm. long and 1.1 cm. in diameter and weighing 0.4 g. were made of quartz wool which easily could be packed into plugs of a reproducible permeability.[6] The quartz wool was obtained from the Thermal-American Fused Quartz Corporation and had an average fiber diameter of 9.5 μ. It was washed first with 95% ethanol, then water, and finally was packed into the streaming cell, washed with 250 cc. of 3% HF solution and then rinsed with distilled water.

Solutions were made by adding Analytical Reagent grade chemicals to distilled water (specific conductivity 1.4 to 2.0 $\times 10^{-6}$ ohm^{-1}cm.$^{-1}$) which had been boiled just before use to remove dissolved gases.

Methods.—An apparatus was designed to use non-polarizing saturated calomel half-cells as electrodes. Agar salt bridges were utilized to couple the generated e.m.f. with the half-cells. The inlet electrode was provided with a counterflow of fresh streaming liquid so that the liquid entering the plug would not be contaminated by the bridge electrolyte. The exit chamber of the cell was designed so that the exit liquid flowed past the sample holder to ensure a constant temperature throughout the plug. The e.m.f. E was read on a Type K Leeds and Northrup potentiometer using a Brown Electronik null indicator. Pressure difference ΔP was determined by a mercury U-tube manometer across the plug. ΔP was plotted as a function of E and the slope of the line was taken as the index of the electrokinetic charge density.

Sediment heights of quartz powder (surface area, 0.44 m.^{2} per gram and a particle diameter of 2 to 5 μ) were measured directly by settling equal amounts (4.0 g.) of quartz powder[7]

(1) Based on the Ph.D. dissertation of Armand F. Lewis, Armstrong Cork Company Fellow, 1958.

(2) V. Pravdic and M. Mirnik, *Croatica Chem. Acta*, **30**, 113 (1958).

(3) A. M. Gaudin and D. W. Fuerstenau, *Mining Eng.*, **7**, 66 (1955).

(4) L. A. Wood, *J. Am. Chem. Soc.*, **68**, 437 (1946).

(5) H. Helmholtz and M. Smoluchowski, *Wied. Ann.*, **7**, 337 (1879). See P. E. Bocquet, "Two Monographs on Electrokinetics," Eng. Res. Inst., Univ. of Mich, Bull. 33, 1951.

(6) M. Z. Nammari, Masters Degree Thesis, Lehigh University, June, 1958.

(7) H. A. Gardner, "Physical and Chemical Examination of Paints, Varnishes, Lacquers and Colors," 9th Ed., Institute of Paints and Varnishes Research, Bethesda, Maryland 1939, p. 216.

in flat bottomed Gardner viscosity tubes[7] 1 cm. in diameter. The ionic strength of the electrolyte solutions was 0.1 mole per liter.

Data Analysis.—A typical ΔP *versus* E relation for quartz is linear, through the origin, and reproducible to within 5%. Slopes ρ of the relation, $\Delta P = \rho E$, were 3.95, 4.85 and 15.0 cm. per volt for KCl concentrations of 8.3, 16.6 and 41.5 μ moles per liter, respectively. Distilled water gave a considerably lower electrokinetic charge density and its value depended upon its quality. In fact, ionic strength becomes a critical parameter in determining streaming potentials in distilled water and must be controlled carefully.

Results

A series of experiments was conducted in which ρ was determined for quartz–electrolyte solution interfaces at various ionic strengths μ and temperatures. Data are given in Fig. 1 for KCl at four temperatures, and in Fig. 2 for the chlorides of lithium and barium and for silver nitrate at 25°. In each case, ρ increases with increasing ionic strength, and decreases with increasing temperature. These plots of ρ *versus* μ are called *Electrokinetic isotherms*. They resemble adsorption isotherms in that they represent the amount adsorbed at the interface (electrokinetic charge density) as a function of the equilibrium concentration of charges in solution.

Many temperature-dependent quantities in physical chemistry obey the relation of Clausius and Clapeyron if they are of thermodynamic, or of Arrhenius if they are of kinetic significance. Such a relation is utilized in the calculation of isosteric heats. In this present study, logarithms of the ionic strength necessary to give a constant charge density were plotted against reciprocal temperature at several different values of ρ. In other words, a procedure is used which is analogous to the determination of isosteric heats of adsorption *via* the slopes of the line. In this case, however, the heat term was called the *isocoulombic heat* since it resembles a differential heat term for the electrokinetic process at a constant surface charge density (constant ρ). The general equation expressing the change in ionic strength with temperature while preserving a given electrokinetic charge density at the interface is

$$\frac{\Delta \log (\mu)_\rho}{\Delta (1/T)} = \frac{H_{isc}}{2.3R}$$

where H_{isc} is the isocoulombic heat, T the absolute temperature, and R the gas constant. The slopes are measures of $H_{isc}/2.3R$. With data taken from electrokinetic isotherms at several temperatures, plots were made of log $(\mu)_\rho$ against $1/T$. Some of the plots exhibited a slight curvature at the lower temperatures (25 to 35°), however, a linear trend was approached for most of the electrolytes studied at the higher temperatures.

H_{isc} values were determined at 25 and 65° and averaged for several values of ρ. Table I shows that for a given charge density, the heat accompanying this electrokinetic process decreases in the order $K^+ > Ag^+ > Ba^{++} \approx Li^+$ at 25°, but in the order $Ba^{++} > K^+ \approx Ag^+ > Li^+$ at 65°. No clear correlation with any property of the ionic species present in the system is evident.

Discussion

The low values of H_{isc} (1 to 5 kcal. per mole) imply that streaming potential generation represents a physical process. This energy value compares to the heat term of 3 kcal. per mole calculated by Grubb[8] for the enthalpy of activation for

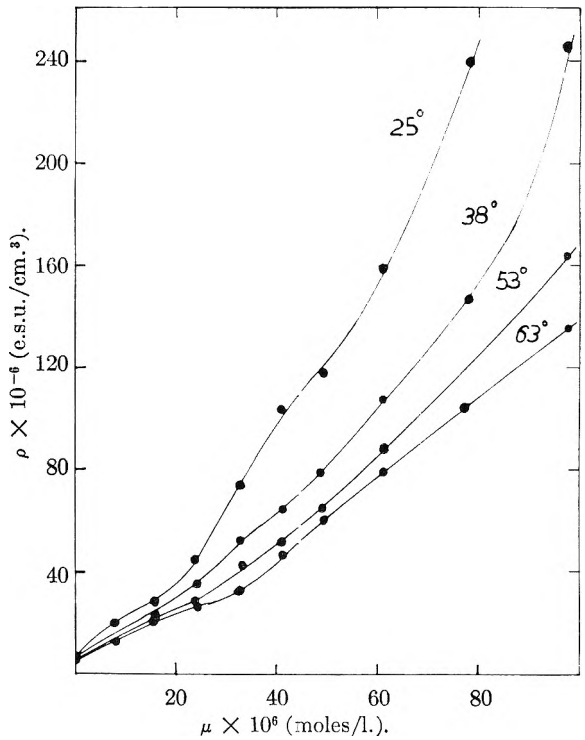

Fig. 1.—Electrokinetic isotherms for potassium chloride solutions on quartz surfaces at several temperatures. (In changing from e.s.u./cm.² to moles (of charges)/l., multiply by 3.35×10^{-12}.)

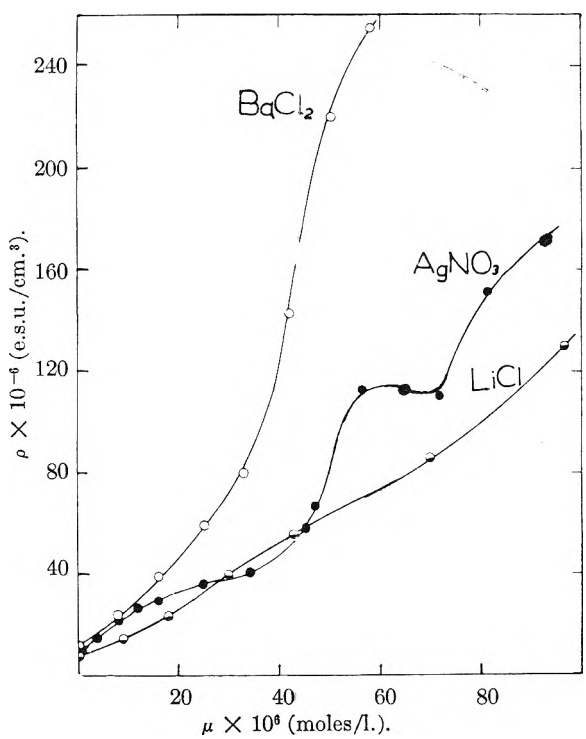

Fig. 2.—Electrokinetic isotherms for several electrolyte solutions on quartz surfaces at 25°.

(8) W. T. Grubb, THIS JOURNAL, **63**, 55 (1959).

TABLE I

AVERAGE ISOCOULOMBIC HEATS AND SEDIMENT VOLUMES AT 25 AND 65° FOR THE QUARTZ–ELECTROLYTE SOLUTION INTERFACE

	25°		65°	
Electrolyte	H_{isc}, kcal./mole[a]	Sediment vol. cm.³/g.[b]	H_{isc}, kcal./mole[a]	Sediment vol. cm.³/g.[b]
LiCl	2.0	0.610	1.3	0.603
KCl	4.4	.711	1.7	.647
$BaCl_2$	2.1	.647	2.5	.654
$AgNO_3$	3.7	.629	1.7	.609

[a] Standard deviation, 0.4 kcal./mole. [b] Standard deviation, 0.008 cm.³/g.

ionic migration in water-saturated ion-exchange membranes. Both approaches apparently reflect energetic properties of double layers.

In order to attach thermodynamic significance to the H_{isc} term herein presented, the nature of the ion transport process must be clearly defined, especially from the point of view of initial and final states. This part is difficult to interpret since little is definitely known about the mechanism of streaming potential generation. However, a review of some possibilities is in order. In a theoretical analysis by Payens,[9] it was shown that a hydrated ion loses part of its hydration shell when placed in the vicinity of an interface of a low dielectric material. A theoretical equation involving the change in free energy of hydration was derived in terms of the distance X from the dielectric surface, $\Delta G = 3N(Zq)^2/4\epsilon X$, where ΔG is the Gibbs free energy, N is Avogadro's number, Z the ionic valence, q the electronic charge, and ϵ the dielectric constant of water. The magnitude of the energy changes occurring in this transition is from 1 kcal./mole when X is 3 Å. to 6 kcal./mole when X is 0.5 Å.

The isocoulombic heats of Table I and the free energies of partial hydration as calculated by the Payens equation are of comparable magnitude since entropy changes in this system would be negligible. This agreement indicates that a possible mechanism of e.m.f. generation in the streaming cell involves the movement of an ion from a region inside the double layer, where it is adsorbed but partially dehydrated, to a more detached region where it is fully hydrated. Whether the new location of the ion is inside the double layer depends on the model chosen. The constancy of the isocoulombic heat with various surface charge densities, implies that all of the electrokinetic activity is confined to layers beyond the first adsorbed layer.

The property represented by H_{isc} may possibly be a composite of energy of desorption partially compensated by energy of hydration. However, as deduced above, the adsorption energy probably plays a less important role in the transition. Furthermore, the adsorption energy would likely be independent of the type of ion associated with the charge. In trying to explain energetic processes in streaming potential generation it must be fully realized that it is a steady-state condition. Therefore any transition in the double layer which is induced by the streaming liquid must be completely reversible.

Sediment volumes also reflect the properties of the wetted surface. Therefore, data for the sediment volumes of the quartz powder at 25 and 65° in electrolytes of ionic strength of 0.1 mole/liter were obtained and are given in Table I for comparison. Higher ionic strength solutions were used in this phase of the work because no temperature dependence of sediment volume was observed in low ionic strength solutions as in distilled water. Analysis of the data in Table I show the similar behavior of the sediment volumes and the isocoulombic heats at the two temperatures. The correlation between these two measurements is apparent, particularly when the same reversal in temperature dependence of the barium ion solution is noted in both measurements. In addition, plots of sediment volume *versus* H_{isc} are found to converge at the sediment volume of quartz powder in distilled water (2.95 cm.).

In general, if the mechanism of streaming potential generation involves a distortion or polarization of the interfacial double layer, the isocoulombic heat may be regarded as a measure of the ease with which the double layer is distorted. Therefore, a less rigid double layer would exhibit a lower isocoulombic heat. Furthermore, a less rigid double layer should also allow a closer approach of two surfaces and consequently would form a more compact sediment. Disregarding the flocculation aspects of suspension stability, this prediction is followed, qualitatively at least, by the parallel behavior of the isocoulombic heats and the sediment volumes of the quartz–electrolyte solution interface.

In summary, a criterion of activity called the electrokinetic charge density appears to reflect the behavior of ions in the electrokinetically sensitive portion of the double layer. This parameter has led to the evaluation of heats of streaming at constant charge density. A physical process appears to be involved. Indications of the usefulness of electrokinetics in interfacial studies are given by comparison of isocoulombic heats and sediment volumes. Both appear to be a measure of double layer rigidity. Dispersion stability, flocculation tendencies of pigments, and flotation of minerals are several fields of endeavor in which the isocoulombic heat concept may prove useful.

Acknowledgments.—The authors are pleased to acknowledge the support of the Armstrong Cork Company whose interest in electrokinetics made this study possible.

(9) T. A. J. Payens, Ph.D. Dissertation, University of Utrecht, 1955.

TRANSPORT PROCESSES IN LIQUID SYSTEMS.[1] III. THERMODYNAMIC COMPLICATIONS IN THE TESTING OF EXISTING DIFFUSIONAL THEORIES

BY R. R. IRANI[2] AND A. W. ADAMSON

Department of Chemistry, University of Southern California, Los Angeles 7, California

Received June 8, 1959

The diffusional and thermodynamic data of the sucrose–water, methanol–benzene and ethanol–benzene systems are used to test and discuss existing diffusion models for liquid systems. The critical dependence of diffusional models on the structure and association in liquids also is discussed. It is shown as well how diffusion data can be interpreted to yield useful information on the structure of solutions.

Introduction

Interest in liquid diffusion has arisen in the last few years, and various theoretical approaches[3–7] have been proposed that tried to relate the measurable two self-diffusion coefficients and the binary (mutual) diffusion coefficient with other thermodynamic properties of a binary system.

Although complete diffusional data are available for a few ideal binary liquid systems,[8] the various models give comparable agreements[7] and no critical evaluation is possible. For example, the ideal benzene–carbon tetrachloride, the toluene–chlorobenzene and the chlorobenzene–bromobenzene systems can be shown to fit any of the theoretical treatments mentioned above. Of the non-ideal binary liquid systems, complete thermodynamic and diffusional data (two self and one binary diffusion coefficients) over all possible concentrations at 25° are available only for the methanol–benzene,[8–9] the ethanol–benzene,[8] and the sucrose–water[10] systems. Using these data, it was therefore undertaken to test and compare the various existing diffusional models. However, it was found that the values of the calculated diffusion coefficients depended in most cases on the assumed degree of association in the liquid mixtures. Thus, a section will be devoted to show the effect of association on the diffusional thermodynamic factors.

Glossary of Symbols

Component 1: water, methanol, ethanol
Component 2: sucrose, benzene

a Activity

A $\left(1 + \frac{\mathrm{d} \ln y}{\mathrm{d} \ln c}\right)$

A^0 Value of A if neither association nor solvolysis is assumed. The superscript ^{0} used above concentration units and other activity coefficients will have the same meaning.

B_i $\left(1 + \frac{\mathrm{d} \ln f_i}{\mathrm{d} \ln N_i}\right)$

C Molarity in moles per liter

k_{ij} Specific rate constant for an i-j coupled motion

f Activity coefficient on the mole fraction basis

F Volume fraction

h Planck's constant

K Boltzmann's constant

m Molality in moles per 100 g. of solvent

n Solvolysis no. (no. of solvent molecules, or component 1, associated with a component 2 molecule)

N Mole fraction

$\bar{V}$ Partial molal volume

T Absolute temp.

y Activity coefficient on the molar basis

ϕ Practical osmotic coefficient

α Association no. for the solvated component 2

β Association no. for component 1

λ_{ij} Distance that species i advances as a result of a coupled motion with component j

$$\Lambda_{ij} = \lambda_{ij}\left(\frac{\bar{V}_1}{\bar{V}_2}\right)^{1/2} = \lambda_{ji}\left(\frac{\bar{V}_2}{\bar{V}_1}\right)^{1/2}$$

η Viscosity in poises

μ Gibbs partial molal free energy (chemical potential)

μ^0_z Standard state chemical potential on the z concentration scale

D^*_i Self-diffusion coefficient of component i

D_{12} Binary diffusion coefficient

Diffusional Thermodynamic Factors with Assumed Association in Liquid Mixtures

General.—The following section will be devoted toward pointing out the sensitive dependence of the diffusional thermodynamic factors on the degree of association in the liquid mixtures involved. The methods of computing these thermodynamic factors for the three binary systems to be discussed in this article also will be considered.

Although in an associated solution of two components Y and Z a large number of species can coexist, forming a distribution function reminiscent of polymeric solutions, three predominant species prevail (or can be thought of as averages of similar species): Y_β, $[ZY_n]_\alpha$ and Z_γ where β, n, α and γ can vary from zero upward, but in no case being all zero. In dilute solutions of Z in Y no Z_γ molecules would be expected, whereas, in dilute solutions of Y in Z, no Y_β would be expected. In concentrated solutions, presently available thermodynamic data on "binary" solutions are not detailed enough to permit the evaluation of the separate thermodynamic contributions of the species discussed above. For the sucrose–water system the assumption of no Z_γ is reasonable inasmuch as no unhydrated associated sucrose molecules are expected. For the methanol–

(1) This investigation was supported in part by contracts with the Office of Ordnance Research and the American Petroleum Institute.

(2) Monsanto Chemical Company, Inorganic Chemicals Division Research Department, St. Louis 66, Missouri.

(3) A. W. Adamson, THIS JOURNAL, **58**, 514 (1954).

(4) L. S. Darken, *Tr. Am. Inst. Mining Met. Engrs.*, **175**, 184 (1948).

(5) O. Lamm, *Acta Chem. Scand.*, **6**, 1331 (1952).

(6) S. Prager, *J. Chem. Phys.*, **21**, 1344 (1953).

(7) A. W. Adamson and R. R. Irani, *J. Chim. Phys.*, **55**, 102 (1958).

(8) P. A. Johnson and A. L. Babb, *ibid.*, **60**, 14 (1956).

(9) C. S. Caldwell and A. L. Babb, THIS JOURNAL, **59**, 1113 (1955).

(10) R. R. Irani and A. W. Adamson, *ibid.*, **62**, 1517 (1958).

benzene and ethanol–benzene systems, the assumption will be made that $\gamma = 0$. However, since n can be chosen to be zero, no assumptions are involved regarding the major component of the $(ZY_n)_\alpha$ molecule.

From the Gibbs–Duhem relationship

$$\sum_j C_i \, d \ln a_i = \sum_j N_i \, d \ln a_i = 0 \qquad (1)$$

and from the definitions given in the glossary of symbols, it can be shown that in general

$$\sum_j A_i \frac{dC_i}{dx} = \sum_j B_i \frac{dN_i}{dx} = 0 \qquad (2)$$

where d/dx is the gradient in the x-direction.

For a multicomponent system

$$\sum_j N_i = \sum_j F_i = \sum_j C_i \bar{V}_i = 1 \qquad (3)$$

If very small concentration changes are chosen, $\bar{V}_i$ can be assumed to stay constant, and differentiation of equation 3 gives

$$\sum_j \bar{V}_i \, dC_i = 0 \qquad (4)$$

For a two component system, it is of interest to note the change in the values of the conventional concentration and thermodynamic units if association and solvolysis are assumed in the absence of associated, unsolvated solute species

$$C_2 = C_2^0/\alpha \qquad (5)$$

$$\bar{V}_1 = \bar{V}_1^0\beta \qquad (6)$$

$$\bar{V}_2 = \alpha(\bar{V}_2^0 + n\bar{V}_1^0) \qquad (7)$$

$$\mu_1 = \beta\mu_1^0 \qquad (8)$$

$$\mu_2 = \alpha(\mu_2^0 + n\mu_1^0) \qquad (9)$$

It follows from equations 2 and 4, that

$$A_1\bar{V}_2 = A_2\bar{V}_1 \qquad (10)$$

$$B_1 = B_2 = B_{12} \qquad (11)$$

Since

$$\mu_i = \mu_{i(c)} + RT \ln \gamma_i C_i = \mu_{i(N)} + RT \ln f_i N_i \qquad (12)$$

then

$$\frac{B_1}{B_1^0} = \frac{B_2}{B_2^0} = \frac{B_{12}}{B_{12}^0} = \left(\frac{\partial\mu_1}{\partial\mu_1^0}\right)\left(\frac{\partial \ln N_1^0}{\partial \ln N_1}\right) \qquad (13)$$

From equations 5, 6, 7 and 8 it follows that

$$\frac{B_{12}}{B_{12}^0} = \alpha \frac{[C_1^0 + (\beta/\alpha - n)C_2^0]}{C_1^0 + C_2^0}[1 - nC_2^0/C_1^0] \qquad (14)$$

In general

$$A_i = B_i \frac{d \ln N_i}{d \ln C_i} \qquad (15)$$

Therefore, for a two component system from equations 5, 6, 7, 14 and 15

$$\frac{A_2}{A_2^0} = \alpha\left[1 - \frac{nC_2^0}{C_1^0}\right] \qquad (16)$$

$$\frac{A_1}{A_2^0} = \frac{\beta\left[1 - \frac{nC_2^0}{C_1^0}\right]}{[n + \bar{V}_2^0/\bar{V}_1^0]}$$

Equations 14, 16 and 17 are true for any binary associated system with the assumptions outlined at the beginning of the section.

Sucrose–Water.—For sucrose–water, Scatchard, *et al.*,[11] tabulated the values of ϕ *vs.* m_2. ϕ for a two component system is defined as

$$\phi = \frac{-\ln a_1}{m_2 M_1/1000} \qquad (17)$$

Equations 1 and 17 can be combined to show that

$$A_2^0 = (d - 0.001C_2^0M_2^0)\frac{d(\phi m_2^0)}{dC_2^0} \qquad (18)$$

Using the data in reference 11, equation 18 and the density (d) data given in "Sugar Analysis"[12] the values of A_2^0 for sugar–water were computed and found to fit the empirical equation

$$A_2^0 = 1 + 0.3695C_2^0 + 0.1388(C_2^0)^2 + 0.0887(C_2^0)^3 \qquad (19)$$

Methanol–Benzene.—For the methanol–benzene system the thermodynamic factors were computed as follows: Scatchard, *et al.*,[13] report analytical expressions for the "corrected" excess free energy of mixing, G_0^E, which at 25° can be represented by the equation

$$G_0^E = N_1^0N_2^0[1205.2 - 157.0(N_1^0 - N_2^0) + 190.7(N_1^0 - N_2^0)^2 - 122.4(N_1^0 - N_2^0)^3 + 92.0(N_1^0 - N_2^0)^4] \qquad (20)$$

where subscript 2 refers to benzene. But

$$G_0^E = RT(N_1^0 \ln f_1^0 + N_2^0 \ln f_2^0) \qquad (21)$$

Therefore

$$B_{12}^0 = 1 + N_1^0N_2^0\left[\frac{d^2(G_0^E/RT)}{d^2N_2^0}\right] \qquad (22)$$

From equations 20 and 22 it follows that at 25° for methanol–benzene

$$B_{12}^0 = 1 + N_1^0N_2^0[-5.372 + 19.704N_2^0 - 70.080(N_2^0)^2 + 115.84(N_2^0)^3 - 74.40(N_2^0)^4] \qquad (23)$$

The complexity of equations 20 and 23 is due to the extreme non-idealities of mixing.

Ethanol–Benzene.—For the ethanol–benzene system, the total vapor pressure P_T over various mixtures is reported[14] at 35, 50, 60 and 66°. A regular log P_T *vs.* $1/T$ plot was made to obtain the values of P_T at 25°. Since fugacities are not available, an ideal vapor mixture is assumed and

$$d \ln a_1^L = d \ln a_1^G = d \ln P_T N_1^G \qquad (24)$$

where a_1^L and a_1^G are the activities of ethanol in the liquid and gas, respectively. Hence

$$A_1^0 = \frac{d \ln P_T N_1^G}{d \ln C_1^0} \qquad (25)$$

Thus $P_TN_1^G$ was plotted *vs.* C_1^0 and at various points the slope was measured and multiplied by $C_1^0/P_TN_1^G$ to yield A_1^0. A_2^0 and B_{12}^0 can be computed from the values of A_1^0 using equations 10 and 15 and are found to agree well with those of Johnson and Babb.[8]

Partial Molal Volumes.—The partial molal volumes for the individual species were computed in a standard procedure.[15] For the three systems under consideration the plot of the molar volume of the mixture *vs.* N_2^0 can be represented within ±4% by straight lines, indicating that when the substances

(11) G. Scatchard, W. J. Hamer and S. E. Wood, *J. Am. Chem. Soc.*, **60**, 3061 (1938).

(12) C. A. Browne and F. W. Zerban, "Sugar Analysis," John Wiley and Sons, New York, N. Y., 1949.

(13) (a) G. Scatchard, S. E. Wood and J. M. Mochel, *J. Am. Chem. Soc.*, **68**, 1957 (1946); (b) G. Scatchard, *Chem. Revs.*, **44**, 7 (1949); (c) G. Scatchard and L. B. Ticknor, *J. Am. Chem. Soc.*, **74**, 3724 (1952).

(14) "The International Critical Tables," Vol. 3, McGraw-Hill Co., Inc., New York, N. Y., 1928, p. 360.

(15) E. A. Guggenheim, "Thermodynamics," Interscience Publishers, Inc., New York, N. Y., 1950, p. 174.

TABLE I

THE SUCROSE–WATER SYSTEM[a] AT 25°

C_2^0	F_1^0	B_{12}^0	$(D_1^* \times 10^6)$ measd.	$(D_2^* \times 10^6)$ measd.	$(D_{12} \times 10^5)$ measd.	$(D_{12} \times 10^6)$[b] calcd.	$(D_{12} \times 10^6)$[c] calcd.	$(D_1^* \times 10^5)$[d] calcd.	$[\beta^1/_2\Lambda_{12e}\Delta S^{0\ddagger}/2R]$[e]
0.0	1.000	1.000	25.8	5.23	5.23	5.23	5.23	25.8	30
.2	0.956	1.024	21.5	4.26	4.55	5.14	4.72	26.3	39
.4	.914	1.075	17.3	3.81	3.97	5.34	4.19	26.6	45
.6	.870	1.135	14.2	3.66	3.39	5.71	3.69	26.4	50
1.0	.785	1.284	8.76	3.21	2.40	5.65	2.78	23.4	62
1.5	.671	1.511	3.50	2.43	1.87	4.35	1.51	17.5	86
2.0	.570	1.800	1.14	1.98	1.34	2.93	0.69	9.8	117
2.2	.526	1.940	0.61	1.65	1.14	2.25	0.43	7.2	277

[a] All D values are in cm.²/sec. [b] Medium-flow treatment. [c] Gordon's equation. [d] Lamm's treatment. [e] In A^0; from the position-exchange treatment, assuming $n = 4.5$.

are mixed, the individual molecules do not change volume, except for possible association.

The Medium Flow Model

Adamson[3] and Prager[6] have generalized the treatment originally proposed by Darken.[4] They considered the case of binary solutions, and assumed a general medium flow to arise due to the non-cancellation of the volume flows of the various species, combined with the restriction of constant volume for the diffusion system. The equation they developed for the case $\partial \bar{V}_i/\partial C_i = 0$ can be written as

$$D_{12} = (F_1 D_2^* + F_2 D_1^*) B_{12} \qquad (26)$$

or

$$D_{12} = D_{12}' B_{12} \qquad (27)$$

The Sucrose–Water System.—Using the data in Article I of this series,[10] equations 26 and 27 and the calculated values of F_1^0, F_2^0 and B_{12}^0, D_{12} was calculated for representative concentrations and shown in Table I, together with the measured binary diffusion coefficients. B_{12} was assumed to be equal to B_{12}^0; however, this assumption is discussed in more detail below.

There is little agreement between the calculated and the measured mutual diffusion coefficients; the agreement becomes worse if the activity coefficient corrections are applied. The tendency to "over correct" the mutual diffusion rate has been reported by Johnson and Babb[8] and Kincaid and Eyring,[16] who indicated that the same phenomenon occurred for systems with positive vapor pressure deviations from ideality, when attempts were made to linearize the diffusion–viscosity data by correcting for solution activity.

However, the fact that the values calculated are much higher than the experimental values indicates that some of the parameters used are in error. A check on the question of the partial molal volumes and whether they are equal to the hydrodynamic volumes shows that unreasonable values have to be assigned to make the experimental values agree with the calculated ones. The assumption that $B_{12} = B_{12}^0$ is probably incorrect, but very unreasonable hydration and association numbers would have to be assumed to impose a fit of the experimental measurements to equation 27. For example, at 1.8 M sucrose, the value of D_{12}' is 2.2×10^{-6} cm.²/sec. immaterial of the values for n, α or β because at that concentration $D_1^* = D_2^* = D_{12}'$ and it does not matter what the values of F_1 and F_2 are; the measured value of D_{12} at 1.8 M sucrose is 1.6×10^{-6} cm.²/sec. To impose an agreement between the measured and calculated mutual diffusion coefficient, B_{12} should be 0.73. According to equation 14, B_{12} is 0.73 if

$$\alpha = \beta = 1 \text{ and } n = 14$$

The choice of a hydration number of 14 is unrealistic because it would mean that at 3.0 molar B_{12} would become negative! From equation 14 it is evident that if one chooses to assign combination values for α and β other than unity, it becomes necessary to assume hydration numbers larger than fourteen to impose the fit.

The real problem then, might lie in the value of the D_i^*. D_i^* is determined by the intrinsic mobility of the species and was assumed in equation 26 to be equal to the self-diffusion coefficient. The intrinsic diffusion coefficients that should be used in the binary equations are the ones that result through the coupling of one of the components with the other. Since in the case of water there are mechanisms of motion not involving sucrose, the measured self-diffusion coefficients do not represent the intrinsic mobilities. Moreover, diffusion of labelled sucrose can occur as a result of a mutual rotation or sliding past each other of two sucrose molecules which come together and subsequently separate. This type of process would contribute to the sucrose self-diffusion, but not to D_{12}, since no net motion is involved. The co-volume of the somewhat elongated sucrose molecule is such that from about one molar on, free rotation is no longer possible and more sucrose–sucrose exchange probably takes place.

Thus, the assumption that the intrinsic and self-diffusion coefficients are the same[3,6] does not apply in the sucrose–water system due to the presence of exchange mechanisms that do not contribute to the binary diffusion mobilities.

The Methanol–Benzene System.—Using the data of Johnson and Babb,[8] equations 26 and 27, and the calculated values of F_1, F_2 and B_{12}^0, D_{12} was computed for representative concentrations with the data shown in Table II, together with the measured binary diffusion coefficients, when no association in the solution is assumed. Better agreement can be shown by the proper choice of n, β and α. From equations 26 and 14 for $n = 0$, the ratio R of the corrected D_{12} with association to D_{12} with no association is

(16) J. F. Kincaid, H. Eyring and E. A. Stearn, *Chem. Revs.*, **28**, 301 (1941).

TABLE II

THE METHANOL–BENZENE SYSTEM AT 25°[a]

N_1^0	Measured $(D_{12} \times 10^5)$	Measured $(D_2^* \times 10^5)$	Measured $(D_1^* \times 10^5)$	F_2^0	B_{12}^0	Calcd. medium-flow $(D_{12} \times 10^5)$[b]	Calcd. medium-flow $(\alpha = \beta)$[c]	Calcd. Lamm's eq.[c] α	Calcd. Lamm's eq.[c] β	Calcd.[b] Gordon's eq. $D_{12} \times 10^5$
0	3.82	2.18	4.16	1.000	1.000	..	1.0	1.0	1.0	..
0.1	1.40	2.29	2.70	0.949	0.193	0.53	2.7	1.0	2.9	1.16
.2	1.00	2.37	2.36	.890	.068	.16	6.2	1.0	6.9	0.56
.3	0.86	2.41	2.09	.830	.119	.26	3.8	1.0	2.8	.40
.4	0.82	2.44	1.99	.755	.136	.29	2.8	1.0	4.0	.37
.5	0.89	2.45	1.96	.674	.147	.31	2.9	1.2	4.4	.41
.6	1.05	2.44	1.96	.578	.186	.40	2.6	1.4	4.6	.55
.7	1.30	2.44	2.00	.465	.277	.62	2.1	1.3	4.1	.74
.8	1.69	2.44	2.09	.339	.420	.98	1.7	1.3	3.8	1.02
.9	2.20	2.45	2.19	.175	.623	1.34	1.6	1.1	3.4	1.46
1.0	2.66	2.46	2.30	.000	1.000	..	1.0	1.0	1.0	..

[a] All D values are in cm.²/sec. [b] Assuming no association. [c] Assuming $n = 0$ and $D_{calcd.} = D_{measd.}$

TABLE III

THE ETHANOL–BENZENE SYSTEM AT 25°[a]

N_1^0	Measured $D_{12} \times 10^5$	Measured $D_2^* \times 10^5$	Measured $D_1 \times 10^5$	F_2^0	B_{12}^0	Calcd. medium flow $(D_{12} \times 10^5)$[b]	Calcd. medium flow $(\alpha = \beta)$[c]	Lamm's eq.[c] α	Lamm's eq.[c] β	Calcd.[b] Gordon's eq. $(D_{12} \times 10^5)$
0.0	3.30	2.18	3.30	1.000	1.000	..	1.0	1.0	1.0	..
.1	1.44	2.26	2.13	0.932	0.550	1.19	1.2	1.0	1.2	1.76
.2	1.05	2.30	1.75	.858	.290	0.54	2.0	1.0	2.0	0.87
.3	0.89	2.32	1.60	.781	.182	.32	2.8	1.2	1.9	.51
.4	0.87	2.31	1.49	.695	.150	.26	3.4	1.7	3.6	.39
.5	0.94	2.25	1.40	.605	.204	.35	2.7	1.6	2.0	.49
.6	1.10	2.21	1.33	.505	.315	.55	2.0	1.3	2.5	.70
.7	1.29	2.12	1.24	.391	.460	.82	1.6	1.2	2.0	.91
.8	1.53	2.02	1.18	.274	.625	1.12	1.4	1.1	1.7	1.09
.9	1.76	1.92	1.10	.146	.830	1.50	1.2	1.0	1.5	1.19
1.0	1.97	1.83	1.02	.000	1.000	..	1.0	1.0	1.0	..

[a] All D values in cm.²/sec. [b] Assuming no association. [c] Assuming $n = 0$ and $D_{calcd.} = D_{measd.}$

$$R = \alpha N_1^0 + \beta N_2^0 \qquad (28)$$

Since experimentally $R > 1$, an equation involving only α and β can be set up at each concentration. Values of α and β in the special case of $\alpha = \beta$ are shown in Table II that would result in perfect agreement between the calculated and measured D_{12}. These association numbers are fairly reasonable.

It is interesting to note that a high degree of association had to be assumed in the concentration region where maximum deviation from ideal mixing was observed. Values of $n > 0$ would have caused higher values of α and β.

The Ethanol–Benzene System.—The data of Johnson and Babb[8] were treated in exactly the same way as those for the methanol–benzene system and the results are shown in Table III. Here again n was assumed to be zero, and equation 28 was utilized to compute values of α and β, assuming $\alpha = \beta$.

The Lamm Treatment

Lamm's[5,17–19] relations between the various diffusion coefficients is based on the concept that there is a different mechanism acting between the interchange of similar and dissimilar molecules. Since self-diffusion is a measure of both types of molecular exchange, the theory cannot be readily tested if the two frictional forces considered are not linearly concentration dependent. Since there is ordinarily no positive way of determining whether such linearity exists, Lamm has proposed a simplified equation based on a volume dependence of the frictional forces involved. The equation can be rearranged into the form

$$D_1^* = \frac{1}{F_1/D_{11}^* + N_2 B_{12}/D_{12}} \qquad (29)$$

where D_1^* and D_{11}^* are the self-diffusion coefficients of component 1 in the presence of component 2 and in the pure state, respectively.

It should be noted that the Lamm treatment, while recognizing the three types of diffusion processes in a binary system, retains the principle of long range coupling. Thus, for the three component system, from which the self-diffusion relationship arises as a special case, the constant volume condition is imposed as a collective coupling of all three types of friction.

The Sucrose–Water System.—In Table I, the values of D_1^* are calculated from equation 29 and compared with the measured data when no association is assumed. It can be seen that the agreement between the calculated and measured values is worse than that from the medium flow treatment and cannot be improved much by assuming reasonable association and hydration numbers. For example, at 1.8 molar sucrose, an association number for the water of about twelve and a hydration number of zero have to be assumed to impose a fit between the measured and calculated D_1^*.

(17) O. Lamm, THIS JOURNAL, **51**, 1063 (1947).
(18) O. Lamm, *Arkiv. f. Kemi*, **17A**, No. 9 (1943).
(19) O. Lamm, *ibid.*, **18A**, No. 2 (1944).

The Alcohol–Benzene Systems.—In the case of the alcohol–benzene systems, the Lamm equation can be tested more fully than in the sucrose–water system, the reason being that both D_{11}^* and D_{22}^* are known. Thus, if equation 29 is combined with the thermodynamic relations for an associated medium, the expressions for the two self-diffusion coefficients become

$$\frac{1}{D_2^*} = \left(\frac{F_2^0 + nC_2^0\bar{V}_1^0}{D_{22}^*}\right) + \frac{\alpha N_1^0 B_{12}^0\left(1 - n\frac{N_2^0}{N_1^0}\right)^2}{D_{12}} \quad (30)$$

$$\frac{1}{D_1^*} = \left(\frac{F_1^0 - nC_2^0\bar{V}_1^0}{D_{11}^*}\right) + \frac{\beta N_2^0 B_{12}^0\left(1 - \frac{nN_2^0}{N_1^0}\right)}{D_{12}} \quad (31)$$

In Table II unique values for α and β are shown for methanol–benzene that would make equations 30 and 31 agree with the experimental results for the case of $n = 0$. If values of n greater than zero are chosen, unrealistic values for α and β result, *e.g.*, fractional α values and/or values of β greater than ten. Similar values of α and β are shown in Table III for the ethanol–benzene system.

Test of Gordon's Equation

Gordon's[20] equation is one of the best known semi-empirical relationships in liquid diffusion

$$D_{12} = D_2^0(\eta_0/\eta)A_2 \quad (32)$$

If for the sucrose–water system the solution viscosities and the values of A_2^0 are inserted in equation 32, it is found that the calculated D_{12} values differ increasingly from the experimental ones with increasing concentration. This is shown in Table I. Quite varying values for β and n have to be assigned to force an agreement with equation 32, because the deviation changes sign around 1.3 molar.

For the methanol–benzene and the ethanol–benzene systems the comparison between the measured and calculated D_{12} is shown in Tables II and III, where deviations up to 55% are observed. Association numbers between one and two would have to be assumed for perfect agreement.

The non-conformity of Gordon's equation with concentrated sugar solutions already has been reported by Van Hook and Russel[21]; they observed up to 300% difference between the measured and calculated D_{12}. Although only reasonable solvolysis numbers have to be assumed for perfect agreement in the alcohol–benzene systems, the main problem is that at high concentrations the simple Stokes law type of relationship between viscosity and diffusional mobility can well be expected to break down; the solution can definitely no longer be considered a continuum, to say nothing of the possible large sizes of associated solvent molecules. Moreover, the viscosity of the medium probably is composed of three types of interactions, comparable to the three diffusion coefficients, and cannot be expected to describe the behavior of D_{12} solely. Moreover, Gordon[22] demonstrated that from a thermodynamic point of view equation 32 cannot be valid over wide ranges of concentration.

(20) A. R. Gordon, *J. Chem. Phys.*, **5**, 522 (1937).

(21) A. Van Hook and H. D. Russel, *J. Am. Chem. Soc.*, **67**, 370 (1945).

(22) A. R. Gordon, *ibid.*, **72**, 4840 (1950).

The Position Exchange Treatment

The "Position Exchange" treatment[7] relates the various diffusion coefficients with specific kinetic jump distance and isosteric exchange during mutual diffusion. Thus

$$D_{12} = \frac{k_{12}\Lambda_{12}^2 B_{12}}{\bar{V}_1\bar{V}_2(C_1 + C_2)} = \frac{k_{12}\Lambda_{12}^2 A_2}{\bar{V}_2} \quad (33)$$

$$D_2^* = k_{22}C_2\Lambda_{22}^2 + F_1 D_{12}/A_2 \quad (34)$$

with a reciprocal expression for D_1^*. The specific rate constant k_{12} is given by

$$k_{12} = \frac{eKT}{h}\frac{\bar{V}_1\bar{V}_2}{\bar{V}_1 + \bar{V}_2}e^{-E/RT}e^{\Delta S^{0\ddagger}/R} \quad (35)$$

and from equations 33 and 35

$$\Lambda_{12}^2 e^{\Delta S^{0\ddagger}/R} = \frac{D_{12}(\bar{V}_1 + \bar{V}_2)(C_1 + C_2)}{B_{12}\frac{eKT}{h}e^{-E/RT}} \quad (36)$$

If association is assumed, then

$$\Lambda_{12}^2 e^{\Delta S^{0\ddagger}/R} = \frac{D_{12}[\beta V_1^0 + \alpha(nV_1^0 + V_2^0)][C_1^0 + C_2^0]}{B_{12}^0\alpha\beta\left(1 - \frac{nC_2^0}{C_1^0}\right)\frac{eKT}{h}e^{-E/RT}} \quad (37)$$

Therefore, equation 37 can be used to calculate coördinated jump distances if n, α and β are known.

For sucrose–water at 25°, n is chosen to 4.5 because such a choice would roughly account for the variation of f with N,[23] while E can be represented by[23,24]

$$E = (4.6 + 1.3C_2^0)\ \text{kcal./mole} \quad (38)$$

In addition the term $\beta V_1^0 << \alpha(nV_1^0 + V_2^0)$ so that in Table I values of $\beta^{1/2}\Lambda_{12}e^{\Delta S^{0\ddagger}/2R}$ are shown. It is evident that either a positive $\Delta S^{0\ddagger}$ and/or a moderate β value must be assumed to get fairly reasonable Λ_{12} values. The large variation in the calculated values with concentration is probably attributable to changes in $\Delta S^{\ddagger}$ and β. λ_{12} and λ_{21} for the separate species can be calculated from the relations

$$\Lambda_{12}^2 = \frac{\bar{V}_1}{\bar{V}_2}\lambda_{12}^2 = \frac{V_2}{V_1}\lambda_{21}^2 \quad (39)$$

Similar calculations can be performed on the methanol–benzene system using experimentally determined activation energies.[9] For the ethanol–benzene system no diffusional activation energies are available.

Equation 34 cannot be used readily because activation energies for self-diffusion are not available at present.

Conclusions

(1) The diffusional thermodynamic factors are highly dependent on the degree of association assumed in liquid solutions. (2) Binary and self-diffusional mobilities are not equivalent due to special interchange mechanisms between molecules. (3) For the methanol–benzene and the ethanol–benzene systems present theories of long range interactions are as successful as the recent model of localized isosteric interchange,[7] whereas for the sucrose–water system where special interchange

(23) A. C. English and M. Dole *ibid.*, **72**, 3261 (1950).

(24) L. Gosting and J. M. Morris, *ibid.*, **71**, 1998 (1949).

mechanisms must exist and marker motion is absent, it is concluded that the sucrose and water clusters interdiffuse through a coördinated isosteric process.

Acknowledgment.—The authors wish to express their sincere appreciation to Dr. Scott E. Wood for helpful suggestions.

DISPERSION OF PLATINUM ON SUPPORTED CATALYSTS

BY LAWRENCE SPENADEL AND MICHEL BOUDART

Esso Research and Engineering Company, Linden, New Jersey

Received June 29, 1959

Hydrogen chemisorption at saturation can be used to determine the specific surface area and an average crystal size for platinum highly dispersed on an alumina support in a range of dispersion not accessible to measurements by X-ray line broadening. For a fresh catalyst containing 0.6 wt. % platinum, the ratio of platinum atoms to adsorbed hydrogen atoms is almost equal to unity. This shows that the metal is very highly dispersed on the support. Platinum crystal growth is brought about by a heat treatment at elevated temperatures. Good agreement is obtained between platinum particle size calculated from chemisorption and from X-ray line broadening in a crystal size range where the latter method becomes applicable.

Introduction

Chemisorption has been used in the past to determine the surface area of catalyst.[1] The method requires that the adsorbate form a chemisorbed monolayer and that there exist a simple relation between the number of molecules adsorbed at saturation and the number of surface atoms. Thus, hydrogen forms an almost complete monolayer on a nickel evaporated film with each adsorbed hydrogen atom corresponding to one surface metal atom.[2]

These special requirements have prevented chemisorption from becoming a general method of surface area determination. Nevertheless, its principle has considerable merit in particular situations.

If, for example, a metal is dispersed on an oxide support in small quantities and in a particle size range that cannot be detected by physical measurements, the problem of determining the dispersion of the supported metal may be solved in principle by selective chemisorption. This has been done by Boreskov and Karnaukhov[3] who studied the preferential chemisorption of hydrogen by platinum supported on silica gel. In this investigation, the average particle size of platinum crystallites calculated from the metal specific surface area was never less than 40 Å.

On the other hand, the dispersion of platinum on acidic bases (acidic aluminas or silica–aluminas) has not been reported until recently.[4–6] Unpublished data obtained in this Laboratory indicate that catalysts containing less than 1 wt. % platinum on η-alumina are characterized by a very high dispersion of the metal. In fact, the crystal size of the platinum is, in most cases, too small to be determined by X-ray line broadening. It can be assumed that the crystal size of the platinum is smaller than about 50 Å. Since X-ray measurements are not applicable in this region, it was decided to study the dispersion of platinum on an alumina support by means of hydrogen chemisorption.

Experimental

A volumetric glass system of standard design[7] was used for the adsorption measurements. The apparatus included a McLeod gauge, a mercury manometer read with the help of a cathetometer, sample and gas storage bulbs, and an oil diffusion pump used in conjunction with a mechanical pump.

The gases used were helium for dead space determinations, hydrogen for catalyst reduction and adsorption, and nitrogen and argon for BET surface area determinations. Commercial cylinder gases were purified as noted: hydrogen by diffusion through a palladium thimble; helium by passing it through a train composed of activated charcoal at liquid nitrogen temperature, a drying column and a liquid nitrogen cold trap; argon by passage through a liquid nitrogen cold trap.

The adsorbents or catalysts used were η-alumina, η-alumina supported platinum catalysts and platinum black. The supported catalysts were reforming catalysts, prepared as described in the literature.[8] The catalysts were made by impregnation of the supports with aqueous chloroplatinic acid and then drying at 550° for one hour. The chloride and platinum are present in near stoichiometric amounts. The surface areas of the alumina supports are given in Table I. The platinum black used (>98% platinum) was obtained from Baker and Co.

Platinum crystal size was determined from the breadth of the (311) X-ray diffraction line, recorded on a Norelco X-ray spectrometer. The standard equation of Patterson[9] with Warren's corrections[10] was used in the calculation of X-ray crystal size.

Before measurement of a hydrogen adsorption isotherm, the adsorbent or catalyst was subjected to a standard pretreatment. First the sample was outgassed *in vacuo* at 500° for a few hours. Then it was kept under about one atmosphere of hydrogen at 500° for 30 minutes in order to reduce the surface adequately. Finally it was outgassed at 500° overnight (16 hours). No difference in adsorption isotherm was detectable if the final outgassing time was increased to 72 hours. In this work, outgassing was considered completed when a pressure of less than 10^{-3} mm. could be maintained for more than 15 minutes in the system cut off from the pumps at the temperature of the experiment.

(1) A. F. Benton, *J. Am. Chem. Soc.*, **48**, 1850 (1926).

(2) O. Beeck, "Advances in Catalysis," Vol. II, Academic Press, Inc., New York, N. Y., 1950, p. 151.

(3) G. K. Boreskov and A. P. Karnaukhov, *Zhur. Fiz. Khim.*, **26**, 1814 (1952).

(4) L. Spenadel and M. Boudart, paper presented at Boston A.C.S. meeting, 1959.

(5) J. J. Keavney and S. F. Adler, paper presented at Boston A.C.S. meeting, 1959.

(6) T. R. Hughes, R. J. Houston and R. P. Sieg, paper presented at Boston A.C.S. meeting, 1959.

(7) G. L. Joyner, "Scientific Glass Blowing," Instruments Publishing Co., Pittsburgh, Pa., 1949, p. 257.

(8) F. G. Ciapetta and C. J. Plank, "Catalysis," Vol. I, Reinhold Publ. Corp., New York, N. Y., 1954, p. 315.

(9) A. C. Patterson, *Phys. Rev.*, **49**, 884 (1936).

(10) B. E. Warren, *J. Amer. Ceramic Soc.*, **21**, 49 (1938).

TABLE I

DATA ON PLATINUM DISPERSION

	BET S.A., $m.^2/g.$	Adsorpt. at 250° 24 cm. in moles $H_2 \times 10^6/g.$ Sample	Support	H atoms ads. per Pt atom in sample	S.A. of Pt, $m.^2/g.$	Pt crystal size from adsorpt., Å.	Pt crystal size from X-ray line broadening, Å.
Pt black	0.55	4.98	..	0.0019	0.54	4,300	..
Pt black[3]	0.17	1.62	..	.00063	0.17	13,700	...
0.60 wt. % Pt on Al_2O_3 (fresh)	195	19.8	4.65	.99	273	<10	<50
0.60 wt. % Pt on Al_2O_3 (heat treated 2 hr., 650°)	135	5.50	3.40	.14	38	61	200
4.46 wt. % Pt on Al_2O_3 (heat treated 24 hr., 650°)	115	8.80	3.45	.047	13	212	255
3.10 wt. % Pt on Al_2O_3 (heat treated 24 hr., 750°)	95	3.50	0.85	.033	9.2	253	255

The outgassing temperature of 500° does not affect the platinum or alumina surface area of the catalyst.

Results

Typical adsorption isotherms at 250° are shown in Fig. 1. More than 90% of the hydrogen adsorption is instantaneous. There is then a slow gas uptake, the rate of which becomes negligible after 30 minutes. The amount of gas taken up slowly never exceeds more than 10% of the total gas uptake. In all experiments 30 to 45 minutes was allowed before a pressure reading was taken.

Results obtained from the adsorption data are summarized in Table I. Column 1 gives conventional BET surface areas measured with nitrogen (15.8 $Å.^2$/molecule) except in the case of Pt black where argon was used (14.6 $Å.^2$/molecule). The values quoted for the supported catalysts refer to the support alone.

Adsorption values at 24 cm. and 250° are reported in columns 2 and 3 because, as discussed below, it is believed that essentially complete surface coverage is reached on platinum at that pressure and temperature. The difference between the values in columns 2 and 3 together with the platinum content of the sample gives the number of H atoms adsorbed per Pt atom in the sample (column 4). Finally, experimental data on Pt crystal size from X-ray line broadening are reported in the last column. Data on the second line of the table are those of Boreskov and Karnaukov.[3]

Discussion

The adsorption method will give a correct surface area of platinum if these various conditions are satisfied: (1) hydrogen taken up by platinum is only adsorbed (surface) and not absorbed (interior); (2) hydrogen adsorption at 250° and 24 cm. corresponds closely to saturation with a hydrogen atom per surface platinum atom; (3) when platinum is dispersed on the support, the support adsorbs the same quantity of hydrogen that it would if platinum were absent.

These points will now be discussed in turn.

1. Adsorption vs. Absorption.—As is well known, absorption of hydrogen in metals is a slow process.[2] Since most of the adsorption (>90%) recorded took place very rapidly, it can be concluded that absorption of hydrogen, if present at all in this work, represents at most a small fraction (<10%) of the total gas uptake. The surface area of platinum calculated on the assumption that the gas uptake corresponds only to adsorption may, therefore, be too high by 10% at the most.

2. Monolayer of Hydrogen on Platinum.—The shape of the isotherm (Fig. 1) suggests that at 250°, a hydrogen pressure of 24 cm. approaches almost complete saturation of the surface.

The adsorption data in the restricted range of pressures covered in the measurements on Pt black are represented in Fig. 2 by means of a Langmuir isotherm with dissociation

$$v = \frac{v_m b p^{1/2}}{1 + b p^{1/2}}$$

where v is the volume adsorbed, v_m the volume corresponding to a monolayer, b a constant, p the hydrogen pressure. From the intercept, v_m can be calculated. The surface coverage $\Theta = v/v_m$ at 250°, 24 cm. on Pt black is then seen to be equal to 0.96.

No claim is made, of course, that hydrogen adsorption on platinum obeys a Langmuir isotherm. The argument presented here merely supports the idea that saturation is closely approached under the conditions selected. The error made here, by assuming complete saturation, would lead to a value for the platinum surface area that is smaller than the actual one. This would tend to compensate for any overestimation of the platinum surface area due to partial absorption of hydrogen in the bulk of the lattice. There is a possibility that some of the slow sorption is actually adsorption on the surface at already high values of coverage.

It is interesting to see the excellent agreement between the results of this work and those of the Russian workers, although samples of Pt black of different origin and surface area were used in both cases. The amount of hydrogen (in micromoles per $m.^2$ of Pt) adsorbed at 250° and 24 cm. is 4.98/0.55 = 9.05 in our work and 1.62/0.17 = 9.53 in the Russian investigation. This agreement demonstrates that proper reduction and evacuation can lead to quite reproducible values of hydrogen adsorption on platinum catalysts.

3. Effect of Platinum on Hydrogen Adsorption on the Support.—It is conceivable that platinum highly dispersed on a support would occupy sites on the support which also are hydrogen adsorption sites in the absence of platinum. While the

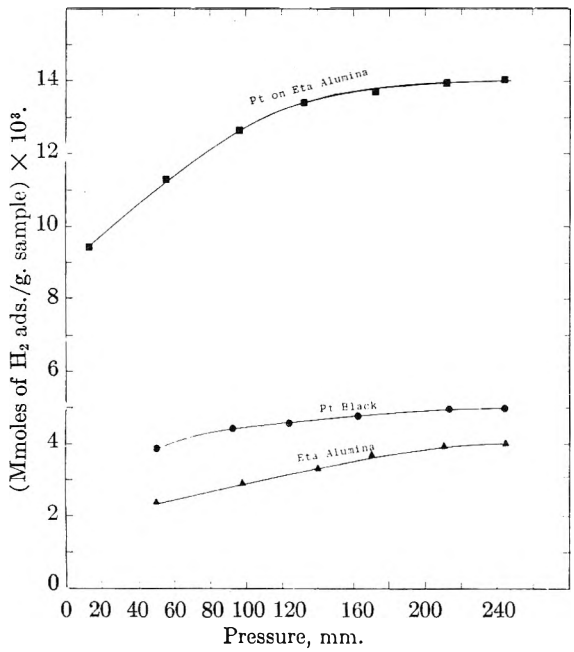

Fig. 1.—Hydrogen adsorption isotherms at 250°.

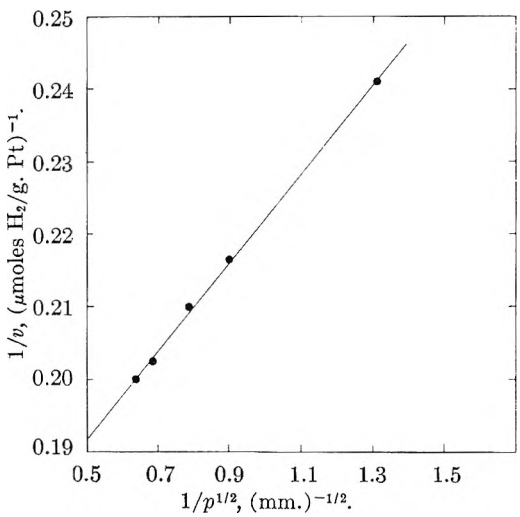

Fig. 2.—Langmuir isotherm for hydrogen adsorbed on a platinum catalyst at 250°.

present data offer no evidence of this, the effect, if it were real, would lead to values which would underestimate the platinum surface areas. On the other hand, hydrogen adsorption might occur on alumina sites in the vicinity of sites occupied by platinum while the same alumina sites might not be able to chemisorb hydrogen in the absence of platinum. If this opposite effect took place, the surface area of platinum at very high dispersion might actually be overestimated. The possibility of this effect will be taken into account in the rest of this discussion.

To sum up, except for the point just made, the conditions for using hydrogen adsorption to determine platinum dispersion seem to be adequately fulfilled, although independent experimental evidence presented below is desirable to support this conclusion.

Platinum Surface Area and Crystal Size.—In order to translate the hydrogen adsorption data (column 4) into platinum specific surface areas (column 5), the reasonable assumption is made that the low index planes (100 and 110) of platinum are equally exposed on the average on the surface. The site densities (number per cm.^{2}) of these planes are 1.31×10^{15} and 0.93×10^{15}, respectively, giving an average of 1.12×10^{15} sites per cm.^{2}. The figures of column 4 have, therefore, to be multiplied by $(6.02 \times 10^{23})/(195.09 \times 1.12 \times 10^{15} \times 10^4)$ in order to obtain specific surface areas of Pt in m.^{2}/g. Note that this gives 0.54 m.^{2}/g. for our platinum black *vs.* 0.55 m.^{2}/g. by the BET method. Hydrogen adsorption under the conditions of this work then corresponds to a surface coverage $\Theta = 0.54/0.55 = 0.98$, in good agreement with the value $\theta = 0.96$ estimated above from the adsorption isotherm and in excellent support of the contention that surface saturation is practically complete. It is also interesting to note (second line of Table I) that the translation from hydrogen adsorption to surface area as proposed here gives complete agreement between BET and hydrogen surface areas in the Russian work.

In the case of the fresh catalyst (line 3), the very large surface area of 273 m.^{2}/g. is obtained. This compares with 276 m.^{2} which is the calculated surface area of 1 gram of platinum in a monatomic layer.[11] Obviously, the platinum on the alumina support is very highly dispersed. However, the absolute value of 273 m.^{2}/g. must not be taken too seriously. Indeed, if the dispersion becomes extreme, as shown by the one-to-one correspondence between adsorbed H atoms and Pt atoms (column 4), the crystallographic concept of density of sites may well lose its meaning. Furthermore, as already discussed, the reported figure may be too high as a result of possible hydrogen adsorption on support sites adjacent to the platinum.

The case of the fresh platinum catalyst deserves some further discussion. If the platinum atoms were dispersed one by one on the support, they would be separated from each other by relatively large patches of alumina and the average distance between them would be about 100 Å. But then, a hydrogen molecule coming down to such an isolated site would dissociate into an atom adsorbed on platinum and another adsorbed on an adjacent alumina site. If the latter diffused along the surface till it finds another vacant isolated platinum site, the main adsorption process should be slow insofar as surface diffusion of adsorbed hydrogen on oxides is believed to be of the slow activated type.[12] But if the second adsorbed H atoms stays in the vicinity of the first, then it is difficult to understand why the ratio of H atoms to Pt atoms did not exceed unity. As a matter of fact, the value of unity for this ratio rather suggests that platinum clusters are still present on the support. These clusters may be two-dimensional. If they are three-dimensional, an upper average crystal

(11) Using 1.12×10^{15} sites/cm.^{2} as the average site density, the corresponding surface area per g. of platinum is $6.02 \times 10^{23}/195.09 \times 10^4 \times 1.12 \times 10^{15} = 276$ m.^{2}/g.

(12) E. Wicke, *Z. Elektrochem.*, **53**, 279 (1949).

size of platinum can be estimated in the following way:

Consider a single unit cell of platinum on alumina. It has thirteen exposed Pt atoms but if the corner atoms in contact with the support can chemisorb hydrogen, the four support sites adjacent to these corners could also chemisorb one hydrogen atom each so that, with this possible interference of the support, the ratio H/Pt would be 17/14 = 1.2 at saturation. If now we consider a crystallite made of eight unit cells, four of which lie in contact with the support, it has 63 Pt atoms, 49 of which are exposed. Eight Pt atoms on the support can conceivably lead to adsorption on the support of eight additional H atoms. Thus, the H/Pt ratio would be, at the most, 57/63 = 0.90 which is less than the experimental figure 0.99. Therefore, if the platinum is in the form of crystallites, the latter must consist on the average of blocks containing less than two unit cells on a side.

Since the edge of a Pt unit cell measures 3.9 Å., the adsorption data indicate that the average crystal size must be smaller than 2 × 3.9 Å., *i.e.*, certainly less than 10 Å., if the platinum is still in crystalline form. Since the argument includes a correction for the possible interference by the support in an unfavorable direction, this conclusion must be viewed as conservative. Of course, it is entirely possible that the platinum is dispersed in the form of two-dimensional patches. While no choice can be made between these two alternatives, namely, crystallites measuring less than 10 Å. on the average or two-dimensional surface patches, this work establishes for the first time the extremely high dispersion of fresh platinum catalysts on alumina supports. Even if the metal is still crystalline, it cannot be detected by X-ray line broadening or other available physical techniques.

Crystal Growth by Heat Treatment.—Except in the case of the fresh catalyst where the platinum dispersion is so extreme, the adsorption data can be translated into an average crystal size. The reasonable assumption is made that the crystal is a cube of side d with five exposed faces, one being in contact with the support. The exposed surface is $5d^2$; the weight is $d^3\rho$ where ρ is the density of Pt. Therefore surface area/g. of Pt = $5/d\rho$. Values of d calculated in this way are shown in column 6 of Table I.

It is seen that even a moderate heat treatment of the catalyst brings about crystal growth. After two hours at 650°, the extreme platinum dispersion has disappeared and the average crystal size has reached about 60 Å. But a rather severe heat treatment is required to obtain agreement between crystal size calculated from adsorption data and crystal size from X-ray line broadening. After only a moderate heat treatment, platinum crystal size values obtained from X-ray line broadening are larger than that obtained from adsorption measurements. This is understandable since hydrogen adsorption detects all platinum atoms on the support while the X-ray method detects only crystals larger than 50 Å. After a moderate heat treatment, there must remain on the support very small crystallites (<50 Å.) besides the larger ones which are the only ones to be detected by the X-ray technique. On the other hand, the remarkable agreement obtained between the crystal sizes from adsorption and from X-ray after adequate crystal growth (253 Å. *vs.* 255 Å.) provides the desirable independent evidence in support of the conclusions reached earlier concerning the validity of using hydrogen adsorption to study dispersion of platinum on alumina.

Conclusions.—Hydrogen chemisorption is a useful and reliable tool to study dispersion of platinum on oxide supports. The extremely high dispersion (<10 Å.) of platinum on alumina has been demonstrated for the first time by hydrogen chemisorption. With platinum crystal sizes larger than 50 Å. but smaller than 1000 Å., hydrogen chemisorption gives values identical with those obtained from X-ray line broadening. With unsupported platinum of still larger crystal size (>1000 Å.), hydrogen chemisorption and BET nitrogen adsorption give practically the same platinum specific surface area.

Acknowledgment.—The authors wish to express their appreciation to Dr. F. Kant for many helpful discussions and Mr. D. L. Baeder for his constant encouragement and advice. The unpublished work of Dr. Z. W. Wilchinsky under whose direction the technique of particle size measurement by X-ray line broadening was perfected in this Laboratory is also gratefully acknowledged.

THE PHYSICAL NATURE OF SUPPORTED PLATINUM

BY STEPHEN F. ADLER AND JAMES J. KEAVNEY

Stamford Laboratories, American Cyanamid Company, Stamford, Connecticut

Received August 12, 1959

Two types of platinum–alumina reforming catalysts, impregnated and cogelled, have been examined by means of H_2 adsorption and X-ray line-broadening techniques. The catalysts were examined (1) fresh, (2) coked, (3) regenerated, (4) mildly sintered, (5) severely sintered and (6) reactivated after the two levels of sintering. The adsorption was shown to decline after coke had been deposited in a naphtha reforming reactor. A careful burn-off of the coke restored the adsorption to at least one-half of its original level. Mild sintering, in a partial steam atmosphere, caused a large decrease in adsorption which was partially recovered after reactivation under a high pressure of oxygen. On the other hand, sintering at one atmosphere of steam caused a decrease in adsorption which was essentially irreversible despite attempts at reactivation. The adsorption results on fresh, sintered and reactivated catalyst are interpreted by assuming (1) the existence of two types of platinum aggregation-monolayer for impregnated catalyst, pseudo-spherical for cogelled catalyst, and (2) that H_2 is adsorbed as atoms at the surface interstices between platinum atoms. Platinum particle sizes are derived that are in good agreement with X-ray line-broadening values. The adsorption of H_2 per gram of platinum was found to be virtually independent of platinum concentration within either of the two groups of catalysts investigated.

Introduction

It has been of interest to this Laboratory to study the nature of platinum supported on alumina, in the concentration range appropriate for a reforming catalyst. One of the properties which most obviously affects the performance of any heterogeneous catalyst is the surface area of the active material. A study was therefore started to determine the surface area of platinum available in supported catalysts of the type used in reforming.

Determination of the surface area of one component in a multiple component catalyst has been done previously by Emmett and Brunauer[1] for iron on a promoted ammonia-synthesis catalyst, by means of carbon monoxide adsorption, and later[2,3] by the same method for cobalt on kieselguhr and for nickel on aluminum oxide. These determinations were made on catalysts in which the active component occupied a large percentage of the surface. Boreskov and Karnaukhov[4] applied the technique to a low concentration (0.2 to 0.5%) of platinum supported on silica gel. They used hydrogen as their adsorbate. Spenadel and Boudart[5] have most recently used hydrogen adsorption to study $Pt–Al_2O_3$ catalysts. Their conclusions regarding Pt dispersion are in general agreement with those presented in this paper.

All previous work compared the adsorption on the catalysts with that on the pure metal, in order to determine the surface area of the metal in the catalyst. Although this is probably valid for large particles, it would seem that surface properties of very small particles must be different from the bulk metal. For this reason, a different approach to the interpretation of adsorption results is presented.

Experimental

1. **Preparation of Catalysts. A. "Impregnated" Catalysts.**—A high purity (99.9%+) γ-alumina, in $1/8'' \times 1/8''$ cylindrical pellet form of *ca.* 250 $m.^2/g.$ surface area (BET) and 0.56 cc./g. water pore volume, was calcined to 593°, cooled to room temperature in a sealed container, and portions of it were impregnated with solutions of chloroplatinic acid (C.P. grade) of sufficient volume to fill the pellet porosity. The platinum content of the solutions was adjusted to give Pt contents, in the finished catalyst, ranging from 0.1 to 0.8%. The material was dried overnight at 120°, calcined from 205 to 593° in four hours and calcined an additional hour at 593°. The finished catalyst was stored in a sealed container.

B. **"Cogelled" Catalysts.**—Alumina sol containing *ca.* 5% solids as Al_2O_3 was cogelled by the simultaneous mixing of the sol and chloroplatinic acid (C.P. grade) with aqueous ammonia. The resulting gel was dried overnight at 120°, and then calcined to 260°. After grinding, blending with a lubricant and pelleting into $1/8'' \times 1/8''$ cylinders, the gel was recalcined to 593° in four hours and held at that temperature for one hour. The platinum content of the catalyst was adjusted by varying the amount of platinum solution used in the cogellation step. The final product had a BET surface area of *ca.* 210 $m.^2/g.$ and a porosity of 0.56 cc./g.

C. **Coking of Catalysts.**—A number of fresh catalyst samples were coked for one or five days in a naphtha reforming reactor operating under the following conditions: feed—Mid-Continent naphtha (93–176° boiling range); liquid hourly space velocity, 2.0 $hr.^{-1}$; av. temp., 483°; pressure, 200 p.s.i.g.; H_2 recycle rate, 5000 S.C.F./bbl. (once-through).

D. **Regeneration of Coked Catalysts.**—Coked catalysts were regenerated by calcining them in a muffle furnace from 200 to 593° in no less than four hours. This allowed the coke to be burned off slowly.

E. **Steaming of Catalysts.**—Two types of steaming procedure were used to sinter the catalyst samples. The mild steaming was performed by injecting water into a circulating air furnace held at 705°. The partial pressure of the water vapor in the furnace was determined to be 0.35 atmosphere. More severe steaming was accomplished by vaporizing water, in the absence of air, into steel tubes packed with catalyst and kept at 750°. Here, the water pressure was necessarily 1.0 atmosphere.

F. **Reactivation of Catalysts.**—A number of steamed catalysts were reactivated by heating them to 620° in a static 60 p.s.i.g. O_2 atmosphere for two hours.

G. **H_2 Adsorption Measurements.**—The chemisorption of hydrogen was measured volumetrically at a pressure of 8–9 mm. The sample holder was a small Pyrex bulb of a size such that the sample completely filled it; it was joined to the rest of the system by a ground glass joint. The supply of reagent grade hydrogen was connected to the system through three stopcocks which served as a dosing system. A similar system was employed for helium. The manometer was of 10 mm. Pyrex tubing, and used dibutyl phthalate as the manometer fluid. The large bulbs were of 500, 1000 and 2000 cc. volumes and were calibrated with water before mounting. They were not thermostated but were well insulated. The system was designed such that adsorption could be measured at constant pressure (within 10%). The initial pressure in the system was 9–10 mm. (about 13 cm. dibutyl phthalate) and before admitting gas to the sample, the volume of the system was adjusted by closing off one or more of the large bulbs. The volume was chosen so that the expected adsorption would cause a drop of 10% or less in the pressure. If the drop exceeded 10%,

(1) P. Emmett and S. Brunauer, *J. Am. Chem. Soc.*, **59**, 310 (1937).
(2) R. Anderson, W. Hall and L. Hofer, *ibid.*, **70**, 2465 (1948).
(3) F. Hill and P. Selwood, *ibid.*, **71**, 2522 (1949).
(4) G. K. Boreskov and A. P. Karnaukhov, *Zhur. Fiz. Khim.*, **26**, 1814 (1952).
(5) L. Spenadel and M. Boudart, THIS JOURNAL, **64**, 204 (1960).

an additional bulb was opened, restoring the pressure to within 10% of the initial value. The dibutyl phthalate manometer was read to 0.05 mm. with a Gaertner cathetometer; this allowed measurement of the amount adsorbed to 0.5%.

All measurements were made at 200 ± 1°. The temperature was controlled by a Leeds and Northrup Electromax Controller. Sample sizes were in general from 7–10 g., with smaller samples taken when quantities were limited.

It was found that after outgassing of the sample at low temperatures (300°) for 16 hours, adsorption of H_2 started at a moderate rate and continued at about this rate even after three hours. It was felt that the more rapid the initial adsorption and the smaller the secondary adsorption, the cleaner the Pt surface. Maxted[6] found that poisoning of Pt with sulfur greatly reduced the initial rate of adsorption of H_2, compared to unpoisoned Pt. Outgassing at 400° or 500° improved the situation in that a rapid initial adsorption was obtained, but a slow adsorption still continued after three hours. A 20 second exposure to hydrogen at 500° and 10 mm. followed by 16 hr. outgassing at 500° gave the best results insofar as eliminating the slow adsorption was concerned. With this treatment, the rate of change of adsorption after two hours was 2% or less per hour. Hydrogen treatment for longer than one minute at 500° did not diminish this rate but did decrease the amount adsorbed, possibly because of sintering. No difference was found for treatment times less than one minute.

The standard treatment, then, for any catalyst sample was: 2–3 hours outgassing, with a mercury diffusion pump, followed by 20 seconds exposure to H_2 at 10 mm., and 16 hours outgassing, all at 500°. The pressure after outgassing was less than 10^{-5} mm. The temperature was then lowered to 200°, the free volume in the sample holder measured with helium, and the hydrogen sorption started. The uptake of hydrogen was followed with time, and the amount adsorbed calculated to STP. The adsorption recorded for a given sample was taken at the two hour point.

In Fig. 1 is shown a typical adsorption *vs.* time curve. Curves obtained at a variety of temperatures with no hydrogen pre-reduction are also shown. A portion of the isotherm is shown in Fig. 2, which indicates that a possible variation of 10% in the region of 9 mm. gives a very small change in adsorption (about 2%).

H. X-Ray Diffraction Line Broadening.—Determinations of the platinum crystallite size in various catalysts were made by means of standard line-broadening techniques. The instrument used was a Phillips diffractometer employing Cu Kα radiation with a Ni filter. Measurements were made on the Pt (111) reflection plane corresponding to a 2.26 Å. lattice spacing.

Results and Discussion

Hydrogen adsorption was measured on several catalysts; the results are shown in Table I. Several blank determinations were made on pure Al_2O_3, on Al_2O_3 impregnated with HCl, and on a coked Al_2O_3. All of these adsorptions were 0.003 cc. (STP)/g. or less. Since this is about the expected experimental error, the adsorption on Al_2O_3 was considered to be zero, and no corrections were made to the catalyst results.

The effect of steaming catalysts as well as subsequent oxygen treatment can be seen from Table I. Steaming at 705° and 0.35 atm. H_2O decreases the adsorption of the cogelled catalyst *ca.* 80%, whereas that of the impregnated catalyst decreases approximately 50%. It is possible by oxygen treatment to restore the cogelled samples to a substantially higher adsorption, but the adsorption of the impregnated catalyst remains at about 50% of the fresh catalyst. More stringent steaming (750°, 1 atm. H_2O) decreases the adsorption by both types of catalysts to a very low value, and oxygen treatment has a negligible effect.

(6) B. Maxted, *J. Chem. Soc.*, 2203 (1931).

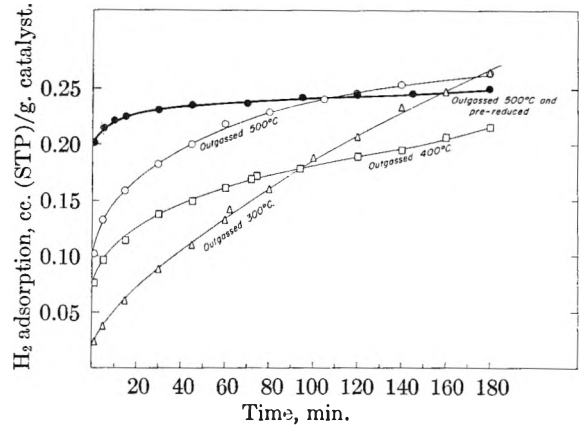

Fig. 1.—Hydrogen adsorption at 200° on 0.58% Pt cogelled catalyst.

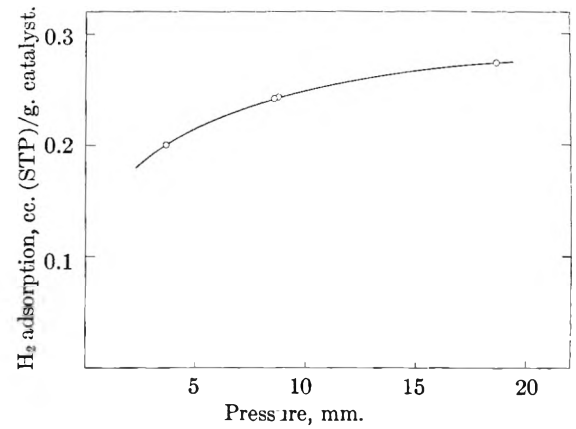

Fig. 2.—Hydrogen adsorption at 200° on 0.58% Pt cogelled catalyst.

TABLE I

HYDROGEN CHEMISORPTION OF PLATINUM CATALYTS
CC. (STP)/G. CATALYST

Treatment	Catalyst: Cogelled 0.58% Pt.	Cogelled 0.30% Pt.	Impregnated 0.30% Pt
Fresh	0.242	0.135	0.248
Coked, 1 day run	.054[a]		.052
regenerated	.191		.231
Coked, 1 day run	.057		
regenerated	.134		
Coked, 5 day run	.073[b]		
regenerated	.197		
Steamed, 0.35 atm., 705°,			
5 hr.	.029	.017	.111
reactivated	.140	.112	.116
Steamed, 1.00 atm., 750°,			
5 hr.	.036		.012
reactivated	.045		.016

[a] 0.92% carbon. [b] 2.50% carbon.

In order to interpret the adsorption measurements in terms of Pt crystallite size, it was desirable to measure the adsorption on pure platinum of known surface area. Two measurements on platinum black were unsuccessful because the platinum sintered under the conditions of the experiment. Measurements were then made on platinum foil with a BET surface area of 2.0 m.^{2}. The amounts adsorbed were 0.135 and 0.133 cc. (STP)/m.^{2}. The Pt foil did not receive any pre-

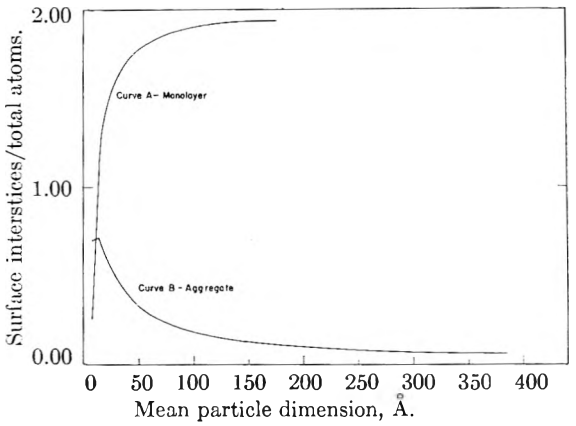

Fig. 3.—Variation of I/T ratio with particle size.

reduction, because the adsorption curve levelled out satisfactorily without it. This is in good agreement with Boreskov and Karnaukhov[4] who found an adsorption of 0.11 cc. (STP)/m.^{2} on sintered platinum sponge at 250° and the same pressure. Their Pt was pre-reduced. Unfortunately, these results do not seem to be applicable to the catalysts under study. If one assumes all (100) faces on the surface of the foil, the observed ratio of H atoms adsorbed to surface Pt atoms is 0.55. In the fresh impregnated catalysts measured, the ratio of H atoms adsorbed to total Pt present is greater than one. It seems clear that finely divided Pt is very much more efficient in hydrogen adsorption than is bulk platinum.

In order to make a correlation, therefore, between the hydrogen chemisorption and the size of the platinum crystallites, it is necessary to consider the probable mode of adsorption of hydrogen on platinum. It is assumed that hydrogen adsorbed on platinum under the conditions cited here exists primarily as atoms.[7] Although Boreskov and Karnaukhov did not find that the adsorption became constant, even up to one atmosphere, their measurements indicate that there is an extremely strong adsorption which is complete at a few millimeters of Hg pressure. This suggests that at the pressure used in this investigation, all of the primary adsorption sites are filled. Since we find that on some catalysts more H atoms are adsorbed than there are Pt atoms present, there must be more than one adsorption site per Pt atom. Mignolet[8] has already indicated that hydrogen is probably adsorbed above the spaces between atoms, rather than on top of each atom. In a hexagonal face there are two such sites per atom, neglecting edge effects. It is concluded, therefore, that at least on some faces two H atoms are adsorbed for each surface Pt atom.

However, because of the wide discrepancy between H/Pt ratios for fresh impregnated and cogelled catalysts, it was felt that there might be a fundamental difference in the manner in which the platinum was arranged on the surface of these catalysts. It is hard to see how the adsorption of chloroplatinic acid on an activated alumina surface at low (<1.0%) concentrations can result in anything other than a discontinuous monolayer of chloroplatinate ions. Reduction of such a surface in a hydrogen atmosphere would necessarily result, at least initially, in a discontinuous monolayer of platinum metal. We believe this to be the case for impregnated catalysts.

Using the previously stated concept that the adsorption of hydrogen atoms occurs at the interstices of the platinum surface, we may calculate the H/Pt ratio to be expected from a monolayer of any given dimensions. For simplicity we shall consider the monolayer to consist of n rows of close-packed platinum atoms, with a radius of 1.39 Å.,[9] the rows containing alternately n and $n - 1$ atoms. Adsorption of the H atoms is assumed not to occur at the platinum–alumina interface. If the opposite assumption is made mean particle dimensions obtained are approximately one-half of those given below in the range of 0 to 20 Å. We have not observed H/Pt ratios corresponding to monolayer particles of a larger size.

The general equations for the number of total atoms T and the number of surface interstices I, were obtained as a function of the number of rows n in the monolayer (1,2).

$$T = n^2 - \frac{n}{2} + \frac{\sin^2 \pi n/2}{2} \quad (1)$$

$$I = 2n^2 - 5n + 3 \quad (2)$$

Curve A in Fig. 3 shows the relationship between the ratio, I/T, and the mean dimension of the monolayer. In future discussion, the ratio, I/T, is taken to be identical to the ratio, H/Pt.

A very likely alternative to the monolayer type of array is a roughly spherical form such as might be expected if a chloroplatinic acid solution were precipitated in the presence of alumina. In this case, one might well expect to produce three-dimensional aggregates of platinum, or of some complex of platinum, which is subsequently reduced to the metal. These aggregates will exhibit a different I/T ratio dependence on particle dimension than was found for the monolayer because of the vastly different surface–volume relationships which characterize these arrays. Specifically, it was assumed that the three-dimensional array was generated as a close-packed cubic mass with a hexagonal base, having N atoms in the side of the hexagon. Successive layers are placed on the base with proper regard for cubic symmetry and tapering off to an approximation of a hexagonal pyramid.

Using such a model, a new set of equations (3,4) can be derived which relate I and T to the variable N, as well as to the mean dimension of the aggregate which was taken as the distance between opposite sides of the base.

$$T = 38 + (N - 3)57 + (N - 3)(N - 4)20 + (N - 3)(N - 4)(N - 5)\,5/3 \quad (3)$$

$$I = 6(N - 1)^2 + 3[(N - 2) + (N - 4) + \ldots + (2 + \sin^2 \pi N/2)] + 2 \sin^2 \pi N/2 + 1 \quad (4)$$

Curve B in Fig. 3 shows how the ratio I/T is related

(7) See, for example (a) D. D. Eley, "Advances in Catalysis," Vol. I, Academic Press, New York, N. Y., 1948, pp. 176–181; (b) J. H. DeBoer, "Advances in Catalysis," Vol. VIII, Academic Press, New York, N. Y., 1956, pp. 68–76.

(8) J. C. P. Mignolet, paper presented at Fall 1958 Meeting, American Chemical Society.

(9) L. Pauling, "Nature of the Chemical Bond," 2nd ed., Cornell University Press, Ithaca, N. Y., 1948, p. 409.

to the mean dimension of the hexagonal aggregate.

From Fig. 3, hydrogen adsorption values for various catalysts were interpreted in terms of either a "monolayer" or "aggregate" array of some mean dimension. Most of these same catalysts were also examined for average Pt crystallite size by X-ray line-broadening measurements. In Tables II and III, a comparison is made between average Pt particle dimensions as determined by the two methods.

TABLE II

LINE-BROADENING AND ADSORPTION DATA—0.30% Pt IMPREGNATED CATALYSTS

Treatment	Relative Pt peak area[a]	Mean particle dimension, Å. X-Ray	H_2 adsorption[b] M	A
Calcined 593°, 1 hr.	..	<50	20	..
Coked, regenerated	..	<50	20	..
0.35 atm. steam, 705°, 5 hr.	210	180–220	..	18
reactivated	..	.....	..	17
1.00 atm. steam, 750°, 5 hr.	370	250–300	..	290
reactivated	370	200–250	..	175

[a] Peak height × half-width (arbitrary units). [b] M, monolayer; A, aggregate.

TABLE III

LINE-BROADENING AND ADSORPTION DATA—COGELLED CATALYSTS

Wt. % Pt	Treatment	Relative Pt peak area[a]	Mean particle dimension, Å. X-Ray	H_2 adsorption[b] M	A
0.30	Calcined 593°, 1 hr.	..	<50	12	12
.30	0.35 atm. steam, 705°, 5 hr.	460	80–120	..	215
.30	reactivated	..	.....	..	22
.58	Calcined 593°, 1 hr.	..	<50	11	14
.58	0.35 atm. steam, 705°, 5 hr.	360	130–150	..	250
.58	reactivated	290	90–130	..	38
.58	1.00 atm. steam, 750°, 5 hr.	350	100–150	..	180
.58	reactivated	490	80–120	..	145

[a] Peak height × half-width; normalized for Pt content. M, monolayer; A, aggregate.

It is seen that there is general agreement between the two methods of determining Pt dimensions including instances where H_2 adsorption data indicate that the particles are too small to be "visible" in X-ray determination. The effective lower limit with our instrument was approximately 50 Å. because (1) we were using the strongest Pt diffraction line which is superimposed on a γ-Al_2O_3 line and (2) the Pt concentration was at most 0.58%. Both of these factors made the line-broadening measurements extremely difficult. The only large discrepancy between values from the two methods is noted for the impregnated catalyst steamed at 0.35 atm. The area under the Pt diffraction peak of this sample is approximately one-half that for either the severely steamed or the reactivated samples. It seems likely that a considerable portion of the platinum in this mildly steamed catalyst is of a particle size too small to be detected by our X-ray technique. H_2 adsorption is, however, not limited in this way; on the contrary, the particle size derived from H_2 adsorption measurements is based on particles of all sizes.

The results for this sample strongly suggest a bimodal particle-size distribution, one mode of which is "invisible" with the X-ray technique. The close agreement between values for the same catalyst after severe steaming indicate that the distribution has reverted to one with a single maximum, and that the bimodal form is a transient one. A similar phenomenon was observed by Selwood, *et al.*,[10] who studied the Ni–SiO_2 system by means of thermomagnetic analysis. Here also, moderate sintering produced a transient bimodal particle-size distribution.

We feel that the dimensional values obtained for fresh and sintered catalyst have a real physical significance. On the other hand, we do not believe that the results obtained on the reactivated catalysts should be taken to indicate a decreased Pt particle size. Considerations of energetics would rule out the possibility of a platinum particle of over 200 Å. dissociating into 20 Å. particles as might be indicated for the cogelled catalyst containing 0.30% Pt. Instead, we interpret the apparent decrease in size after reactivation as due to a disruption of the platinum lattice by oxygen atoms. These are removed by subsequent hydrogen dosing, leaving fissures in the sintered particle. These fissures are then responsible for an increase in Pt surface area which accounts for increased H_2 sorption. At the same time, the degree of ordering in the lattice is reduced and this accounts for the line broadening results.

If we assume that the state of sub-division of the Pt controls the H/Pt ratio, then within each group of catalysts, this does not vary much with the concentration of Pt. The number of cc. (STP) per gram of Pt present goes from 41.6 to 45.0 in going from 0.30 to 0.58% cogelled catalyst. For impregnated catalysts the numbers are 82.0 for 0.10%, 82.6 for 0.30%, and 94.7 for 0.80%.

Effect of Coking.—It can be seen that the coke deposited on a catalyst during reforming diminishes the hydrogen adsorption sharply, but that subsequent regeneration restores it almost to the value of the fresh catalysts in most cases. This indicates that the coke is concentrated on the surface of the platinum, since the carbon present is as low as 0.9% which is only enough to cover at most 5% of the total surface area of the catalyst in monolayer form. It is surprising, perhaps, that a sample coked for five days, with 2.5% carbon on it, has a slightly higher adsorption than the one day sample with only 0.9%. It may be that the carbon is at first finely divided but then forms aggregates which allow greater diffusion of H_2.

Despite the low H_2 adsorption displayed by coked catalysts, it is well-known that one, and even five, days of coke lay-down are not sufficient to deactivate the "total" activity of such catalysts. Weisz[11] has already pointed out that only a min-

(10) P. W. Selwood, S. Adler and T. R. Phillips, *J. Am. Chem. Soc.*, **77**, 1462 (1955).

(11) P. B. Weisz and C. D. Prater, "Advances in Catalysis," Vol. IX, Academic Press, Inc., New York, N. Y., 1957, pp. 575–586.

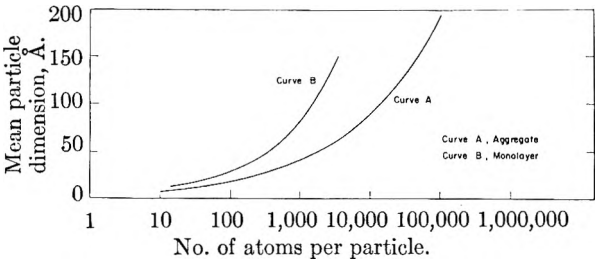

Fig. 4.—Number of platinum atoms per particle *vs.* mean particle dimension.

imal level of dehydrogenation activity is necessary to produce normal levels of "total" activity, and therefore, we interpret these results as indicative of the existence on the coked catalyst of the necessary "steady-state" level of exposed Pt sites. Further, we believe that one of the functions of the high-pressure hydrogen atmosphere in a reforming reactor is to maintain that "steady-state" level of sites by continuous hydrogenation of coke-precursor fragments.

It is noteworthy that two samples of regenerated cogelled catalyst, after 1-day coking, displayed two distinct levels (Table I) of H_2 adsorption despite the fact that the samples were essentially replicates, and other replicates were much more reproducible. We feel that this may be due to the fact that slight differences in local temperatures during regeneration can lead to different levels of sintering in cogelled catalyst.

It is interesting to speculate further about the meaning of the adsorption data on mildly sintered and on regenerated samples in terms of particle growth. One can estimate the number of particles that participate in such a phenomenon and thus arrive at a qualitative description of the distribution of the platinum on the catalyst surface. Figure 4 shows the relationship between platinum particle dimension and the number of atoms per particle as derived from the equations discussed previously. From this plot, we were able to calculate the average number of Pt atoms per particle for various catalysts as shown in Table IV.

TABLE IV

PLATINUM ATOMS PER PARTICLE

Catalyst	No. of atoms per particle Fresh	Regenerated	Steamed[a]	Growth factor Reg./Fr.	Std./Fr.
Cogelled—0.30% Pt	20	..	200,000	..	10,000
0.58% Pt	30	500	100,000	20	3,000
Impregnated 0.30% Pt	50	50	100	1	2

[a] Five hr. at 705°, 0.35 atm. H_2O.

We have suggested earlier that the methods of preparation used for the cogelled and impregnated catalysts could lead, respectively, to aggregated and monolayer types of platinum arrays. A further difference may be in the manner in which the particles are distributed on the catalyst surface. Cogellation will, most likely, produce widely separated surface localities in which the platinum spheroids, precipitated from chloroplatinic acid solution, will cluster. The bulk of the catalyst surface area is, after all, produced after the platinum particles are lodged in the alumina matrix. By contrast, impregnation of alumina with chloroplatinic acid should lead to a random distribution of platinum "rugs."

These arrangements serve to explain how a moderate amount of energy, as supplied by careful regeneration or mild steaming will produce a larger degree of "polymerization" in the cogelled catalyst. Given the thermal energy produced during a regeneration, cogelled catalyst sinters slightly and impregnated catalyst not at all. Mild steaming allows the Pt clusters in cogelled catalyst to coalesce completely; in the impregnated catalyst only a portion of the particles are sintered by this treatment, while the balance remain apparently unaffected. Severe steaming causes complete sintering in both types of catalyst.

Acknowledgments.—We wish to thank Mr. George Yates, who made the hydrogen adsorption measurements, and Mr. William Doughman, who provided the X-ray diffraction patterns.

α-PARTICLE RADIOLYSIS OF CARBON MONOXIDE

BY A. C. STEWART AND H. J. BOWLDEN

Parma Research Laboratory, Union Carbide Corporation, Cleveland, Ohio

Received July 30, 1959

The present paper presents a theoretical analysis of new and old experimental work on the α-radiolysis of carbon monoxide. Specific attention is given to the effects of adding non-reactive gases. A model is presented, and the resulting equations are fitted to the data by a least-squares technique. A value is obtained for the reaction cross section in pure CO. Evidence is presented to support the hypothesis that ionization plays a large role in the process.

Introduction

Studies of the influence of inert gases on chemical reactions induced in gases by the absorption of energy from highly ionizing radiation are being continued.[1-6] In the present work we have examined reactions in which energy transfer must be important and have speculated about details of

(1) S. C. Lind and D. C. Bardwell, *Science*, **62**, 422, 593 (1925); **63**, 310 (1926); *J. Am. Chem. Soc.*, **47**, 2684 (1925); **48**, 1575 (1926).

(2) S. C. Lind, "The Chemical Effects of Alpha Particles and Electrons," 2nd ed., Am. Chem. Soc. Monograph, Reinhold Publ. Corp., New York, N. Y., 1928, p. 189.

(3) S. C. Lind, THIS JOURNAL, **56**, 920 (1952).

(4) S. C. Lind, *ibid.*, **58**, 800 (1954).

(5) S. C. Lind and P. S. Rudolph, *J. Chem. Phys.*, **26**, 1768 (1957).

(6) R. C. Palmer, D. C. Bardwell and M. D. Peterson, *ibid.*, **28**, 167 (1958).

the absorption process. When α-particles act at room temperature on carbon monoxide, the resulting products are carbon dioxide, carbon and a solid polymer $(C_3O_2)_x$. In early experiments,[7] the products of the reaction were established and the solids, C and $(C_3O_2)_x$ characterized. The present work was to determine whether mixing a single inert or chemically unreactive gas (CO_2, Ar, He, Kr, Ne, N_2, Xe) with irradiated CO would increase the rate of reaction.

Experimental

Experimental procedures have been previously described.[8] Alpha particles (5.48 mev.) from Rn 222 (half-life, 3.825 d) were used. Irradiations were carried out in Pyrex bulbs of ~ 2 cm. diameter so that α-particles (range 3.9 cm. at 0°, 760 mm.) traversed them. Gamma rays were measured to determine dose rates and external shielding was provided to reduce the background in the laboratory. Reaction was followed by pressure change.

Carbon monoxide was obtained from reaction of formic acid and hot concentrated reagent-grade sulfuric acid.[9] Radon was collected from an acid radium chloride solution. Both were purified by usual procedures. Spectrographic grade additive gases were used without further purification.

Description and Analysis of the Model.—Lind defines a velocity constant, $k\mu/\lambda$.[10]

$$\frac{k\mu}{\lambda} = \frac{\log (P/P_0)}{E_0(e^{-\lambda t} - 1)}$$

where

P_0 = initial total pressure
P = total pressure at time, t
E_0 = initial charge of radon
λ = decay constant for radon

In these experiments the constants did not show whether a particular foreign gas added to CO increased, or retarded, the rate of reaction. Consequently, the kinetic treatment which follows was undertaken. We have adopted the following sequence of reactions to represent the processes occurring

$$CO \xrightarrow{(\alpha)} C^* + O^* \quad (1)$$
$$CO_2 \xrightarrow{(\alpha)} CO + O^* \quad (2)$$
$$O^* + CO \longrightarrow CO_2^* \quad (3)$$
$$CO_2^* \longrightarrow CO + O^* \quad (4)$$
$$C^* + 2CO \longrightarrow C_3O_2 \quad (5)$$
$$C^* \longrightarrow C\ (\text{solid}) \quad (6)$$
$$CO_2^* \longrightarrow CO_2 \quad (7)$$

The rate equations derived from the above sequence are

$$\dot{x} = a_1 y + a_2 v - a_3 xy + a_4 u \quad (8)$$
$$\dot{y} = -a_1 y - a_3 xy - 2a_5 y^2 z + a_2 v + a_4 u \quad (9)$$
$$\dot{z} = a_1 y - a_5 y^2 z - a_6 z \quad (10)$$
$$\dot{u} = a_3 xy - (a_4 + a_7)u \quad (11)$$
$$\dot{v} = -a_2 v + a_7 u \quad (12)$$

In these equations x, y, z, u, v represent the partial pressures of O*, CO, C*, CO_2* and CO_2, respectively. The a's are the respective rate "constants" for equations 1-7. The dot represents differentiation with respect to time. The quantities y and P (total pressure) $\simeq y + v$ represent the measured pressure changes.

(7) Ref. 2, p. 152.
(8) Ref. 2, Chap. 7.
(9) W. C. Fernelius, ed., "Inorganic Syntheses," Vol. II, McGraw-Hill Book Co., Inc., New York, N. Y., 1946, p. 81.
(10) Ref. 2, p. 116.

Applying the usual steady state (or "secular equilibrium") hypothesis,[11] and setting $\dot{x} = \dot{z} = \dot{u} = 0$, we obtain the relations

$$\dot{y} = -4a_1 y + \frac{2a_1 y}{1 + \frac{a_5}{a_6} y^2} \quad (13)$$
$$\dot{v} = a_1 y$$

The parameter a_1 is not constant but is proportional to the flux of α-particles and contains a factor $e^{-\lambda t}$.

Let

$$w = e^{-\lambda t} \quad (14)$$

and

$$a_1 = \alpha_1 w$$

Thus, α_1 is the initial value of the rate "constant" a_1. Its units are sec.$^{-1}$. If we define the quantity

$$\sigma_1 = \frac{\alpha_1}{\phi} \quad (15)$$

where ϕ is the initial α-particle flux, measured in particles per cm.^{2} sec., the quantity σ_1 has the unit cm.^{2}. It will be called the reaction cross section[12] for process 1 and may be expected to have a value of the order of the cross-sectional area of a CO molecule ($\sim 10^{-15}$ cm.^{2}). If the sphere is sufficiently large compared with the range of the α-particles (this condition is met reasonably well in the present experiments), we find that

$$\phi = \frac{9Q}{16\pi R^2} \quad (16)$$

where Q is the total radon concentration in curies times 3.7×10^{10} (*i.e.*, in disintegrations per second), and R is the radius of the (spherical) vessel in cm.

We now transform equations 13 using 14, making w the independent variable. This leads to the relations

$$\frac{dy}{dw} = \frac{1}{2} \vartheta y \frac{\beta_5^2 + 2y^2}{\beta_5^2 + y^2} \quad (17)$$

and

$$\frac{dv}{dw} = -\frac{1}{4} \beta y$$

where

$$\beta = 4c_1/\lambda \quad (18)$$

and

$$\beta_5 = (a_6/a_5)^{1/2}$$

The integrals of these equations are

$$y = \beta_5[\zeta^2 + \zeta(1 + \zeta^2)^{1/2}]^{1/2}$$

and

$$P(= y + v) = -\frac{\beta_5}{4} \int_0^\zeta \left[1 + \left(1 + \frac{1}{\zeta^2}\right)^{1/2}\right]^{1/2} d\zeta + P_1 + y \quad (19)$$

where

$$\zeta = e^{\beta(w - w_1)} \quad (20)$$

and P_1 and w_1 are constants of integration.

Fitting the Data.—The results of the preceding

(11) See, for example, A. A. Frost and R. G. Pearson, "Kinetics and Mechanism," John Wiley and Sons, Inc., New York, N. Y., 1953, p. 159.
(12) See, for example, I. Kaplan, "Nuclear Physics," Addison-Wesley, Cambridge, Mass., 1955, pp. 369 ff.

TABLE I

CO CROSS SECTIONS

	Case	$\sigma(10^{-15}$ cm.$^2)$	β	β_5 (mm.)	w_1	P_1 (mm.)	V (mm.)
1	Pure CO (i)	1.084	0.61783	220.13	−0.14709	242.37	1.31
2	(ii)[a]	1.084	0.67802	406.97	+0.84000	282.25	0.65
3	CO + CO_2	1.154	0.56077	315.66	+0.52480	368.99	0.39
4	CO + Ar	1.63	1.70	385	+1.00	321	2.43
5	CO + He (i)	1.357	1.24127	71.75	−0.200	401.64	3.05
6	(ii)	1.334	0.83843	271.66	+0.56884	209.45	1.59
7	(iii)	1.160	0.80402	232.18	+0.220	226.41	1.56
8	CO + Kr	1.398	0.82025	350.30	+0.80847	271.09	0.49
9	CO + Ne[b]	1.63	1.50	12	−1.00	259	0.83
10	CO + N_2	1.485	0.81689	6.01	−4.28091	182.51	0.71
11	CO + Xe (i)[a]	1.084	0.72635	129.38	+0.31000	153.36	0.24
12	(ii)	1.084	0.68736	363.87	+0.82000	261.38	0.67

[a] S. C. Lind and P. S. Rudolph, private communication. [b] S. C. Lind and M. Vanpee, THIS JOURNAL, 53, 898 (1949); private communication.

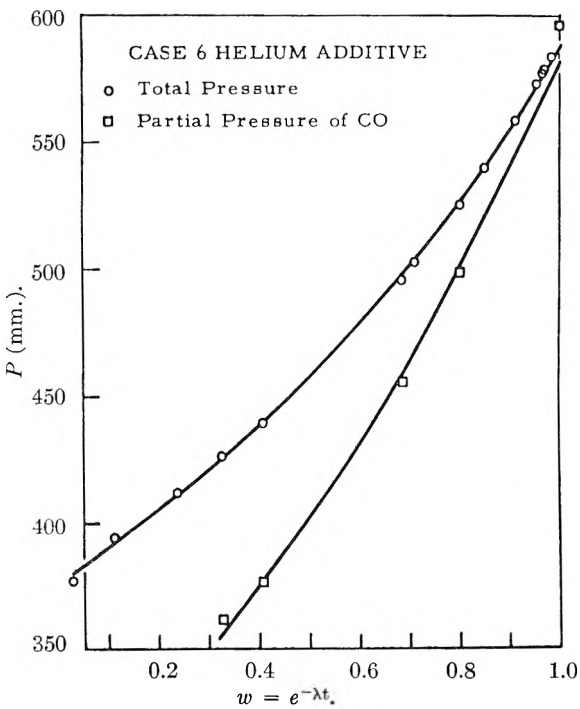

Fig. 1.—A typical plot of total pressure P and partial pressure y as functions of $w = e^{-\lambda t}$. Case 6, helium added to 475.2 mm. (this is subtracted from the total pressures plotted). The continuous curves represent the values computed by the present methods.

section are too complex for use in handfitting the experimental data. A program was written for fitting the data with equations 19 and 20 by the method of least squares, using an IBM-704 electronic computer.

The procedure was to obtain values of the four constants β, β_5, w_1 and P_1 which gave the best fit for each experiment. Since two of these parameters, β and w_1 appear non-linearly, it was not possible to use standard least-squares techniques. An iterative method was developed which obtains the best values by successive approximations. After values for the parameters were obtained by this method for each individual experiment, they were re-examined for possible correlations and new fits were obtained which demonstrated these correlations.

Results of the Curve Fitting.—Data obtained from curves similar to Fig. 1 can be fitted satisfactorily with the values for the constants shown in Table I. This table lists the values for the four constants in equations 19 and 20 together with the cross section σ_1 and the RMS deviation $\bar{V}$ between observed and calculated values. To obtain this RMS deviation, the measurements of y (partial pressure of CO) were given a relative weight of 0.09 to allow for the necessary uncertainties in reducing these measurements to room temperature, and the experimental difficulties associated with the measurement. Most of the σ-values in Table I reflect the "best fit" for the data. However, in case 2 the "best fit" value of σ_1 was 1.011. It was found, however, that σ_1 could be made equal to the value (1.084) from case I, and the data from case 2 still fitted more closely than those from case 1. The same procedure was used in cases 11 and 12.

Table II contains the results of reducing the differences in cross section with and without the added gas to terms of 1% (by pressure) of added gas. Three runs of helium experiments were available (cases 5, 6 and 7) and, consequently, a test was made on the proportionality of $\Delta\sigma$ to added gas. The value of σ for case 6 was used as a base, and values of σ for cases 5 and 7 were then chosen by proportionality to the pressure of helium added. It is observed that case 7 is fit by this value as well as case 6. The data of case 5 were regarded as unreliable because of a probable error in the vital initial pressure reading.

TABLE II

INCREASE IN CROSS SECTION FOR 1% (BY PRESSURE) INERT GAS ADDITIVE

Gas	$\Delta\sigma(10^{-15}$ cm.$^2)$
CO_2	0.006 ± 0.002
A	.021 ± .010
He	.0034 ± .001
Kr	.024 ± .002
Ne	.005 ± .002
N_2	.015 ± .001
Xe	.000 ± .001

Typical plots of direct comparisons between experimental points and values calculated using the constants in Table I are presented graphically in Fig. 2. The points represent differences between experiment and theory, and show the transients very clearly.

Discussion of Results

The elimination of most of the rate constants in the derivation of equations 13 indicates that they cannot be determined from the data available. Equation 2 could have been left out. The reactions in equation 3, 4 and 7 are possible mechanisms for removing the atomic oxygen from the system as rapidly as it is formed. These requirements may be met by requiring that the rate constants for reactions 3 and 7 be much larger than the others.

We have obtained σ_1, the cross section for reaction 1, and β_5, which gives the relative importance of reactions 5 and 6 in removing free atomic carbon from the reaction. From experiments 1, 2, 11 and 12 we conclude that the basic reaction cross section for the dissociation of CO by α-particles is

$$\sigma_1 = (1.084 \pm 0.005) \times 10^{-16} \text{ cm.}^2 \qquad (21)$$

If we multiply this by the number of molecules per unit volume, we obtain 2900 events per millimeter path length per α-particle. Since the initial specific ionization value for radon alphas in air is about 3000 ion pairs per millimeter, our value suggests that the events are ionizations.

The effects of adding an inert gas may be of two types. First, by acting as an intermediary in the transfer of energy to CO it may increase the apparent value of the cross section σ_1. Second, it may provide an alternate path for the removal of C* from the system, thus increasing the apparent value of β_5. The first effect is evidenced in the figures of Table II. The mechanism postulated for this energy transfer depends on the mechanism of the immediate α + CO reaction itself. The results of Table II afford a clue to this mechanism. In Fig. 3 we plot the increase in cross section as a function of the ionization potential of the added gas. The shape of the resultant curve indicates that ionization is the primary event in this reaction. The continuous curve in Fig. 3 is obtained by plotting a quantity proportional to $[E_I - E_I(CO)]^{-1/2}$, and smoothing this to zero at $E_I(CO) = 14.00$ e.v. with a width roughly equal to the thermal energy (0.025 e.v.). This is a reasonable form for an ionization transfer collision process, modified by thermal broadening. The process corresponds to the equations

$$\begin{aligned} M &\xrightarrow{(\alpha)} M^+ \\ M^+ + CO &\longrightarrow CO^+ + M \end{aligned} \qquad (22)$$

The conclusion that ionization is the primary event is not necessarily in conflict with equation 1. If that equation is expanded into any number of forms, such as

$$CO \xrightarrow{(\alpha)} CO^+ + e \longrightarrow CO^* \longrightarrow C + O$$

or

$$CO \xrightarrow{(\alpha)} CO^+ + e \longrightarrow C + O^+ + e$$

or

$$CO \xrightarrow{(\alpha)} CO^+ + e \longrightarrow C^+ + O + e$$

etc., the existence of the intermediate step does not interfere if there is no other path to or from the intermediate step.

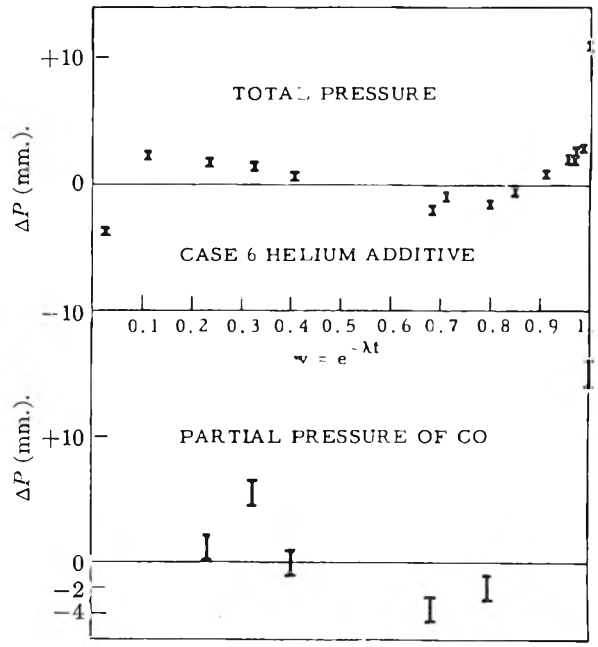

Fig. 2.—Measure of agreement between experiment and the present theory. The symbols give differences, P (observed) − P (computed), with probable errors (mostly experimental). Case 6, as in Fig. 1.

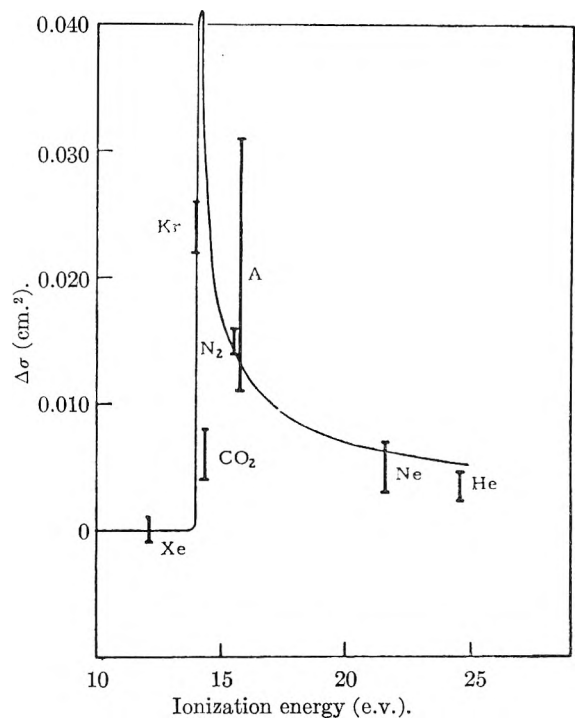

Fig. 3.—Increase in reaction cross section caused by a 1% (by pressure) addition of various gases, plotted as a function of the ionization energy of the additive. The continuous curve represents a suggested form for an ionization mechanism (see text).

The value for CO_2 falls considerably below the curve in Fig. 3. This is not surprising, since any addition of CO_2 merely supplements the CO_2 produced in the reaction. If the true contribution of CO_2 is large, then it would appear that in a more refined analysis the system 1–7 should be supplemented by the equations 22 (with M replaced by CO_2).

The over-all stoichiometry gives a proportionality of 3:1 in the ratio of decrease in CO to increase in CO_2, but the rates of change of these two components can be obtained from equations 17 and 18.

$$-\frac{dy}{dv} = 2\frac{\beta_5^2 + 2y^2}{\beta_5^2 + y^2}$$

This is not 3, but varies as the experiment proceeds (through its dependence on y). It may take on any values between 2 and 4, depending on the ratio y/β_5. Consequently, a derivation of partial pressures from an assumption of constant stoichiometry is subject to question.

The "transient" near the beginning of the experiment (w near 1) has not yet been explained. An examination of equations 1–7 shows that the rate of removal of CO depends on the balance between processes 5 and 6, *i.e.*, on the value of β_5. If β_5 is small, (5) is the main process, while for larger β_5, (6) becomes important. The mechanism of (6) is not clear, but since solid carbon is produced in the bulbs in a very finely divided state, it could be a process of nucleation and agglomeration. If it is assumed that during the "transient" solid carbon nuclei are being generated, while after the transient no more are produced, those present merely growing, then it is possible to explain the transient qualitatively. A value of 0 for β_5 would increase the slope dP/dw in equation 17, which goes from $^1/_4\ \beta y$ at $\beta_5 = \infty$ to $^3/_4\ \beta y$ at $\beta_5 = 0$. If, then β_5 increases from zero to the steady value shown in Table I during this period, the features of the transient become qualitatively understood. Quantitatively, however, this picture is not so satisfactory. Actual slopes at $t = 0$ are as much as five times the "maximum" value $^3/_4\ \beta y$ obtained by the above reasoning. It may very well be that the steady-state assumption used here is not satisfactory in the early stages of the process. A technique is being developed to extend the computational method used in the present work into a more general program, in which the steady-state approximation will not be necessary. With such a technique this point may be investigated further. It is also possible that the addition of reactions involving charge transfer between CO and CO_2 may help in providing a better fit. The specific nature of the mathematical reduction used here makes it difficult to add such a possibility but a general program will remove this difficulty, and enable us to make a more thorough analysis of these factors.

We have no explanation for the variation of the steady-state values of β_5 in Table I. The small values of β_5 in the argon and nitrogen experiments are particularly noteworthy. This implies correspondingly small production of solid carbon nuclei.

Summary.—A model has been presented which satisfactorily explains many features of the experimental data. In particular, fits to the data may be made with physically reasonable values of the reaction cross section for ionization of CO by α-particles. This cross section is apparently increased by many additive gases, and the dependence of the increase upon the ionization energies supports the hypothesis that ionization is the primary event involved. The initial "transient" remains unexplained.

Acknowledgments.—The experimental work for this study was performed in the Chemistry Division of the Oak Ridge National Laboratory operated for the U. S. Atomic Energy Commission by Union Carbide Nuclear Company, Division of Union Carbide Corporation. The authors wish to thank Dr. S. C. Lind for introducing one of us (A. C. Stewart) to the problem and for his invaluable counsel. They also wish to thank Dr. P. S. Rudolph for aid in performing the experiments and for many helpful discussions.

THE INFRARED SPECTRA OF POLYMERS. III. THE INFRARED AND RAMAN SPECTRA OF ISOTACTIC POLYPROPYLENE[1]

BY MARVIN C. TOBIN

Central Research Division, American Cyanamid Company, Stamford, Connecticut

Received July 31, 1959

The infrared and Raman spectra of isotactic and the infrared spectrum of amorphous polypropylene are reported. The spectra are used to establish the positions of standard tertiary methyl frequencies for spectra–structure correlations and the demonstration that simple methyl branching is absent in polyethylene. The observed spectra are compared with those predicted from various proposed crystal structures.

Introduction

Polypropylene is of great spectroscopic interest as the model "tertiary methyl" hydrocarbon, just as is polyethylene as the model linear hydrocarbon. Unfortunately, the complex structure of polypropylene in the crystal, and the difficulty of associating group frequencies with normal modes make interpretation of the spectra a matter of some difficulty. In the present paper, the infrared and Raman spectra of polypropylene are analyzed from two viewpoints. First, the spectra are examined to locate frequencies characteristic of tertiary methyl groups. Then, the spectra are compared with those predicted from various possible crystal structures.

The X-ray diffraction pattern of crystalline polypropylene has been analyzed by Natta, Corradini and Ceseari.[2] The polymer chains occur

(1) Presented before the Cellulose Chemistry Division of the American Chemical Society in Boston in April, 1959.

as helices with three monomer units per turn. Left- and right-handed helices are distributed regularly in pairs throughout the crystal. Further than this, a certain ambiguity remains in the structure, for the following reason. Since the methyl branches are not perpendicular to the helix axis, on a given site the C–CH_3 bonds can make an angle less than 90° ("up") or more than 90° ("down") with a fixed direction in the crystal. (An "up" chain may be converted to a "down" chain by a simple rotation perpendicular to the helix axis.)

The crystal structure is such that if all sites contained "up" chains, the left- and right-handed helices in each pair would have a glide plane of symmetry between them. If the left-handed helices were "up" and the righ-handed helices "down" or *vice versa*, the helices in a pair would have a center of symmetry between them. A third possibility and the one favored by Natta, Corradini and Ceseari,[2] is that the "up-down" property be distributed at random, even though the "left-right" property remains regular. This last structure would have a statistical space group C_{2h}^6, with four chains per unit cell. While the X-ray results of Natta, Corradini and Ceseari definitely eliminate the regular, centrosymmetric "up-down" structure, the "up-up" structure having glide plane symmetry remains a possibility.[3]

Experimental

Infrared spectra of Montecatini polypropylene film and of a polypropylene oil were obtained on a Beckman IR-4 spectrometer, using NaCl and CsBr optics. The oil was isolated from isotactic material, prepared at these laboratories, by extraction with heptane, followed by extraction of the heptane extract with acetone. To obtain infrared spectra of the melted film, a strip of film was sandwiched between rock salt plates in a standard demountable holder. This fitted into a small furnace, which heated the entire assembly to the desired temperature (about 185°). Measurements in the CsBr region were made on the oil and on the unmelted film only. Thicknesses of these latter of 0.5–2.0 mm. were used in the 300–700 cm.$^{-1}$ and 1600–2700 cm.$^{-1}$ regions and of 0.05–0.1 mm. in the 700–1600 and 2700–3100 cm.$^{-1}$ regions.

Samples of stretched film were prepared by holding a strip of film a small distance above a hot plate, and stretching as soon as the film softened. Infrared spectra of the stretched film were obtained using a six-plate AgCl polarizer on a Perkin–Elmer Model 21 spectrometer. The polarizer was placed so that the electric vector of the transmitted radiation remained perpendicular to the spectrometer base, orientation being changed by rotating the sample.

Raman spectra were obtained on commercial Montecatini polypropylene pellets, using a cyrstal powder source constructed at these laboratories.[4] The pellets were held in a standard Raman tube. Four-hour exposures were used. Since the pellets had a yellowish tinge and were weakly fluorescent, very weak lines may have been missed. Complete Raman spectra of DYNH and Marlex 50 polyethylenes[5] were recorded at the same time, again with four-hour exposures. These are given in Table I. The spectrum for Marlex 50 given there agrees with that of Nielsen and Woollett. The infrared and Raman spectra recorded for polypropylene are given in Table II, along with the standard tertiary methyl frequencies proposed by Sheppard and Simpson.[6,7] Since no marked differences between the infrared spectra of melt and oil could be discerned, only the spectrum of the latter is given. No bands could be found in the 1600–2700 cm.$^{-1}$ region of the infrared spectrum of the oil.

Tertiary Methyl Bands.—The monomeric repeat unit of polypropylene should give rise to 23 normal modes of which six are CH stretchings, one a CH_2 bending and three CH_3 bendings. Assuming the spectrum of amorphous polypropylene to resemble that of the hypothetical isolated, extended chain, one would expect to find 13 moderately strong bands below 1350 cm.$^{-1}$. Roughly this number is found, considering that the broad band around 550 cm.$^{-1}$ may contain several fundamentals.

TABLE I

RAMAN SPECTRA OF MARLEX 50 AND DYNH POLYETHYLENES

Marlex 50	DYNH
1062s	1062s
1126s	1126s
1177w	1177w
1293s	1293s
1412w	1412vvw
1435s	1435s
1458w	1458w
2718w	2718w
2845s	2845s
2890s	2890s
2926w,br	2926w,br

It does not seem possible to give any assignment of frequencies to normal modes, since the form of these is not known, and the group frequency approximation almost certainly does not hold for most of the modes. A normal coördinate analysis would require solution of a 14 × 14 secular equation, taking the methyl group as a point mass. In this situation, it seems best to follow earlier workers[6,7] and attempt to classify the observed frequencies as CH, CH_2 and tertiary methyl (including "skeletal") modes.

The standard tertiary methyl bands given by Sheppard and Simpson[6] are listed in Table II as 430, 830, 1010, 1040, 1155 and 1360 cm.$^{-1}$. If we examine our Raman spectrum, and the infrared spectrum of the amorphous polymer, we find bands at ~500 (IR), 808 (IR, R), 975 (IR), 1157 (IR, R), 1333 (R) and 1382 (IR) cm.$^{-1}$. The two sets of bands agree well except near 1000 cm.$^{-1}$. We find a strong infrared band at 975 cm.$^{-1}$, but no marked infrared or Raman bands at 1010 or 1040 cm.$^{-1}$. Therefore, 975 cm.$^{-1}$ is chosen as the tertiary methyl frequency in this region. This choice agrees with a recent classification given by Sushinskii,[7] who gives 800–900, 955 and 1150–1170 cm.$^{-1}$ for standard tertiary methyl frequencies. It is particularly noteworthy that, as in short chain hydrocarbons, the 1382 cm.$^{-1}$ band is absent in the Raman spectrum, and the 1333 cm.$^{-1}$ band is absent in the infrared spectrum. No Raman bands were observed near 500 or 975 cm.$^{-1}$, even though bands appear at these positions in short-chain compounds. It is possible that these bands were present, but obscured by background. In any event, they must be an order of magnitude weaker than those bands which were observed.

(2) G. Natta, P. Corradini and M. Ceseari, *Atti. accad. naz. Lincei Rendi. Classe di sci. fis. mat. e nat.*, **21**, 365 (1956).

(3) Professor G. Natta, private communication.

(4) M. C. Tobin, *J. Opt. Soc. Am.*, **49**, 850 (1959).

(5) J. R. Nielsen and A. Woollett, *J. Chem. Phys.*, **26**, 1391 (1957).

(6) N. Sheppard and D. Simpson, *Quart. Rev.*, **7**, 19 (1953).

(7) M. M. Sushinskii, *Spectrochim. Acta*, **14**, 271 (1959).

TABLE II

INFRARED AND RAMAN SPECTRA OF POLYPROPYLENE,[a] CM.$^{-1}$

Isotactic[d]	Infrared Oil	Raman[b]	Sheppard and Simpson	Assignment
408vw	460–620 br with peak at 542 w	( )	(430)	Skeletal[c]
460w, 537w ⊥	542w			
580vw				
742 barely detectable	738, 742 vw			CH_2 rocking
808m, 842m ⊥ ∥	800–860vw	808m	(830)	Skeletal[c]
900w ⊥	895vw			
942vw ⊥				
975m, 998m ∥	975m	( )	(1010)	Skeletal[c]
	1000vww?		(1040)	
1045vw ∥				
1102vw ⊥				
1155m sh, 1170m ⊥ ∥	1160m	1157s	(1155)	Skeletal[c]
1222vw, 1260w ⊥ ∥	1230–60vw, br			CH_2 wagging
1295, 1308 ⊥ ∥	1300vvw			CH_2 twisting
1330w ⊥		1333s	(1360)	CH bending[c]
1364s, 1382vs ⊥	1382vs			CH_3 sym. bending[c]
1446vs sh ⊥	1450 vs	1457s,br		CH_3 asym. bending
1462vs ⊥	1460 vs			CH_3 asym. bending
1466vs ⊥	1470 vs			CH_2 bending
1647w				2 × 810
1690w				2 × 840
1755w				810 + 975 (?)
1840w				460 + 1382
1905, 1925sh w				460 + 1450
1970, 2010 vw				810 + 1157
2060vvw, br				810 + 1260 (?)
2125sh, 2155 vw				810 + 1333
2195, 2210sh w				810 + 1382
2284w				2 × 1157
2350–2425w, br				975 × 1460
2720w				1333 + 1382
2820vs ⊥	2825 vs	2831 s		CH_2 sym. stretching
2880vs ⊥	2875 vs	2884 s		CH_3 sym. stretching
2915vs ⊥	2920 vs	2921 s		CH_2 asym. stretching
2960vs ⊥	2960 vs	2968 s		CH_3 asym. stretching

[a] s, strong; m, medium; w, weak; vw, very weak; vvw, very, very weak; sh, shoulder; br, broad. [b] Empty parentheses in Raman spectrum indicate presumably missed bands. [c] Standard tertiary methyl frequencies. [d] ∥ = greatest absorption with electric vector of polarized radiation parallel to stretch direction of film; ⊥ = greatest absorption perpendicular to stretch direction of film.

The methylene frequencies are assigned at 740, 1260 and 1300 cm.$^{-1}$, by analogy with short-chain compounds.[5,6] The CH_2 rocking near 740 cm.$^{-1}$ has vanishingly small intensity in the crystal, so that the 738–742 cm.$^{-1}$ amorphous doublet may be useful for crystallinity measurements. It is not clear why this band, if the assignment is correct, should be a doublet.

The author believes that this treatment points up a generally ignored usefulness of polymer spectra in establishing spectra-structure correlations. Polymer spectra are perturbed to a much lesser extent than those of short chain compounds by rotational isomerism.

An immediate use may be made of the tertiary methyl correlations established here. Bryant and

Voter[8] have suggested that short chain branching in polyethylene consists entirely of ethyl or longer branches. Examination of Table II and the infrared spectrum of polyethylene[9,10] confirms this view. While polyethylene has absorptions at 888 and 1375 cm.$^{-1}$, characteristic of terminal methyl, there is no absorption at all at 975 cm.$^{-1}$, a standard tertiary methyl position.

Spectra and Crystal Structure.—With helical polymers such as polypropylene, the usual line-site-space group correlation[11] cannot be made, but must be replaced by the extended chain-helix-space group sequence. Since the helix has factor-group symmetry C_3, each normal mode of the extended chain will split into three modes in the helix.[11] Two of these will be degenerate. The factor group analysis for the possible space groups shows that the degeneracy will split in the crystal, so that each mode of the extended chain should give rise to six or twelve distinct modes in the crystal, depending on the number of chains per unit cell.

None of these predictions, based on group theory, is borne out. If we take, as before, the spectrum of the amorphous polymer as that of the extended chain, each band of the extended chain appears to split into two bands in the infrared spectrum of the crystal. The Raman spectrum of the polymer shows no splittings at all. While unresolved splittings are not uncommon in the Raman spectra of crystals (compare reference 5), bands separated by more than 3–4 cm.$^{-1}$ should have been resolved in our infrared spectra. One must conclude that either intrachain coupling between monomer unit modes in the helix is weak, and that the observed splitting is an interchain effect, or that interchain splitting is weak and that the observed components in the crystal infrared spectrum are the A_1 and E bands of line group C_3 arising from each extended chain mode. This latter splitting would be solely an intrachain effect.

(8) W. Bryant and R. Voter, *J. Am. Chem. Soc.*, **75**, 6113 (1953).
(9) M. C. Tobin and M. J. Carrano, *J. Chem. Phys.*, **25**, 1044 (1956).
(10) S. Krimm, C. Liang and G. B. B. M. Sutherland, *ibid.*, **25**, 549 (1956).
(11) M. C. Tobin, *ibid.*, **23**, 819 (1955).

Lacking a firmly established crystal structure, it is not possible to decide conclusively between these two possibilities on the basis of our spectra. Nevertheless, an indication is given by the polarizations of the crystal components. The four cases which we have to consider are (1) a single helix free of interchain perturbation, (2) two chains with glide-plane symmetry, (3) two chains with a center of symmetry and (4) a crystal structure with no short-range order (see Introduction). In the last three, intrachain splitting is assumed absent.

In cases (1) and (2), where symmetry elements C_3 or σ_h are present, no observed doublet could have both components parallel, since symmetry requires one transition moment to be perpendicular to the helical axes, and thus experimentally to the stretch direction of the film. The observed parallel dichroisms of both components of the 975–998 cm.$^{-1}$ doublet are in conflict with this. Case (3), as was remarked in the Introduction, is ruled out by the X-ray analysis. The observed violations of the mutual exclusion rule at 808 and 1157 cm.$^{-1}$ are consistent with this X-ray result. Structure (4), with no short-range order and thus no selection rules, is not inconsistent with the observed 975–998 cm.$^{-1}$ dichroisms or the violations of the mutual exclusion rule. Nevertheless, the spectra certainly cannot be said to prove this structure, although they tend to support it, as well as interpretation of the splitting as an interchain effect.

The question of interchain *versus* intrachain coupling could be settled by spectra of mixed crystals of polypropylene and completely deuterated polypropylene. If the splittings persisted in bands of one present in a large amount of the other, the splittings could certainly be assigned to intrachain coupling. Otherwise, interchain coupling would be indicated.

Acknowledgment.—The author wishes to thank Professor Giulio Natta for illuminating discussions of the crystal structure of polypropylene. He also wishes to extend his thanks to Mr. Norman B. Cothup for discussions of tertiary methyl group frequencies.

THE ACTION OF HYDROGEN ATOMS ON THE FERRO-FERRICYANIDE SYSTEM IN AQUEOUS SOLUTIONS

BY GIDEON CZAPSKI AND GABRIEL STEIN

Department of Physical Chemistry, The Hebrew University of Jerusalem, Israel

Received August 6, 1959

The action of H atoms—generated in an electrodeless HF discharge—on the ferro-ferricyanide system in aqueous solution was investigated. In the *p*H range 1–13 ferricyanide is reduced at a rate independent of *p*H or added ferrocyanide. The final ratio of ferro/ferricyanide is of the order of 10^3 at $[K_4Fe(CN)_6] = 0.1$ *M*. These results are satisfactorily explained if the reduction of ferricyanide by H atoms is a relatively fast reaction with a specific velocity constant of the order of 10^7 liter mole^{-1} sec.$^{-1}$.

In previous papers it was shown that hydrogen atoms produced in an electrodeless high frequency discharge and introduced into aqueous solutions are capable, in acid solution, of oxidizing ferrous ions to ferric[1,2] and iodide ions to iodine.[3] The oxidation of ferrous ions to ferric by H atoms was also observed by Davis, Gordon and Hart.[4] The re-

(1) G. Czapski and G. Stein, *Nature*, **182**, 598 (1958).
(2) G. Czapski and G. Stein, THIS JOURNAL, **63**, 850 (1959).
(3) G. Czapski, J. Jortner and G. Stein, *ibid.*, **63**, 1769 (1959).

sults were in good agreement[3] with results obtained in the action of ionizing radiations on such solutions[5,6] and were interpreted by us[3] as supporting the assumption[6,7] that H atoms oxidize through the intermediate formation of $H_2^+{}_{aq}$ which acts as the actual electron acceptor. In the radiation chemistry of the ferro-ferricyanide system however results were obtained[8,9] which could be interpreted[10] as not being in agreement with this assumption. Namely Fricke and Hart[8] found that in air-free solutions ferrocyanide was oxidized by ionizing radiations with a low G-value of $\sim$1 compared with a value of approximately 7 for solutions containing ferrous ions. Moreover this low value of $G\sim$1 remained constant, independent of pH in the range of pH 2 - 11. Tarrago, Masri and Lefort[9] confirmed these results.

We have therefore examined the action of H atoms on this system.

Experimental

The apparatus and procedure for the generation of H atoms was described previously.[1-3] In the present work we used a H_2 pressure of 27 mm. and the high frequency discharge was of 27 Mc. with an output of about 900 watt. Twenty-five ml. of solution, in triply distilled water, was used for each experiment and all chemicals were of analytical grade.

Ferricyanide was determined by measuring the optical density of the solution at 420 mμ where ϵ 1000 $\pm$ 20 was found at 25°. At the same wave length $\epsilon \sim 1$ for ferrocyanide. A Beckman Model B spectrophotometer was used. The molar extinction coefficient of ferricyanide was found to be constant in the pH range 1–13.

Experiments were carried out in 0.3 N H_2SO_4 (pH $\sim$ 1), 0.1 N NaOH (pH $\sim$ 13) and in pure aqueous solution (pH $\sim$ 7).

Results

Reduction of Ferricyanide.—Hydrogen atoms at a constant rate of 5×10^{-7} mole min.$^{-1}$ (*i.e.*, 2.4×10^{-6} mole l.$^{-1}$min.$^{-1}$) were passed through the solution at different initial concentrations of ferricyanide and at different pH values. The results are shown in Table I.

The results in Table I show that the reduction yield is indeed independent of pH in the range 1–13, and independent of initial concentration, down to concentrations of 2.6×10^{-4} M. Thus under these conditions neither the recombination of H atoms, nor the reoxidation of ferrocyanide formed appears to be able to compete for the available H atoms with the process of ferricyanide reduction.

In further experiments we investigated the effect of added ferrocyanide on the reduction. Under all conditions the reduction proceeded to over 99% ferrocyanide being present, the limit of observation. For example in 0.001 N H_2SO_4 in the presence of initially added 0.1 M $K_4Fe(CN)_6$, ferricyanide was reduced from an initial concentration of 1.3×10^{-4} M to a final concentration of 5×10^{-5} M,

(4) T. W. Davis, S. Gordon and E. J. Hart, *J. Am. Chem. Soc.*, **80**, 4487 (1958).

(5) T. Rigg, G. Stein and J. Weiss, *Proc. Roy. Soc.* (*London*), **A211**, 375 (1952).

(6) W. G. Rothschild and A. O. Allen, *Rad. Res.*, **8**, 101 (1958).

(7) J. Weiss, *Nature*, **165**, 728 (1950).

(8) H. Fricke and E. J. Hart, *J. Chem. Phys.*, **3**, 596 (1935).

(9) X. Tarrago, E. Masri and M. Lefort, *Compt. rend.*, **244**, 343 (1957).

(10) M. Lefort, *Ann. Rev. Phys. Chem.*, **9**, 143 (1958).

TABLE I

REDUCTION OF $K_3Fe(CN)_6$

Duration of expt., min.	$[K_3Fe(CN)_6]_0 \times 10^4$, M	Solvent	Approx. pH	$[K_4Fe(CN)_6] \times 10^4$, M	% reduced	Rate of reductn., μmole min.$^{-1}$ l.$^{-1}$
20	8	Water	7	4	49	20
20	8	Water	7	3.9	51	20.5
20	8	Water	7	4.4	45	18
20	8	0.3 N H_2SO_4	1	3.9	51	20.5
20	8	.3 N H_2SO_4	1	4.1	49	19.5
20	8	.3 N H_2SO_4	1	4.3	46	18.5
20	10.5	Water	7	5.6	47	24.5
20	10.1	0.3 N H_2SO_4	1	4.8	52	26.5
20	11.0	.1 N NaOH	13	6.5	41	22.5
20	100	.3 N H_2SO_4	1	95	5	25
10	2.6	.3 N H_2SO_4	1	0.4	85	22.1
10	2.6	Water	7	0.2	90	24

so that the final ratio of ferro/ferricyanide was of the order of 2×10^3.

Oxidation of Ferrocyanide.—Experiments were carried out on pure 0.1 M $K_4Fe(CN)_6$ solutions, in 0.3 N H_2SO_4. The maximum difference in optical density at 420 mμ observed would corrrespond to the oxidation of 0.3% only. Owing to the large experimental error we may only say that these experiments support the results of the previous section.

Discussion

The results obtained by us correspond to the results obtained in radiation chemistry. The low G-value obtained there corresponds[10] to $G_{Fe(CN)_6^{-4}} = G(OH) - G_H + 2G(H_2O_2)$, if all H atoms are utilized efficiently in the reduction of ferricyanide. That this is so appears from the present work too. We may now account for the difference between this system and the ferrous-ferric ion system[2] in the following manner. The fact that the presence of a very large excess of ferrocyanide has no effect on the reduction process is consistent with the view that it is not H atoms that are capable of oxidizing but the $H_2^+{}_{aq}$ ions formed from them according to

$$H + H^+{}_{aq} \longrightarrow H_2^+{}_{aq}\ k_1 \qquad (1)$$

This process has to compete with the process

$$H + Fe(CN)_6^{3-} \longrightarrow H^+{}_{aq} + Fe(CN)_6^{4-} \qquad (2)$$

It is only if reaction 1 can successfully compete with reaction 2 that an oxidizing species will be available at all. Increasing the concentration of ferrocyanide can have thus no primary effect, but may react with H_2^+, if formed.

We have previously shown[2] that reaction 1 is a relatively slow process, k_1 having a value of the order of 10^2 liter mole^{-1} sec.$^{-1}$. Thus assuming that all H_2^+ formed is utilized for oxidizing ferrocyanide our results for the ratio of $k_1[H][H^+]/k_2[H]$[ferricyanide] obtained in the previous section both for the oxidation of ferro- and for the reduction of ferricyanide, indicate that k_2 has a value of the order of 10^7 l. mole^{-1} sec.$^{-1}$. As the ferro-ferricyanide system is not stable in strongly acid solutions, one cannot attempt to obtain experimental conditions, where the formation of H_2^+ would prevail. Thus the velocity of the oxidation reaction could not be investigated.

In our previous work we found that the *p*H dependence of the reduction of ferric ions indicates that in that case it is the species $(FeOH)^{2+}$ that reacts with H atoms and the mechanism is probably one of group transfer

$$(FeOH)^{2+} + H \longrightarrow Fe^{2+} + HOH \qquad (3)$$

This would be a relatively slower process, so that in that case reaction 1 could proceed to a considerable extent. Indeed oxidation of ferrous to ferric ion was observed. Our views regarding group transfer in that case are in agreement with those of Schwarz.[11]

In the present case however the reduction would proceed through a relatively fast electron transfer step so that at the *p*H values practicable in the ferro–ferricyanide system reaction 1 is of small extent.

It may be remarked that as the reduction rate is independent of concentration, the reduction of ferricyanide shows advantages as a dosimeter in this type of work over, *e.g.* silver nitrate solutions.[12]

(11) H. A. Schwarz, *J. Am. Chem. Soc.*, **79**, 534 (1957).

(12) F. E. Littman, E. M. Carr and A. P. Brady, *Rad. Res.*, **7**, 107 (1957).

ELECTRIC MOMENTS AND ROTATIONAL CONFORMATIONS OF THE PENTAERYTHRITYL HALIDES AND RELATED COMPOUNDS[1]

BY H. BRADFORD THOMPSON AND CAROL C. SWEENEY

Contribution from the Department of Chemistry, Gustavus Adolphus College, St. Peter, Minnesota

Received August 10, 1959

The very small electric moments of pentaerythrityl chloride and bromide have been verified and explained on the basis of threefold rotational barriers, plus steric exclusion of some rotational isomers. The picture thus developed successfully predicts electric moments for 1,1,3,3-tetrachloropropane (experimental: 0.75 *D*), 1,3-dichloro-2,2-dimethylpropane (2.27 *D*) and 1,3-dichloro-2-chloromethyl-2-methylpropane (2.10 *D*). The model is also in accord with reported moments for pentaerythrityl fluoride and iodide and 1,3-dibromo-2-bromomethyl-2-methylpropane.

Among the earlier electric dipole moments determined were those of the pentaerythrityl halides (1,3-dihalo-2,2-bis-(halomethyl)-propanes), $C(CH_2X)_4$.[2] There was at the time a lively interest in these compounds, since it appeared that the bond arrangement about the central carbon might be planar rather than tetrahedral. Following resolution of this question, the zero electric moments reported for the chloride, bromide and iodide appear to have occasioned little note until Franklin[3] pointed out that these compounds should have very sizeable moments, assuming free rotation about the carbon–carbon bonds. Large moments would also be expected assuming threefold rotational barriers.

We therefore undertook to verify these moments, to examine a series of related halides and to seek an explanation of the apparent anomaly. It is our purpose here to demonstrate that these electric moments can be explained on steric grounds alone, in light of current knowledge of rotational conformations.

Results and Discussion

Pentaerythrityl Halides.—We have re-examined the electric moments of pentaerythrityl chloride and bromide in benzene solution at 25° and have studied the bromide in *p*-xylene at temperatures up to 119° (Table I). In every case, the total polarization does not exceed the molar refraction by 10%. Thus the permanent electric moments in these molecules must be small or zero as previously reported.

(1) Presented in part before the Division of Physical Chemistry at the 135th Meeting of the American Chemical Society, Boston, April, 1959.

(2) L. Ebert, R. Eisenschitz and H. v. Hartel, *Z. physik. Chem.*, **B1**, 94 (1928); I. Estermann and M. Wohlwill, *ibid.*, **B20**, 195 (1933).

(3) A. D. Franklin, *J. Am. Chem. Soc.*, **73**, 3512 (1951).

Expected electric moments assuming free rotation, calculated by Eyring's procedure,[4] are given in Table II. The discrepancy between our values and those of Franklin appears to result from the values chosen for the C–X bond moments. We have assumed throughout that any permanent moment results from replacement of hydrogen with halogen and that the best source of bond or group moments is an experimental moment for a compound containing that group. The reference data used is indicated in Table II. We have further assumed that in a halogen-substituted group the moment is along the C–X bond and that all bond angles are tetrahedral.

Calculations for symmetrical threefold rotational barriers will give the same expected moments as for free rotation.[5] Thus interactions of some sort between halomethyl groups in these molecules must strongly restrain these groups in symmetrical mutual orientations.

Expected Steric Effect.—The nature of this restriction can be seen by examination of Fig. 1, showing the neopentane structure. Each methyl group is in the staggered rotational position relative to the central carbon. Then, assuming tetrahedral bond angles, the bonds from the four external carbons are similarly oriented in space. The twelve C–H and C–X bonds may be divided into four *directional groups* of three parallel bonds each. For example, the three bonds marked A are parallel and are the only bonds in that direction.

Assuming a C–C bond distance of 1.54 Å., the carbons in any two halomethyl groups will be 2.51 Å. apart. This is then also the distance be-

(4) H. Eyring, *Phys. Rev.*, **39**, 746 (1932).

(5) E. F. Westrum, Jr., and D. H. Payne, personal communication.

TABLE I

EMPIRICAL CONSTANTS, MOLAR REFRACTIONS, MOLAR POLARIZATIONS AND ELECTRIC MOMENTS OF PENTAERYTHRITYL HALIDES AND RELATED COMPOUNDS

Compound	T, °C.	Solvent	Empirical constants[a] ϵ_1	α	v_1	β	P_2[a]	MR_D[a]	μ[a]
$C(CH_2Cl)_4$	25	Benzene	2.2736	0.072	1.1450	−0.413	48.6	44.76	0.43
$C(CH_2Br)_4$	25	Benzene	2.2740	.230	1.1448	− .759	61.4	56.35	.50
	96	*p*-Xylene	2.2285	.166	1.2650	− .850	60.4	56.35	.49
	119	*p*-Xylene	2.1830	.179	1.2920	− .869	61.8	56.35	.59
$CH_2(CHCl_2)_2$	25	Benzene	2.2740	.285	1.1449	− .460	46.9	35.44	.75
$CMe(CH_2Cl)_3$	25	Benzene	2.2740	2.70	1.1449	− .365	129.9	39.69	2.10
$CMe_2(CH_2Cl)_2$	25	Benzene	2.2744	3.83	1.1448	− .232	140.0	34.70	2.27

[a] Empirical constants and symbols are as defined by Halverstadt and Kumler.[19] α and β are wt. fraction rather than mole fraction coefficients.

TABLE II

OBSERVED AND FREE ROTATION ELECTRIC MOMENTS

Compound	Electric moments: Obsd. This paper	Obsd. Others	Calcd. This paper	Calcd. Franklin	Basis for calcn. (this paper)
$C(CH_2F)_4$		2.2[5]	3.62		C_2H_5F, 1.92[7]
$C(CH_2Cl)_4$	0.43	0[3]	3.71	2.8	n-C_3H_7Cl, 1.97[8]
$C(CH_2Br)_4$	0.50	0[3]	3.64	2.6	n-C_3H_7Br, 1.93[6]
$C(CH_2I)_4$		0[3]	3.47	2.3	n-C_3H_7I, 1.84[6]

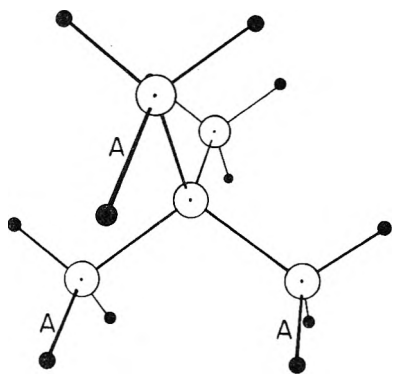

Fig. 1.—Neopentane structure: the three bonds A are parallel and constitute one of four directional groups.

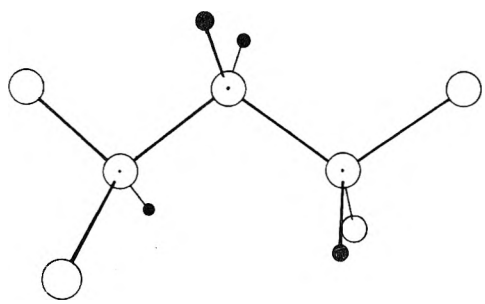

Fig. 2.—Structure of 1,1,3,3-tetrachloropropane.

tween, for example, the parallel bonds A, and between halogen nuclei terminating these bonds. As the van der Waals radius for chlorine is about 1.8 Å.,[10] this is much too close for chlorines, bromines or iodines. Thus in each directional group there should be only one carbon–halogen bond, and each C–X bond in the molecule must point in a different direction. The vector sum of the four bond moments is then zero. Accordingly, steric considerations combined with the assumption of a threefold rotational barrier can completely explain the absence of large moments for pentaerythrityl chloride, bromide and iodide.

Atomic Polarizations.—The orientation polarizations for pentaerythrityl chloride and bromide are sufficiently small that if the electronic polarization had been increased by 10% (the once popular manner of approximating the atomic polarization), a zero electric moment could have been reported. As pointed out by Smyth,[11a] it is probably better in most cases to assume that the molar refraction for sodium-D light approximates the electronic plus atomic polarizations. Molecules with large opposed dipoles, however, commonly have large atomic polarizations, since small distortions of the molecular frame lead to sizeable instantaneous electric moments. Torsional motions should make the molecules considered here quite flexible, and in comparison with known atomic polarizations[11b] a 5 cc. polarization due to torsion does not seem unreasonable. Thus the small electric moments for pentaerythrityl chloride and bromide in Tables I and II may well represent torsional oscillations. It seems unnecessary to suppose the presence of any large population of unsymmetrical rotational isomer.

1,1,3,3-Tetrachloropropane.—Steric exclusion as outlined above should also function in the 1,1,3,3-tetrahalopropanes, restricting them to the rotational isomer shown in Fig. 2. This should provide a test of our model, since these compounds might not otherwise be expected to have a low electric moment. In the conformation shown, the four C–X bonds are again so oriented that their vector sum is zero. Accordingly, we synthesized the only known compound of this series,[12] the chloride. The electric moment in benzene is included in Tables I and III. Here again, the calculated moment is very much smaller than that for free rotation.

The tabulated moment in this case must also reflect oscillatory motions about the C–C axes. Here, however, there may be an additional permanent moment due to the non-equivalence of the four C–H bonds. The C–H bond moments in the central methylene can hardly be expected to equal

(6) E. G. Cowley and J. R. Partington, *J. Chem. Soc.*, 977 (1938).
(7) C. P. Smyth and K. B. McAlpine, *J. Chem. Phys.*, **2**, 499 (1934).
(8) A. Niini, *Ann. Acad. Sci. Fennicae*, **A46**, No. 1 (1936).
(9) H. B. Thompson, THIS JOURNAL, **64**, 280 (1960).
(10) L. Pauling, "The Nature of the Chemical Bond," 2d Ed., Cornell University Press, Ithaca, N. Y., 1945, p. 189.
(11) C. P. Smyth, "Dielectric Behavior and Structure," McGraw-Hill Book Co., Inc., New York, N. Y., 1955; (a) p. 222; (b) p. 421.
(12) A. M. Whaley and H. W. Davis, *J. Am. Chem. Soc.*, **73**, 1382 (1951).

those in the dichloromethyl groups. Here, too, it seems unnecessary to assume any important contribution from rotational isomers of higher permanent moment.

Other Halogenated Neopentanes.—Steric exclusion should also function in the related di- and trihalogenated neopentanes. The electric moment of one such halide, 1,3-dibromo-2-bromomethyl-2-methylpropane, has previously been reported.[13] We have studied, in addition, the di- and trichloro compounds. In each case, as seen in Table III, the experimental moment agrees much more closely with our model than with the free rotation value.

In these cases also, polarization due to torsional oscillation will occur. However, the small values will make little difference in the presence of a sizeable polarization associated with a large permanent moment. For instance, one might expect 5 cc. $\times$ $^3/_4$ as the approximate torsional-motion polarization for 1,3-dichloro-2-chloromethyl-2-methylpropane, since this compound has three rather than four oscillating chloromethyl groups. This correction would increase the calculated moment from 1.97 to 2.01 Debye.

TABLE III

OBSERVED AND CALCULATED ELECTRIC MOMENTS

	Electric moments		
		Calcd. for:	
Compound	Obsd.	free rotation	fixed positions
$C(CH_2Cl)_4$	0.43	3.71	0
$CMe(CH_2Cl)_3$	2.10	3.28	1.97
$CMe_2(CH_2Cl)_2$	2.27	2.73	2.27
$CH_2(CHCl_2)_2$	0.75	2.75[14]	0
$C(CH_2Br)_4$	0.50	3.64	0
$CMe(CH_2Br)_3$	1.83[13]	3.22	1.93

Pentaerythrityl Fluoride.—Since the non-bonded radius for fluorine is about 1.35 Å., or only slightly over half the distance (2.51 Å.) between bonds of a directional group, non-symmetric rotational isomers might not be entirely excluded in pentaerythrityl fluoride. Westrum and Payne[5] have determined this moment, 2.2 Debye. This falls short of the free rotation value, indicating that non-symetrical isomers are important but are less stable than symmetrical isomers.

If the higher energy of the non-symmetrical isomers is due to close F–F approach, an estimate of this energy can be made. For threefold barriers, there will be 3^4 or 81 rotational isomers (not, of course, all distinguishable). These may be divided according to electric moment as indicated in Table IV. Assuming an energy E for two fluorine atoms in the same directional group, isomers of the second, third or fourth type listed in Table IV will have energies, respectively, E, $2E$ or $3E$ above the energy of isomers of group one. The observed electric moment will then be given by

$$\frac{\mu}{m^2} = \frac{384/3e^{-E/RT} + 192/3e^{-2E/RT} + 288/3e^{-3E/RT}}{9 + 48e^{-E/RT} + 12e^{-2E/RT} + 12e^{-3E/RT}}$$

where m is the $-CH_2F$ group moment. If μ = 2.2 Debye, m = 1.92 Debye, and RT = 590 cal., then E = 1175 cal.

TABLE IV

ROTATIONAL ISOMERS IN PENTAERYTHRITYL FLUORIDE

No. of parallel C–F bonds	No. of isomers	Electric moment squared
0	9	0
2	48	$8/3\ m^2$
2 and 2	12	$16/3\ m^2$
3	12	$24/3\ m^2$

It is, of course, likely that isomers having more than one set of two parallel bonds have energies somewhat different from $2E$ or $3E$. However, these make relatively little contribution to the above calculation. If terms in $2E$ and $3E$ are neglected entirely, E is found to be 1110 cal. A somewhat more serious source of error lies in the assumption (implicit above) that the wells in the potential function are the same shape for the differing isomers. This is approximately correct for a simple barrier of the form

$$V = A \cos \phi + B \cos 3\phi$$

if B is considerably greater than A. However, the potential function as two or more fluorines approach must be much more complicated. If the potential wells are indeed somewhat steeper for non-symmetrical states, E will be smaller than that calculated above. Thus one should probably say only that E is in the neighborhood of 1 kcal.

Experimental

Materials.—Pentaerythrityl chloride (m.p. 97°) was prepared as described by Mooradian and Cloke.[15] The product was twice recrystallized from 95% ethanol. Pentaerythrityl bromide (m.p. 172°) was made by the procedure of Schurink.[16] The product was recrystallized from 95% ethanol and sublimed under reduced pressure. White flakes were obtained.

1,1,3,3-Tetrachloropropane was made as described by Whaley and Davis.[12] The crude product was distilled at 100 mm., and the fraction boiling at 94–98° was twice redistilled using a column of about six theoretical plates. A sample of the final product distilled over the range 70.0–170.2° at 746 mm., d^{25}_4 1.4613 (lit. 1.4612); $n^{25}D$ 1.4813 (lit. 1.4813).

1,3-Dichloro-2-chloromethyl-2-methylpropane was prepared from the corresponding alcohol using $SOCl_2$ in pyridine, as described by Urry and Eiszner.[17] The fraction boiling at 68–69° at 10 mm. was refractionated. d^{20}_4 1.2641 (lit. 1.264), $b^{20}D$ 1.4834 (lit. 1.4837).

1,3-Dichloro-2,2-dimethylpropane was prepared in the same way from the appropriate diol. No literature reference to this compound was discovered. *Anal.* Cl, 49.9% (theor. Cl, 50.3%). Molar refraction: 34.70 cc. (theor. 35.02). Molecular wt. (micro Dumas): 142.4 (theor. 141.05). d^{25}_4 1.0839, $n^{25}D$ 1.4460, b.p. 45° at 18 mm., 144–145° at 730 mm.

Apparatus and Method.—The capacitance-measuring circuit has been described previously.[18] The present model employs voltage regulation on both plate and heater supplies. The cell is of glass and consists of two concentric cylinders, silver plated on the facing surfaces.

The electric moments were calculated according to Halverstadt and Kumler, using in each case five solutions with concentrations in the range 0.002 to 0.01 wt. fraction

(13) E. N. Gur'yanova, *Zhur. Fiz. Khim.*, **24**, 479 (1950); *C. A.*, **44**, 8181 (1950).

(14) Based on a moment of 2.06 Debye for the $-CHCl_2$ group, as observed for 1,1-dichloropropane. P. Gross, *Physik. Z.*, **32**, 587 (1931).

(15) A. Mooradian and J. B. Cloke, *J. Am. Chem. Soc.*, **39**, 943 (1945).

(16) H. B. Schurink, *Org. Syntheses*, **17**, 73 (1937).

(17) W. H. Urry and J. R. Eiszner, *J. Am. Chem. Soc.*, **74**, 5822 (1952).

(18) H. B. Thompson and M. T. Rogers, *J. Chem. Ed.*, **32**, 20 (1955).

solute.[19] Coefficients determined are included in Table I. Molar refractions for solids were calculated using the atomic refractions of Eisenlohr.[20] Values for liquids were computed from the experimental densities and refractive indices.

(19) I. F. Halverstadt and W. D. Kumler, *J. Am. Chem. Soc.*, **64**, 2988 (1942).

(20) F. Eisenlohr, *Z. physik. Chem.*, **75**, 585 (1910).

Acknowledgment.—The authors are grateful to Research Corporation for a grant supporting this work.

ADSORPTION STUDIES ON CLAY MINERALS. VII. YTTRIUM–CESIUM AND CERIUM (III)–CESIUM ON MONTMORILLONITE[1]

BY GALEN R. FRYSINGER[2] AND HENRY C. THOMAS[2]

Contribution No. 1512 from the Sterling Chemistry Laboratory, Yale University, New Haven, Conn.

Received August 12, 1959

Exchange–adsorption of cesium and the nominally tripositive ions of yttrium and cerium on Chambers, Arizona, montmorillonite (from solutions of the nitrates) has been studied at different concentrations and temperatures. The isotherms obtained with the two trivalent ions are closely similar but are very much more complicated in character than those previously found for ions of lower charge. Reversals in selectivity occur at compositions which depend on total concentration and temperature. The average charge of the sorbed trivalent ions is shown to be nearly three. Thermodynamic data for the exchange reactions are computed. The composition of the clay as regards the sorbed species is independent of the *p*H of the equilibrating solution over a wide range (3–4 *p*H units).

In earlier papers of this series we have reported studies of the exchange–adsorption behavior of the alkali and alkaline earth ions on montmorillonite and of the alkalis on attapulgite. We now extend the survey to tripositive ions. The results of all the earlier work are qualitatively similar. With cesium as the reference ion the adsorption behavior shows no particular anomalies and differs from system to system principally in the degree of selectivity for cesium at low cesium content of the solution. The adsorption isotherms (except possibly for solutions containing only trace quantities of one or the other of the elements) are all concave down over the whole composition range. With the tripositive ions this simple behavior disappears; the isotherms become much more complex in character. It is shown that the adsorbed trivalent species actually have a charge near three. The complex shape of the isotherms appears to be characteristic of the sorbing surface and little if at all dependent on the ionic species in solution, since the composition of the surface is scarcely affected by changing the *p*H of the equilibrating solutions.

Experimental

The techniques used in this work are essentially the same as those described by Gaines and Thomas,[3] *i.e.*, the "equilibrium column" method. In this procedure the adsorbent is brought to chemical equilibrium with a mixed electrolyte solution of known composition. The solutions used in equilibrating the columns carried isotopic tracers; when the activity of the effluent became identical with that of the input solution, equilibrium was presumed to have been reached. Analysis of the column was done by isotopic exchange: the radioactive tracer was displaced by non-radioactive solution of the same chemical composition, and thus disturbances in the adsorption equilibrium were avoided. The information obtained on the distribution of traced element between solution and adsorbent is independent of the nature of the molecular species present in the solution or on the adsorbent, provided only that these come to isotopic equilibrium. This last we may safely suppose to be true in our cases.

The montmorillonite used was a portion of the material prepared and described by Gaines.[3] Determinations of loss in weight on ignition were done periodically in order to bring all weighings to a common basis. The columns contained about 2 g. of clay dispersed on 3 g. of an asbestos fiber shown to have a capacity of less than 0.002 meq./g.

The cesium nitrate was stated by the supplier[4] to be 99.9 + % pure. Solutions were prepared by direct weighing of the material dried at 110°.

Carrier-free Cs^{137} from the Oak Ridge National Laboratory was obtained in HCl solution. A volume of about 2 ml. containing 10 mc. was diluted to one liter and a few milliliters of this solution used as a "spike" for the cesium nitrate solutions, the chloride thus introduced being entirely negligible.

The rare earth oxides from our sample of yttrium nitrate[5] were found by radioactivation analysis[6] to contain a minimum of 99.5 % Y_2O_3, the impurities being rare earths and probably present only as traces. Solutions were prepared by dissolving the hydrated yttrium nitrate in very dilute nitric acid (*p*H 4–5). The resulting solution was passed through a column of Dowex-1 in the OH form. By carefully controlling the flow rate it was possible to obtain a stable solution of yttrium nitrate of *p*H *ca.* 6.8 after bubbling with nitrogen. These solutions would stand for weeks without showing evidences of precipitation. It was not possible to accomplish this with solutions of the chlorides, hence our choice of the nitrate systems.

The Y^{91} isotope was used as a tracer. It was received in 1.5 *N* HCl and treated as follows: A solution containing 10 mc. of Y^{91} was washed into a polystyrene beaker and a small portion of previously prepared $Y(NO_3)_3$ solution added. The solution was made basic with NaOH and the resulting

(1) The material for this paper is taken largely from the dissertation submitted in 1956 by Galen R. Frysinger to the Faculty of the Graduate School of Yale University in partial fulfillment of the requirements for the degree of Doctor of Philosophy and, as regards cerium, work done by Galen R. Frysinger in post-doctoral capacity at Yale. The work was supported by the Nuclear Engineering Department of Brookhaven National Laboratory, to which we again offer our thanks.

(2) Venable Hall, University of North Carolina, Chapel Hill, North Carolina.

(3) G. L. Gaines and H. C. Thomas, *J. Chem. Phys.*, **23**, 2322 (1955). In this publication a factor of 2 was omitted in the definition of K_c' on page 2325 as well as in the calculations with this formula. All the values of K_c' given in Table V must be multiplied by 2 and the points in Fig. 1 shifted down by 0.693. The heading in Table VI is also in error; actually values of $-\int_0^1 \ln K_c' \mathrm{d}(q/q_0)$ are tabulated, and these must be decreased by 0.69. These changes give $\Delta F^0 = 3700$ cal. and $\Delta S^0 = +9$ e.u.; ΔH^0 and the activity coefficients remain unchanged.

(4) A. D. Mackay, Inc., New York, N. Y.,

(5) From the Lindsay Chemical Co., West Chicago, Ill.

(6) We are indebted to the Oak Ridge National Laboratory for this analysis.

precipitate collected on a small circle of Whatman No. 40 filter paper. The filtrate contained negligible activity and was discarded. The precipitate was treated with 3-ml. portions of 0.1 N HNO_3 until only a small amount of activity remained on the paper. The nitric acid solution was diluted to 500 ml.

Stock solutions of yttrium nitrate were analyzed by the slow precipitation of the hydroxide. About 0.3 mmole of Y and 0.4 g. of urea in 200 ml. of water were heated on the steam-bath. After a few hours the precipitate appeared and and the digestion was continued overnight. The precipitate was collected on a Whatman No. 42 filter, washed with faintly basic NH_4NO_3 solution, dried, ignited in platinum and weighed as Y_2O_3. Solutions containing tracer were, of course, analyzed only after the preparation was completed.

Cerium nitrate,[5] stated to have a purity of 98% was dissolved and adjusted to pH near seven as described for yttrium. These solutions were analyzed by precipitation and repeated evaporation in platinum with HF. The residue was dried at 300° and weighed as CeF_3.

The eluates of the columns were analyzed for cesium or for the trivalent metals by standard counting techniques using glass jacketed Geiger counters, all appropriate corrections being applied. A sufficient number of counts was recorded to keep the statistical uncertainty in the neighborhood of 0.5 %. When solutions containing tracers for both elements were used in some of the experiments with yttrium, the yttrium was separated by a double precipitation as the hydroxide. The efficacy of this separation was demonstrated.

The clay compositions were generally determined by the isotopic exchange $Cs^0 \rightarrow Cs^*$. These exchanges gave relatively sharp break-through curves. The hold-up volumes of the columns were determined by weight. These volumes amounted to 10–15 ml. It is impossible to state with what accuracy the pertinent, *i.e.*, final, hold-up volume was known. Fortunately, however, errors of as much as 20% in these volumes have little or no effect on the measured isotherms. The matter is of more significance in attempting to determine the true charge number of the adsorbed trivalent species. We shall return to this point.

The exchange capacity of the montmorillonite was redetermined for the nitrate system. Five isotopic cesium exchanges and a Cs → (natural ion) exchange gave 1.377 meq. per g. backbone with a maximum difference from this average of 0.014. Gaines[3] measurements, with the chlorides, gave 1.362 ± 0.009 meq./g. As would be supposed, the nature of the anion is without effect.

Results

The exchange isotherms are given in Fig. 1 and 2. These are deviation plots; the fraction of sites occupied by cesium (q/q_0) in excess of the equivalent fraction of cesium in the solution is given as the ordinate and the equivalent fraction of cesium in solution (c/c_0) as the abscissa. Positive values thus indicate selectivity for cesium. The complex nature of the results is quite evident. It might be remarked that the work with cerium was done later and entirely independently of the work with yttrium. The qualitative agreement between the two cases supplies a desirable check.

The results given in Fig. 1 and 2 were obtained with solutions initially adjusted to about pH 6.8 and without further attempt at pH control. To determine the possible effect of small variations in pH, a series of experiments in the cesium–yttrium system was carried out in which the pH was deliberately varied over a range of nearly four units (as measured with a glass electrode) by the addition of small amounts of concentrated nitric acid to the solutions. The pH of the effluent equilibrium solution differed from that of the input solution by no more than 0.15 pH unit. These results are given in Table I. The experiments were done in duplicate or triplicate, and from these data the character of the precision obtainable in this work

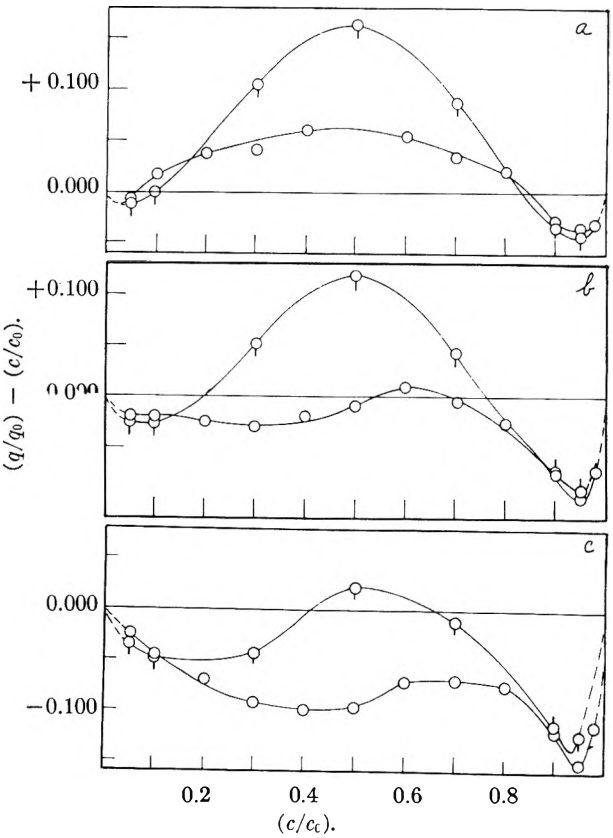

Fig. 1.—Exchange adsorption isotherms, Cs–RE, on montmorillonite at 0.02 N: ○, yttrium; ♂ or ♀ cerium, (a) 30°; (b) 50°; (c) 75°.

may be seen. The exchange capacities of the mineral were determined before and after the exposure to the acidified solutions. The values obtained (1.008 meq./g. and 0.980 meq./g., respectively) indicate the possibility of a small loss due to acid attack. No trends, however, are observable in the extent of adsorption. To within the precision of these experiments the exchange sorption of yttrium–cesium is entirely unaffected by the pH of the solution in the range 3–7. It is clear that whatever may be the variation of the yttrium species in the solution the proportion of yttrium on the sorbent is unaffected by changes in pH. We assume that cerium exhibits similar behavior.

TABLE I

EFFECT OF pH ON THE CESIUM–YTTRIUM EXCHANGE ON MONTMORILLONITE

Temp. 50°; c_0 = 0.04 N

c/c_0 (Cs)	pH (30°)	q/q_0 (Cs)
0.30	6.8	0.367, 0.378, 0.364
	4.5	.378, .386
	3.2	.374, .380
0.70	6.9	.814, .822, 0.824
	4.5	.814, .814
	3.2	.811, .805

The agreement with the data of Fig. 2b is entirely satisfactory at $c/c_0 = 0.70$; at $c/c_0 = 0.30$, on the steep part of the isotherm, the agreement is perhaps as good as could be expected.

At low total concentration the clay is selective for the trivalent ion both when this ion is present

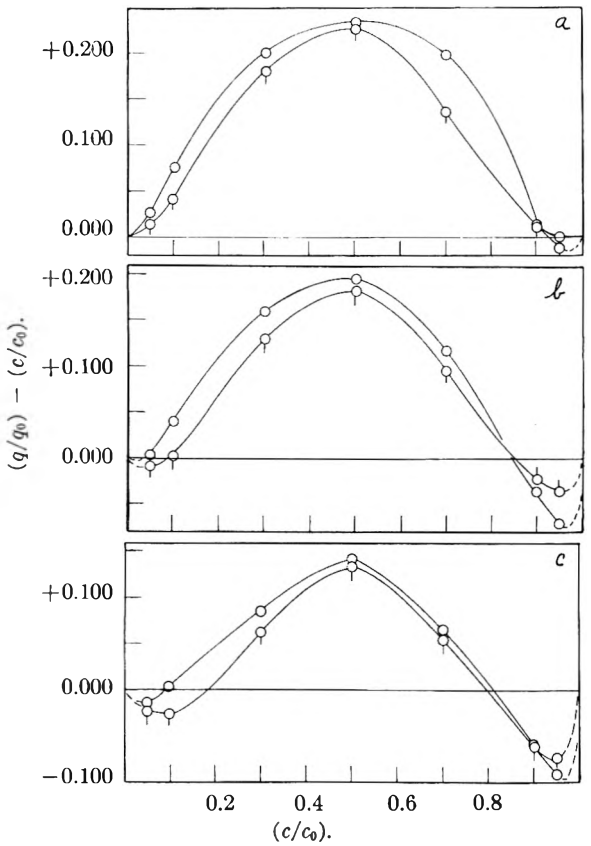

Fig. 2.—Exchange adsorption isotherms, Cs–RE, on montmorillonite at 0.04 *N*: ○, yttrium; ♂ or ♀ cerium, (a) 30°; (b) 50°; (c) 75°.

in small proportion and when it is present in large proportion. In the middle range of composition the clay selectively sorbs cesium, except at high temperatures and low concentrations; this selectivity decreases rapidly with the temperature. Certainly in the case of yttrium at low total concentration the maximum selectivity for cesium shifts toward higher cesium content with increase in temperatures. The data for cerium are not sufficiently detailed to show if this effect also occurs with this element.

All of the data presented in Fig. 1 and 2 are based on determinations of cesium *via* the displacement $Cs^0 \rightarrow Cs^*$. The reproducibility of these results as determined from independent experiments designed to be identical is about 0.006 in q/q_0 regardless of its magnitude.

In one series of experiments with yttrium both metals were traced. Knowing the hold-up volume of the column and assuming a constant capacity of the clay, we can calculate from the results with these "double-isotopic" columns the average charge number of the sorbed yttrium. Errors accumulate badly in this computation, but the results point clearly to an increase in the extent of hydrolysis of the sorbed trivalent metal with increasing temperature. A series of six experiments (at different cesium contents) gave the following charge numbers: 30°, 2.96 ± 0.16; 50°, 2.84 ± 0.15; 75°, 2.65 ± 0.14. (The maximum differences from the average are given.) There is no clear evidence of an effect due to cesium content. To check this conclusion as to the charge number a series of ten columns was run, $Y^* \rightarrow$ (natural clay), $Y^0 \rightarrow Y^*$, at 75°. The measured capacity (assuming tripositive Y, 1.108 ± 0.006 meq./g. clay as weighed) corresponds to a charge number of 2.8. This result must be considered more accurate than that from the double tracer experiments. The self-consistency of these results shows clearly that whatever may be the nature of the species in the nearly neutral yttrium solutions, the clay prefers its trivalent ions at the highest possible charge. The nature of the experiment leaves no room for doubt that true exchange adsorption is involved in the association of the trivalent metal and the clay.

In the case of the cerous ions similar experiments (with no cesium) gave charge numbers 2.82 ± 0.02, 2.74 ± 0.02, 2.81 ± 0.04 at 30, 50 and 75°, respectively, again indicating hydrolysis, without, however, an observable temperature dependence.

Thermodynamics

Using the definition and conventions adopted by Gaines and Thomas[7] we define an equilibrium ratio by

$$K_c' = \frac{M_{Cs}{}^3 N_{RE}}{M_{RE} N_{Cs}{}^3} = 3c_0 \frac{(c/c_0)^2(1 - q/q_0)}{(1 - c/c_0)(q/q_0)^3} \qquad (1)$$

in which M and N refer to molalities and fraction-of-sites for the indicated substances; in the second form all quantities refer to cesium, and molarities and molalities are identified for the dilute solutions in question.

The calculation of the thermodynamic equilibrium constant is summarized in the formula

$$\ln K = -2 + \ln \left[\frac{f_{RE}(a)}{f_{Cs}{}^3(b)}\right] + \int_0^1 \ln K_c \, dN_{Cs} - 3 \int_a^b n_{H_2O} \, d \ln a_{H_2O} \qquad (2)$$

in which

$$K_c = K_c' \frac{\gamma_{\pm}{}^6{}_{CsNO_3}}{\gamma_{\pm}{}^4{}_{RE(NO_3)_3}} \qquad (3)$$

and the f's are the activity coefficients in the mono-ion clay phases at the molalities in use. The f's are defined as unity in the mono-ion clays in equilibrium with infinitely dilute solutions. These situations are taken as the standard states of the solid phases.

We dispose of the complications in formula (2) as follows: According to (3) we need measurements of the mean activity coefficients in mixed solutions of the rare earths and cesium. These are not available. In pure cesium nitrate solutions measured activity coefficients are available[8] only down to 0.1 M, and we can find no data for pure yttrium nitrate. Therefore we use the Debye–Hückel expression for the activity coefficient, taking the a parameter for $CsNO_3$ equal to that for CsCl, namely 3.0 Å.[9]; for both rare earths we use 4.95 Å. as given by Glueckauf[10] for yttrium. The Gug-

(7) G. L. Gaines, Jr., and H. C. Thomas, *J. Chem. Phys.*, **21**, 714 (1953).

(8) R. A. Robinson and R. H. Stokes, "Electrolytic Solutions," Butterworth, London, 1955, p. 480.

(9) H. S. Harned and B. B. Owen, "The Physical Chemistry of Electrolytic Solutions," Reinhold Publ. Corp., New York, N. Y., 2nd Ed., 1950, p. 381.

(10) E. Glueckauf, *Nature*, **163**, 414 (1949).

genheim equation as modified by Glueckauf gives essentially identical results at 25°, and since the data for using this equation at other temperatures are lacking, no further attempt was made to improve upon the simple Debye–Hückel calculation. The computations of the activity coefficient ratios were made for the various compositions at the three temperatures. The contribution of this term to (2) is far from negligible; it amounts to about 1.1 in ln K.

The last term in (2) gives the contribution to the free energy due to the change in water activity in going from (a) (that is, c_0N, $Y(NO_3)_3$) to (b)(c_0N, $CsNO_3$). Since detailed data on the water compositions of these clays are not available, we write

$$3\int_a^b n_{H_2O}\, d \ln a_{H_2O} = \bar{n}_{H_2O} \ln \frac{a_{H_2O}(a)}{a_{H_2O}(b)} \qquad (4)$$

where $\bar{n}_{H_2O}$ is an average water content in moles per exchange equivalent. A number of investigators[11-15] have made studies of the montmorillonite–water system, from which we may get estimates for $\bar{n}_{H_2O}$. With increasing water activity the c-axis spacing of montmorillonite increases by integral steps, corresponding to mono-layer increments of water molecules. This "crystalline swelling" brings the spacing to about 20 Å. for 99% humidity, corresponding to four layers and a total interlayer water content of about 0.5 g./g. clay. No direct experimental data are available for the water content of the montmorillonites in our solutions. Norrish,[15] however, gives a c-axis spacing of 13.8 Å., for a cesium montmorillonite in equilibrium with water and 19.4 Å. for aluminum montmorillonite in equilibrium with 0.01 N $Al_2(SO_4)_3$. These spacings correspond to a water content of 0.3–0.4 g./g. clay. In the absence of any better data we take 0.5 g. as an upper limit for the average water content. This corresponds to $\bar{n}_{H_2O} \leq 26.6$ moles per exchange equivalent. We calculate the ratio of the activities of the solvent in the two electrolytes from the osmotic coefficient, using the Debye–Hückel approximation. The contribution of the water term is, of course, small for our dilute solutions, the largest value being 0.049 in ln K (at 0.04 N, 75°). In any case, in the approximation to which we are forced to work, the contribution will be seen to cancel.

The first non-constant term in (2) gives the contribution to the standard free energy of the process of bringing the mono-ion clays from their standard states into equilibrium with solutions of normality c_0. In the model we use, the effects, if any, of sorbed anion are entirely disregarded. This activity coefficient ratio is then determined entirely by the properties of the solvent. Neglecting the molal volume of the solvent in comparison with that of the vapor and assuming, perforce, a constant water content, we find

$$\ln f_{RE}(a) = -3\bar{n}_{H_2O} \ln a_{H_2O}(a)$$
$$\ln f_{Cs^3}(b) = -3\bar{n}_{H_2O} \ln a_{H_2O}(b) \qquad (5)$$

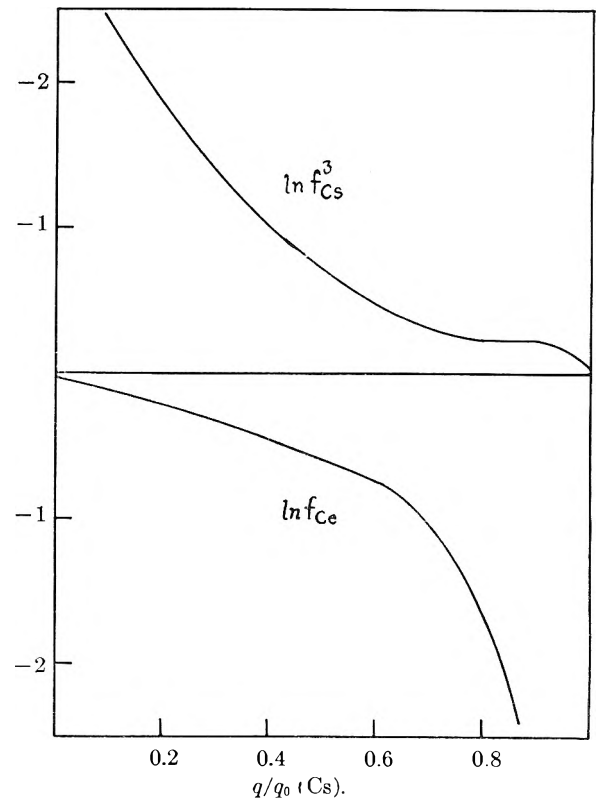

Fig. 3.—Solid phase activity coefficients, 30°, 0.02 N.

The resulting expression (approximate) for ln $[f_{RE}(a)/f_{Cs}{}^3(b)]$ cancels the contribution of (4) in ln K. These "zero-point" contributions must, however, be retained in the computation of the solid phase activity coefficients. When the small term due to the variation of the water activity is neglected, these activity coefficients are given by, *e.g.*

$$\ln f_Y(x) = \ln f_Y(a) - 2(q/q_0)_x - (q/q_0)_x \ln K_c(x) + \int_0^{(q/q_0)_x} \ln K_c'\, d(q/q_0) + \int_0^{(q/q_0)_x} \ln \left(\frac{\gamma_{Cs^3}}{\gamma_Y}\right) d(q/q_0) \qquad (6)$$

Complete calculations of the equilibrium constants and activity coefficients have been made for yttrium and for cerium.[16] The general behavior of the activity coefficients is illustrated in Fig. 3, in which as is seen, the complicated nature of the adsorption process is reflected in the relatively enormous deviations from unity of these quantities.

In Table II the values of the standard free energies are given for the different temperatures.

TABLE II

STANDARD FREE ENERGY CHANGES FOR THE REACTIONS

$$Cs_3M + (RE)^{+++}(N) = 3Cs^+(N) + (RE)M$$

	$\Delta F°$ (kcal./mole RE)			
	Yttrium		Cerium	
T (°K.)	0.02 N	0.04 N	0.02 N	0.04 N
303	4.81	4.68	5.01	4.49
323	4.65	4.52	4.93	4.38
348	4.52	4.40	4.80	4.23

Insofar as yttrium is concerned the agreement between the results for the two concentrations is satisfactory, the difference being but little outside

(11) J. Mering, *Trans. Faraday Soc.* **B42**, 205 (1946).
(12) R. C. Mackenzie, *Clay Miner. Bull.*, **1**, 115 (1950).
(13) I. Barshad, *Amer. Miner.*, **35**, 225 (1950).
(14) R. W. Mooney, A. G. Keenan and L. A. Wood, *J. Am. Chem. Soc.*, **74**, 1371 (1952).
(15) K. Norrish, *Disc. Faraday Soc.*, **18**, 120 (1954).
(16) The authors will be pleased to make these detailed results available to anyone interested.

estimates based on an error of 0.006 in q/q_0. When the computations are repeated deliberately altering the values of q/q_0 by 0.006, the value of ΔF^0 at 30° is changed by about 50 cal. The discrepancy in the case of cerium is consistently about 500 cal. We are unable to account for this apparent difference in the behavior of yttrium and cerium and must suppose that our calculated values of ΔF^0 are reliable only to 500 cal. It is possible that the thermodynamic model is inadequate in its omission of effects due to adsorption of anion. We have no data on which to base a convincing discussion of this point. In any case this approach does not appear promising: the valence numbers as determined imply only a small anion content, nor do they show a significant difference between the two elements. The high specificity of the clay surface for the tripositive ions and, by comparison, its very low specificity for the hydrogen ion make understandable the absence of effects due to changes in *p*H

Plots of $\Delta F^0/T$ *vs.* $1/T$, as calculated for the two concentrations give nearly parallel straight lines; the enthalpies are all essentially identical. In Table III average values for the two concentrations are given.

TABLE III

THERMODYNAMIC DATA FOR THE REACTIONS

$Cs_3M + (RE)^{+++} = 3Cs^+ + (RE)M$

	At 30°	
	Yttrium	Cerium
ΔF^0 kcal.	4.7	4.8
ΔH^0, kcal.	6.6	6.3
ΔS^0, cal./deg.	6.3	5.0

The results reported here indicated clearly the very complicated nature of the adsorption effects which may be expected whenever a tripositive ion must be taken into account. We would expect aluminum to behave in a manner very similar to yttrium and cerium. Thus the adsorption phenomena in any clay bed exposed to acid solutions will show effects apparently due to a large decrease in capacity because of selective adsorption of aluminum and this effect will be particularly apparent at relatively low aluminum content.

THE SOLUBILIZATION OF ISOÖCTANE BY COMPLEXES OF SERUM ALBUMIN AND SODIUM DODECYL SULFATE

BY M. BREUER[1] AND U. P. STRAUSS

School of Chemistry, Rutgers, The State University, New Brunswick, New Jersey

Received August 13, 1959

The solubilization of isoöctane by complexes of sodium dodecyl sulfate and bovine serum albumin in aqueous solution was studied at 25° by vapor pressure measurements. The vapor pressure isotherms were similar to those observed with micellar detergent in the absence of protein, but less highly curved. Significant amounts of isoöctane were solubilized below the critical micelle concentration of the detergent, indicating that the protein–detergent complex was the solubilizing agent. Over the whole range of protein and detergent concentrations investigated, the solubilizing efficiency of a bound detergent molecule was found to be a single-valued function of the number of detergent molecules bound per protein molecule. When this number was below a certain value, no solubilization occurred, suggesting that clusters of bound detergent molecules are necessary for isoöctane solubilization. Above this critical value, one molecule of isoöctane was solubilized for each additional three bound detergent molecules.

Introduction

The solubilization of oils, fats and other substances of normally low water solubility by colloidal electrolytes has been studied extensively but is still not completely understood.[2] In the case of soaps and detergents, the phenomenon has been observed only above the critical micelle concentration (c.m.c.), and it is generally believed that aggregation of the soap or detergent molecules into micelles is a necessary condition for the occurrence of solubilization.[3] In order to study this interesting phenomenon further, we decided to investigate solubilization by detergent molecules which are bound to proteins. Evidence for such solubilization can be found in the literature.[4,5] Besides throwing light on the characteristics of the solubilization by protein–detergent complexes, such a study would also illuminate the manner in which detergent molecules are bound by proteins. Furthermore, Ekwall has pointed out that an understanding of solubilization by protein–detergent complexes may provide an insight into the nature of physiological lipid transport and of the penetration of carcinogenic molecules into the living cell.[4]

The system chosen for our investigation consisted of bovine serum albumin (BSA), sodium dodecyl sulfate (SDS) and 2,2,4-trimethylpentane (isooctane). There were three reasons for this choice: (1) The binding of SDS by BSA in the absence of electrolytes has previously been studied, and the number of SDS molecules bound per molecule of BSA is known as a function of the concentration of free SDS.[6] (2) Isoöctane is not solubilized by BSA[6] or by free SDS molecules alone. (3) It has been shown that polysoaps such as poly-4-vinylpyridine

(1) Colgate Post-Doctoral Fellow, 1958–1959.

(2) For a thorough discussion of the subject and a review of the literature, see M. E. McBain and E. Hutchinson, "Solubilization," Academic Press, Inc., New York, N. Y., 1955.

(3) There is some evidence that limited aggregation and solubilization already occurs at concentrations lower than the c.m.c. [P. Ekwall and I. Danielson, *Acta Chim. Scand.*, **5**, 973 (1951); J. W. McBain and H. Huff, *J. Am. Chem. Soc.*, **70**, 3838 (1948)], but the amounts solubilized under these conditions are small compared to the amounts solubilized by micelles.

(4) P. Ekwall, *Acta Unio Contra Cancrum*, **10**, 44 (1954).

(5) I. Blei, *J. Colloid Sci.*, **14**, 358 (1959).

(6) G. Strauss and U. P. Strauss, THIS JOURNAL, **62**, 1321 (1958).

quaternized with *n*-dodecyl bromide, which should be quite similar to BSA–SDS complexes, must contain a minimum-sized region of dodecyl groups to solubilize aliphatic hydrocarbons.[7] No such minimum-sized region has been demonstrated for aromatic and polar–non-polar solubilizates.[7] Thus, the solubilization of an aliphatic hydrocarbon might serve as an indicator for the bunching of bound SDS molecules.

Experimental

Materials.—Crystallized BSA was Lot. No. T68204 obtained from Armour Laboratories. It was freed of fatty acids by Goodman's method[8] and lyophilized.

Pure crystalline SDS was provided by the Colgate–Palmolive Company.

Isoöctane (Phillips Petroleum Co., pure grade, minimum purity 99 mole per cent.) was redistilled.

Conductivity water, prepared as described previously,[6] was boiled before use to prevent bacterial and other growth. The specific conductivity never exceeded 1×10^{-6} ohm^{-1} cm.$^{-1}$.

Methods.—The BSA concentration was determined by measuring the optical density at 278 mμ in a Beckman DU spectrophotometer. A Beckman Model G *p*H meter was used for the *p*H measurements. The electrical conductance was determined as previously described.[6] In both the *p*H and conductance measurements care was taken to avoid the evaporation of solubilized isoöctane.

The solubilization experiments were carried out by measuring the absolute vapor pressure of isoöctane at 25.0° using a modification of the method of McBain and O'Connor.[9] The apparatus was constructed by H. Dragun in this Laboratory and will be described elsewhere. The chief improvement over the McBain–O'Connor apparatus was the use of mercury valves in place of stopcocks. Similar types of apparatus have been described.[10,11] All parts of the apparatus except the flask containing the solution and the small bore tube containing the hydrocarbon were thermostated about two degrees above the desired temperature to avoid condensation of the isoöctane. The amount of solubilized isoöctane was calculated by subtracting the amount in the known gas phase volume from the total amount transferred from the small bore tube of known cross section. All standard corrections, customary in vapor pressure measurements, were applied.[12] The results of Strauss and Strauss[6] were used to calculate the amount of bound SDS per BSA molecule.

Results and Discussion

Typical vapor pressure curves are shown in Fig. 1 where, for convenience, a, the activity of isoöctane[13] is represented as a function of x, the number of isoöctane molecules solubilized per bound detergent molecule.[14] For comparison results obtained with a 0.1 *M* SDS solution containing no protein are also included.[15] All the curves have similar shapes, with the pure detergent curve having somewhat greater curvature than the BSA–SDS

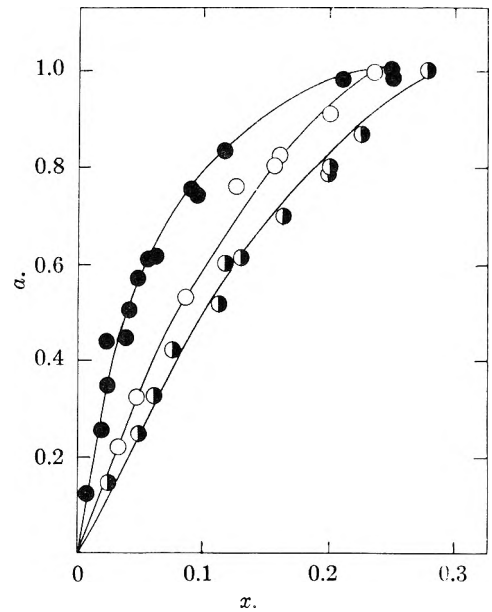

Fig. 1.—Vapor pressure of isooctane over aqueous solutions of sodium dodecyl sulfate and bovine serum albumin: ●, 0.1 M SDS; ○, 3×10^{-4} M BSA + 2.52×10^{-2} M SDS (r = 80); ◑, 3×10^{-4} M BSA + 4.55×10^{-2} M SDS (r = 140). For meaning of a and x, see text.

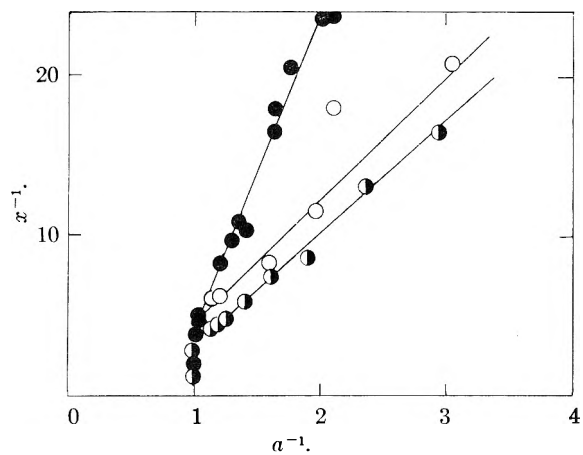

Fig. 2.—Reciprocal plots for sodium dodecyl sulfate and bovine serum albumin: ●, 0.1 M SDS; ○, 3×10^{-4} M BSA + 2.52×10^{-2} M SDS (r = 80); ◑, 3×10^{-4} M BSA + 4.55×10^{-2} M SDS (r = 140). For the meaning of a and x, see text.

curves. The value of the abscissa where the ordinate is unity corresponds to the isoöctane solubility. While the curves in Fig. 1 are difficult to extrapolate to $a = 1$, it has been shown that if the reciprocal of the ordinate is plotted against the reciprocal of the abscissa the resulting plots are linear near $a = 1$ and can easily be extrapolated to give the desired isoöctane solubility.[11] Representative plots of this type are shown in Fig. 2, and the results are presented in Table I. The first two columns contain the stoichiometric BSA and SDS molarities, denoted by (BSA) and $(SDS)_t$, respectively, the third column $(SDS)_b$, the molarity of bound SDS, and the fourth column r, the number of SDS molecules bound per protein molecule. The next column contains K_s, the solubility of solubilized isoöctane, in moles per liter, obtained by

(7) U. P. Strauss and N. L. Gershfeld, *ibid.*, **58**, 747 (1954).

(8) D. S. Goodman, *Science*, **125**, 1296 (1957).

(9) J. W. McBain and J. J. O'Connor, *J. Am. Chem. Soc.*, **58**, 2610 (1936).

(10) U. P. Strauss and E. J. Jackson, *J. Polymer Sci.*, **6**, 649 (1951).

(11) A. P. Brady and H. Huff, THIS JOURNAL, **62**, 644 (1958).

(12) G. W. Thompson in "Physical Methods of Organic Chemistry," A. Weissberger, ed., Vol. 1, Interscience Publishers, Inc., New York, N. Y., 1949, pp. 141–251.

(13) The activity is defined by the relation, $a = p/p_0$, where p_0 and p are the vapor pressures of isoöctane over the pure liquid and over the solution, respectively.

(14) The extent of detergent binding by the protein is assumed to be unaffected by the solubilized isoöctane. For support of this assumption by conductivity and *p*H measurements, see below.

(15) Since the SDS molarity (0.1) is very large compared to the c.m.c. (0.0082), almost all the SDS is in micellar form. The abscissa is taken as the number of isoöctane molecules per micellar SDS molecule for this case.

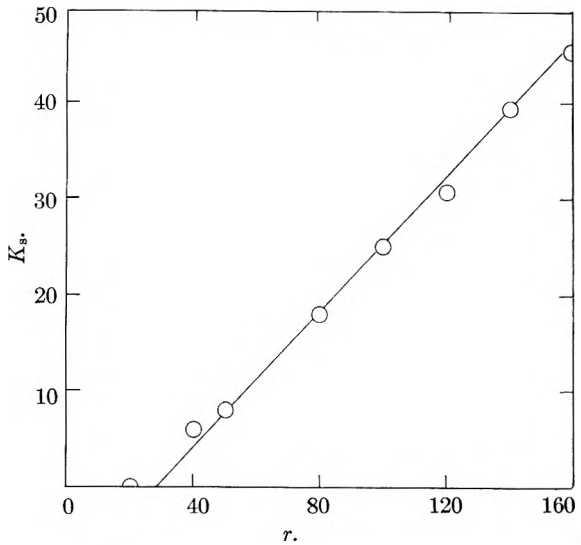

Fig. 3.—Isoöctane solubilized per mole of protein as a function of the degree of binding of sodium dodecyl sulfate.

multiplying the reciprocals of the abscissas corresponding to the breakpoints in Fig. 2 by the molarity of bound SDS.[16] The sixth column contains x_s, the maximum number of isoöctane molecules solubilized per bound (or, in the absence of BSA, micellar[14]) SDS molecule, obtained directly from Fig. 2.

TABLE I

(BSA) × 10⁴	(SDS)t × 10⁴	(SDS)b × 10⁴	r	K_s × 10⁴	x_s	k^{-1}
0.00	75	0	..	0.0	0.000	...
0.00	1000	917	..	229	.250	0.048
0.70	38	28	40	3.9	.140	.118
1.00	50	40	40	6.2	.155	.050
1.20	58	48	40	6.7	.140	.083
1.50	205	180	120	45.0	.250	.160
3.00	70	60	20	0.0	.000	...
3.00	130	120	40	18.0	.150	.202
3.00	161	150	50	24.0	.160	.110
3.00	252	240	80	56.9	.237	.128
3.00	318	300	100	75.6	.252	.104
3.00	385	360	120	91.8	.255	.100
3.00	455	420	140	118	.280	.140
3.00	558	480	160	137	.285	.160

The following conclusions can be drawn from Table I. (1) The first row illustrates that in the absence of BSA, there is no solubilization of isooctane detectable below the c.m.c. (82×10^{-4} M). (2) In the presence of BSA, solubilization is possible when the stoichiometric molarity of detergent is below the c.m.c. (rows 3–5). This result furnishes proof that the SDS bound by the protein does the solubilizing. (3) At a given value of r, the maximum amount of isoöctane solubilized per bound detergent molecule is the same, within the limits of experimental error, regardless of the stoichiometric concentrations of BSA and SDS. Since in all the experiments with BSA the concentration of free SDS was below the c.m.c., the above result lends support to the view that, below its c.m.c., the free SDS does not contribute to the solubilization. (4) When the BSA is saturated with detergent, the solubilizing efficiency of an SDS molecule is somewhat greater than when it is part of a micelle. This is apparent from a comparison of the last and the second rows of Table I. Similar results have been obtained with a polysoap.[10] (5) Below a certain value of r there is no solubilization. This behavior is illustrated graphically in Fig. 3, where the number of isoöctane molecules solubilized per BSA molecules is represented as a function of r.[17] The plot is linear and leads to the equation

$$K_s/(\mathrm{SDS})_b = (r - 24)/3.0;\ r \geq 24 \qquad (1)$$

The lower limit of 24 for r indicates that a critical concentration of detergent molecules bound by a protein molecule is necessary for isoöctane solubilization. This result means that the binding of a single SDS molecule is not sufficient for solubilization, but that a certain minimum number of SDS molecules have to be clustered together inside or on the surface of the BSA molecule. A similar finding with polysoaps[7] has already been mentioned in the Introduction to this paper. Calculations show that if the SDS molecules are assumed to be randomly distributed over the binding sites on the protein, the observed intercept is of the right order of magnitude for a minimum cluster size of 3 or 4 SDS molecules.[18] The slope of the line in Fig. 3 indicates that once r has reached the value of 24, one molecule of isoöctane is solubilized for each three additional bound SDS molecules.

Since x_s, the solubilizing efficiency of a bound SDS molecule, is equal to $K_s/r(\mathrm{SDS})_b$, it follows from equation 1 that x_s may be represented by the expression

$$x_s = (r - 24)/3.0r;\ r \geq 24 \qquad (2)$$

This function rises rapidly when r exceeds 24 and levels off toward a horizontal asymptote when r becomes large compared to 24.

While so far we have focused our attention on the solubilizing efficiency of the bound detergent at isoöctane saturation, it is also of interest to consider the number of isoöctane molecules solubilized per SDS molecule in the initial stage of solubilization. A measure of this quantity is the reciprocal of Henry's Law constant k, defined here as the initial slope of the a *vs.* x curves given in Fig. 1. The values of this quantity, obtained from the intercepts of x/a *vs.* x plots, are given in the seventh column of Table I. By comparing these values with the corresponding saturation values in the sixth column, it is seen that the solubilizing efficiency of a bound detergent molecule increases with increasing isoöctane solubilization.[19] However, this increase is much less pronounced for BSA–SDS complexes than for SDS micelles (second

(16) These values could have been obtained more directly by using the reciprocal of the isoöctane molarity as the abscissa in Fig. 2. Since r is assumed to remain constant as isoöctane is solubilized, the two methods are equivalent. The present method has been chosen because it is more appropriate for another point to be discussed later.

(17) While all our results would have fallen on the curve, for the sake of clarity, only the results corresponding to a BSA molarity of 3.00×10^{-4} are used in Fig. 3.

(18) Based on the same consideration one would not predict a linear relationship, but instead a curve with an inflection point; however, this curve may lie so close to the line as to be experimentally indistinguishable from it.

(19) The experimental uncertainty at the lower values of r is large, and not too much significance should be attached to the values at r = 40 and 50.

row) where the initial solubilizing efficiency is comparatively very low.

If the reciprocal plots in Fig. 2 are examined along the lines indicated by Brady and Huff,[11] one finds that our slopes are positive, but somewhat smaller than theirs, and that our intercepts are between 0 and +1. Our isotherms are qualitatively similar to theirs, obtained with benzene and SDS, and fit the mathematical form of their equation 8. For SDS without BSA, our values of their interaction constant k_{12} and their quantity f are 1.15 and 0.051, respectively. For the BSA curves, k_{12} ranges from 1.4 to 2.5 and f from 0.12 to 0.40. It is not surprising that our values of f, which may formally be regarded as a measure of the fraction of the moles of detergent available for solubilization, should be smaller than theirs, since isoöctane is generally solubilized to a much smaller extent than benzene. In view of the general similarity of our isotherms and theirs, we may adopt their conclusion that solubilization is a coöperative phenomenon,—as opposed to adsorption on existing sites,—also in the case where the solubilizing agent is a protein–detergent complex.

The effect of isoöctane solubilization on the electrical conductivity of solutions containing BSA (3.00×10^{-4} M) and varying amounts of detergent corresponding to values of r equal to 50, 80, 100, 130 and 160 was found to be measurable but very small. The percentage increases in the conductivities of the above solutions due to saturation with isoöctane were 1.5, 1.7, 2.8, −0.4 and −2.4, respectively. These results suggest that the solubilization of isoöctane has very little effect on r and on the local dielectric constant near the ionizable groups.[20] The same conclusions are also borne out by the observation that isoöctane solubilization had no measurable effect on the pH of the BSA–SDS solutions.

Acknowledgment.—We wish to express our thanks to the Colgate–Palmolive Company for the financial support of this research and for a postdoctoral fellowship for one of us (M. B.).

(20) While it is conceivable that these two effects are large but opposite in sign, such a hypothesis is highly unlikely. It has previously been shown that with a polyscap (where the number of ionizable groups on the macro-ion is constant) the effect of solubilization of an aliphatic hydrocarbon on the conductance is very small, indicating little, if any, change in the local dielectric constant [U. P. Strauss and S. S. Slowata, THIS JOURNAL, **31**, 411 (1957)]. It has also been shown that a change in the value of r would have a significant effect on the conductivity of the BSA–SDS complex.[6]

RADIOLYSIS OF n-PARAFFINS: MECHANISM OF FORMATION OF THE HEAVY PRODUCTS

BY C. D. WAGNER

Shell Development Company, Emeryville, California

Received August 19, 1959

n-Pentane in liquid phase was irradiated with high energy electrons and photons and the products analyzed. The C_6–C_{10} iso- and n-paraffins are formed in the early stages by free radical recombination, involving methyl, ethyl, n-propyl, n-butyl, 1-pentyl, 2-pentyl and 3-pentyl radicals. Relative steady-state concentrations of these radicals were determined from the product distribution. Absolute total free radical concentration at the dose rate used is of the order of 10^{-7} mole per liter, with mean lifetimes of slightly less than a millisecond at 25°. 1-Pentene and *cis*- and *trans*-2-pentenes are major products, formed by a reaction independent of temperature and of the presence of radical scavengers. Formation of *cis*-olefin had not previously been observed. The product pentenes react at nearly equal ratios by a mechanism as yet unknown. This reaction of the olefins is not important in the formation of heavy products below doses of the order of 3×10^7 rads, but becomes increasingly important above this level. All major products and nearly all minor ones evidently originate from simple bond-breaking processes. Isomerizations and complicated concerted processes are essentially absent. Alkyl free radical disproportionations, decompositions, and hydrogen abstraction reactions are absent.

Introduction

Radiolysis of n-alkanes by high energy electrons or photons gives hydrogen plus four groups of hydrocarbon products[1]: (1) paraffins and olefins of carbon number $<n$, where n is the carbon number of the feed, (2) olefins of carbon number n, (3) hydrocarbons of carbon number $n+1$ through $2n-1$, and (4) hydrocarbons (dimer) of carbon number $2n$. This study concerns the detailed mechanism of formation of the heavier products, C_{n+1}-C_{2n}, and represents an extension of previous studies by Dewhurst[2] and de Vries and Allen.[3]

(1) H. A. Dewhurst and E. H. Winslow, *J. Chem. Phys.*, **26**, 969 (1957), designated class (1) as C_1, Class (3) as C_i, and Class (4) as C_d.

(2) H. A. Dewhurst, THIS JOURNAL, **62**, 15 (1958); *J. Am. Chem. Soc.*, **80**, 5607 (1958).

(3) A. De Vries and A. O. Allen, THIS JOURNAL, **63**, 879 (1959).

Experimental

Feed.—n-Pentane was Phillips Research Grade, treated by passage through silica gel followed by distillation. It was 99.97% pure. The detectable impurity is thought to be neohexane, since its g.l.c. (gas–liquid chromatography) retention time agrees with that of neohexane on both silicone and Ucon-filled columns.

Photon Irradiations.—The feed was carefully degassed and distilled into a previously flamed and evacuated 8×100 mm. glass tube. The sealed-off tube with its 0.4 g. sample was irradiated beneath a slanting high intensity target.[4] The appropriate temperature was maintained by suspending the ampule in a thin-walled 10 mm. diam. titanium tube and passing nitrogen through the tube at the required temperature. Dose, determined by ceric dosimetry, was 3.8×10^7 rads. in the 30 minute irradiation time.

Hydrogen and methane were collected and measured by opening *in vacuo* and pumping off by Toepler, and the col-

(4) C. D. Wagner and V. A. Campanile, *Nucleonics*, **17** [7], 99 (1959).

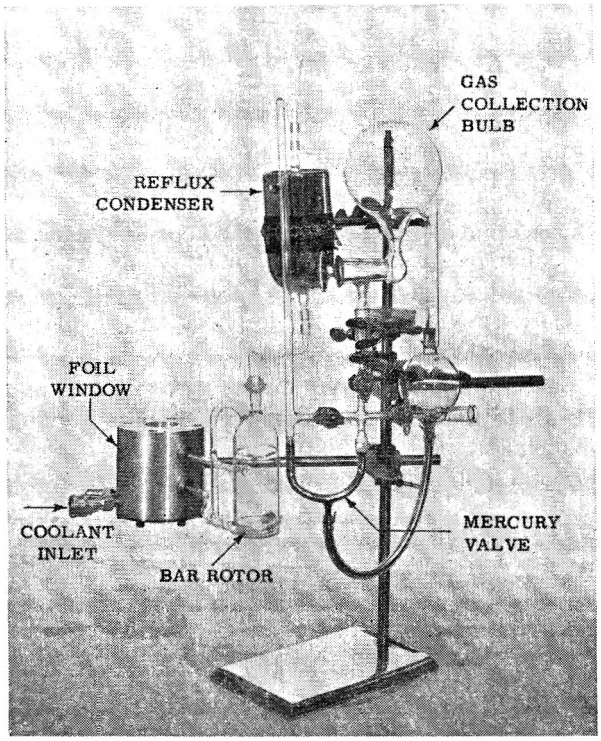

Fig. 1.—Apparatus for electron irradiations.

lected gas was analyzed by mass spectrometry. The liquid was analyzed by gas chromatography at 50° for pentenes and at 155° for C_6-C_{10}. For the low temperature analysis a $^1/_4 \times$ 40-foot tube with Ucon filling was used; this gave complete resolution of all pentenes. Retention times were checked with authentic samples on both 40-foot Ucon and silicone-filled columns. A $^1/_4 \times$ 20-foot silicone column was used for the high-temperature analysis. Relative peak areas were converted to weight per cent. by using previously determined factors varying from 1.00 for C_5 to 1.21 for C_{10}. Examination of particular products by mass spectrometry was done on samples trapped in the g.l.c. effluent by a U-tube in liquid nitrogen.

Electron Irradiation for Product Distribution.—The apparatus shown in Fig. 1 was used. The 64.2 g. of feed was distilled into the vessel *in vacuo*, and pressure was brought to 760 mm. by addition of helium. (The helium was passed through charcoal at −193° before it was introduced.) With rapid centrifugal stirring by the magnetic pump, the hydrocarbon was irradiated in the cell with a vertical beam of 3 Mev. electrons for 1284 seconds. Beam current collected in the cell was 20 microamperes. A collimating pipe was used to ensure centering of the beam at the surface of the sample. The temperature of irradiation was *ca.* 20°, maintained by circulating ice-water. Dry Ice in the reflux condenser prevented loss of feed, and gas produced was vented through the mercury valve.

The calculated dose, based on beam current, irradiation time and electron energy, was 1.05×10^8 rads. The calculation required a correction factor of 14% to allow for electron back scattering and degradation of energy in passing through the foils. This was checked within 5% by two simulated systems, one involving an aluminum calorimeter and the other a stirred solution of ceric ion (ceric ion solution may not be used directly in the aluminum cell). The results (*cf.* Table I) indicate that this calculated dose is too high, by about 80%. The explanation may lie in gas evolution in the cell being great enough to depress the liquid level so that some of the electrons lost energy in the cell wall beneath.

The liquid product of the electron irradiation was analyzed like that above, except that a $^1/_4 \times$ 20-foot Ucon column was used for analysis of C_5-C_7. In addition, a portion was hydrogenated over PtO_2, separated on a silicone gas chromatography column into its constituents, and analyzed by mass spectrometry to identify each compound. The purpose of the hydrogenation was to prevent interferences by the small amounts of olefins normally present.

TABLE I

PRODUCTS FROM PENTANE RADIOLYSIS

Form of radiation	Photons		Electrons
Dose rate, rads/hr.	10^8		*ca.* 4×10^9
Dose, rads	3.8×10^7		10.5×10^7
Temp., °C.	−115°	25°	20° (hydrogenated products)
Products	G-Values		
Hydrogen	3.8	4.1	
Isopentane	0.05	0.05	0.04
1-Pentene	0.45	0.47	
trans-2-Pentene	1.00	1.00	
cis-2-Pentene	0.30	0.37	
ΣC_6			0.14
n-Hexane			0.052
2-Methylpentane			0.047
3-Methylpentane			0.034
ΣC_7	0.34	0.47	0.33
n-Heptane			0.09
2-Methylhexane			0.16
3-Ethylpentane			0.07
ΣC_8	0.33	0.43	0.28
n-Octane			0.07
Isoöctanes			0.22
ΣC_9	0.04	0.05	0.05
n-Nonane			0.014
Isononanes			0.039
ΣC_{10}	1.00	1.45	0.80
n-Decane			0.06
Isodecanes			0.74

Electron Irradiation for Kinetics of Pentene Formation.—A radically different irradiation technique was used in this experiment. Pentane was distilled into several melting point tubes 1.0 mm. i.d. × 80 mm. long, and the tubes were sealed off under vacuum. The *ca.* 20 μl. samples were irradiated in the 3 Mev. electron beam at a point 20 cm. below the 5 mil thick aluminum window. It was previously determined that the current density for a 10 μ ampere beam at this point is 0.345 μamp./cm.^{2}. Since the energy loss for 3 Mev. electrons in a very thin hydrocarbon sample is given as 2.00 Mev./g./cm.^{2},[5] the dose rate should be 2.45×10^8 rads/hr. On this basis the tubes were removed one by one so that the doses were 10, 20, 40, 100 and 220 megarads.

The tubes were then opened and the contents injected directly into a $^1/_4'' \times 40'$ Ucon gas chromatography column. Areas of completely-resolved peaks for 1-pentene, *trans*-2-pentene and *cis*-2-pentene were measured.

Results

Analysis of the product distributions from the photon and electron irradiations are shown in Table I. Data for the light hydrocarbons are omitted because no special effort was made to ensure against their losses in handling.

Most data in the table should be accurate to well within 10%. Those for the C_6 compounds are not quite this accurate because of their small peak areas. However, all three C_6 and three C_7 products were completely resolved in the 50° analysis. At 140°, on silicone, resolution was achieved in C_8-C_{10} only between branched and straight-chain products in each carbon number. Relative *G*-values for the C_8-C_{10} products agree well with

(5) Ann T. Nelms, NBS Circ. 577, "Energy Loss and Range of Electrons and Positrons.

those of de Vries and Allen[3]; otherwise the agreement is rather poor.

Mass spectra obtained in the various carbon-number fractions (before hydrogenation) are shown in Table II. Data for the photon and electron irradiations are similar, and except for the m/q = 140 peak in the dimer, are believed to be within experimental error (the samples, and therefore the M.S. peak heights, were very small). The higher value for m/q = 140 in the electron irradiation is believed to be due to higher olefin content at the higher dose level.

TABLE II

MASS SPECTRA OF C_8–C_{10} PRODUCTS

	ΣC8		ΣC9		ΣC10	
m/q	Electrons	Photons[a]	Electrons	Photons	Electrons	Photons
142					1.00	1.00
140					0.5	0.3
128			1.00	1.00		
127					0.07	0.1
126			0.5	0.6	0.04	0.1
114	1.00	1.00				
113			0.19	2.0	1.8	
112	0.3	0.2		0.23	1.2	1.2
99	0.2	0.2	1.7	1.4	1.9	1.8
98	0.35		2.3	2.1	2.5	2.3
85	3.8	2.9	4.6	4.0	0.9	0.7
84	2.2	1.7	3.7	3.3	1.0	0.8
71	8.1	6.5	7.6	6.0		
70	8.5	6.7	10.6	8.4		

[a] From an experiment with dose = 2.6×10^7 rads. The electron irradiation was that cited, with dose = 10.5×10^7 rads.

Discussion

Isomerization.—It is clear from the low yield of isopentane that skeletal isomerization is a very minor process. Whether the isopentane is formed by an intramolecular rearrangement is not clear. It appears that the reactions that are prevalent are characterized by simple cleavage or condensation. Complex reactions involving concerted migrations of groups are apparently of negligible importance.

Unsaturation. Light Hydrocarbons.—The light hydrocarbon products ($<C_5$) consist of both saturated and unsaturated compounds, the latter amounting to roughly 20%. Yields and mechanism are to be discussed in a forthcoming publication.

Heavy Products.—Unsaturation is also present in the heavier products (C_6-C_{10}) from *n*-pentane. Unsaturation was noted at high dose levels by Keenan, Lincoln, Rogers and Burwasser[6] with *n*-butane and by Snow and Moyer[7] with C_{27} paraffin, but at dose levels comparable to this present study unsaturation was not observed by Dewhurst[2] with *n*-hexane nor by de Vries and Allen[3] with *n*-pentane.

It is believed that this olefin is a secondary product involving first-formed pentene or pentadiene. The prevalence of olefins in the high dose study in ref. 6 is consistent with this; here the difference in ratio of ion intensity at m/q = 140 to that at m/q = 142 in the photon and electron irradiations is believed to be due to difference in dose and the fraction of C_{10} product derived from intermediate olefin.

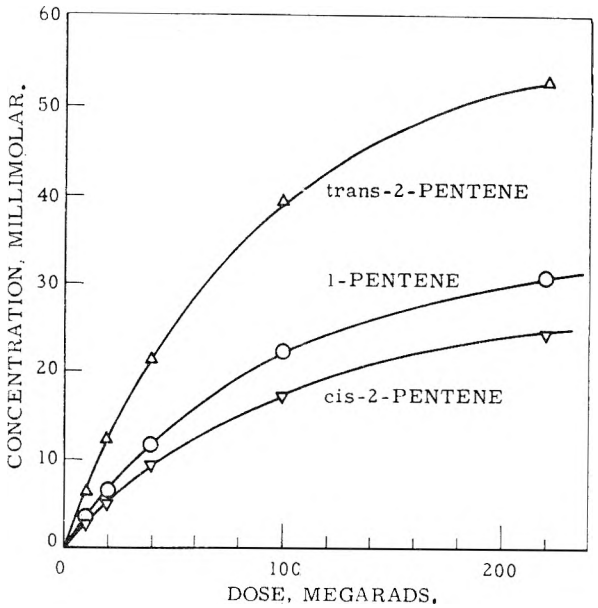

Fig. 2.—Rise in pentene concentration with dose.

Pentenes.—The three *n*-pentenes are major products. From pure *n*-pentane their rate of formation is linearly dependent on dose rate, and from independent experiments not yet reported it has been found that they react at a rate first order in their concentration. Thus, the rate of rise of concentration with respect to dose is given by

$$\frac{d[X]}{dD} = k_0 - k_1[X] \qquad (1)$$

where [X] represents olefin concentration and D represents dose.

The olefin concentration is given by the integrated form:

$$[X] = \frac{k_0}{k_1}(1 - e^{-k_1 D}) \qquad (2)$$

Olefin concentrations determined in the electron irradiations of pentane in capillary tubes are shown in Fig. 2. From the slope of the concentration–dose curve at zero dose, values for k_0 were calculated, shown in Table III. Then from the concentrations at 220 megarads the values for k_1 were calculated. The curves calculated from these constants are plotted in Fig. 2 along with the experimental points. *G*-Values for olefin production are calculated from k_0.

TABLE III

RATE CONSTANTS FOR OLEFIN FORMATION AND REACTION

	k_0, moles l.$^{-1}$ megarad^{-1}	$G_{(pentene)}$	k_1, megarad^{-1}
1-Pentene	0.00037	0.54	0.011
trans-2-Pentene	.00067	.97	.0117
cis-2-Pentene	.00028	.41	.010

Forming the double bond at the end position is less favored by a factor of 2.5, reflecting the greater energy of a methyl C–H bond over a methylene

(6) V. J. Keenan, R. M. Lincoln, R. L. Rogers and H. Burwasser, *J. Am. Chem. Soc.*, **79**, 5125 (1957).

(7) A. I. Snow and H. C. Moyer, *J. Chem. Phys.*, **27**, 1222 (1957).

C–H. *trans*-Olefin is formed faster than *cis*-olefin in a ratio 2.4. The *G*-value for total pentene formation is 1.9. This compares with Dewhurst's[2] value of 1.5 for hexene from hexane. However, his value does not include *cis*-hexenes. *cis*-Olefin products have apparently not been observed before from either low or high molecular weight hydrocarbons. This is due to the difficulty of detection by infrared spectrophotometry. This observation suggests that new consideration be given to the formation of *cis*-unsaturation in irradiation of hydrocarbon polymers; to date this possibility has not been adequately considered.

The olefin formation reaction has been shown by Dewhurst to be independent of temperature and of the presence of radical scavengers, so olefin must not be formed by any thermal reaction requiring significant activation energy or by thermal radical disproportionation. Data obtained here on temperature dependence demonstrated that all three isomers are formed at the same rate at −115° as they are at 25°. Thus, it is believed that the olefins are formed by an intramolecular decomposition from vibrationally-excited states not in thermal equilibrium. Any correspondence with thermodynamically-expected concentrations must be fortuitous.

The close correspondence in the rates of disappearance of olefin is striking, and may indicate that the rate is a general function of an isolated double bond, independent of the groups attached to it. It hardly appears that olefin reacts by thermal radical addition, for the work of Buckley and Szwarc[8] indicates the rate constants then should differ by factors up to 3–4.

If we assume heavy products can result from this reaction, it is of interest to calculate the apparent *G*-values for products derived from olefin at various dose levels. From equations 1 and 2 for olefin formation and concentration, equation 3 may be derived for the concentration of product, X_1, formed from the olefin. (We assume that first-order disappearance requires that $[X_1] = [X_0] - [X]$.)

$$[X_1] = k_0\left[D - \frac{1 - e^{-k_1 D}}{k_1}\right] \qquad (3)$$

From $k_0 = 0.00132$, representing rate of formation of total pentenes, and $k_1 = 0.011$ representing an average rate of reaction, *G*-values for formation of products from olefin are calculated to be 0.01, 0.09, 0.76 and 4.1 for doses of 10^7, 3×10^7, 10^8 and 3×10^8 rads, respectively. Thus, such reactions cannot be important in the formation of the observed heavy products at low doses, but may become significant above 3×10^7 rads. Substantially this conclusion was reached by Dewhurst[2] on the basis of linearity of heavy product formation.

Free Radicals in Heavy Product Formation.—The work of Dewhurst[2] makes it rather evident that the heavier products are formed from thermal free radicals, for he found that they are not formed in the presence of iodine, and alkyl iodides are formed instead. de Vries and Allen[3] obtained a rather good fit (except for C_7) between calculated and observed yields of branched and straight-chain C_6-C_{10} products, with an assumed radical distribution. Since the product analysis shown in Table II of this study for the electron irradiation of *n*-pentane is considerably more detailed, a similar but more complete treatment is presented.

There are several assumptions involved. It is assumed first that the olefin content is small enough to be ignored. Second, it is assumed that radicals are produced by action of the radiation in some way as yet undefined, by simple C–C and C–H splits to form 1-pentyl, 2-pentyl, 3-pentyl, *n*-butyl, *n*-propyl, ethyl and methyl radicals. Third, it is assumed that these radicals disappear by radical recombination with collision efficiencies independent of radical structure. (It is known that ΔE is very close to zero. Thus this assumption requires that diffusion and steric factors in their reaction also be independent of structure). Fourth, it is assumed that recombinations in the track before diffusion give the same product distribution as that to be expected from a homogeneous solution of free radicals. With these assumptions the rates of formation of the products of various carbon numbers are given by the following, where R_n refers to a concentration of radical of carbon number n, and M_n refers to a concentration of a hydrocarbon product of carbon number n

$$\frac{dM_{10}}{dt} = KR_5^2$$

$$\frac{dM_9}{dt} = 2kR_5R_4$$

$$\frac{dM_8}{dt} = 2kR_5R_3 + kR_4^2$$

$$\frac{dM_7}{dt} = 2kR_5R_2 + 2kR_4R_3$$

$$\frac{dM_6}{dt} = 2kR_5R_1 + 2kR_4R_2 + kR_3^2$$

In this case k is the rate constant for recombination of two like species, while the rate constant for recombination of unlike species must include the factor two in the collision frequency factor.

From the above and from product ratios there can be derived relative free radical concentrations. In this we assume that a true steady-state exists independent of dose, so that final product distribution reflects relative production rates. This assumption must be valid, for the concentrations are closely linear with dose

$$\frac{M_{10}}{M_9} = 15.3 \qquad R_4 = 0.0327R_5$$

$$\frac{M_{10}}{M_8} = 2.82 \qquad R_3 = 0.177R_5$$

$$\frac{M_{10}}{M_7} = 2.48 \qquad R_2 = 0.190R_5$$

$$\frac{M_{10}}{M_6} = 5.8 \qquad R_1 = 0.064R_5$$

The relative concentrations turn out to be reasonable. The ethyl nearly equals the propyl concentration, and both are much larger than methyl and butyl, indicating much more frequent split away from the terminal bonds, as one would expect from the energetics of the two reactions. The higher yield of methyl than *n*-butyl is not under-

(8) R. P. Buckley and M. Szwarc, *Proc. Roy. Soc.* (*London*), **A240**, 396 (1957).

stood. This effect has been observed before by iodine scavenging.[2,9,10]

The isomer distribution in the C_7 product was more reproducible and accurate than that of the C_6, and all three isomers were resolved in contrast to those in the C_8 and C_9 product. Therefore we use the C_7 distribution to determine the relative concentrations of 1-pentyl, 2-pentyl and 3-pentyl radicals

$$\frac{d(3\text{-methylhexane})}{dt} = 2kR_2R_{52}$$

$$\frac{d(3\text{-ethylpentane})}{dt} = 2kR_2R_{53}$$

$$\frac{d(n\text{-heptane})}{dt} = 2kR_2R_{51} + 2kR_4R_3$$

where in R_{5a} the position of the free valence is denoted by a. From those data, the relative concentrations of the three pentyl radicals were found to be

$$\text{1-pentyl} = 0.25R_5$$
$$\text{2-pentyl} = 0.51R_5$$
$$\text{3-pentyl} = 0.24R_5$$

It is gratifying to observe that the concentration of 2-pentyl appears to be about twice that of 3-pentyl, consistent with the relative number of hydrogen atoms at each of these types of secondary carbon atoms, and the concentration of 1-pentyl is about the same as 3-pentyl, although the hydrogen atom ratio is 3:1. This is consistent with a much lower probability of splitting the primary C–H bond. Such a relationship could not be obtained if the C_7 product were formed by a mechanism involving free radical addition to a mixture of 1-pentene and 2-pentene; also such a specific relation would hardly be expected from an ion-molecule reaction which has very high collision efficiency, and accordingly, low selectivity.

The final test is the check of the isomer distribution in all of the product groups. Since the total in each carbon number must agree (these quantities were used in calculating the relative radical concentrations), the meaningful data are limited to those in Table IV.

TABLE IV

COMPARISON OF CALCULATED AND OBSERVED PRODUCT RATIOS

Product ratio	Calcd.	Obsd.
2-Methylpentane/ΣC_6	0.38	0.3–0.4
3-Methylpentane/ΣC_6	.18	0.2–0.3
n-Hexane/ΣC_6	.44	0.4
n-Octane/ΣC_8	.25	.23
n-Nonane/ΣC_9	.25	.26
n-Decane/ΣC_{10}	.062	.073

This agreement is regarded as good, and confirms that the major mode of formation of C_6-C_{10} product is by thermal free radical recombination.

It is worth noting also that the C_7 product contains only three isomers. Thus, *n*-butyl plus *n*-propyl gives *n*-heptane, and there is no product of isopropyl and *sec*-butyl. This is consistent with the alkyl iodides formed from alkanes in the presence of iodine.[2,9] Therefore, as expected, the radicals do not isomerize under these conditions.

Free Radical Production Rate.—Weber, Forsyth and Schuler[11] used iodine as a free radical scavenger and found a G-value of 8.0 ± 0.2 for free radical production from a large variety of open chain compounds. Values obtained by Prevost-Bernas, *et al.*,[12] using diphenylpicrylhydrazyl are in essential agreement.[11] By use of unit conversion factors this may easily be translated into rate of production, if the actual dose rate is known. Thus, if the reaction is

$$\frac{1}{2}\,M \xrightarrow{k_iI} R\cdot \qquad (1)$$

k_i is 5.16×10^{-9} mole/l. rad, and k_iI, where I is in rads per hour, is $5.16 \times 10^{-9}I$ mole/l. hour or $1.43 \times 10^{-12}I$ mole/l. sec. (Density of *n*-pentane used in this conversion was 0.62 g./ml.)

In the X-ray experiment it is estimated that the effective instantaneous dose rate in the scanning photon beam is 10^8 rads/hour. This gives a value for k_iI of 1.4×10^{-4} mole/l. sec. It is more difficult to estimate the effective dose rate to that portion of the solution being irradiated at any instant in the *n*-pentane electron irradiation, but 4×10^4 rads./hr. seems a reasonable value. This gives 5.8×10^{-3} mole/l sec. for the free radical formation rate for the electron irradiation.

Free Radical Concentration.—In order to estimate the steady-state free radical concentration we assume the important reactions are

$$\frac{1}{2}\,M \xrightarrow{k_iI} R\cdot \qquad (1)$$

$$2R\cdot \xrightarrow{k_r} R_2 \qquad (2)$$

where (*1*) specifies only that radicals are produced at a rate k_iI. Then, the radical concentration is given by

$$[R] = \left(\frac{k_iI}{k_r}\right)^{1/2} \qquad (4)$$

assuming that the system can be treated as a homogeneous solution. If some of the free radicals recombine before they diffuse away from the track the calculated bulk concentration will be too high. However, iodine scavenging experiments by Schuler[13], using heavy particles, demonstrate that recombination in the track is not an important effect.

There are no direct data available on the rate constant for recombination of heavier alkyl radicals in hydrocarbon solution. Gomer and Kistiakowsky[14] found the gas phase rate constant at 25° for methyl radicals to be 3.6×10^{10} l./mole sec. Ivin and Steacie[15] obtained 2.0×10^{10} l./mole sec. for the combined rates in gas phase of disproportionation and recombination of ethyl radicals.

(9) C. E. McCauley and R. H. Schuler, *J. Am. Chem. Soc.*, **79**, 4008 (1957).

(10) L. H. Gevantman and R. R. Williams, THIS JOURNAL, **56**, 569 (1952).

(11) E. M. Weber, P. F. Forsyth and R. H. Schuler, *Rad. Research* **3** [1], 68 (1955).

(12) A. Prevost-Bernas, A. Chapiro, C. Cousin, Y. Landler and M. Magat, *Disc. Faraday So.*, **12**, 98 1952).

(13) R. H. Schuler, THIS JOURNAL, **63**, 925 (1959).

(14) R. Gomer and G. B. Kistiakowsky, *J. Chem. Phys.*, **19**, 85 (1951).

(15) K. J. Ivin and E. W. R. Steacie, *Proc. Roy. Soc.* (*London*), **A208**, 52 (1951).

Heller[16] found that the collision efficiencies for methyl-methyl, methyl-ethyl and ethyl-ethyl are identical at 100° in gas phase. Aditya and Willard[17] summarize data on iodine atom recombination in hydrocarbon solution; values range from 1.0 to 2.2 $\times$ 10^{10} l./mole sec. as a reasonable value for the rate constant. It is hardly likely that the rate constant for alkyl radicals can be larger than that for iodine atoms.

From this, and the values for free radical formation rate, the free radical steady-state concentration is calculated to be 1.0, and 6.2 $\times$ 10^{-7} for the photon and electron irradiations of *n*-pentane, respectively.

Free Radical Lifetimes.—The average free radical lifetimes are obtained by dividing the free radical concentrations by their rates of production. In terms of dose rate, this is given by

$$\tau = (k_i k_r I)^{1/2} \qquad (5)$$

for 10^8 rads/hour, the lifetime is 0.7 msec.; for 4×10^9 rads/hour, it is 0.11 msec.

The lifetimes of those radicals that recombine in the track will be very much shorter. The concentration in the bulk of the larger fraction that escape from the track will be slightly lower than that calculated by equation 4 and therefore the average lifetimes of the escaping radicals will be longer than that calculated above.

Hydrogen Abstraction Reactions.—It is of interest to determine whether radicals react by hydrogen abstraction

$$R\cdot + C_5H_{12} \xrightarrow{k_a} RH + C_5H_{11}\cdot \qquad (3)$$

before they recombine. Such a reaction would shift the steady-state distribution of free radicals by increasing pentyl radical concentration at the expense of smaller radicals. In the extreme, if the rate of abstraction were very much faster than recombination, essentially only pentyl radicals would be present and the product distribution would consist only of light hydrocarbons and decanes, with no intermediate C_6, C_7, C_8 and C_9 products. Thus, abstraction must not be dominant in this system, but it is of interest to determine whether it is significant.

Since abstraction requires 8 kcal. of activation energy per mole, while recombination requires no activation energy, a study of the effect of radiolysis temperature on product distribution should disclose the prevalence of abstraction at room temperature. Viewing the system as a homogeneous solution of free radicals in hydrocarbon, we can derive the following relation between the ratio of intermediate and dimer products and the relative free radical concentrations: If $r = ([C_6] + [C_7] + [C_8] + [C_9])/[C_{10}]$, $[R_5]$ = pentyl concentration and $[R_s] = [R_1] + [R_2] + [R_3] + [R_4]$

$$\frac{[R_5]}{[R_5] + [R_s]} = \frac{1}{\sqrt{1 + r}} \qquad (6)$$

From the data of Table I, r = 1.00 and 0.79 and $[R_5]/[R_5] + [R_s]$ = 0.71 and 0.75 for the electron and photon irradiations, respectively. In the pair of experiments designed to test temperature dependence, the ratio $([C_7] + [C_8])/[C_{10}]$ at 25 and −115° was 0.63 and 0.67, respectively. This agreement (within experimental error) demonstrates conclusively that hydrogen abstraction by free radicals is negligible under these conditions.

It is of interest to check this result against that to be expected from values for the appropriate rate constants for thermal free radicals. We can express the above result as a probability that a radical abstracts hydrogen before recombining. That is, using k_a from reaction *3* and k_r for the recombination reaction *2*

$$P_a = \frac{k_a[M]}{k_r[R] + k_a[M]}$$

and this equals zero in our system. In this equation [M] for pentane is 8.7, and the quantity $k_r[R]$ derived from equation 4 (for the free radical concentration) is equal to $(k_r k_i I)^{1/2}$. Values for k_r and k_i are given above, and $(k_r k_i I)^{1/2}$ = 0.146 $I^{1/2}$ sec.$^{-1}$.

There are no direct data on k_a for radicals other than methyl, and some data treatment is required. Trotman-Dickenson, Birchard and Steacie[18] found the rate constant for the hydrogen abstraction reaction of methyl radicals on *n*-pentane at 25° to be 121 l./mole sec. Smid and Szwarc[19] conducted competitive rate experiments in isooctane solution with free radicals and concluded that the rate constant for abstraction by ethyl and propyl radicals from paraffins is about one-tenth that for methyl. If we assume the absolute gas phase value is the same in liquid phase we may adopt 12 l./mole sec. as a reasonable value for k_a for the radicals we are concerned with. Values of P_a so calculated when plotted against log I give a sigmoidal curve, with P_a = 0.9 at 6 $\times$ 10^3 rads hr., 0.5 at 5 $\times$ 10^5 rads hr., and 0.1 at 4 $\times$ 10^7 rads hr. It is evident from this that no significant abstraction is expected at a dose rate of $>10^8$ rads per hour.

It is then of interest to inquire whether there is evidence for the validity of the sigmoidal curve from experiments at lower dose rate. Dewhurst and Winslow[1] obtained data on the ratio of "intermediate" to "dimer" in *n*-hexane at a photon dose rate of 2 $\times$ 10^5 rads per hour and an electron dose rate estimated at 8 $\times$ 10^8 rads per hour. Later Dewhurst[2] presented similar data for another electron irradiation at 8 $\times$ 10^8 rads per hour. Values of $[R_6]/([R_8] + [R_6])$ calculated from their data were 0.88, 0.81 and 0.75, respectively. It is gratifying to observe that the ratio is considerably shifted at the very low dose rate and is in the direction to indicate that hydrogen abstraction becomes significant at lower dose rates.[20] Further evidence for this has been obtained by Schuler and Muccini[21] from the radiolysis of cyclopentane-cyclohexane mixtures at various dose rates.

(16) C. A. Heller, *J. Chem. Phys.*, **28**, 1255 (1958).

(17) S. Aditya and J. E. Willard, *J. Am. Chem. Soc.*, **79**, 2680 (1957).

(18) A. F. Trotman-Dickenson, J. R. Birchard and E. W. R. Steacie, *J. Chem. Phys.*, **19**, 163 (1951).

(19) J. Smid and M. Szwarc, *J. Am. Chem. Soc.*, **78**, 3322 (1956).

(20) Since this paper was written R. A. Back and N. Miller (*Trans. Faraday Soc.*, **55**, 911 (1959)), reported on gas phase radiolysis of *n*-pentane and other hydrocarbons. They attribute some of the products under their experimental conditions to hydrogen abstraction reactions and addition of free radicals to olefins.

Role of the Hydrogen Atom.—Since pentyl radicals comprise about 70% of the alkyl present in the steady state, and since they do not arise by hydrogen abstraction, they must either be formed by a direct decomposition

$$M \longrightarrow R_s^{\cdot} + H \qquad (4)$$

or by some bimolecular process such as

$$M^+ \text{ or } M^* + M \longrightarrow 2R\cdot + H_2 \qquad (5)$$

Evidence for production of hydrogen atoms by reaction *4* has been obtained by iodine scavenging methods; evidence by Dewhurst[2] was indirect, while that by Meshitsuka and Burton[22] involved direct isolation of hydrogen iodide. One or both of processes *4* and *5* are more probable than the process

$$M \longrightarrow 2R_s^{\cdot} \qquad (6)$$

We might examine the rate constants for thermal hydrogen atoms to see what they are likely to do if they are formed by reaction *4*. We may consider three reactions at zero time (in absence of olefin product)

$$H\cdot + M \xrightarrow{k_{ha}} R\cdot + H_2 \qquad (7)$$

$$H\cdot + R\cdot \xrightarrow{k_{hr}} RH \qquad (8)$$

$$H\cdot + H\cdot \longrightarrow H_2 \qquad (9)$$

Since hydrogen atoms are very reactive, their concentration must be very low, and reaction *9* is excluded. (This can easily be proved from the rate constants below). The rate constant for reaction *8*, k_{hr}, may be taken to be 3×10^9 l./mole sec., derived from the $CH_3 + CH_3$ rate constant, diminished to compensate for the lower collision frequency with the small hydrogen atoms. The rate constant for reaction 7 can be derived from the work of Schiff and Steacie,[23] who found the collision yield in gas phase at 25° to be 7×10^{-8}. The collision frequency Z at this temperature should be about 1.5×10^{11} l./mole sec., giving a rate constant of about 10,000 l./mole sec., about 80 times the constant for abstraction by methyl radicals. The probability that the hydrogen atom would react by hydrogen abstraction before addition to R· is then approximately

$$\frac{k_{ha}[M]}{k_{ha}[M] + k_{hr}[R]} = 0.98$$

Thus, if hydrogen atoms are formed by reaction *4*, they react by hydrogen abstraction to form H_2 and pentyl. It is apparent that the over-all processes to form pentyl radicals are 2.3 times as probable as carbon–carbon scission, reaction *6*.

Disproportionation and Decomposition of Radicals.—Thus far only recombination and hydrogen abstraction reaction of free radicals have been considered. Decomposition of a free radical to a smaller radical and olefin is endothermic by over 20 kcal., and at ordinary temperatures is not important. Disproportionation, however, is important in gas phase. For example, Back[24] found, on the basis of kinetic analysis of mercury-photosensitized decomposition of gaseous *n*-pentane at 25°, that the ratio of the rate constants for disproportionation and recombination, k_d/k_r, for pentyl radicals is 0.7. Kraus and Calvert[25] found this ratio at 100° to be 4.6, 0.42 and 2.3 for *t*-butyl, isobutyl, and *sec*-butyl respectively, and concluded that the ratio is roughly proportional to the number of hydrogens on α-carbon atoms. Thus straight chain *n*-alkyl and *sec*-alkyl radicals should have ratios of about 0.9 and 1.8, respectively. Activation energies for disproportionation are very close to zero, like recombination, so that these ratios should not change appreciably as the temperature is lowered. Thus disproportionation should be important in radiolysis, at least in the gas phase.

However, as pointed out above, Dewhurst[2] found the rate of hexene production from hexane to be unaffected in the presence of radical scavengers. Thus, it is difficult to see how a significant fraction of it can be formed by radical disproportionation of *sec*- or *n*-alkyl radicals. Phibbs and Darwent[26] photolyzed *n*-decane in liquid phase in the presence of mercury at 0 −134° and found only eicosanes plus hydrogen. Thus it appears that disproportionation actually does not contribute in liquid phase, but is important in gas phase. It seems reasonable that disproportionation is a consequence of the energy released on recombination, in which the radicals rebound and separate with transfer of a hydrogen atom; in liquid phase collisional deactivation must reduce the probability of disproportionation essentially to zero.

Ion–molecule Reactions.—While the origin of much of the observed product can be explained in terms of conventional free radical mechanisms, the product of bulk 1-hexene radiolysis could not.[27] There the predominance of straight chain and 5-methylundecane skeletons with one double bond instead of diolefin with C_2 and C_3 branches was explained by a mechanism involving an ion-molecule condensation. The reaction may be favored by the significant electron affinity of the olefin, which by momentarily trapping the ejected electron can prolong the life of the ion. With saturated paraffins, on the other hand, such stabilization is lacking, and there is no direct evidence for such a reaction.

One ion–molecule reaction that has been postulated frequently is the hydrogen abstraction reaction

$$C_5H_{12}^+ + C_5H_{12} \longrightarrow C_5H_{13}^+ + C_5H_{11} \qquad (10)$$

analogous to the known reaction with methane ion and methane. The product ion could decompose on neutralization by

$$C_5H_{13}^+ + \epsilon^- \longrightarrow C_5H_{11} + H_2 \qquad (11)$$

This could be the bimolecular reaction mentioned in outline as reaction *5*.

(21) R. H. Schuler and G. A. Muccini, *J. Am. Chem. Soc.*, **81**, 4116 (1959).

(22) G. Meshitsuka and M. Burton, *Rad. Research*, **10** [5], 499 (1959).

(23) H. I. Schiff and E. W. R. Steacie, *Can. J. Chem.*, **29**, 1 (1951).

(24) R. A. Back, *Trans. Faraday Soc.*, **54**, 512 (1958).

(25) J. W. Kraus and J. G. Calvert, *J. Am. Chem. Soc.*, **79**, 5921 (1957).

(26) M. K. Phibbs and B. de B. Darwent, *J. Chem. Phys.*, **18**, 679 (1950).

(27) P. C. Chang, N. C. Yang and C. D. Wagner, *J. Am. Chem. Soc.*, **81**, 2060 (1959).

CRYOSCOPIC STUDIES IN THE MOLTEN BISMUTH–BISMUTH CHLORIDE SYSTEM[1]

BY S. W. MAYER, S. J. YOSIM AND L. E. TOPOL

Atomics International, A Division of North American Aviation, Inc., Canoga Park, California

Received August 19, 1959

A series of freezing point depression measurements has been made in the metal-rich and salt-rich regions of the Bi–$BiCl_3$ system. $BiCl_3$ was found to have a cryoscopic effect of 3.02 ± 0.07 when dissolved in molten bismuth. This effect can be explained by dissociation of $BiCl_3$ solute or by reaction of $BiCl_3$ with Bi to form the monochloride. In the case of the salt-rich region, the results suggest that Bi dissolves in $BiCl_3$ as Bi_2Cl_2.

Introduction

Cryoscopic measurements of metals dissolved in fused salts have been carried out on solutions of Cd,[2] Ni[3] and alkali metals[4] dissolved in their chlorides. However, no cryoscopic studies of a halide dissolved in a molten metal have hitherto been reported. Although the solubility of salts in metals is usually very low near the latter's freezing point,[5] molten bismuth metal appeared to be a suitable solvent for such a study since Eggink[6] reported that the solubility of $BiCl_3$ in Bi at the eutectic temperature was 2.0 mole %. Consequently, a series of freezing point depression measurements was made in the metal-rich region of the Bi–$BiCl_3$ system.

A cryoscopic study was also carried out in the salt-rich region of this system in an attempt to obtain information about the species existing in solutions of bismuth dissolved in $BiCl_3$. Some of these data have, in fact, been used in a recent publication[7] to support deductions concerning species formed in Bi–$BiCl_3$ solutions.

Experimental

Materials.—High purity bismuth metal, obtained from Belmont Refining and Smelting Company and reported to be 99.999% pure on the basis of spectrochemical analysis, was used throughout these studies. Before use the bismuth was melted in an atmosphere of dry helium and filtered through dry Pyrex wool to remove any bismuth oxide present. The freezing point was found in 6 replicate measurements to be 271.01 ± 0.06°, compared with the literature value of 271.3°.[8] Reagent grade bismuth trichloride was dried under a current of HCl gas and distilled under HCl and then under argon. The first and last eighths of the distillate were discarded. Analysis showed the resulting product to be anhydrous, with a chlorine to bismuth ratio of 3.00. The melting point of the salt was 233.6°.

Apparatus and Procedure.—The mixtures of bismuth and $BiCl_3$ were prepared under argon in a dry-box. They were sealed in 18-mm. Pyrex ampules which had a thin-walled thermocouple well sealed into the bottom of the tube. Temperatures were measured with a calibrated chromel-alumel thermocouple using a Rubicon B precision potentiometer. The cold junction of the thermocouple was maintained in an oil-filled tube, placed in a distilled water–ice-bath. The sample was heated in a Marshall furnace which was automatically regulated by a West Gardsman temperature controller operating through a variable transformer.

While supercooling was not a problem with the metal-rich samples, in the case of salt-rich samples supercooling occurred and became severe in the 20–30 mole% Bi concentration range. However, prior addition of dry powdered Pyrex to act as a nucleating agent for the $BiCl_3$ solvent, when accompanied by vigorous shaking, was effective in reducing supercooling. In later experiments, it was found that blowing a jet of cold air on top of the tube for a moment resulted in crystallization of a small amount of $BiCl_3$ which served as a nucleating agent.

Results and Discussion

Molten Bismuth Solvent.—Figure 1 shows the freezing point depressions of molten bismuth solutions produced by $BiCl_3$ solute. The cryoscopic number n (the number of particles formed in molten bismuth per molecule of solute) was calculated in accordance with the Raoult–van't Hoff equation

$$n = \frac{\Delta H_f \Delta T}{R T_f T N_2} \qquad (1)$$

where

ΔT is the freezing point depression
T_f and T are the freezing points of pure bismuth, 544.1°K. and the solution, respectively
N_2 is the mole fraction of solute
ΔH_f is the molar heat of fusion of bismuth at its m.p., 2.60 kcal.[8]

A least squares treatment of the freezing point depression data yielded a mean cryoscopic number of 3.02 with a standard deviation of 0.07. The eutectic composition, determined by the intersection of the least squares line with the mean eutectic temperature of 267.3 ± 0.1°, was found to be 0.54 mole %. This value for the eutectic composition is considerably lower than the value of 2.0 mole % found by Eggink.[6] However, his method of determining this composition, namely withdrawing a sample of metal through the salt phase, could easily result in contamination of the metal phase. Sokolova's[9] phase diagram, which was determined by the cooling curve method, showed the eutectic at 0.7 mole % bismuth, more in agreement with this study than with Eggink's. However, Sokolova's data are inadequate for a cryoscopic study since only one point was obtained for the liquidus curve in the metal-rich region and the probable error of the freezing point measurement is one degree or more.

The observed cryoscopic number of 3.0 indicates that $BiCl_3$ does not dissolve in a molecular form,

(1) This work was supported by the Atomic Energy Commission. This paper has been presented in part before the Division of Physical Chemistry at the National Meeting of the A.C.S. in September, 1957.

(2) K. Grjotheim, F. Grönvold and J. Krogh-Moe, *J. Am. Chem. Soc.*, **77**, 5824 (1955).

(3) J. W. Johnson, D. Cubicciotti and C. Kelley, THIS JOURNAL, **62**, 1107 (1958).

(4) M. A. Bredig, J. W. Johnson and W. T. Smith, Jr., *J. Am. Chem. Soc.*, **77**, 307 (1955).

(5) S. J. Yosim and E. B. Luchsinger, *Ann. N. Y. Acad. Sci.*, in press.

(6) B. G. Eggink, *Z. physik. Chem.*, **64**, 449 (1908).

(7) M. A. Bredig, THIS JOURNAL, **63**, 978 (1959).

(8) D. Stull and G. Sinke, "Thermodynamic Properties of the Elements," Am. Chem. Soc., Washington, D. C., 1956.

(9) M. A. Sokolova, G. G. Urazov and V. G. Kuznetsov, *Akad. Nauk, S.S.S.R., Inst. Gen. Inorg. Chem.*, **1**, 102 (1954).

since a cryoscopic number of one would then be expected. However, there are at least four apparent mechanisms which would yield a cryoscopic number of three. The first of these is one in which $BiCl_3$ dissociates into 4 particles upon dissolving and the bismuth from $BiCl_3$ becomes indistinguishable from the bismuth particles of the molten metal. When Bi^{+3} dissolves in a good conductor such as molten bismuth, the charge on Bi^{+3} would not be expected to remain localized but would distribute itself throughout the conductor, resulting in equivalent bismuth particles. The bismuth ion from the $BiCl_3$ then would not depress the freezing point of bismuth metal, and the three chlorine atoms or ions of the $BiCl_3$ solute would contribute the observed cryoscopic effect of three particles.

The second mechanism is again a dissociation of $BiCl_3$ into 4 particles with the bismuth from $BiCl_3$ distinguishable from the bismuth metal particles. The observed cryoscopic number of 3.0 could then be interpreted in terms of deviation of the bismuth solvent from Raoult's law. This mechanism is a less likely one since it appears improbable that the activity coefficient of the solvent would vary in just such a manner as to have the cryoscopic number remain a constant integer over the range studied.

A third process is one in which the $BiCl_3$ reacts with the bismuth solvent to form undissociated BiCl molecules, as shown below

$$BiCl_3 + 2Bi = 3BiCl \qquad (2)$$

The fourth mechanism is the dissociation of BiCl or $(BiCl)_x$ yielding bismuth particles indistinguishable from the bismuth metal particles just as in the first mechanism. The first and fourth mechanisms cannot be differentiated cryoscopically since the final compositions are identical.

In principle, mechanism 3 can be distinguished from 1 or 4 by the fact that there is a different concentration of bismuth solvent resulting from each process. However, due to the low solubility of $BiCl_3$ in Bi, the cryoscopic technique is not sufficiently accurate to permit a choice between them.

Molten $BiCl_3$ Solvent.—Because equation 1 is not intended for use at higher solute concentrations, the following equation was used to interpret the freezing point data

$$\ln a_{BiCl_3} = \frac{-\Delta H_f \Delta T}{RTT_f} \qquad (3)$$

where ΔH_f is the molar heat of fusion of $BiCl_3$ (5.68 kcal./mole),[10] and a_{BiCl_3} is the activity of $BiCl_3$. The assumptions included in equation 3 are that the heat of fusion is constant over the temperature range studied and that there is no solid solution. Also, the use of equation 3 in interpreting the freezing point results involves the assumption that the activity coefficient of the solvent is unity and that accordingly the heat of mixing is negligible. There is no direct information on the heat of mixing at these temperatures; however at 328° the partial molal heat of solution of $BiCl_3$ in a solution containing bismuth is nearly zero at concentrations up to approximately 20 mole % bismuth.[11]

(10) L. E. Topol, S. W. Mayer and L. D. Ransom, THIS JOURNAL, in press.

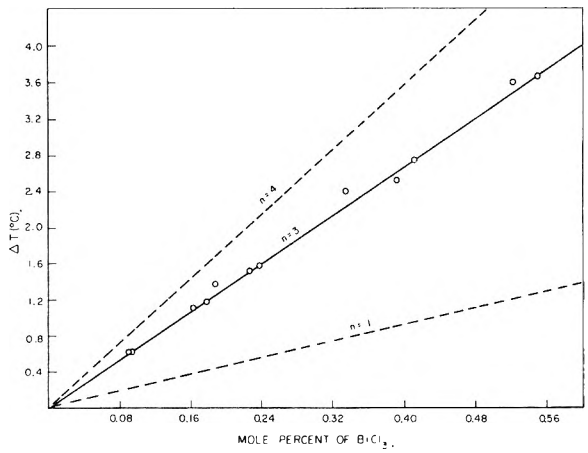

Fig. 1.—Freezing point depression of Bi by $BiCl_3$.

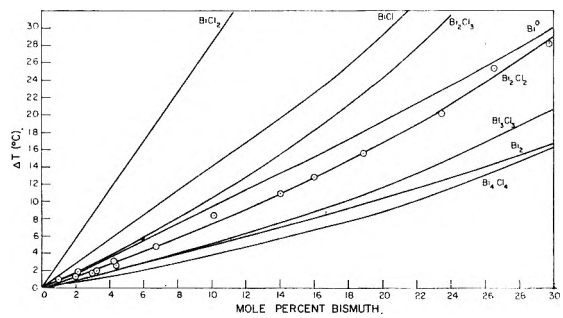

Fig. 2.—Comparison of experimental freezing point depressions of $BiCl_3$ with those calculated for various bismuth species.

In order to determine the most probable bismuth species, based on this cryoscopy work, the mole fraction of $BiCl_3$ in these solutions was calculated on the basis of each of the mechanisms

$$Bi \longrightarrow Bi \text{ atoms} \qquad (4)$$
$$2Bi \longrightarrow Bi_2 \qquad (5)$$
$$2Bi + BiCl_3 \longrightarrow 3BiCl \qquad (6)$$
$$4Bi + 2BiCl_3 \longrightarrow 3Bi_2Cl_2 \qquad (7)$$
$$2Bi + BiCl_3 \longrightarrow Bi_3Cl_3 \qquad (8)$$
$$8Bi + 4BiCl_3 \longrightarrow 3Bi_4Cl_4 \qquad (9)$$
$$Bi + 2BiCl_3 \longrightarrow 3BiCl_2 \qquad (10)$$
$$Bi + BiCl_3 \longrightarrow Bi_2Cl_3 \qquad (11)$$

The resulting freezing point curves are shown in Fig. 2. Based on these results, it can be seen that reaction 7, or formation of Bi_2Cl_2, appears to be the most likely mechanism for solution, in agreement with Bredig's[7] conclusions. The agreement between the experimental freezing point depressions and those calculated on the basis of formation of Bi_2Cl_2 is good for the entire $BiCl_3$ liquidus range. It can also be seen that formation of Bi_2Cl_2 is a much more likely mechanism than the formation of Bi_4Cl_4 suggested by Corbett[12] who based his interpretation on vapor pressure results[11] of Bi–$BiCl_3$ solutions. The conclusion that Bi_2Cl_2 is the species formed when bismuth metal is added to $BiCl_3$ is consistent with, but not proven by, the existence of $(BiCl)_x$ in the solid and with the fact that these solutions are diamagnetic.[13]

(11) D. Cubicciotti, F. J. Keneshea, Jr., and C. M. Kelley, *ibid.*, **62**, 463 (1958).

(12) J. D. Corbett, *ibid.*, **62**, 1149 (1958).

(13) J. D. Corbett, S. Winbush and F. C. Albers, *J. Am. Chem. Soc.*, **79**, 3020 (1957).

It is interesting to note that if the literature value for the heat of fusion of $BiCl_3$ (2.6 kcal./mole)[14] is used, the data reported here would be most consistent with mechanisms 7 and 8, *i.e.*, formation of Bi_2 and Bi_3Cl_3. However, the value of 2.6 kcal. for ΔH_f of $BiCl_3$ is based on phase diagram results while the value of 5.68 kcal.[10] used in this work is the result of a calorimetric determination and is, therefore, regarded as more accurate.

If one assumes mechanism 4 (solution as Bi atoms) to be correct and calculates the activity coefficient of $BiCl_3$, it is found that γ_{BiCl_3} is between 1.00 and 1.03 over the entire range (up to 30 mole %). Since bismuth and $BiCl_3$ are so different, one would expect a much greater deviation of the solvent from ideality at least in the more concentrated solutions. Therefore, it is not likely that the formation of Bi atoms is the sole mechanism.

A possibility which must not be overlooked is that a combination of 2 or more species could yield the observed freezing point depressions. Evidence supporting the latter, especially at higher temperatures, is the presence of retrograde solubility in the region of the miscibility gap of the Bi–$BiCl_3$ system[15]; *i.e.*, the solubility of molten bismuth in liquid $BiCl_3$ decreases as the temperature increases from 320 to 550° and then increases with increasing temperature. This retrograde solubility might be the resultant of 2 processes. However, near the melting point of $BiCl_3$, it is not known whether these two processes are taking place or whether there is only a single process.

Thus, while the results of these experiments indicate that Bi_2Cl_2 is the most likely species, the possibility that a combination of other species can explain these results cannot be neglected. Other experiments of a non-thermodynamic nature would be desirable before any firm conclusion can be drawn as to the species existing in these solutions.

(14) K. K. Kelley, U. S. Bureau of Mines, Bulletin 393, Washington, D. C., 1936.

(15) S. J. Yosim, A. J. Darnell, W. G. Gehman and S. W. Mayer, THIS JOURNAL, **63**, 230 (1959).

CALCIUM POLYPHOSPHATE—RATE AND MECHANISM OF ITS HYDROLYTIC DEGRADATION

BY E. O. HUFFMAN AND J. D. FLEMING

Division of Chemical Development, Tennessee Valley Authority, Wilson Dam, Alabama

Received August 24, 1959

The rate and mechanism of the hydrolytic degradation of vitreous calcium polyphosphate were studied experimentally. Despite limitations imposed by the presence of calcium, paper chromatography proved useful for the analytical separations. Degradation of the highly condensed calcium polymer follows, at a higher rate, essentially the mechanism reported for the vitreous sodium phosphate known as Graham's salt. The energy of activation over the temperature range 25 to 100° ranges from 15 to 22 kcal. Rates of degradation at 25, 50 and 100° are expressed as functions of *p*H. The presence of soil accelerates the degradation. Results of the study help to explain the behavior of calcium polyphosphate as a fertilizer and serve as background information in the development of hydrolytic processes for its conversion to other fertilizer materials.

Vitreous calcium polyphosphate is of interest as a fertilizer and as an intermediate in the manufacture of other fertilizers. In either use, the rate and mechanism of its hydrolytic degradation are of interest. A study[1] of the gross rate of its conversion to orthophosphate antedated the development of methods for following the intermediate steps in the conversion.

In a re-examination of the degradation process, advantage was taken of methods recently developed for determining the average size of polyphosphate molecules[2] and the distribution of different phosphate species.[3-6] Certain characteristics of calcium polyphosphate necessitated modification of the methods, however, and limited the precision of the results. The average size of the polyphosphate molecules dissolved by use of an ion-exchange resin was determined by *p*H titration, and the rate and mechanism of the hydrolytic degradation of dissolved calcium polyphosphate were studied by use of paper chromatography.

(1) W. H. MacIntire, L. J. Hardin and F. D. Oldham, *Ind. Eng. Chem.*, **29**, 224 (1937).

(2) O. Samuelson, *Svensk Kem. Tid.*, **56**, 343 (1944); **61**, 76 (1949).

(3) J. P. Ebel and Y. Volmar, *Compt. rend.*, **233**, 415 (1951).

(4) J. P. Ebel, *Bull. soc. chim. France*, 991 (1953).

(5) J. Crowther, *Anal. Chem.*, **26**, 1383 (1954).

(6) E. Karl-Kroupa, *ibid.*, **28**, 1091 (1956).

Methods

Preparation of Phosphate Glass.—Calcium polyphosphate glass was prepared from monocalcium phosphate monohydrate essentially as described by Hill, Faust and Reynolds.[7] Instead of multiple fusion of the products obtained from the dehydration step, however, small batches were fused once. Refractive index measurements indicated that the glasses were homogeneous. The crushed β-calcium metaphosphate in 10-g. batches was heated rapidly to 1020°, held for 20 minutes, then quenched. The mole ratio CaO: P_2O_5 of the glass was 1.0 ± 0.01—the summation CaO + P_2O_5, 99.98%.

Chain-length Titration.—The solubility of calcium polyphosphate glass in water proved too low to yield solutions suitable for determination of average chain length by *p*H titration. Suitable solutions were prepared at ice-bath temperature by stirring for several hours 1-g. portions of −325-mesh glass in 100 ml. of distilled water containing 20 g. of Amberlite IR-120 resin in its sodium form. The resultant solutions contained from 1.5 to 3.3 g. P_2O_5/l. as sodium polyphosphate.

The solutions prepared by cation exchange were analyzed by the Samuelson titration method.[2] The *p*H meter here, and throughout the study, was a Beckman Model H2.

Paper Chromatography.—The method for chromatographic analysis of the calcium phosphate solutions was similar to methods used with sodium phosphate solutions.[3,6] Problems of streaking and degradation on the paper were more pronounced with the calcium phosphates, however, and minor, though important, modifications of the methods were

(7) W. L. Hill, G. T. Faust and D. S. Reynolds, *Am. J. Sci.*, **242**, 457 (1944).

necessary. Preliminary tests showed that exchange between the calcium polyphosphate solution and the sodium resin yielded a sodium solution whose chromatographic behavior was like that reported[3,4,6] for sodium phosphate solutions. Furthermore, when calcium chloride was added to a dilute solution of known sodium poly- and metaphosphates, neither the appearance nor disappearance of any species was detected chromatographically. The presence or absence of non-moving cyclic species, as reported by Thilo,[8] was not determined; all the phosphate that did not move sufficiently for identification on the chromatograms was designated simply as "non-moving" phosphate.

Ring compounds identified in the degradation products by conventional two-dimensional chromatography[4,8,9] were tri- and tetrametaphosphates, predominantly trimetaphosphate. The other degradation species that were identified were tetra- and tripolyphosphates, pyrophosphate and orthophosphate. Two-dimensional chromatography could not be used for quantitative analysis of the solutions in the rate studies, because the acidic solution caused virtually complete degradation of the non-moving phosphates after the sample had been in the basic solution. Two-dimensional chromatography thus was suitable only for qualitative identification of the readily moving degradation species.

The chromatographic method finally used in the rate study was essentially the band placement, one-dimensional, ascending method[6] with Ebel's[4] acidic solvent. Separations were made at 25 ± 1°. The analytical sample, 50 to 100γ of phosphorus, required as much as 500 μl. of solution. The solution was added to the paper in 50-μl. portions, and the paper was dried at room temperature between additions. The elution time was 4 hours. The sections of paper containing the separates were digested in a nitric–perchloric acid mixture, and the phosphorus was determined by a modification of Hague and Bright[10] method.

The rates of change of concentration of the several species were represented adequately by smooth curves, although a few analytical results were scattered rather widely. The quantities reported for a species are correct within a few per cent. Recovery of the phosphorus placed on the paper usually was 95% or more.

Rate Measurements.—Most of the solutions for the rate studies were prepared by stirring vigorously 20 g. of −35 +60-mesh glass in 50 ml. of water in an ice-bath for 24 hours. The solutions contained approximately 1 g. of polymer per liter; their *p*H was about 4.0. They usually contained no significant amount of degradation products. By the time *p*H adjustments were made and a rate experiment was started, however, appreciable degradation had occurred.

Solutions containing 10 to 12 g. of polymer per liter were obtained by stirring 20 g. of −200-mesh glass in 50 ml. of water for 24 hours at 25°. From 10 to 20% of the phosphate in these solutions was present as degradation products when the rate measurements were begun.

Solutions for rate measurements were adjusted to the required *p*H with 0.5 *N* HCl or saturated limewater. Samples for 25 and 50° hydrolyses were placed in stoppered 100-ml. test-tubes; for the 100° hydrolyses, the test-tubes were fitted with 6-mm. glass reflux tubes to prevent loss of water. The 25° water-bath held the temperature constant within ±0.01°—the 50° oil-bath, within ±0.1°. The temperature was held between 99.6 and 100° by a rapidly boiling water-bath for the studies at 100°.

During the hydrolysis at 25°, the *p*H was checked with the meter. Solutions for study at 50 and 100° were adjusted by the meter prior to heating, and the *p*H during the hydrolysis was measured with Accutint papers. Measurements with the papers were considered reliable to about 0.2 *p*H unit.

When the temperature of the solutions at *p*H 6.0 was raised above about 35°, a viscous coacervate of the calcium salt[11] was precipitated. Removal of most of this precipitate by rapid filtration introduced some uncertainty in the zero time for the hydrolysis and lowered the concentration of the salt in solution.

Samples from the 25° hydrolyzates were pipetted directly to the chromatographic paper. Those from the 50 and 100° runs were placed in small test-tubes and chilled immediately in an ice-bath.

Results and Discussion

Average Chain Length.—Values are shown in Table I for the average chain length $\bar{n}$ of the phosphate solubilized through cation exchange with the sodium resin. The near constancy of $\bar{n}$ through four successive resin treatments of the same sample shows that no species was solubilized preferentially, although dissolution was 80% complete. The solutions prepared at ice-bath temperature contained no species small enough to move on a chromatogram. With an $\bar{n}$ of 23 and no species as small as tetramer, it is evident that the solutions contained no very long chains. Further evidence of the absence of very long chains in the solubilized material was found in a measurement of $\bar{n}$ for a sample of calcium polyphosphate coacervate[11] containing 50% water; a value of 33 indicated that the larger molecules were precipitated preferentially in the viscous coacervate.

TABLE I

AVERAGE CHAIN LENGTH OF PHOSPHATE SOLUBILIZED BY CATION EXCHANGE WITH SODIUM RESIN

Exchange period	Cumulative exchange time, hr.	Cumulative fraction, %, of phosphate extracted	Av. chain length, $\bar{n}$
Exchanged at ice-bath temp.			
1	5	22.5	22
2	24	52.9	25
3	48	72.1	23
4	72	80.1	24
Exchanged at room temp.			
1	96	90	20

The one sample prepared by exchange-dissolution at room temperature ($\bar{n}$ = 20, Table I) contained degradation products observable on a paper chromatogram.

Degradation on the Paper.—The graph in Fig. 1 shows a rather rapid decrease in the proportion of non-moving phosphate, with concomitant increase in the ring (tri- and tetrameta) phosphates, during elution on the chromatographic paper. The proportions of ortho- and pyrophosphates, as well as of tripolyphosphate (not shown in Fig. 1), remained constant during the elution. Similar measurements on about 25 samples, with variation of the elution time from 2 to 5 hours, gave a basis for corrections for degradation occurring on the paper and led to the adoption of the 4-hour elution time. The correction for a 4-hour elution comprised a 10% addition to the amount of non-moving phosphate found on the paper and a corresponding subtraction from the amount found as rings.

The necessity for limiting the elution time to 4 hours perhaps was a factor in preventing the identification of individual species containing more than 4 phosphorus atoms or the isolation (by the one-dimensional technique) of tetrameta- and tetrapolyphosphates from the trimetaphosphate found predominant in the two-dimensional tests. The rate and mechanism study thus hinged on observa-

(8) E. Thilo and I. Grunze, *Z. anorg. allgem. Chem.*, **290**, 223 (1957).

(9) J. P. Ebel, *Mikrochim. Acta*, 679 (1954).

(10) J. L. Hague and H. A. Bright, *J. Research Natl. Bur. Standards*, **26**, 405 (1941).

(11) E. H. Brown, J. R. Lehr, J. P. Smith, W. E. Brown and A. W. Frazier, THIS JOURNAL, **61**, 1669 (1957).

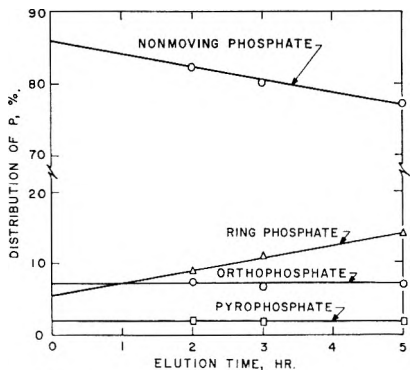

Fig. 1.—Degradation on the paper at 25°.

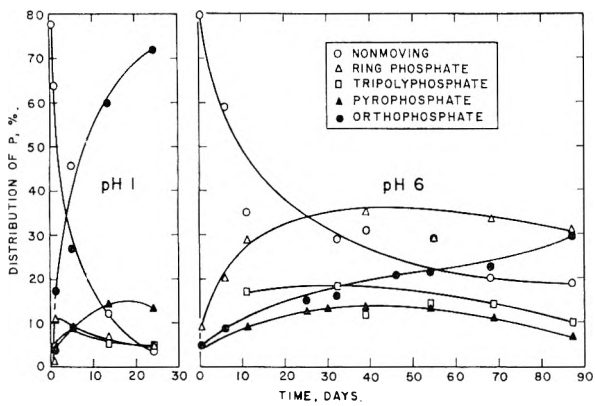

Fig. 2.—Distribution of species in the hydrolytic degradation of calcium polyphosphate at 25°.

tions of the disappearance of non-moving phosphate with formation of degradation products comprising rings, tripoly-, pyro- and orthophosphates.

A recent investigation[12] by use of light scattering and of dilute-solvent chromatography, indicated that the phosphate designated here as non-moving comprises a distribution of chain sizes in qualitative agreement with the average chain length of 23 reported here for the "undegraded" calcium polyphosphate. Other recent advances in chromatography[13–15] might also be applied profitably to the degradation of calcium polyphosphates.

Rate and Mechanism.—Rate data were obtained at *p*H's of 1 to 6 and at 25, 50 and 100°. At 25° the degradation was observed for 3 months; at 100° the longest experimental time was 5 hours. The experimental data are available.[16]

The rates of change in quantities of the identifiable species and the non-moving phosphate at 25°, *p*H 1 and 6, are shown in Fig. 2. The rates of degradation of all the species increase markedly with decrease in *p*H, some more than others. Although the rate of degradation of the non-moving phosphate is considerably slower at *p*H 6 than at *p*H 1, the rate of degradation of the rings is very much slower at the higher *p*H, as is shown by the buildup of ring species. This relationship also shows that rings (primarily trimetaphosphate) are a principal degradation product of the non-moving phosphate. Whether these identifiable rings are derived from degradation of non-moving interlocked rings, from long chains, or from both, is not proved here. Figure 2 shows also that orthophosphate is not derived primarily from scission at the ends of long chains; instead, it is derived largely through degradation of the shorter intermediate species, because a considerable buildup of orthophosphate is attained only when the intermediates are largely degraded. These results show that the calcium polyphosphate degrades through the same three paths found[17] for the degradation of Graham's salt: splitting off of end groups, random scission along the chain, and ring formation (tri- and tetrametaphosphates).

The rate data are summarized in Table II, where the time of appearance of the maximum amount of each intermediate, and the corresponding fraction of the phosphorus are shown as functions of *p*H and of temperature. These data were taken from curves like those in Fig. 2. At the higher *p*H's, longer times were required to reach the maxima for intermediates, and generally the fractions of the phosphorus at the maxima were higher. Elevation of temperature increased all the rates, with no significant differences apparent in the temperature dependence of the several species.

TABLE II

TIME OF OCCURRENCE OF MAXIMA AND FRACTION (%) OF THE PHOSPHATE AS DIFFERENT SPECIES AT THEIR MAXIMA

	Rings[a]		Tripolyphosphate		Pyrophosphate	
*p*H	Time of max.	Fraction %	Time of max.	Fraction, %	Time of max.	Fraction, %
			25°			
1.0	4 days	12	8 days	7	10 days	15
2.6	20 days	23	15 days	9	10 days	5
3.0	20 days	15	20–30 days	10	15–20 days	10
4.7	25 days	28	25–35 days	12	>50 days	>10
6.0	35 days	34	.....	..	>50 days	>10
			50°			
1.0	20 hr.	7	.....	..	25 hr.	14
2.0	40 hr.	15	30 hr.	8	60 hr.	20
4.0	90 hr.	33	>140 hr.	..	140 hr.	12
6.0	>100 hr.	>30	.....	..	.....	..
			100°			
1.0	5 min.	21	8 min.	16	10 min.	15
2.0	20 min.	16	10 min.	9	70 min.	16
4.0	20 min.	32	75 min.	6	.....	..
6.0	ca. 60 min.	33	>100 min.	>18	110 min.	28

[a] Mostly trimeta with some tetrameta and tetrapoly.

Although a qualitative picture of the rate and mechanism of the degradation is provided, it is not yet possible to write a complete rate equation for the total of the consecutive first-order processes involved, including the values of the rate constants for the degradation of all species. Kinetic studies on the intermediate species would be helpful for this. Nevertheless, progress was made in evalua-

(12) S. Ohashi and J. R. Van Wazer, *J. Am. Chem. Soc.*, **81**, 830 (1959).

(13) K. Grassner, *Mikrochim. Acta*, (3–4), 594 (1957).

(14) H. J. McDonald, E. W. Bermes, Jr., and H. G. Shepherd, Jr., *Chromatog. Methods*, **2**, No. 2, 1 (1957).

(15) M. J. Smith, *Anal. Chem.*, **31**, 1023 (1959).

(16) Material supplementary to this article has been deposited as Document number 6074 with the ADI Auxiliary Publications Project, Photoduplication Service, Library of Congress, Washington 25, D. C. A copy may be secured by citing the Document number and by remitting $1.25 for photoprints, or $1.25 for 35 mm. microfilm. Advance payment is required. Make checks or money orders payable to: Chief, Photoduplication Service, Library of Congress.

(17) J. F. McCullough, J. R. Van Wazer and E. J. Griffith, *J. Am. Chem. Soc.*, **78**, 4528 (1956).

tion of the kinetics of the degradation of the non-moving phosphate. The data for the rate of degradation of the non-moving phosphate are plotted as first-order rates in Fig. 3.

The displacement of the curves for *p*H 6 (and to some extent all the curves for 100°) results from precipitation of phosphate after the experiment was started.

To prevent its dissolution during the rate experiment, precipitated phosphate was removed by filtration and the experiment was continued with the more dilute solution. The effect of concentration was tested in separate experiments with solutions containing 1 and 11 g. of polymer per liter at 25° and at the same *p*H. The rates were proportional to the concentration, but the first-order rate constants were not appreciably different. Rate constants derived from the lines in Fig. 3 thus should show correctly the effects of *p*H and temperature.

First-order rate constants calculated from the slopes of the lines in Fig. 3 are shown as experimental constants in Table III, along with smoothed values obtained from equations representing the constants as functions of *p*H

At 25°	$\log k = -2.00 - 0.30\ p\mathrm{H}$
At 50°	$\log k = -1.13 - 0.30\ p\mathrm{H}$
At 100°	$\log k = 0.93 - 0.30\ p\mathrm{H}$

The half-life periods in Table III are based on the smoothed constants. The calcium salt degrades 5 to 10 times as fast as the sodium (Graham's) salt[17] under comparable conditions.

TABLE III

RATE OF HYDROLYSIS OF NON-MOVING CALCIUM POLYPHOSPHATE (1 G. OF POLYMER PER LITER)

Temp., °C.	*p*H	$k \times 10^2$, hr.$^{-1}$ Exptl.	$k \times 10^2$, hr.$^{-1}$ Smoothed	$t_{1/2}$, hr.
25	1	0.55	0.50	139
	2	..	.25	277
	3	.04	.12	578
	4	..	.063	1100
	6	.03	.016	4330
50	1	3.0	3.7	19
	2	2.5	1.9	37
	4	0.25	0.46	151
	6	0.14	0.12	578
100	1	460	426	0.16
	2	160	214	0.32
	4	42	53	1.31
	6	23	14	4.95

The rate of degradation is not uniformly dependent on temperature over the range 25 to 100° (Fig. 4). Activation energies calculated from Fig. 4 are 15 kcal. for the temperature interval 25 to 50° and 22 kcal. for 50 to 100°. The average value for 25 to 100° is 19 kcal. One factor which probably contributes to this trend in activation energy is a decrease in *p*H with increase in temperature.

The average value of 19 kcal. for the activation energy is significantly lower than the value 26 kcal. calculated from the data[17] for Graham's salt—a difference in line with the difference in rates of degradation of the calcium and sodium polymers. The average value for the calcium salt

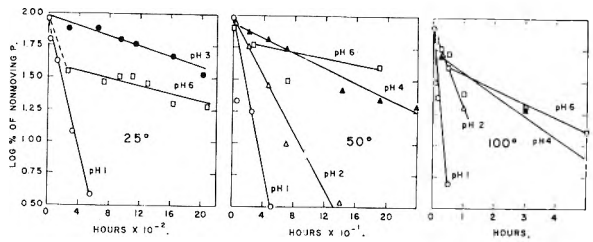

Fig. 3.—Rate of degradation of calcium polyphosphate.

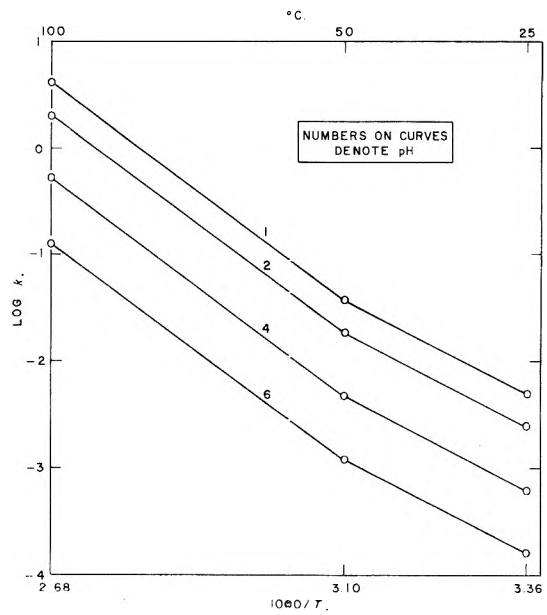

Fig. 4.—Effect of temperature and *p*H on the rate of degradation of calcium polyphosphate.

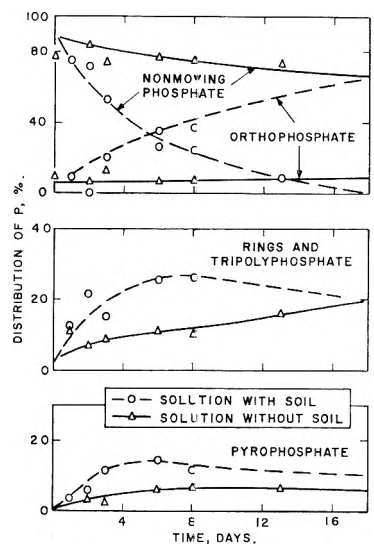

Fig. 5.—Effect of soil on rate of hydrolysis of calcium polyphosphate solution at 25° (1 g. of polymer per liter).

is the same as that reported[18] for scission at branch points in Graham's salt The lower activation energy for breaking at branch points is attributed[18] to a closer approach of the water dipole as a result of the phosphorus atoms being more nearly neutral at the branch points. The calcium polyphosphate

(18) U. P. Strauss and T. L. Treitler, *ibid.*, **78**, 3553 (1956).

is less ionized[19] (more nearly neutral) than sodium polyphosphate[20] and thus premits closer approach of the water dipole with resultant lower activation energy than that for Graham's salt.

The rate constants in Table III do not apply to calcium polyphosphate in soil, as constituents in soil are known to accelerate the degradation of polyphosphates.[21,22] This was demonstrated in one experiment with calcium polyphosphate. Hartsells soil (20 g.) was added to 1 liter of solution containing 1 g. of polymer. The degradation rate curves for the non-moving and the several identified species in the presence and absence of soil are shown in Fig. 5. The half-lives for the degradation of the non-moving phosphate were 83 and 1050 hours in the presence and absence of soil, respectively, a difference roughly equivalent to that obtained by lowering the *p*H from 4 to 0. Although the effect of soil probably is proportional to the extent of contact between soil and phosphate solution, the curves in Fig. 5 show that, insofar as the kinds and proportions of intermediates are concerned, the degradation mechanism is not changed by the soil.

(19) J. A. Gray and K. E. Lemmerman (reported by O. T. Quimby), THIS JOURNAL, **58**, 603 (1954).

(20) J. I. Watters, S. M. Lambert and E. D. Loughran, *J. Am. Chem. Soc.*, **79**, 3651 (1957).

(21) E. Bamann and E. Heumüller, *Naturwissenschaften*, **28**, 535 (1940).

(22) E. Karl-Kroupa, C. F. Callis and E. Scifter, *Ind. Eng. Chem.*, **49**, 2061 (1957).

Acknowledgment.—J. W. Williard and R. D. Duncan made the chemical analyses.

THE KINETICS OF THE REACTION BETWEEN Pu(IV) AND Fe(II)[1]

BY T. W. NEWTON AND H. D. COWAN

University of California, Los Alamos Scientific Laboratory, Los Alamos, New Mexico

Received August 28, 1959

The kinetics of the reaction between Pu(IV) and Fe(II) has been studied in perchlorate media containing up to 0.10 *M* chloride. The rate law indicates that the most important activated complexes are formed from water, Pu^{+4} and Fe^{+2} with the prior loss of one hydrogen ion, and from Pu^{+4}, Fe^{+2} and Cl^-. The formulas and the heats, free energies and entropies of formation of these activated complexes from the principal reactants were found to be: $(Pu{\cdot}OH{\cdot}Fe^{+5})^{\ddagger}$, $\Delta H^{\ddagger}$ = 19.1 kcal./mole, $\Delta F^{\ddagger}$ = 15.1 kcal./mole and $\Delta S^{\ddagger}$ = 13.3 e.u. and $(Pu{\cdot}Cl{\cdot}Fe^{+5})^{\ddagger}$, $\Delta H^{\ddagger}$ = 14.4 kcal./mole $\Delta F^{\ddagger}$ = 14.2 kcal./mole and $\Delta S^{\ddagger}$ = 0.6 e.u. The relation between the kinetics of this reaction and similar ones is discussed. Small amounts of H_2SO_4 were found greatly to accelerate the reaction.

Introduction

This paper is one of a series in which the kinetics of various oxidation-reduction reactions of plutonium are described. The rate laws and thermodynamic quantities of activation are being determined for sets of similar reactions in order to learn more about the factors which influence the rates of such reactions. Studies have been made of the kinetics of reduction of Pu(IV) by Pu(V),[2] Ti(III),[3] V(III)[4] and U(IV).[5] In the present work the reducing agent is Fe(II) which provides an ion of a charge type different from those listed above.

Experimental Part

Reagents.—Solutions of $Pu(ClO_4)_3$, $K_2Cr_2O_7$, $LiClO_4$, $HClO_4$ and $NaClO_4$ were prepared as previously described.[5] A stock solution of $Fe(ClO_4)_2$ was prepared by the dissolution of a weighed sample of pure iron in enough standardized 1.5 *M* $HClO_4$ to make a final solution which was 0.08 *M* in iron and 0.500 *M* in $HClO_4$. The small amount of insoluble residue was removed by filtration. Stock solutions of HCl and H_2SO_4 were prepared by the dilution of analytical reagent grade acids and were analyzed by titration.

Procedure.—Rate runs were made spectrophotometrically by following the absorbance at 4695 Å. where Pu(IV) absorbs relatively strongly. The general procedure used was essentially the same as described previously[5] except that solutions of Fe(II) were used instead of U(IV).

The concentration units employed in this paper are moles per liter (*M*) at 23°. The actual volume concentrations will be different at the different temperatures, for example being about 1% greater at 2.5°.

Catalytic Impurities.—The possibility that catalytic impurities were present in the various solutions was examined. All solutions except the Pu(III) solutions were found to be essentially free of catalysts.

Runs were made in which the ordinary stock solutions were compared with specially purified material. The HCl was specially purified by distillation, the $HClO_4$ by vacuum distillation and the $LiClO_4$ by electrolysis as previously described.[6] In all cases the two rate constants agreed to within 0.5%. This is well within the experimental error; duplicate runs usually agreed to within 1 to 2%.

Absence of catalytic impurities in the Fe(II) and $K_2Cr_2O_7$ stock solutions was shown by mixing equivalent amounts of the two and adding the resulting Fe(III)–Cr(III) mixture to the solutions for a rate run. In this way it was shown that increasing the total iron by a factor of four and the total chromium by a factor of seven changed the rate by less than 1.5%.

As in the previous work on Pu(IV)[5] evidence for a small amount of catalytic impurity was found in some of the plutonium stock solutions. Runs which had the same concentrations of acid, Fe(II) and Pu(IV) but differing concentrations of total plutonium gave different apparent second-order rate constants. Solutions prepared from two different lots of plutonium metal both gave rate constants which were essentially linear from 2.5×10^{-3} to 1×10^{-2} *M* total plutonium. For lot A: $k' = (102.0 \pm 2.0) + (997 \pm 270)$ (Σ Pu) M^{-1} min.$^{-1}$ and for lot B: $k' = (102.1 \pm 1.0) + (548 \pm 154)$ (Σ Pu) M^{-1} min.$^{-1}$, where k' is the apparent second-order rate constant, (Σ Pu) is the total plutonim concentration in *M*, and the uncertainties are the standard deviations determined by least squares. The presence of this catalysis makes it impossible to be sure that Pu(III) does not appear in the rate law.

Stoichiometry.—When Pu(IV) and Fe(II) are mixed in acid solution, the oxidation potentials indicate that the principal reaction will be

(1) This work was done under the auspices of the U. S. Atomic Energy Commission.

(2) S. W. Rabideau and R. J. Kline, THIS JOURNAL, **62**, 617 (1958).

(3) S. W. Rabideau and R. J. Kline, *ibid.*, **64**, 193 (1960).

(4) S. W. Rabideau and R. J. Kline, *J. Inorg. and Nucl. Chem.*, in press.

(5) T. W. Newton, THIS JOURNAL, **63**, 1493 (1959).

(6) T. W. Newton, *ibid.*, **62**, 943 (1958).

$$Pu(IV) + Fe(II) = Pu(III) + Fe(III) \quad (1)$$

That no other reactions are important was shown by the following experiment. Two solutions were prepared which differed only in the order of addition of the reagents. In the first, 0.8 meq. of Cr(VI) was added to 1.3 meq. of Pu(III) and after these had reacted 0.4 meq. of Fe(II) was added and the reaction allowed to go to completion. For the second solution, 0.8 meq. of Cr(VI) was added to 0.4 meq. of Fe (II) and then 1.3 meq. of Pu(III) was added. Both solutions had the same final concentrations since both had the same absorbance at 4695 Å. where Pu(IV) absorbs strongly. This indicates that the Fe(II) reduced the same amount of Pu(IV) in the first solution as it reduced Cr(VI) in the second. Since analytical experience indicates that the reaction between Fe(II) and Cr(VI) is stoichiometric, it has been concluded that the reaction between Fe(II) and Pu(IV) is stoichiometric also.

Results and Discussion

The Rate Law.—The rate was found to be first order in each of the reactants, Pu(IV) and Fe(II); that is, when all the other concentrations were constant the rate was given by $-d[Pu(IV)]/dt = -d[Fe(II)]/dt = k'[Pu(IV)][Fe(II)]$ M min.$^{-1}$, where k' is the apparent second-order rate constant and the quantities in brackets represent concentrations. This was shown by the good linearity of plots of log $\{[Fe(II)]/[Pu(IV)]\}$ *versus* time or of plots of $[Pu(IV)]^{-1}$ *versus* time for those runs in which the concentrations of Pu(IV) and Fe(II) were essentially equal. In most of the runs the reaction was followed to about 80% completion and a straight line fit the appropriate plot of the data to within 0.002 absorbance unit. The apparent second-order rate constants were determined from the slopes of these straight lines.

The reaction product Fe(III) has no effect on the rate; this was shown by one of the results mentioned in the section on catalytic impurities. It cannot be stated with certainty that Pu(III) does not appear in the rate law; if it does, it is in the form of a small additional term $k''[Pu(III)][Pu(IV)][Fe(II)]$.

The effect of hydrogen ion concentration on the rate was studied extensively at 2.5° in $LiClO_4$ solutions of ionic strength equal 2.03 M. The data obtained are shown in Table I. The apparent second-order rate constants k' were found to be essentially inversely proportional to the hydrogen ion concentration; so the rate law was provisionally formulated as

$$-d[Pu(IV)]/dt = k_2[Pu^{+4}][Fe^{+2}][H^+]^{-1} \quad (2)$$

which is written in terms of the principal species present in solution. Since $[Pu^{+4}] = [Pu(IV)][H^+]([H^+] + K)^{-1}$ and $[Fe^{+2}] = [Fe(II)]$, the rate constant k_2 in equation 2, is given by $k_2 = k'([H^+] + K)$, where k' is the apparent second-order rate constant and K is the hydrolysis quotient for Pu(IV). The values for $k'([H^+] + K)$ given in Table I were calculated under the assumption that $K = 0.021$ M at 2.5°, this value was obtained by extrapolating the data of Rabideau.[7]

It is seen that the apparent values of k_2 are nearly constant but seem to show a slight trend. It was found that these values are given by the expression: $k'([H^+] + K) = (187.2 \pm 4.4) + (10.6 \pm 4)[H^+]$, where the uncertainties are twice the standard deviations as determined by least squares. It is possible that this trend is due to a minor path such that the rate law would be

$$-d[Pu(IV)]/dt = k_1[Pu^{+4}][Fe^{+2}] + k_2[Pu^{+4}][Fe^{+2}][H^+]^{-1} \quad (3)$$

with $k_1 = 10.6$ M^{-1} min.$^{-1}$ and $k_2 = 187$ min.$^{-1}$ at 2.5°. It is also quite possible that the trend is due to changes in activity coefficients as the medium is changed from 2 M $HClO_4$ to 1.75 M $LiClO_4$ + 0.25 M $HClO_4$. This possibility is supported by the change in k' when $NaClO_4$ is substituted for $LiClO_4$. (See section on ionic strength and medium effects.) In any case, it may be concluded that the reaction occurs primarily by the path described by the k_2 term in rate law 3.

TABLE I

EFFECT OF HYDROGEN ION CONCENTRATION ON THE RATE AT 2.5° IN $LiClO_4$-$HClO_4$ SOLUTIONS WITH $\mu = 2.03$

Initial concentrations, $M \times 10^3$				k', M^{-1} min.$^{-1}$	$k'([H^+] + K)$, min.$^{-1}$
$HClO_4$	Pu(III)	Pu(IV)	Fe(II)		
250	1.34	1.14	1.18	720	195
250	1.34	1.14	1.18	712	193
438	1.34	1.14	1.18	416	191
625	1.34	1.14	1.18	292	189
812	1.34	1.14	1.18	232	193
1000	1.34	1.14	1.18	189	193
1000	1.25	1.15	2.32	191	195
1000	1.25	1.15	2.32	197	201
1250	1.25	1.15	2.32	158	201
1500	1.25	1.15	2.32	135	205
1750	1.25	1.15	2.32	115	204
2000	1.25	1.15	2.32	105	212

The Effect of Chloride.—Chloride ion was found to cause a marked increase in the rate of the reaction. The results of the rate determinations at 20.2° are summarized in Table II.

TABLE II

EFFECT OF CHLORIDE CONCENTRATION ON THE RATE

Conditions: 20.2°, $\mu = 2.03$ made up with $LiClO_4$, initial reactant concentrations 1.15×10^{-3} M Pu(IV) and 1.17×10^{-3} M Fe(II)

Acid concn., M	Chloride concn., M	k' obsd., M^{-1} min.$^{-1}$	k', calcd.,[a] M^{-1} min.$^{-1}$	k', calcd.,[b] M^{-1} min.$^{-1}$
2.00	0.00	876	872	872
2.00	.05	1370	1359	1340
2.00	.10	1840	1798	1807
1.25	.00	1310	1335	1335
1.25	.05	1830	1865	1844
1.25	.10	2280	2341	2354
0.50	.00	3070	3065	3065
.50	.05	3810	3759	3731
.50	.10	4400	4387	4397

[a] Calcd. from: $k' = (1 + 0.048/[H^+] + 1.15[Cl^-])^{-1}(71 + 1644/[H^+] + 8880[Cl^-] + 5330[Cl^-]/[H^+])$. [b] Calcd. from: $k' = (1 + 0.048/[H^+])^{-1}(71 + 1644/[H^+] + 7900[Cl^-] + 3350[Cl^-]/[H^+])$.

A rate law in the form

$$-d[Pu(IV)]/dt = k_1[Pu^{+4}][Fe^{+2}] + k_2[Pu^{+4}][Fe^{+2}][H^+]^{-1} + k_3[Pu^{+4}][Fe^{+2}][Cl^-] + k_4[Pu^{+4}][Fe^{+2}][Cl^-][H^+]^{-1} \quad (4)$$

may be used to describe the data. A quantitative interpretation of the data requires a knowledge of the association quotient for $PuCl^{+3}$ as well as

(7) S. W. Rabideau, *J. Am. Chem. Soc.*, **79**, 3675 (1957).

the hydrolysis quotient since the concentration of Pu^{+4} is related to the stoichiometric concentration by the relation $[Pu^{+4}] = [Pu(IV)](1 + K/[H^+] + \beta[Cl^-])^{-1}$ where K is the hydrolysis quotient and β is the association quotient. This association quotient is quite small and is not known with certainty. Rabideau, *et al.*,[8] give the value 1.38 M^{-1} for 25°, this number has been provisionally accepted and the values have been calculated at other temperatures under the reasonable assumption that the aqueous entropy of $PuCl^{+3}$ is the same as that of $PuOH^{+3}$. This gives 1.15 M^{-1} for β at 20.2° and leads to $k_1 = 71\ M^{-1}$ min.$^{-1}$, $k_2 = 1644$ min.$^{-1}$, $k_3 = 8880\ M^{-2}$ min.$^{-1}$ and $k_4 = 5330\ M^{-1}$ min.$^{-1}$. The agreement between the observed and calculated second-order rate constants shows that rate law 4 is satisfactory. To show the lack of sensitivity of k_3 and k_4 on the choice of β, the calculation was repeated assuming no complexing by chloride. Under this assumption $k_3 = 7900\ M^{-2}$ min.$^{-1}$ and $k_4 = 3350\ M^{-1}$ min.$^{-1}$. Thus, in spite of uncertainty in the value of β, it may be concluded that the paths described by the k_2, k_3, and k_4 terms in rate law 4 are all important in the solutions studied.

The Effect of Sulfate.—A preliminary series of experiments showed that small amounts of H_2SO_4 greatly accelerate the reaction. In 2 M $HClO_4$ at 2.5°, 9×10^{-4} M H_2SO_4 increased the rate a factor of 5.13. The data cannot be analyzed quantitatively because the association quotient of $PuSO_4^{+2}$ is unknown at 2.5°. It is possible to conclude, however, that the free sulfate concentration appears in the rate law to the first power only. This is to be contrasted with the result for the U(IV) reaction where it was found that sulfate appeared in the rate law to both first and second powers.[5]

Ionic Strength and Medium Effects.—The effect of varying the ionic strength was determined in a short series of experiments in which the $HClO_4$ concentration was varied without the addition of salt. The results are given in Table III. It is seen that the value of $k'([H^+] + K)$, which is nearly equal to the value of k_2, doubles when the ionic strength is increased from 0.52 to 2.02.

TABLE III

EFFECT OF $HClO_4$ ON THE RATE AT 15.4° WITHOUT ADDED SALT

μ	$HClO_4$, M	k', M^{-1} min.$^{-1}$	K, M[a]	$k'([H^+] + K)$
0.52	0.50	921	0.057	513
1.02	1.00	648	.046	678
2.02	2.00	511	.039	1040

[a] Ionic strength effect on the hydrolysis quotient estimated using the Debye–Hückel expression with $\hat{a} = 7.5$ Å.

The effect of substituting $NaClO_4$ for $LiClO_4$ was studied in 0.5 M $HClO_4$ solutions with $\mu = 2$ at 2.5, 6.2 and 15.4°. It was found that the rate was decreased an average of 16%.

Temperature Dependence.—Rate runs were made at hydrogen ion concentrations from 0.5 to 2 M and total plutonium concentrations from 1.9×10^{-3} to 7.6×10^{-3} M at five temperatures ranging from 2.5 to 20.2°. The data were extrapolated to zero total plutonium concentration to remove the effects of possible catalysts in the plutonium and values of k_1 and k_2 were determined as described in connection with the discussion of rate law 3. The results of this procedure are given in columns 3 and 4 of Table IV.

TABLE IV

THE EFFECT OF TEMPERATURE IN 2.00 M PERCHLORATE SOLUTIONS

Temp., °C.	K[a], M	k_1, M^{-1} min.$^{-1}$	k_2, min.$^{-1}$	k_2 (calcd.),[b] min.$^{-1}$	$k_2(2\ M\ [H^+])$,[c] min.$^{-1}$	$k_2(2\ M\ [H^+])$ calcd.),[d] min.$^{-1}$
2.5	0.021	10	186	185	207	206
6.2	.026	13	296	299	323	330
10.2	.031	34	494	493	563	545
15.4	039	53	934	927	1040	1022
20.2	048	76	1620	1627	1770	1790

[a] Hydrolysis quotient obtained from the data of Rabideau.[7] [b] Calcd. from: $\log k_2 = 17.903 - 4310/T$. [c] This is $k'([H^+] + K)$ observed in 2.00 M $HClO_4$. [d] Calcd. from: $\log k_2 = 17.908 - 4299/T$.

The values of k_1 are small, ranging between 4.4 and 6.9% of the values of k_2. As mentioned previously, it is quite possible that the effect here attributed to k_1 is actually a medium effect. If this is true, the values tabulated for k_2 apply to the reaction as it would occur in 2 M $LiClO_4$ solutions. The values which apply in 2 M $HClO_4$ solutions are listed in column 6 of Table IV.

For both sets of data plots of $\log k_2$ *versus* $1/T$ give good straight lines. The method of least squares was used to find the Arrhenius equations

for 2 M $LiClO_4$

$$\log k_2 = (17.903 \pm 0.128) - (19{,}720 \pm 170)/2.303RT \quad (5)$$

for 2 M $HClO_4$

$$\log k_2 = (17.908 \pm 0.446) - (19{,}670 \pm 580)/2.303RT \quad (6)$$

where the uncertainties given are twice the standard deviations, the units of k_2 are min.$^{-1}$ and R is in cal. deg.$^{-1}$ mole^{-1}. Since the constants in equations 5 and 6 are the same within their uncertainties, the conclusions to be reached about the principal path do not depend on whether k_1 implies an actual path for the reaction or not.

TABLE V

THE VARIATION OF THE RATE CONSTANTS WITH TEMPERATURE

Temp., °C.	k_1, M^{-1} min.$^{-1}$	k_2, min.$^{-1}$	β,[a] M^{-1}	k_3, M^{-2} min.$^{-1}$	k_4, M^{-1} min.$^{-1}$	k_3,[b] M^{-2} min.$^{-1}$	k_4,[b] M^{-1} min.$^{-1}$
2.5	12	183	0.56	1810	110	1750	0
6.2	10	303	.66	2300	590	2200	370
10.2	25	508	.78	3840	970	3580	560
15.4	48	942	.96	6150	2130	5610	1190
20.2	71	1644	1.15	8880	5330	7900	3350

[a] The association quotient for $PuCl^{+3}$, calculated assuming $\Delta H = 6.5$ kcal./mole and $\Delta S = 22.5$ e.u. [b] Calculated assuming $\beta = 0$ at all temperatures.

In order to determine the temperature dependence of the paths involving chloride ion, series of runs were made at hydrogen ion concentrations between 0.5 and 2.0 M, chloride concentrations up to

(8) S. W. Rabideau, L. B. Asprey, T. K. Keenan and T. W. Newton, "Proceedings of the Second United Nations International Conference on the Peaceful Uses of Atomic Energy," Vol. XXVIII, United Nations, Geneva, 1958, P/2247, p. 361.

TABLE VI

THERMODYNAMIC QUANTITIES OF ACTIVATION AT 25°

	Net activation process	$\Delta F^{\ddagger}$, kcal./mole	$\Delta H^{\ddagger}$, kcal./mole	$\Delta S^{\ddagger}$, e.u.	$S^{\ddagger}$ complex, e.u.
(1)	$Pu^{+4} + Fe^{+2} + H_2O = (Pu{\cdot}OH{\cdot}Fe^{+5})^{\ddagger} + H^{+}$	15.1	19.1 ± 0.6	13.3 ± 1.3	−82
	or				
(2)	$Pu^{+4} + Fe^{+2} + OH^{-} = (Pu{\cdot}OH{\cdot}Fe^{+5})^{\ddagger}$	−3.9	5.8 ± 0.6	32.5 ± 1.3	−82
(3)	$Pu^{+4} + Fe^{+2} + Cl^{-} = (Pu{\cdot}Cl{\cdot}Fe^{+5})^{\ddagger}$	14.2	14.4 ± 1.5	0.6 ± 5.2	−98
(4)	$Pu^{+4} + Fe^{+2} + Cl^{-} + H_2O = (Pu{\cdot}OH{\cdot}Fe{\cdot}Cl^{+4})^{\ddagger} + H^{+}$	..	31 ± 8	.....	..
(5)	$Fe^{+3} + Fe^{+2} + OH^{-} = (Fe{\cdot}OH{\cdot}Fe^{+4})^{\ddagger}$	−2.0	6.6	29	−70
(6)	$Fe^{+3} + Fe^{+2} + Cl^{-} = (Fe{\cdot}Cl{\cdot}Fe^{+4})^{\ddagger}$	13.3	16.6	7	−77

0.10 M and total plutonium concentrations of about 1.9×10^{-3} M. In treating the data from these runs, it has been assumed that the small effect due to possible catalysts in the plutonium is not enhanced by chloride. The data taken at each temperature were analyzed in terms of the four constants in rate law 4. The calculation was made under two different assumptions with respect to chloride complexing. First, that $\beta = 1.38\ M^{-1}$ at 25° and second, that $\beta = 0$ at all the temperatures. The results of these calculations are given in Table V.

The values of k_1 and k_2 given in Table V differ from those given in Table IV in that they are based on data extrapolated to zero chloride but not to zero total plutonium concentrations. These k_1 values are more discordant than those in Table IV but the k_2 values are not inconsistent with the others since they may be represented by the equation

$$\log k_2 = (18.028 \pm 0.279) - (19{,}880 \pm 360)/2.303RT \quad (7)$$

which is in good agreement with equations 5 and 6.

A plot of log k_3 *versus* $1/T$ shows more scatter than similar plots of log k_2. This is not unexpected since the determination of k_3 involves differences between measured rate constants and involves the simultaneous determination of k_4. The k_3 values which were calculated assuming the β values in Table V are given by

$$\text{og } k_3 = (15.132 \pm 1.14) - (15{,}000 \pm 1{,}480)/2.303RT \quad (8)$$

On the other hand, if it is assumed that there is no chloride complexing, the analogous expression is not very different

$$\log k_3 = (14.508 \pm 1.09) - (14{,}230 \pm 1{,}420)/2.303RT \quad (9)$$

A plot of log k_4 *versus* $1/T$ shows serious scatter; all that can be said with certainty about the temperature coefficient of k_4 is that it is larger than that of k_2.

Thermodynamic Quantities of Activation.—Rate law 4 indicates that the reaction in chloride solutions proceeds by at least three parallel paths. The three activated complexes which are definitely indicated may be considered to be formed in the net activation processes given in Table VI. The formulas of the activated complexes are those required by the rate law but the structures indicated are merely plausible ones. The thermodynamic quantities, $\Delta F^{\ddagger}$, $\Delta H^{\ddagger}$ and $\Delta S^{\ddagger}$ which are associated with the net activation processes were calculated from the experimentally determined constants in equations 5 or 6 and 8 according to the absolute reaction rate theory.[9]

Discussion

The formal ionic entropies, $S^{\ddagger}_{\text{complex}}$, of a number of activated complexes with a charge of +5 have been tabulated for reactions involving actinide ions.[10] The range of values was from −72 to −108 e.u. The values found in the present work fall within this range.

Net activation processes for two of the activated complexes involved in the Fe(II)–Fe(III) exchange reaction have been included in Table VI for comparison with the analogous processes listed for the Fe(II)–Pu(IV) reaction. The thermodynamic quantities of activation were computed from the data of Silverman and Dodson.[11] By comparing processes 2 and 3 with 5 and 6 it is seen that the substitution of Cl^- for OH^- increases the $\Delta H^{\ddagger}$ values by about 10 kcal. for both reactions. However, the same substitution reduces $\Delta S^{\ddagger}$ by 32 ± 5 e.u. for the Fe(II)–Pu(IV) reaction but by 22 e.u. for the Fe(II)–Fe(III) exchange. It is not known what significance to attach to this difference.

It is of interest that Cl^- has a large effect on the rate of the reduction of Pu(IV) by Fe(II) but only a small effect on the reduction by Ti(III),[3] V(III)[4] or U(IV).[5] These latter reducing agents must form metal–oxygen bonds and the activated complexes may well involve bridging by OH. If this is true, the small Cl^- effect may be pictured as the ligand effect discussed by Taube, *et al.*[12]

Acknowledgments.—The authors wish to acknowledge many helpful discussions with Dr. C. E. Holley, Jr., and especially with Dr. J. F. Lemons, under whose general direction this work was done.

(9) S. Glasstone, K. Laidler and H. Eyring, "The Theory of Rate Processes," McGraw–Hill Book Co., New York, N. Y., 1941, p. 195–199.

(10) T. W. Newton and S. W. Rabideau, THIS JOURNAL, **63**, 365 (1959).

(11) J. Silverman and R. W. Dodson, *ibid.*, **56**, 846 (1952).

(12) R. K. Murmann, H. Taube and F. A. Posey, *J. Am. Chem. Soc.*, **79**, 262 (1957).

DIELECTRIC DISPERSION IN GASES AT 400 MEGACYCLES[1]

BY JAMES E. BOGGS AND A. P. DEAM

Electrical Engineering Research Laboratory and Department of Chemistry, The University of Texas, Austin 12, Texas

Received August 31, 1959

An apparatus has been constructed for measuring the dielectric constant of gases as a function of pressure at 402.1 Mc. Measurements have been made on CH_3Cl, CH_3Br, C_2H_5Cl and $CHCl_2F$ at 40°. In all cases the dispersion was of the non-resonant type and was adequately represented by the Cole–Cole dispersion curve. The measurements have been correlated with previous work on microwave absorption and with dielectric constant measurements at 9400 Mc. and at low frequency.

Recent papers from this Laboratory[2-5] have reported measurements of the dielectric constant of numerous gases at a frequency of 9400 Mc. For certain molecules the dielectric constant at 9400 Mc. is lower than that at low-frequency due to a non-resonant relaxation-type dispersion. The values of the dielectric constant at high and at low frequencies have been correlated[4,6-9] with absorption measurements and with fundamental theory for the case of symmetric top molecules.

The measured dielectric constants at 9400 Mc. were well on the low side of the dispersion curve, and the dispersion itself has never been observed. At 9400 Mc., theory indicates[4] that the dispersion could be observed directly at higher pressures, but experimental difficulties obviate this approach. At lower frequencies the dispersion curve should be observable at more convenient pressures. A frequency in the region of 400 Mc. was chosen as being convenient for most gases. The experiments of sweeping frequency at a constant gas pressure or of sweeping pressure at a constant frequency are entirely equivalent, and the latter has been chosen as easier experimentally.

For asymmetric top molecules, it has never been shown clearly that the difference between the dielectric constant at 9400 Mc. and that at low frequency is due entirely to non-resonant dispersion.[6] For some such molecules there are rotational transitions at very low frequencies which can give rise to non-resonant dispersion. In addition, there are transitions within the microwave region which might distort the dispersion curve. If the entire dispersion curve could be observed at 400 Mc., this question also could be resolved.

Experimental

Apparatus.—The apparatus used in conducting the experiments reported in this paper consisted of a silver-plated Invar coaxial resonator immersed in a temperature-controlled oil-bath. The resonator operated in the dominant TEM mode and exhibited an unloaded figure of merit of approximately 4,000. The resonator length was approximately $\lambda/4$. The resonant frequency of the resonator varies as $\epsilon^{-1/2}$, where ϵ is the dielectric constant of the medium.[10]

An oscillator, through a regulating system, was caused to operate at the self-resonant frequency of the resonator, thus transferring this frequency to an active measurable frequency. In order to provide sufficient resolution (0.25 p.p.m.), a crystal oscillator, temperature controlled, generated a frequency nominally 22 Mc. away from the resonator frequency. Thus, as gas was introduced into the resonator, the difference frequency between the crystal reference and the resonator frequency varied and was monitored to give the desired information. The difference frequency was generated with a crystal rectifier and detected with a Gertsch FM-3 frequency meter.

At all times the frequency of the controlled generator was mechanically tuned to provide near zero static error with the sampling resonator. This was done since no automatic integration had been incorporated in the control servo.

It has been shown[10] that the stabilized frequency that is generated is not entirely dependent on the resonant frequency of the measuring cavity. This is due primarily to the nature of the hybrid network used to obtain an error voltage from the measuring cavity. Unavoidable reflections in this device combine with the reflected error at the measuring cavity to establish the over-all error signal. Such secondary reflections may vary in phase and magnitude to produce an error in the apparent frequency shift as the dielectric constant within the cavity varies in magnitude. Therefore if the reference output voltage is held at that recorded for the evacuated cavity, an error in the calculated dielectric constant may result. Errors of the nature discussed here vary inversely with the Q of the measuring cavity. For a given instrument these errors should be reasonably constant in time and should depend only on the dielectric constant within the cavity, being of greater significance if this dielectric constant is small.

To evaluate the magnitude of the error discussed, measurements were made on CCl_2F_2, a gas for which the molar polarization is independent of gas pressure.[5,8] At medium and high gas pressures the molar polarization was found to be constant at a value of 24.992 ± 0.003. At lower pressures the apparent dielectric constant rose increasing by 1% when the dielectric constant fell to 1.000165. An error curve was plotted and the appropriate correction was applied to the measurements made on other gases. The correction was significant only at low gas pressures, reaching 1% only when the gas pressure was lowered to 20 to 30 mm.

Gas pressure was measured to ±0.05 mm. with a mercury manometer in conjunction with a cathetometer. The temperature of the resonator was controlled to ±0.05°.

Materials.—With the exception of $CHCl_2F$, all of the gases were used directly as they were obtained from commercial sources. The $CHCl_2F$ was frozen down to remove non-condensible impurities. All of the gases were analyzed on a Consolidated 21-102 mass spectrometer, and corrections were made in calculating the dielectric constants for the small amounts of impurities found. This correction was negligible except for non-polar impurities, and in no case did the correction exceed 0.2% of the molar polarization.

Procedure.—The procedure followed was basically that used earlier at 9400 Mc. Measurements were made at 40.0° over a pressure range of 20 to 780 mm. The molar volume, in liters, was calculated from the equation $V = RT/P - B$, where B = 0.337 for CCl_2F_2,[11] 0.395 for CH_3Cl,[12] 0.452 for CH_3Br,[12] 0.512 for $CHCl_2F$[13] and 0.620 for C_2H_5Cl [14]

(1) This work has been supported by Air Force Contract AF 33-(616)-5581.

(2) J. E. Boggs, C. M. Crain and J. E. Whiteford, THIS JOURNAL, **61**, 482 (1957).

(3) J. E. Boggs, C. M. Thompson and C. M. Crain, *ibid.*, **61**, 1625 (1957).

(4) J. E. Boggs, *J. Am. Chem. Soc.*, **80**, 4235 (1958).

(5) J. E. Boggs, J. E. Whiteford and C. M. Thompson, THIS JOURNAL, **63**, 713 (1959).

(6) J. E. Boggs and J. C. Agnew, THIS JOURNAL, **63**, 1127 (1959).

(7) G. Birnbaum, *J. Chem. Phys.*, **27**, 360 (1957).

(8) E. B. Wilson, Jr., THIS JOURNAL, **63**, 1329 (1959).

(9) W. Maier and H. K. Wimmel, *Z. Physik*, **153**, 297 (1958); **154**, 133 (1959).

(10) R. V. Pound, *Proc. I.R.E.*, **35**, 1405 (1947).

(11) "Thermodynamic Properties of Dichlorodifluoromethane," Circular No. 12, Am. Soc. Refrig. Eng., (1931).

(12) P. G. T. Fogg, P. A. Hanks and J. D. Lambert, *Proc. Roy. Soc. (London)*, **A219**, 490 (1953).

Results

The molar polarization, measured at 40.0° and 402.1 Mc., is shown as a function of gas pressure in Fig. 1 for CH_3Cl and CH_3Br, in Fig. 2 for C_2H_5Cl and in Fig. 3 for $CHCl_2F$.

According to the theory previously developed[4,7] for Debye-type dispersion, the dielectric constant of a gas in the dispersion region is given by

$$\epsilon = \epsilon_\infty + \frac{\epsilon_0 - \epsilon_\infty}{1 + (\nu/\nu_M)^2} \qquad (1)$$

where ϵ_0 is the value of the dielectric constant at zero frequency, ϵ_∞ is the value the dielectric constant approaches at frequencies well above those at which non-resonant dispersion occurs (but below those at which rotational dispersion sets in), ν is the frequency of the measuring radiation and ν_m is the critical frequency for which absorption is a maximum.

Since frequency and pressure are reciprocal quantities[7] and $(\epsilon - \epsilon_\infty)/(\epsilon_0 - \epsilon_\infty) = (P - P_\infty)/(P_0 - P_\infty)$ with a negligibly small error, equation 1 may be rewritten

$$\frac{P - P_\infty}{P_0 - P_\infty} = \frac{1}{1 + (p_M/p)^2} \qquad (2)$$

where p_M is the pressure at which $P = P_0 + (P_0 - P_\infty)/2$. Attempts to fit this equation to the experimental data did not, in general, succeed, regardless of the values which were chosen for P_0 and P_∞. The experimental data indicated that the dispersion was spread out over a slightly greater frequency range than is indicated by the Debye equation.

The Debye equation is based on the assumption that a single line-broadening parameter is involved in the dispersion. Birnbaum[7] found, however, that to explain his experiments on microwave absorption by similar gases a distribution of line widths needed to be assumed. The Cole–Cole equation,[15] which by substitutions similar to those used above may be written

$$\frac{P - P_\infty}{P_0 - P_\infty} = \frac{1 + (p/p_M)^{\alpha-1} \sin(\alpha\pi/2)}{1 + 2(p/p_M)^{\alpha-1} \sin(\alpha\pi/2) + (p/p_M)^{2(\alpha-1)}}$$

where α is a measure of the spread of line widths, gave good agreement with the absorption experiments. The solid lines in Figs. 1, 2 and 3 are plots of this equation using the values of the parameters shown in Table I. The average deviation of the experimental points from the line, including runs made on different days with different samples of gas, ranges from about 0.05% at high and medium pressures to about 0.2% at the lowest pressure.

TABLE I

Gas	P_0 (cc.)	P_∞ (cc.)	$\Delta\nu/p$ (mc./mm.)	α
CH_3Cl	81.6	75.0	4.2	0.05
CH_3Br	78.57	73.6	3.4	.03
C_2H_5Cl	100.9	91.6	4.1	.00
$CHCl_2F$	51.5	42.2	2.7	.03

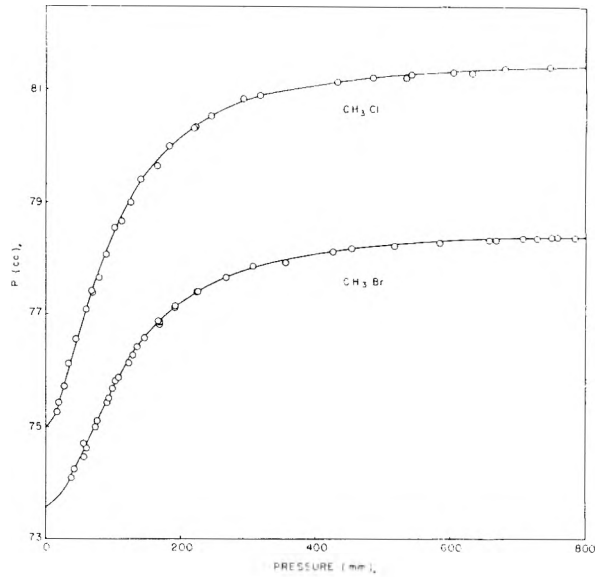

Fig. 1.—Molar polarization of CH_3Cl and CH_3Br as a function of pressure at 402 Mc. and 40°.

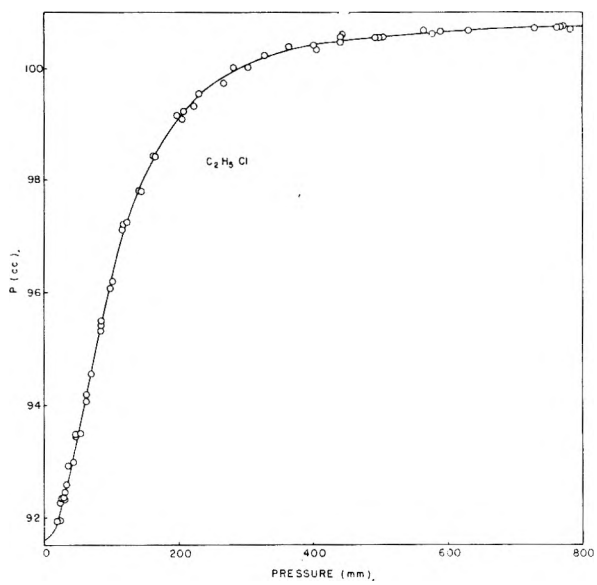

Fig. 2.—Molar polarization of C_2H_5Cl as a function of pressure at 402 Mc. and 40°.

Discussion

For CH_3Cl, values of 81.5,[16] 82.1[17] and 81.2 cc.[18] have been obtained for P_0 by measurements at low frequency. Our value of 81.6 cc. is in satisfactory agreement with these earlier measurements. Our previous measurement of the molar polarization of CH_3Cl at 9400 Mc. (P_∞) was 76.0 cc.[2] The present value of 75.0 cc. should be considerably more accurate.

For non-resonant dispersion, the quantity $(P_0 - P_\infty)/(P_0 - P_D)$ where P_D is the distortion polarization should be given by $\sum_{J,K} f_{JK}|\mu_{JK}|^2/\mu^2$, where f_{JK} is the fractional number of molecules occupying

(13) A. F. Benning and R. C. McHarness, *Ind. Eng. Chem.*, **32**, 698 (1940).

(14) J. D. Lambert, G. A. H. Roberts, J. S. Rowlinson and V. J. Wilkinson, *Proc. Roy. Soc.* (*London*), **A196**, 113 (1949).

(15) K. S. Cole and R. H. Cole, *J. Chem. Phys.*, **9**, 341 (1941).

(16) Calculated from the results of O. Fuchs, *Z. Physik*, **63**, 824 (1930).

(17) Calculated from the results of R. Sanger, O. Steiger and K. Gächter, *Helv. Phys. Acta*, **5**, 200 (1932).

(18) Calculated from the results of K. L. Ramaswamy, *Proc. Indian Acad. Sci.*, **A4**, 108 (1936).

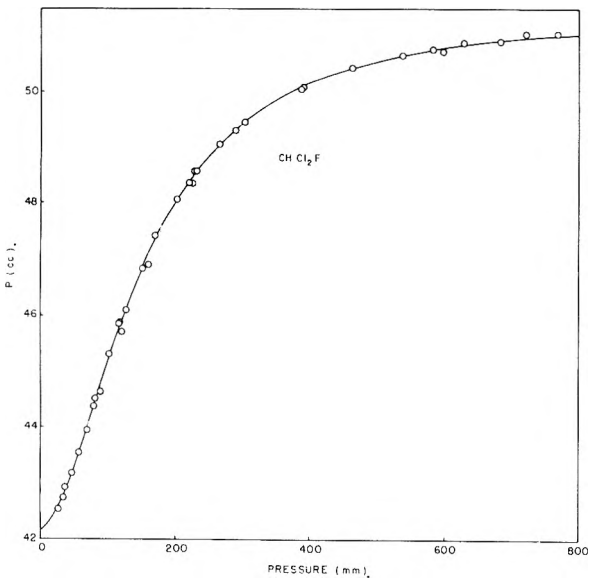

Fig. 3.—Molar polarization of $CHCl_2F$ as a function of pressure at 402 Mc. and 40°.

the J,K rotational energy level and $|\mu_{JK}|^2$ is the square of the dipole moment matrix element.[4] The summation can be evaluated from spectral data for symmetric top molecules. For CH_3Cl, a value of 0.097 has been obtained by direct summation.[7] Using 13.8 cc. for the distortion polarization of CH_3Cl (the average of the values of Fuchs[16] and Sanger[17]), our data give $(P_0 - P_\infty)/(P_0 - P_D) = 0.097$.

Our value of the line-broadening parameter, $\Delta\nu/p$, for CH_3Cl is 4.2 Mc./mm. Of the numerous measurements of this quantity from microwave absorption studies, the most accurate appears to be that of Birnbaum,[7] who has obtained a value of 4.5 Mc./mm. at 26°. If $\Delta\nu/p$ varies as $T^{-1.59}$ as indicated by Birnbaum and Maryott,[19] the absorption value is equivalent to 4.3 Mc./mm. at the temperature of our measurement.

Birnbaum[7] found a value of the Cole–Cole parameter α for CH_3Cl of 0.051 in agreement with our value of 0.05.

For CH_3Br, previously reported values of P_0 are 78.2,[20] 78.3[18] and 78.0 cc.,[21] compared with our value of 78.57 cc. Our previous measurement of P_∞ at 9400 Mc. was 74.2 cc., compared with the present value of 73.6 cc. By direct summation,[7] $\sum_{J,K} f_{JK}|\mu_{JK}|^2/\mu^2 = 0.076$. Our value for $(P_0 - P_\infty)/(P_0 - P_D)$ is 0.080 if the average of the values of Smyth[20] and Groves[21] is used for P_D. Birnbaum's value[7] for $\Delta\nu/p$ of 3.8 Mc./mm. is equivalent to a value at 40° of 3.6 Mc./mm., compared with our value of 3.4 Mc./mm.

For the two symmetric top molecules CH_3Cl and CH_3Br, the dielectric dispersion curves are in good agreement with theory, and the values obtained for the parameters check well with those obtained from dielectric constant measurements at low frequency and at 9400 Mc. and from experiments on microwave absorption. The other two gases studied, C_2H_5Cl and $CHCl_2F$, are composed of asymmetric top molecules for which the theory is not so complete.

For C_2H_5Cl, previously reported values of P_0 are 100.4[16], 101.1[17] and 99.7 cc.[18] compared with our value of 100.9 cc. Our previous value of P_∞ measured 9400 Mc. was 91.0 cc.[5] compared with the present value of 91.6 cc.

This gas was the only one measured for which the Cole–Cole parameter was equal to zero, indicating that its dispersion is represented adequately by the Debye equation.

Previous measurements of the static molar polarization of $CHCl_2F$ have given values of 49.7[22] and 55.2 cc.[23] Our value of 51.5 cc. falls between these two rather divergent results. Our previous measurement of P_∞ for $CHCl_2F$ at 40° was 42.7 cc., compared with the present value of 42.2 cc.

The dielectric dispersion of the asymmetric top molecules C_2H_5Cl and $CHCl_2F$ appears to be of the same non-resonant type observed for symmetric top molecules. This does not, however, mean that the cause of the dispersion is necessarily the same. An asymmetric top molecule may have rotational sublevels that are nearly degenerate with transitions permitted between certain alternate pairs of adjacent levels. Thus, Krishnaji and Srivastava[24] have attributed the absorption of microwaves at 8,000 Mc. in C_2H_5Cl exclusively to transitions between rotational sublevels, low-frequency Q-branch transitions being most important.

(19) G. Birnbaum and A. A. Maryott, *J. Chem. Phys.*, **29**, 1422 (1958).

(20) Calculated from the results of C. P. Smyth and K. B. McAlpine, *ibid.*, **2**, 499 (1934).

(21) Calculated from the results of L. G. Groves and S. Sugden, *J. Chem. Soc.*, 158 (1937).

(22) Calculated from the results of C. P. Smyth and K. B. McAlpine, *J. Chem. Phys.*, **1**, 190 (1933).

(23) Calculated from the results of R. M. Fuoss, *J. Am. Chem. Soc.*, **60**, 1633 (1938).

(24) Krishnaji and G. P. Srivastava, *Phys. Rev.*, **106**, 1186 (1957).

THE MEASUREMENT OF THE HEATS OF SUBLIMATION OF ZINC AND CADMIUM WITH THE MASS SPECTROMETER[1]

By K. H. Mann[2] and A. W. Tickner

Division of Applied Chemistry, National Research Council, Ottawa, Canada

Received September 1, 1959

A sample of the metal being studied was enclosed in a heated mass spectrometer ion source of special design. In this way the ion source was filled with vapor in equilibrium with the metal whose temperature could be controlled and measured independently of that of the ionizing region. The variation of the vapor pressure with temperature was measured for zinc from 399 to 538°K. and for cadmium from 393 to 469°K. ΔH_{298} was found to be 30.05 ± 0.42 kcal. per mole for zinc and 26.48 ± 0.20 kcal. per mole for cadmium.

Introduction

Since in general it is possible to measure individually the ion currents due to each of a number of substances present in a vapor, the mass spectrometer can be used to follow variations in the partial pressure of one component in the presence of a number of others. Thus, the mass spectrometer is useful in measuring low vapor pressures under conditions where the contributions of volatile impurities become important. It has been used to measure the vapor pressures of the lower hydrocarbons in the region below one mm.[3]

For involatile materials, such as the metallic elements, it becomes necessary to generate the vapor close to the mass spectrometer ion source. The method as it is commonly used employs an effusion cell or crucible mounted so that a molecular beam enters the ionizing region.[4]

For the more volatile metals however, it should be practical to maintain the ion source at a temperature higher than that of the specimen, in order to avoid condensation, and to connect it directly to a heated vessel containing the metal. In this way the ion source would be filled with vapor in equilibrium with the condensed phase, the pressure being controlled directly by the temperature of the metal specimen. Such an arrangement would allow the measurement of the variation of the vapor pressure with temperature for vapor pressures up to about 10^{-3} mm. and for temperatures up to a few hundred degrees above the usual operating temperature of the ion source.

While the proposed method could be used to measure the variation of vapor pressure with temperature, and thus the heat of sublimation, the measurements would lead to absolute values of the vapor pressure only when the ionization cross-section is known. For most metals the ionization cross-sections are not known with any accuracy. However, the method should allow the measurement of the variation of vapor pressure with temperature over a fairly wide range which, in general, should extend to much lower pressures than can be used with the effusion technique. In common with other methods using the mass spectrometer it should be possible to estimate the concentration of any molecular species present in the vapor.

In order to explore the possibilities of the proposed method, the measurement of the heats of sublimation of zinc and cadmium was undertaken.

Experimental

The ion source of a conventional 90° magnetic sector mass spectrometer was modified as shown in Fig. 1. In addition to the normal pumping on the mass spectrometer tube the source chamber was pumped by a 70 l./sec. mercury diffusion pump equipped with a liquid nitrogen trap. Copper cooling coils were added to the ends of the source chamber to prevent the O-rings from being overheated.

The entire furnace assembly was mounted on plate P_1 which was attached to the same mounting posts as the focussing and collimating plates of the mass spectrometer. Plate P_2 was supported with respect to P_1 by four rods. All of the plates and supporting rods were made of Chromel A.

The electron beam was supplied by a tungsten filament F. It entered the ion source furnace through a hole 1 mm. in diameter and emerged through a hole 1.5 mm. in diameter to be measured by means of the trap T. Permanent magnets mounted externally supplied a collimating field of about 100 gauss. An exit slit 0.5 × 6 mm. was provided in the end of the furnace and a circular hole 1 cm. in diameter in plate P_1 opposite the slit allowed sufficient penetration of the field from the focussing plates to withdraw the ions. Three tool steel pins 0.5 mm. in diameter mounted on P_1 and corresponding holes in the end of the ion source furnace located the exit slit with respect to the collimating slits of the mass spectrometer. Electrons from the filament were accelerated by a potential of 50 volts between the filament and the furnace.

The furnaces were machined from molybdenum which, in addition to its low vapor pressure and high melting point, possessed high thermal conductivity and was not attacked by the vapors of the metals to be examined. Each furnace had its own heating element of a non-inductive type cut from Chromel A sheet and wound on with mica insulation. Since it was not necessary to know the temperature of the ion source furnace with great accuracy, it was convenient to place a thermocouple on its wall inside the heating element. The radiation shields were made of tantalum and were supported by stainless steel screws and Pyrex spacers. All electrical leads were brought out at the end of the ion source chamber by means of feed-through insulators.

A regulated a.c. power supply with an output voltage constant to 0.1% was used to supply power for heating the furnaces. Each furnace received its power from the secondary winding of an isolating transformer which allowed the furnace heating elements to operate at the potential of the ion source, approximately 2000 volts above ground. The temperature of each furnace was controlled manually by adjusting a variable autotransformer which supplied the voltage to the primary winding. This arrangement allowed different temperatures to be maintained in the two furnaces over a sufficiently wide range.

The metal samples were cylindrical in form and were mounted on a support machined from boron nitride[5] as shown in Fig. 1. Additional holes were drilled in the sample to increase its surface area, the total area of the openings

(1) Contribution No. 5520 from the National Research Council, Ottawa, Canada.

(2) Holder of a National Research Council Postdoctorate Fellowship.

(3) A. W. Tickner and F. P. Lossing, This Journal, **55**, 733 (1951).

(4) R. E. Honig, *J. Chem. Phys.*, **22**, 1610 (1954); W. A. Chupka and M. G. Inghram, This Journal, **59**, 100 (1955); R. G. Johnson, D. E. Hudson, W. C. Caldwell, F. H. Spedding and W. R. Savage, *J. Chem. Phys.*, **25**, 917 (1956).

(5) Manufactured by The Carborundum Company, Niagara Falls, N. Y.

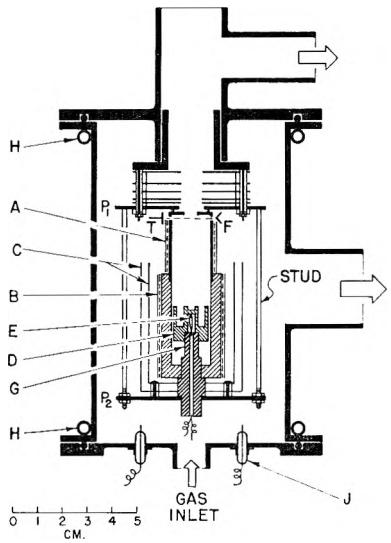

Fig. 1.—Mass spectrometer ion source: A, ion source furnace; B, sample furnace; C, radiation shields; D, metal sample; E, thermocouple; F, filament; G, sample support; H, cooling coils; J, feed-through insulators; P_1, P_2, mounting plates; T, electron beam trap.

in the ion source furnace being less than 0.5% of the exposed surface area of the sample. A hole drilled along the axis of the sample support allowed the insertion of a Chromel P–Alumel thermocouple which measured the sample temperature. The thermocouple wires were brought out of the vacuum without joints through tubular insulators sealed with Apiezon W. The thermocouple was calibrated at the melting points of zinc, lead and tin and at the boiling point of water. Recalibration after use showed that the calibrations had changed by less than 0.6° in all cases. The e.m.f.'s were measured on a potentiometer with an accuracy of ±0.002 mv.

Temperature equilibrium could be attained in a few minutes and the temperature was held constant to within 0.5° while the ion currents were being measured. It was found that the amount by which the temperature of the ion source furnace exceeded that of the sample furnace had little effect on the results. Since the temperatures of the two furnaces were interdependent to some extent, a relatively small temperature difference of about 25° was used in most of the experiments in order to extend the range of the sample furnace temperature to as low a value as possible. Experiments 3 and 4 with zinc were carried out using a constant ion source furnace temperature about 25° higher than the highest sample furnace temperature.

In order to correct for any variation in the over-all efficiency of the ion source during a series of measurements a small reference pressure of krypton was maintained in the ion source chamber by allowing the gas to leak in from a reservoir in the sample line. Krypton was chosen because it was chemically inert and had approximately the same atomic weight as that of the metals to be studied. At each temperature the ion current corresponding to Kr^{84} was measured as well as the ion current due to the metal. The isotope ratios of the metals were checked at several temperatures in order to detect any contributions from impurities.

The zinc and cadmium used were obtained from the Consolidated Mining and Smelting Co. of Canada Ltd., Trail, B. C. According to the supplier their purity was 99.99% or better.

Results and Discussion

The treatment of the results is similar to that of Barrow, *et al.*[6] The heat of sublimation at any temperature T can be represented by

$$\Delta H_T = \Delta H_0' + \Delta a T + {}^1/_2 b T^2 \qquad (1)$$

where $\Delta H_0'$ is an integration constant. By combining (1) with the Clausius-Clapeyron equation and dividing through by $-2.3026R$ we obtain

$$\log P - \frac{\Delta a}{R}\log T - \frac{\Delta b}{4.6052R}T = \frac{-\Delta H_0'}{2.3026RT} + I \qquad (2)$$

where I is another integration constant. The term

$$-\frac{\Delta a}{R}\log T - \frac{\Delta b}{4.6052R}T$$

is designated by $A(T)$ in the following discussion. It can be evaluated graphically using the theoretical heat capacities for the monatomic gaseous metals and the values of Kelley[7] for the solid metals.

The ion current due to the metal can be used as a quantity proportional to P in equation 2 as long as conditions in the ion source do not change. In practice the efficiency of the ion source varies considerably with temperature and to correct for this the ion current due to Kr^{84} at each temperature is used to relate all of the metal ion currents to a constant value of the krypton ion current. Thus

$$P = KI_m \frac{I^0_{Kr}}{I_{Kr}} \qquad (3)$$

where K is a constant, I_m is the metal ion current at temperature T, I_{Kr} is the Kr ion current at temperature T, and I^0_{Kr} is the Kr ion current at the reference temperature. The ion currents have been corrected for the effect of temperature on the concentrations in the ion source furnace.[8]

In addition, the decay of krypton pressure with time was allowed for. The decay was logarithmic and was given by

$$\frac{d(\log p)}{dt} = 5.8 \times 10^{-3}\ \text{hr.}^{-1} \qquad (4)$$

From (2), (3) and (4) we obtain

$$\log I_m + \log I^0_{Kr} - \log I_{Kr} - 5.8 \times 10^{-3}t + A(T) = -\frac{\Delta H_0'}{4.575T} + I - \log K \qquad (5)$$

where t is the time in hours. The left side of the equation is designated Σ' and $\Delta H_0'$ is obtained by plotting Σ' against $1/T$. ΔH_{298} then is obtained from equation 1.

The measured values and the corrections are shown for one series of measurements with zinc in Table I. All of the results for zinc have been summarized in Table II and those for cadmium in Table III. The experimental points obtained in each experiment were treated by the method of least squares. Since there appears to be no correlation between the standard deviation of an experiment and the amount by which ΔH_{298} differs from the mean, each experiment has been treated as a single measurement, the arithmetic mean taken and the standard deviation calculated. For cadmium the results were calculated for both Cd^{112} and Cd^{114} since the two isotopes occur in approximately equal amounts.

The accuracy of the measurements probably is

(6) R. F. Barrow, P. G. Dodsworth, A. R. Downie, E. A. N. S. Jeffries, A. C. P. Pugh, F. J. Smith and J. M. Swinstead, *Trans. Faraday Soc.*, **51**, 1354 (1955).

(7) K. K. Kelley, U. S. Bur. Mines, Bull. 476, 1949.

(8) The measured ion currents are proportional to the concentration in the ion source. At a steady state, under conditions of molecular flow, equal numbers of molecules effuse in each direction through openings connecting the ion source furnace to the region containing the pressure being measured. For two interconnected regions at different temperatures the concentrations will be related by $C_1/C_2 = (T_2/T_1)^{1/2}$.

TABLE I

ZINC—EXPERIMENT No. 6

Temp., °K.	Ion currents, arbitrary units Zn^{64}	Kr^{84}	Log $\frac{I_{64}I^{0}_{84}}{I_{84}}$	$A(T)$	5.8 $\times 10^{-4}t$	Σ'
411.9	0.6	17.7	−0.222	0.608	0.004	0.382
440.9	7.2	17.4	+0.850	.621	.007	1.464
463.2	31.8	14.2	1.573	.631	.010	2.194
492.7	159	9.85	2.417	.644	.012	3.049
522.5	457	4.9	3.167	.657	.014	3.810
504.3	230	7.1	2.713	.649	.019	3.343
477.5	72.5	11.8	2.004	.638	.022	2.620
453.5	20.9	17.1	1.315	.627	.026	1.916
433.9	2.5	9.3	0.666	.618	.029	1.255

TABLE II

HEAT OF SUBLIMATION OF Zn

Expt. no.	No. of observn.	Temp. range, °K.	ΔH_{298}, kcal./mole	Stand. dev.
1	6	400–506	29.81	0.21
2	9	415–520	29.31	.14
3	12	436–523	29.45	.14
4	10	460–538	30.37	.06
5	9	399–526	29.95	.08
6	9	412–522	30.10	.08
7	6	453–515	31.36	.10
		Mean	30.05 ± 0.42	

TABLE III

HEAT OF SUBLIMATION OF Cd

Expt. no.	No. of ob-servn.	Temp. range, °K.	Iso-tope	ΔH_{298}, kcal./mole		Stand. dev.
1	5	400–451	114	26.14	26.15	0.06
			112	26.16		.06
2	5	413–460	114	26.52	26.54	.08
			112	26.56		.09
3	5	408–469	114	26.63	26.67	.04
			112	26.71		.05
4	6	393–464	114	26.54	26.54	.12
			112	26.53		.11
			Mean		26.48 ±	.20

limited more by the extent to which equilibrium can be maintained during the time of an observation (3 to 4 minutes) than by the accuracy with which the readings can be made. We estimate the uncertainty in a single experimental point to be less than 2%. Since changes in the calibration of the thermocouple during the measurements were less than 0.6° the uncertainty in the heat of sublimation due to this cause is less than 1%.

No ion current due to Zn_2 could be detected at any temperature up to 520°K. From this observation we estimate that the ratio Zn_2/Zn is less than 2×10^{-4} at this temperature.

The value of $\Delta H_{298} = 30.05 \pm 0.42$ kcal./mole obtained for zinc from the present measurements is somewhat lower than that of 31.18 ± 0.1 kcal./mole which Barrow, *et al.*,[6] have designated as the "best" value on the basis of their analysis of the earlier work. Their own results, obtained for the temperature range 512 to 649°K., support this value. More recently, however, Nesmeyanov and Ilicheva[9] have measured the vapor pressures of zinc and cadmium by following the exchange of isotopes between two metal specimens through an orifice. Their results for the temperature range 493 to 633°K. lead to a value for zinc of $\Delta H_0 = 30.30 \pm 0.6$ kcal./mole. When recalculated using the heat capacity data of Kelley[7] this gives $\Delta H_{298} = 30.08 \pm 0.6$ kcal./mole in reasonable agreement with our value. Since Barrow's value is based on data for liquid zinc it is possible that the difference is at least partly due to discrepancies in the thermal data.

O'Donnell[10] has measured the vapor pressure of cadmium by an effusion method over the temperature range 482–524°K. and obtains $\Delta H_{500} = 27.8 \pm 0.4$ kcal./mole, corresponding to a value of $\Delta H_{298} = 28.1 \pm 0.4$ kcal./mole. The results of Nesmeyanov and Ilicheva[9] for the temperature range 411–481°K. give a value of $\Delta H_0 = 26.55 \pm 0.13$ kcal./mole which corresponds to $\Delta H_{298} = 26.32 \pm 0.13$ kcal./mole. Our value of $\Delta H_{298} = 26.48 \pm 0.20$ kcal./mole is in reasonably good agreement with that of Nesmeyanov and Ilicheva and with the value of 26.75 kcal./mole given by Brewer.[11] O'Donnell's value appears to be too high.

Conclusion

On the basis of the results obtained the proposed method of measuring the heats of sublimation seems to be a satisfactory one for use with the volatile metals. It should also be possible to apply the method to studies of the vapor properties of other substances of similar volatility.

(9) A. N. Nesmeyanov and I. A. Ilicheva, *Zhur. Fiz. Khim.*, **32**, 422 (1958).

(10) T. A. O'Donnell, *Australian J. Chem.*, **8**, 485 (1955).

(11) L. Brewer, "Chemistry and Metallurgy of Miscellaneous Materials," edited by L. L. Quill, McGraw-Hill Book Co., Inc., New York, N. Y., 1950.

THE PHYSICAL PROPERTIES OF CERTAIN ORGANIC FLUORIDES

BY W. A. T. MACEY[1]

Contribution from the National College of Food Technology, Weybridge, Surrey, England

Received September 8, 1959

The boiling points, densities and refractive indices of a number of liquid organic fluorides have been determined. From these data the molar refractions, specific refractions, specific dispersions, (C–F) bond refractions and (CH_2) group refractions have been calculated. The (C–F) bond refraction (D-line at 20°) in 1-fluoroalkanes is established as 1.55 cc. Similar values for (C–F) are obtained in fluoroesters and fluoroalcohols provided that the substituent fluorine atom is sufficiently far removed from the polarizable group.

Introduction

In a preliminary report[2] some physical properties of the 1-fluoroalkanes (*n*-alkyl fluorides) were described. The present communication records the physical properties of 30 liquid organic fluorides which were prepared in order to obtain bond and group constants for (C–F) and (CH_2).

The pure organic fluorides available were: ten 1-fluoroalkanes; five 3-fluoropropanol carboxylate esters; five *n*-alkyl 3-fluoropropionates; five *n*-alkyl trifluoroacetates; miscellaneous compounds included 3-fluoropropanol-1, 3-fluoropropionic acid, ethyl 5-fluorovalerate and trifluoroacetic acid.

Preparation and Purification.—The 1-fluoroalkanes were prepared from alkyl bromides by treatment with potassium fluoride in ethylene or diethylene glycol.[3-6] 3-Fluoropropanol[4] was prepared from the 3-chloropropanol by treatment with potassium fluoride in ethylene glycol and the 3-fluoropropanol esters by interaction between the fluoroalcohol and acyl chlorides in dry carbon tetrachloride.

3-Fluoropropionic acid[7] was obtained by oxidation of 3-fluoropropanol and the *n*-alkyl fluoropropionates from the alcohols and 3-fluoropropionyl chloride.

The *n*-alkyl trifluoroacetates were prepared from trifluoroacetic acid and the alcohols.

Synthesis of ethyl 5-fluorovalerate was achieved by

$$\text{Tetrahydrofuran} \xrightarrow{HCl} Cl(CH_2)_4OH \xrightarrow{Br_2} Cl(CH_2)_4Br \xrightarrow{NaCN} Cl(CH_2)_4CN \xrightarrow{EtOH} Cl(CH_2)_4CO_2Et \xrightarrow{KF} F(CH_2)_4CO_2Et$$

All the compounds were refractionated immediately before the measurements were made and a check on purity was maintained by microanalyses and by vapor phase chromatography.

Physical Measurements

Density.—Standard methods were used with pycnometers of *ca.* 1 ml. capacity, and water thermostats with temperature control to ±0.05°.

Refractive Index.—The refractive index measurements were made at 20 ± 0.05° in either a Zeiss Pulfrich or a Bellingham and Stanley Pulfrich refractometer. An electric sodium lamp was used for the D-line, and a hydrogen-tube for the C and F lines.

Boiling Point.—All boiling points are corrected.

Calculations

The values shown in Table II for the specific refraction *r* have been calculated from the Lorentz–Lorenz expression

$$r = \frac{n^2 - 1}{n^2 + 2} \times \frac{1}{d}$$

using $n^{20}D$ and d^{20}_4. The values for the specific dispersions *S* shown in the same table have been calculated from the expression

$$S = \frac{n_1 - n_2}{d}$$

where n_1 and n_2 are refractive indices of a compound at two different wave lengths and *d* is the density, all at 20°.

A detailed description of calculations of the bond constants is not included in this report. In general the guiding principle has been the use from the literature of refractometric data for unfluorinated alkanes, alcohols, acids or esters. The (C–F) bond constants were obtained from the molar refraction of each fluoro-compound by subtracting the molar refraction of the unfluorinated homolog *minus* the appropriate number of (C–H) bond values.

Physical Constants.—Examination of Tables I, II and III shows several generalizations

1. (a) The mean (C–F) bond refraction is 1.55 in the fluoroalkanes, 1.55 in carboxylic esters of 3-fluoropropanol. The mean bond refraction rises to 1.76 in *n*-alkyl esters of 3-fluoropropionic acid (where F is in close proximity to carboxyl), falls to 1.53 in ethyl 5-fluorovalerate (where the F atom is remote from carboxyl) and rises to 1.88 in the *n*-alkyl esters of trifluoroacetic acid (where three F atoms are attached to a single carbon).

(b) There is a close correlation between the (isomeric) esters of 3-fluoropropanol and esters of 3-fluoropropionic acid. Both series show, with increasing molecular weight, a regular increase in specific refraction from 0.22 to 0.26; a regular decrease in density from 1.05 to 0.97 and specific dispersions which lie between 58 and 70.

(c) Ethyl 5-fluorovalerate (no. 23) is isomeric with 3-fluoropropyl butyrate (no. 13) and butyl 3-fluoropropionate (no. 20) and has a similar specific refraction, 0.243 (0.243 and 0.244); similar density, 1.002 (0.998 and 0.993), but a much higher specific dispersion, 91, (64 and 66).

(d) The acetylation of 3-fluoropropanol causes very little alteration in many of its physical constants. Thus, the fluoroalcohol and its acetate have comparable densities (1.04, 1.05); specific refraction (0.2236, 0.2230); specific dispersions (56, 58); refractive indices (1.381, 1.387); and (C–F) bond refractions (1.60, 1.52).

2. (a) The densities of all the ester series show a small regular *decrease* with increasing molecular weight.

(1) Croydon Technical College, Croydon, Surrey, England.

(2) G. H. Jeffery, J. Leicester, W. A. T. Macey and A. I. Vogel, *Chemistry & Industry*, 1045 (1954).

(3) F. W. Hoffman, *J. Am. Chem. Soc.*, **70**, 2596 (1948).

(4) F. W. Hoffmann, *J. Org. Chem.*, **15**, 425 (1950).

(5) J. Leicester, W. A. T. Macey and A. I. Vogel, *Org. Syntheses*, **36**, 40 (1956).

(6) F. L. M. Pattison and J. F. Millington, *Can. J. Chem.*, **34**, 757 (1956).

(7) E. Gryszkiewicz-Trochimowski, *Rec. trav. chim.*, **66**, 430 (1947).

TABLE I

PHYSICAL PROPERTIES OF LIQUID ORGANIC FLUORIDES

Compounds listed here are those designated by corresponding numbers in Table II.

	Compound	Formula	B.p., °C.	Pressure, mm.	Density d^{20}_4, g./cc.	Refractive index (20°) C	D	F
(1)	1-Fluoropentane[a]	$CH_3(CH_2)_4F$	64.1	760	0.7917	1.35818	1.35974	1.36385
(2)	1-Fluorohexane[b]	$CH_3(CH_2)_5F$	92.1	760	.8011	1.37308	1.37499	1.37920
(3)	1-Fluoroheptane[c]	$CH_3(CH_2)_6F$	119.3	760	.8060	1.38442	1.38611	1.39080
(4)	1-Fluorooctane[d]	$CH_3(CH_2)_7F$	144.4	760	.8137	1.39383	1.39552	1.40036
(5)	1-Fluorononane	$CH_3(CH_2)_8F$	167.9	760	.8159	1.40134	1.40330	1.40807
(6)	1-Fluorodecane	$CH_3(CH_2)_9F$	187.0	760	.8197	1.40745	1.40949	1.41439
(7)	1-Fluoroundecane[e]	$CH_3(CH_2)_{10}F$	71.2	3	.8239	1.41301	1.41507	1.42004
(8)	1-Fluorododecane	$CH_3(CH_2)_{11}F$	93.9	3	.8257	1.41714	1.41919	1.42424
(9)	1-Fluorotetradecane	$CH_3(CH_2)_{12}F$	120.4	2	.8277	1.42425	1.42639	1.43152
(10)	1-Fluorohexadecane[f]	$CH_3(CH_2)_{15}F$	150.8	2	.8313	1.43005	1.43222	1.43744
(11)	3-Fluoropropyl acetate[g]	$CH_3COO(CH_2)_3F$	137.6	760	1.0549	1.38488	1.38671	1.39107
(12)	3-Fluoropropyl propionate	$CH_3(CH_2)COO(CH_2)_3F$	153.7	760	1.0248	1.39192	1.39382	1.39827
(13)	3-Fluoropropyl butyrate	$CH_3(CH_2)_2COO(CH_2)_3F$	53.3	6	0.9985	1.39853	1.40076	1.40492
(14)	3-Fluoropropyl valerate	$CH_3(CH_2)_3COO(CH_2)_3F$	56.7	3	.9824	1.40523	1.40721	1.41195
(15)	3-Fluoropropyl caproate	$CH_3(CH_2)_4COO(CH_2)_3F$	72.2	3	.9684	1.41017	1.41216	1.41702
(16)	3-Fluoropropanol-1[h]	$FCH_2CH_2CH_2OH$	128.2	760	1.0393	1.37978	1.38150	1.38563
(17)	3-Fluoropropionic acid[i]	FCH_2CH_2COOH	78.4	8	1.2406	1.38927	1.39115	1.39557
(18)	Ethyl 3-fluoropropionate	$FCH_2CH_2COOCH_2CH_3$	133.1	760	1.0502	1.38391	1.38575	1.39015
(19)	*n*-Propyl 3-fluoropropionate	$FCH_2CH_2COO(CH_2)_2CH_3$	32.5	5	1.0160	1.39092	1.39280	1.39731
(20)	*n*-Butyl 3-fluoropropionate	$FCH_2CH_2COO(CH_2)_3CH_3$	44.1	4	0.9931	1.39808	1.40003	1.40465
(21)	*n*-Pentyl 3-fluoropropionate	$FCH_2CH_2COO(CH_2)_4CH_3$	60.2	4	0.9729	1.40392	1.40592	1.41068
(22)	*n*-Hexyl 3-fluoropropionate	$FCH_2CH_2COO(CH_2)_5CH_3$	74.5	5	0.9623	1.41050	1.41246	1.41729
(23)	Ethyl 5-fluorovalerate[j]	$F(CH_2)_4COOC_2H_5$	68.1	13	1.0022	1.40012	1.40209	1.40679
(24)	Ethyl trifluoroacetate[k]	$CF_3COOC_2H_5$	61.6	760	1.1908	1.30527	1.30657	1.30999
(25)	*n*-Propyl trifluoroacetate[l]	$CF_3COO(CH_2)_2CH_3$	82.5	760	1.1373	1.32224	1.32364	1.32705
(26)	*n*-Butyl trifluoroacetate[m]	$CF_3COO(CH_2)_3CH_3$	104.8	760	1.1085	1.33744	1.33906	1.34294
(27)	*n*-Pentyl trifluoroacetate	$CF_3COO(CH_2)_4CH_3$	64.7	79	1.0813	1.34972	1.35141	1.35531
(28)	*n*-Hexyl trifluoroacetate	$CF_3COO(CH_2)_5CH_3$	68.9	49	1.0623	1.35978	1.36153	1.36573
(29)	4-Chlorobutyl trifluoroacetate[o]	$CF_3COO(CH_2)_3CH_2Cl$	54.2	7	1.2695	1.38664	1.38845	1.39301
(30)	Trifluoroacetic acid[p]	CF_3COOH	72.2	760	1.4885	1.28317	1.28426	1.28693

[a] Hoffmann[8] reports b.p. 64.4°. [b] Hoffmann[3] reports b.p. 91.0–93.5°. [c] Swarts[9] reports b.p. 119°, $n^{21}D$ 1.3855 and d^{21}_4 0.8029. [d] Swarts[9-10] reports b.p. 142.5°, $n^{14}D$ 1.3970 and d^{14}_4 0.8120. [e] Gryszkiewicz-Trochimowski, *et al.*,[11] report b.p. 89–91° (12 mm.). [f] Swarts[9] reports b.p. 181° (24 mm.) and d^{13}_4 0.809. [g] Gryszkiewicz-Trochimowski, *et al.*,[11] report b.p. 137–138°. [h] Hoffmann[8] reports b.p. 127.5–128.0°, $n^{25}D$ 1.3771 and d^{25}_4 1.0390. [i] Gryszkiewicz-Trochimowski[7] reports b.p. 51–52° (2 mm.). [j] Saunders, *et al.*,[12] report b.p. 56–60° (16 mm.). [k] Swarts[13] reports b.p. 61.7°, $n^{15}D$ 1.30783 and d^{15}_4 1.19529. [l] Norton[14] reports b.p. 82.5°, $n^{22}D$ 1.3233, d^{25}_{25} 1.1285. [o] Because of some decomposition, physical constants should be regarded only as approximate. [p] Swarts[13] reports b.p. 72.4–72.5° and d^0_4 1.53515.

TABLE II

OPTICAL PROPERTIES OF LIQUID ORGANIC FLUORIDES

Compd. no.	Mol. wt.	Specific refraction r	Molar refraction MR_D	Specific dispersion $S \times 10^4$	(C–F) bond refraction (D-line at 20°)
1	90.14	0.2783	25.11	72	1.51
2	104.16	.2857	29.76	76	1.55
3	118.19	.2915	34.45	79	1.55
4	132.22	.2949	39.00	80	1.52
5	146.24	.2991	43.75	82	1.58
6	160.27	.3019	48.39	84	1.57
7	174.29	.3039	52.98	85	1.51
8	188.32	.3058	57.60	86	1.57
9	216.37	.3097	67.02	88	1.60
10	244.42	.3119	76.25	89	1.66
11	120.12	.2230	26.79	58	1.52
12	134.15	.2333	31.30	62	1.54
13	148.17	.2432	36.04	64	1.58
14	162.20	.2506	40.66	68	1.57
15	172.66	.2571	45.30	70	1.56
16	78.09	.2236	17.46	56	1.60
17	92.07	.1916	17.64	51	1.81
18	120.12	.2235	26.84	59	1.75
19	134.15	.2348	31.50	63	1.74
20	148.17	.2441	36.17	66	1.70
21	162.20	.2524	40.94	69	1.77
22	176.22	.2589	45.61	70	1.81
23	148.17	.2430	36.01	91	1.53
24	142.08	.1602	22.76	40	1.87
25	156.11	.1762	27.51	58	1.90
26	170.14	.1886	32.09	43	1.88
27	184.17	.1997	36.78	52	1.90
28	198.20	.2085	41.33	56	1.87
29	204.58	.1860	38.06	50	2.24
30	114.03	.1195	13.63	25	1.89

(b) A small regular *increase* in density with increasing molecular weight occurs in the fluoroalkanes.

(8) F. W. Hoffmann, *J. Org. Chem.*, **15**, 425 (1950).
(9) F. Swarts, *Bull. Acad. roy. Belg.*, **7**, 451 (1921).
(10) F. Swarts, *J. chim. phys.*, **17**, 68 (1921).
(11) E. Gryszkiewicz-Trochimowski, A. Sporzynski and J. Wnuk, *Rec. trav. chim.*, **66**, 413 (1947).
(12) F. J. Buckle, F. L. M. Pattison and B. C. Saunders, *J. Chem. Soc.*, 1471 (1949).
(13) F. Swarts, *Bull. Acad. roy. Belg.*, **8**, 343 (1922).
(14) T. R. Norton, *J. Am. Chem. Soc.*, **72**, 3527 (1950).
(15) R. N. Haszeldine, *Nature*, **168**, 1028 (1951).
(16) G. Rappaport, M. Hauptschein, J. F. O'Brien and R. Filler, *J. Am. Chem. Soc.*, **75**, 2695 (1953).

TABLE III

BOND AND GROUP CONSTANTS FOR (C–F) AND (CH_2); D-LINE AT 20°

Bond refractions (miscellaneous compounds): 3-fluoropropanol-1, 1.60; 3-fluoropropionic acid, 1.81; ethyl 5-fluorovalerate 1.53; trifluoroacetic acid, 1.89.

Series	Formula	No. compd. examined	Mean (C–F) bond refraction (cc.)	Stand dev. (cc.)	Mean (CH_2) group refraction (cc.)
n-Fluoroalkanes	RCH_2F	9	1.55	±0.03	4.646
Esters of 3-fluoropropanol	$RCH_2CO_2(CH_2)_3F$	5	1.55	± .02	4.638
Esters of 3-fluoropropionic acid	$F(CH_2)_2CO_2CH_2R$	5	1.76	± .01	4.660
Esters of trifluoroacetic acid	$CF_3CO_2CH_2R$	5	1.88	± .04	4.641

TABLE IV

INFRARED ABSORPTION FOR ALKYL TRIFLUOROACETATES

Ester	C=O group frequency (cm.$^{-1}$)
n-Propyl trifluoroacetate	1787
n-Butyl trifluoroacetate	1785
n-Pentyl trifluoroacetate	1787
n-Hexyl trifluoroacetate	1788

3. The specific refractions r as calculated by the Lorentz–Lorenz formula, using $n^{20}D$ and d^{20}_4, show definite trends in both mono- and trifluorides.

(a) For fluoroalkanes the specific refractions lie mainly between 0.28 and 0.31.

(b) For esters of 3-fluoropropanol and 3-fluoropropionic acid (all isomeric) the r values are slightly lower than for fluoroalkanes and show a gradual increase from 0.22 to 0.26. Ethyl 5-fluorovalerate also has an r value within this range.

(c) The specific refractions for *n*-alkyl esters of trifluoroacetic acid (0.16 to 0.20) are definitely lower than for monofluorides of comparable molecular weight.

4. The specific dispersions S were calculated from the expression

$$S = \frac{n_F - n_C}{d} \times 10^4$$

where n_F and n_C were the refractive indices at 20° taken for the F and C lines of the hydrogen spectra (6563 and 4861 Å., respectively), and d the density (d^{20}_4).

Like the refractions the specific dispersion values show definite trends in the compounds examined. (a) The fluoroalkanes have specific dispersions which increase fairly regularly from 72 to 89. (b) The S values for esters of 3-fluoropropanol and 3-fluoropropionic acid all lie between 58 and 70. (c) The introduction of three fluorine atoms on a single carbon as in the alkyl trifluoroacetates lowers the specific dispersion to values between 40–58, while trifluoroacetic acid itself has the very low value of 25.

Infrared Spectra.—Table IV gives the infrared spectra of the *n*-alkyl trifluoroacetates. A relatively large shift to higher frequencies of the carbonyl band when compared with the normal C=O band in unfluorinated esters is shown. There is a common absorption band at the region of 1788–1785 cm.$^{-1}$ (5.59 μ), whereas the normal band for C=O in unfluorinated esters is 1739 cm.$^{-1}$.

Similar shifts have been noted by Haszeldine in fluorocarbons containing a carbonyl group,[15] and by Hauptschein and co-workers[16] in an examination of esters formed from acids or alcohols, either or both of which had fluorocarbon groups. This shift is an accentuation of the shift observed when any electronegative group is attached to the carbonyl carbon and is explained in the simplest terms by the concept that the normal polarization of the carbonyl group as $\overset{\delta+}{C}=\overset{\delta-}{O}$ is cut down by the electronegative group attached to the carbon. The carbon–oxygen bond becomes less polar and consequently shows its stretching vibration at lower wave length.

Bond Refractions (D-line at 20°).—Examination of Table III shows that the "normal" value for the (C–F) bond refraction as derived from nine 1-fluoroalkanes is 1.55 (by normal value is meant a value applicable to systems where interactions between the functional groups are absent or small). The mean (CH_2) group refraction value (from least squares) for the fluoroalkane series is 4.646. This compares very well with the value 4.647 derived by Vogel from a series of alkanes.[17]

The mean value 1.55 for (C–F) derived from five esters of 3-fluoropropanol-1 shows excellent agreement with that determined from the fluoroalkanes. The mean (CH_2) group refraction for this series is 4.638.

The (C–F) bond refraction derived from 3-fluoropropionic acid and five of its *n*-alkyl esters was 1.76. The difference in (C–F) bond refraction in the fluoropropionates over that in the fluoroalkanes is 0.2[illegible] cc. and this increase is most readily explained in terms of the inductive effect of the fluorine substituent.

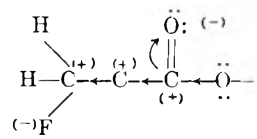

The inductive effect can act through the carbon chain and the enhanced positive character of the carbonyl carbon atom results in the mobile electrons of the alkoxy-bond (C–O) and to a certain extent, those of the carbonyl (>C=O) bond, being made available in the transmission of the inductive effect along the chain. The net result as evidenced by the bond refractions must be a looser electronic system than in the unfluorinated homologs. The mean (CH_2) group refraction for the series is 4.660.

The substitution of H by F in an ester produces an increase in molar refraction which is probably due to the inductive effect of the fluorine atom on the polarizable carboxylate group. If this is so, it follows that, because of the falling off in the in-

(17) A. L. Vogel, *J. Chem. Soc.*, 133 (1946).

ductive effect along the chain, the longer the chain the smaller is the increase in refraction. Ethyl 5-fluorovalerate was therefore selected as a compound in which a good separation of fluorine and the carboxylate group was present. It is of interest for this discussion to compare the (C–F) bond refraction for this fluoroester (1.53) with values obtained from 1-fluoroalkanes and some monofluoro-alcohols and esters:

Compound(s) R is alkyl	(C–F) bond refraction	Line	Ref.
RCH_2F	1.55	D	Present work
$RCO_2(CH_2)_2CH_2F$	1.55	D	Present work
$FCH_2(CH_2)_2OH$	1.60	C & D	Present work
$FCH_2(CH_2)_3CO_2C_2H_5$	1.53	D	Present work
FCH_2CH_2OH	1.59	C	Swarts[19]
$CH_3CO_2CH_2CH_2F$	1.71	D	Swarts[19]
$FCH_2CO_2C_2H_5$	1.75	D	Swarts[19]
$FCH_2CH_2CO_2R$	1.76	D	Present work

Of special interest in this comparison are the values for 2-fluoroethanol and its acetate. The (C–F) bond refraction in 2-fluoroethanol, 1.59, agrees with that for 3-fluoropropanol, 1.60. However, in their esters this agreement is lost. Thus, the mean (C–F) value in the 3-fluoropropyl carboxylates is 1.55 (1.52 for 3-fluoropropyl acetate itself), whereas for 2-fluoroethyl acetate it is 1.71. Evidently the influence on the carboxylate group of the fluorine substituent in the alcoholic portion of the molecule can extend over one methylene group, so approaching the (C–F) bond refraction value when F is present in the acid portion, but cannot extend over two methylene groups.

It is also evident that when a fluorine atom is present in the acidic function the (C–F) bond refraction is greater than when it is in an alcoholic function. This is so when the fluorine atom in the acid portion of an ester is (a) in the α-position to the carboxylate group, as in ethyl monofluoroacetate, or (b) in the β-position to the carboxylate group, as in the alkyl 3-fluoropropionates. The lower refraction in the alcoholic molecules is illustrated when fluorine is (c) β to the hydroxyl group, as in 2-fluoroethanol, or (d) γ- to the hydroxyl group, as in 3-fluoropropanol.

Since the (C–F) bond refraction in ethyl 5-fluorovalerate is 1.53, *i.e.*, close to the 1.55 value, it can be assumed that normal refraction values are to be expected in fluoroesters in which the substituent fluorine atom is at least three methylene groups removed from the carboxylate group.

The first refractometric study of fluorine compounds was made by Swarts[19] who studied a large number of simple fluoro-compounds. More recent studies[20–22] have been concerned with fluorocarbons. Grosse and Cady[22] have shown how the atomic refraction varies with the type of compound. From these values the corresponding (C–F) bond refractions can be calculated and are here added to the original table:

TABLE V

VARIATION OF ATOMIC REFRACTION WITH SUCCESSIVE FLUORINE SUBSTITUTION

						Aliphatic perfluoro compd.
No. of F atoms/mole	1	2	3	4	5	
Atomic refraction (AR_F)	0.95	0.99	1.02	1.08	1.14	1.23
(C–F) bond refraction	1.60	1.64	1.67	1.73	1.79	1.88

A study of the CF_3– group in the alkyl trifluoroacetates was made in order to obtain values for the (C–F) bond refraction when three fluorine atoms are attached to one carbon. Thus, the (C–F) bond refraction (from one-third of the trifluoromethyl group refraction in the trifluoroacetates) is 1.88.

The difference in (C–F) bond refraction in the trifluoroacetates over that in the fluoroalkanes is 0.33 cc. Now if the CF_3– group is not attached to carboxylate then the (C–F) refraction is lower than when it is so attached. Thus, the additional molar, and hence the bond refraction resulting from the presence of adjacent electron-attracting CF_3– and CO_2R groups is present in a non-carboxylic compound such as 2,2,2-trifluoroethanol. The (C–F) bond refraction calculated from data[18] for CF_3CH_2OH is 1.79 whereas in the present work a mean (C–F) bond value of 1.88 was obtained from five alkyl trifluoroacetates, CF_3CO_2R. Two effects must operate in giving increased (C–F) bond refractions in these esters. These are the inductive influence of CF_3– on the carboxylate group and the increase, as shown in Table V, which follows the progressive substitution of hydrogen by fluorine in a molecule. Presumably the increase in the number of adjacent negative charges, due to the fluorine atoms, must loosen the electronic system and so give rise to an increase in the refraction while the large inductive effect of CF_3–, as with a single fluorine in the 3-fluoropropionates, adds still further to this refraction increase.

Acknowledgments.—The author is indebted to Dr. J. D. Mounfield of the National College of Food Technology and Dr. A. I. Vogel of The Woolwich Polytechnic for the provision of materials and research facilities; to Dr. W. E. Silberman and Mr. P. Snelling for technical help; and Professor R. N. Haszeldine for micro-analysis of the trifluoroacetates.

(18) A. Henne and C. J. Fox, *J. Am. Chem. Soc.*, **76**, 479 (1954).
(19) F. Swarts, *J. chim. phys.*, **20**, 30 (1923).
(20) R. N. Haszeldine and F. Smith, *J. Chem. Soc.*, 603 (1951).
(21) R. D. Fowler, J. M. Hamilton, J. S. Kasper, C. E. Weber, W. B. Burford and H. C. Anderson, *Ind. Eng. Chem.*, **39**, 375 (1947).
(22) A. V. Grosse and G. H. Cady, *ibid.*, **39**, 367 (1947).

A STUDY OF SILVER IODIDE COMPLEXES IN WATER SOLUTIONS BY SELF-DIFFUSION MEASUREMENTS

BY E. BERNE AND M. J. WEILL

Contribution from the Department of Inorganic Chemistry, Chalmers Institute of Technology, and the Swedish Institute of Silicate Research, Gothenberg, Sweden

Received November 21, 1958

The silver iodide complexes Ag_mI_n have been studied by means of self-diffusion measurements, at an approximately constant ionic strength equal to 4 *M*. It was shown that there is no condensation into polynuclear complexes on the cationic complexes side of the system. The plot of *D vs.* c_{Ag} for the anionic complexes exhibits a minimum for $c_{Ag} = 0.60$ *M*. This result could be interpreted in terms of the model suggested in earlier works: a series of polynuclear complexes $Ag_mI_{2m+2}^{(m+2)-}$ is formed as the silver concentration increases, but the chain formation is cut off by a ring closure of the type $Ag_mI_{2m}^{m-}$. Evidence is given here that no greater ion than $Ag_4I_8^{4-}$ exists in saturated solutions and that, consequently, it is probable that the chain formation does not exceed the term $Ag_4I_{10}^{6-}$, contrary to what has been claimed in other papers. This condensation model is in agreement with recent X-ray scattering studies.

The silver iodide complexes Ag_mI_n have been studied mainly by Leden, who made potentiometric[1] and solubility[2,3] measurements in aqueous solutions at 25°, and by Nilsson who investigated water solutions of the complexes by X-ray scattering.[4] The cationic complexes ($m > n$) have only been studied with solubility measurements. Therefore, the question of the condensation into polynuclear complexes has not yet been elucidated for this system. On the anionic complexes side, ($n > m$), the potentiometric and solubility data have shown that a condensation phenomenon takes place as the silver concentration increases, but both methods failed to resolve completely the structure of the polynuclear complexes.

We have therefore studied the mobility of these complexes in aqueous solutions, by means of self-diffusion measurements, in order to see whether further information about the structure of Ag_mI_n complexes could be obtained in that way.

Starting from Fick's fundamental diffusion equations, it can be shown that, if the isotopic exchange equilibrium is instantaneously established, the self-diffusion coefficient $\bar{D}$ measured in a mixture of various complexes AB_i (the molar fraction of which is respectively α_i) is a mean value of the self-diffusion coefficients D_i of each pure species

$$\bar{D} = \Sigma \alpha_i D_i$$

The purpose of the following work was then to study, by means of the open-ended capillary method, the variations of $\bar{D}$ at 25°, when the iodide (or silver) concentration increases continually up to saturation, the total silver (or iodide) concentration being kept constant and equal to 4 *M*.

Experiments on the cationic complexes side were performed with ^{131}I as tracer, and on the anionic complexes side with ^{110}Ag.

Experimental

Diffusion Cells.—The open-ended capillary method, as modified by Wang[5] and by Mills[6] requires very large volumes of inactive solution. In order to decrease this volume when expensive solutions, such as 4 *M* $AgClO_4$, are involved, we have adopted in this work a modified type of diffusion cell, in which the required volume of inactive solution is reduced to 50 ml.

The cells, made of ordinary glass, consist of 2 superimposed coaxial cylinders, fitted together by a conical section. The upper cylinder (diameter 3.5 cm., length 7.5 cm.) contains the inactive solution, and the lower one (diameter 1 cm., length 2 cm.) contains the capillary and keeps it in a vertical position. The cells were covered with a glass top, and immersed in a conventional thermostat at 25 ± 0.01°.

A very important problem, which has been discussed by most of the authors, is that of the stirring. In order to fulfill one of the boundary conditions of the method, *i.e.*, to keep the concentration of the radioactive isotope equal to zero at the mouth of the capillary, all authors have come to the conclusion that it is necessary to stir the outer solution. But an important source of error can arise if the stirring is too rapid or turbulent, in which case part of the active solution can be swept out of the capillary by mechanical convection. This phenomenon has been called by Wang the "Δl-effect," as it may be primarily looked upon as a change in the effective diffusion path. A negative "Δl-effect," arising from excessive or turbulent sitrring, leads to a measured value of the diffusion coefficient which is too high. On the other hand, a positive "Δl-effect" provoked by insufficient stirring, leads to a measured value which is too low. It must be noted however that the "Δl-effect" errors are of the same order of magnitude as the precision of the method itself (1 to 2%) and that no appropriate method of measuring it accurately has been suggested up to now.

Preliminary experiments have been made in order to investigate the influence of the stirring speed on the measured value of $\bar{D}$, for the geometrical conditions of our cells. For this purpose, a glass stirrer was placed along the axis of the cell, its lower extremity being 3 cm. above the upper end of the capillary. No difference in $\bar{D}$ has been observed, inside the limits of error of the method (±1%), whether the outer solution was stirred mechanically (50–60 r.p.m.) or when a slight thermal convection was established in the bath (the small temperature gradient was created by keeping the liquid level in the cell 1 cm. higher than the water level in the thermostat. It did not affect the temperature of the capillary in the bottom of the cell, but was sufficient for maintaining the required boundary condition). Hence, all further experiments have been performed without mechanical stirring but with thermal convection.

Manipulations.—The capillaries had internal and external diameters of 0.08 and 0.9 cm., respectively, and a length of *ca.* 4 cm. Before use, each capillary was examined under a microscope to ensure that the bore was uniform. A glass seal was then made at one extremity and the length was measured with a micrometer to an accuracy of 0.1 mm. The capillary was filled with the radioactive solution by means of a thin capillary pipet operated with a medical syringe. A small drop of active solution was deposited on the top of the capillary in order to avoid, as far as possible, convection disturbances during the lowering of the tube in the bath. At first, only 1/5th of the capillary length was immersed in the cell, for half an hour, in order to establish temperature equilibrium. Finally, the tube was gently lowered to the bottom of the cell. After 9 or 10 days, the capillary was taken out of the cell and its contents, with-

(1) I. Leden, *Acta Chem. Scand.*, **10**, 540 (1956).
(2) I. Leden, *ibid.*, **10**, 812 (1956).
(3) I. Leden and C. Parck, *ibid.*, **10**, 535 (1956).
(4) R. O. Nilsson, *Arkiv Kemi*, **12**, 513 (1958).
(5) J. H. Wang, *J. Am. Chem. Soc.*, **73**, 510 (1951).
(6) R. Mills, *ibid.*, **77**, 6116 (1955).

drawn by means of a capillary pipet, were transferred to a special test-tube fitting into the well crystal of a conventional scintillation counter. Five rinsing fractions were added to the test-tube, the liquid level of which then was adjusted to a standard height.

The initial capillary activity was measured by refilling the capillary with the active solution, after having rinsed it five times with the same active solution. The withdrawal of the capillary contents was made as previously described. This operation was repeated 3 times for each capillary, since the deviation between 2 such refillings can amount to 1%. The mean value was adopted for the calculation of $\bar{D}$ according to equation 1

$$\bar{D} = \frac{4l^2}{\pi^2 t} \ln\left(\frac{8}{\pi^2} \times \frac{c_0}{\bar{c}}\right) \qquad (1)$$

l being the capillary length, $\bar{c}$ the average concentration of the radioactive isotope in the capillary after the time t, and c_0 the initial concentration. $\bar{c}$ and c_0 were measured after one another in order to avoid corrections for radioactivity decay, and for apparatus stability.

Solutions.—As solubility and potentiometric data are related to complex solutions of constant ionic strength equal to 4 M, self-diffusion also has been measured in identical media. All experimental operations (preparation of solutions and diffusion runs) were performed in a dark room, because of the instability of concentrated $AgClO_4$ and NaI in day light.

a. **Cationic Complexes Region.**—4 to 5 M silver perchlorate solutions were prepared by precipitating Ag_2O from a hot $AgNO_3$ solution with NaOH. The precipitate was filtered on fritted glass, washed 10 times with water and dissolved in 70% $HClO_4$. After filtration, the solution was titrated with a cationic exchange method (Dowex). The measured solutions had a total silver concentration equal to 4 M and a total iodide concentration up to 0.1 M. Iodide ions were introduced as NaI.

The active solutions were prepared by adding 5 μl. of a carrier-free ^{131}I solution (specific activity 5 mc./ml.) provided by The Isotope Division AERE, Harwell, England, to 10 ml. of the complex solution. Preliminary experiments have shown that the isotopic exchange equilibrium is established instantaneously and, hence, that the observed value of $\bar{D}$ does not depend on the age of the solutions investigated.

b. **Anionic Complexes Region.**—The complexes solutions had an iodide concentration equal to 4 M (I^- was introduced as NaI) and a silver concentration varying from 0.01 to 0.65 M (Ag^+ was introduced as $AgNO_3$). The silver concentration of the saturated solution is 0.7 M.

^{110}Ag was delivered by the Isotopes Division, AERE, Harwell, England, as metallic silver. The silver was first dissolved in hot concentrated nitric acid, and the solution evaporated 5 times to dryness. The pure radioactive silver nitrate then was dissolved in water. The radioactive complexes solutions were prepared by adding 5 μl. of the $^{110}AgNO_3$ solution (concentration 0.93 M, specific activity 1 mc./ml.) to 10 ml. of the complex solutions. The active silver thus added amounted to 5×10^{-4} mole Ag/l. As this quantity is not negligible when the total silver concentration is 0.01 M, the same relative amount of inactive $AgNO_3$ was added to the inactive solutions.

Results

In Tables I and II are listed the self-diffusion coefficients of cationic and anionic complexes, respectively. Each value reported is the average value of 3 to 4 measurements, and the error tabulated corresponds to the root mean square deviation between them. Figure 1 represents the plot of $\bar{D}$ *vs.* c_{Ag} for the anionic complexes.

TABLE I

SELF-DIFFUSION COEFFICIENTS AT 25° OF SILVER IODIDE CATIONIC COMPLEXES IN WATER SOLUTIONS, OF TOTAL SILVER CONCENTRATION 4 M

Iodide concn., moles/l. NaI	$D \times 10^5$, cm.²/sec.
0.01	0.539 ± 0.006
0.10	0.526 ± 0.014

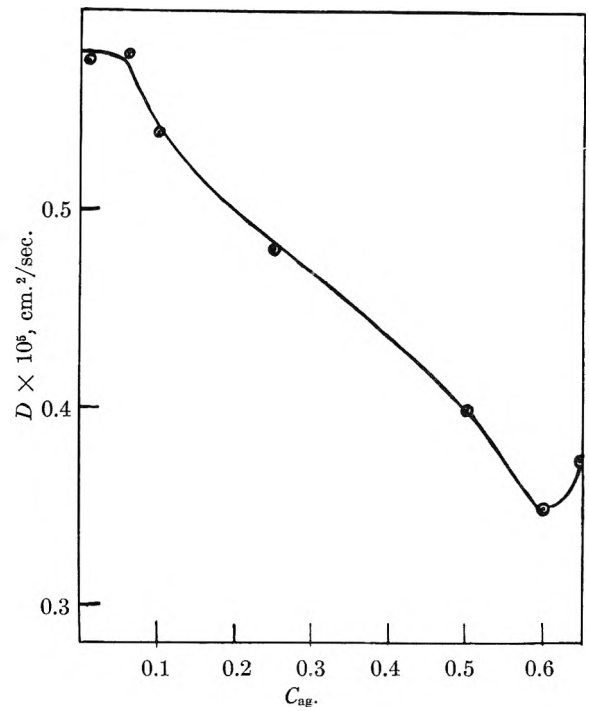

Fig. 1.—Self-diffusion coefficients at 25° of silver iodide anionic complexes in aqueous solutions of total iodide concentration 4 M.

TABLE II

SELF-DIFFUSION COEFFICIENTS AT 25° OF SILVER IODIDE ANIONIC COMPLEXES IN WATER SOLUTIONS OF TOTAL IODIDE CONCENTRATION 4 M

Silver concn., moles/l. $AgNO_3$	$D \times 10^5$, cm.²/sec.
0.01	0.575 ± 0.004
.06	.579 ± .005
.10	.539 ± .003
.25	.480 ± .003
.50	.399 ± .009
.60	.349 ± .001
.65	.374 ± .006

Discussion

Cationic Complexes.—On the cationic complexes side, an unexpected experimental difficulty arose, since in spite of all care taken the solutions were still unstable, and deposited micrograins of metallic silver in the capillaries during the diffusion runs. Hence the accuracy of the measurements was somewhat lower than that corresponding to the usual precision of the method.

Our results show, however, that in the concentration range 0.01 to 0.1 M in iodide, the diffusing particles have the same mobility and hence the same size. One may then conclude that no condensation phenomenon takes place, as the composition of the solutions increases up to saturation. This conclusion is further corroborated by the fact that orientation experiments performed in solutions of concentration 10^{-5} M in iodide yielded approximately the same diffusion coefficient.

Anionic Complexes.—The mean diffusion coefficient $\bar{D}$ is approximately constant in the concentration range $0.01 \leqslant c_{Ag} \leqslant 0.06$ M. As the silver concentration increases from 0.06 up to 0.60 M, the mean mobility of the complexes decreases

regularly, as may be seen in Fig. 1. In the most concentrated solutions ($c_{Ag} > 0.50\ M$), the self-diffusion coefficients exhibit a tendency to increase slightly again. Although this increase is relatively small (from 0.35 to 0.37 $\times$ 10^{-5} cm.^{2}/sec.), it corresponds to a deviation in $\bar{D}$ which is higher than the root mean square deviation of our measurements. One may then conclude that this unexpected result corresponds to a real phenomenon.

Leden's potentiometric and solubility measurements gave evidence for the formation of polynuclear complexes. The potentiometric measurements, performed only in the low concentration range $0.003 \leqslant c_{Ag} \leqslant 0.08$, could be interpreted by assuming the presence of AgI_3^{2-}, AgI_4^{3-}, $Ag_2I_6^{4-}$ and $Ag_3I_8^{5-}$. In saturated solutions, solubility measurements gave evidence for the presence of more condensed complexes. But the method failed to show whether an infinite series of complexes $Ag_mI_{2m+2}^{(m+2)-}$ was formed, or a series of such complexes, cut off at some high condensation step, by a ring closure of the type $Ag_mI_{2m}^{m-}$. Existence of such high complexes as $Ag_{12}I_{24}^{12-}$ has been discussed. Nilsson's X-ray scattering data could be interpreted in terms of both models suggested by Leden with the same accuracy: one of them was a chain model built up by tetrahedra sharing edges, and the other was a symmetrical ion $Ag_4I_8^{4-}$ built up from 4 silver iodine tetrahedra, each sharing three edges with the others.

From his potentiometric data, Leden has calculated that the complexes distribution in a solution of silver concentration $c_{Ag} = 0.01\ M$ is: AgI_4^{3-} = 90% and AgI_3^{2-} = 10%. As both complexes have the same type of structure, the use of Riecke–Graham's formula

$$D\sqrt{M} = \text{constant} \qquad (2)$$

may be justified in our case.

Although this law is only fully valid for the limiting cases of molecules diffusing in a gas, and colloidal particles in a solution, it may be extended, in first approximation, to the case of ions diffusing in electrolytic solutions, as has been done by Andersson and Saddington.[7]

With the help of equations 1 and 2 it is then possible to calculate a rough approach of the true self-diffusion coefficients of the pure complexes. The value of $\bar{D}$ computed for this calculation was $\bar{D} = 0.57\ 7 \times 10^{-5}$ cm.^{2}/sec. We found in that way

$$D_{AgI_3^{2-}} = 0.640 \times 10^{-5} \text{ cm.}^2/\text{sec.}$$
$$D_{AgI_4^{3-}} = 0.570 \times 10^{-5} \text{ cm.}^2/\text{sec.}$$

Since the ion $Ag_4I_8^{4-}$ has also a tetrahedral structure, it is possible to calculate in the same way what its own self-diffusion coefficient would be. The value thus obtained is 0.370×10^{-5} cm.^{2}/sec., and agrees fairly well with the experimental value of $\bar{D}$ found in the solutions of silver concentration 0.65 M, *i.e.*, 0.374×10^{-5} cm.^{2}/sec. Although one must be very careful in applying the formula $D\sqrt{M}$ = Constant if the complexes involved have a chain structure, since the mobility of a chain aggregate is probably lower than the one of a spherical ion of the same weight, one may, however, calculate an upper limit for $\bar{D}$ when the presence of more condensed ions is assumed. For example, a mixture of 80% $Ag_4I_8^{4-}$ and 20% $Ag_4I_{10}^{5-}$ should diffuse with a maximum mean velocity corresponding to $\bar{D} = 0.360 \times 10^{-5}$ cm.$^-$/sec., which is notably lower than our experimental value for $c_{Ag} = 0.65\ M$. One then may conclude that no complex greater than $Ag_4I_8^{4-}$ exists in saturated solutions.

The minimum observed in $\bar{D}$ can be explained in the following way. As the silver concentration increases, there first occurs a condensation into polynuclear complexes $Ag_mI_{2m+2}^{(m+2)-}$ which have a chain structure. When c_{Ag} reaches 0.60 M, the chain formation is cut off, and the symmetrical ion $Ag_4I_8^{4-}$ gradually is formed. The minimum $\bar{D}$ value 0.35×10^{-5} cm.^{2}/sec. is inferior to the self-diffusion coefficient of $Ag_3I_8^{5-}$ calculated in the same way as previously described: 0.39×10^{-5} cm.^{2}/sec. This fact may be attributed to two factors. Firstly, since $Ag_3I_8^{5-}$ has a chain structure, its self-diffusion coefficient probably is lower than the one calculated here. It is however impossible to say how much lower it really is. Secondly, the presence of higher terms of the condensation series is not excluded. From the value itself of $\bar{D}_{min}$ it is not possible to deduce any indication about the upper limit of m. But, as $\bar{D}$ increases after the minimum until a value fitting very well $D_{Ag_4I_8^{4-}}$ it may be probable that the chain formation is already cut off at the early step $m = 4$, since the most plausible mechanism leading to the formation of $Ag_4I_8^{4-}$ is, as previously suggested by Leden

$$Ag_4I_{10}^{6-} \rightleftharpoons Ag_4I_8^{4-} + 2I^-$$

The question might arise whether the increasing amounts of high valency ions lead to an important change in the ionic strength of the investigated media, and to what extent this variation of the diffusing ions environment affected the diffusion coefficients. It is impossible to evaluate the magnitude of such an effect but, in our experiments, the relative variations of the total ionic strength are small enough to allow us to neglect them, in comparison with the consistant variations in D arising from the mass variation of the diffusing ions.

The model suggested above is in agreement with Nilsson's results.

But Leden's solubility measurements cannot be interpreted in terms of $Ag_4I_8^{4-}$. One must, however, keep in mind that the validity of the solubility measurements is dependent on the constancy of the ionic strength of the media. In Leden's work, it may be doubtful if this condition could be regarded having been fulfilled. The present work supports this argument. If one assumes that only AgI_4^{3-} and $Ag_4I_8^{4-}$ are to be found in a solution of silver concentration 0.65 M, it is possible to calculate a rough upper limit for the concentration of AgI_4^{3-} existing in solution. The presence of such ions as $Ag_2I_6^{4-}$ or $Ag_3I_8^{5-}$ could only decrease the result thus obtained. It was found in that

(7) J. S. Andersson and K. Saddington, *J. Chem. Soc.*, 5381 (1949).

way that the maximum proportion of AgI_4^{3-} is only 2% for $c_{Ag} = 0.65\ M$, whilst Leden reports a value of 10% in a saturated solution corresponding to $c_{Ag} = 0.70\ M$.

Acknowledgments.—The authors are grateful to Professor C. Brosset for his constant interest in the present work. They also wish to thank Dr. R. Nilsson who kindly allowed them to use his ion-exchange titration equipment, and Mr. Åkeström who constructed the thermostat.

THE DETERMINATION OF ACTIVITY COEFFICIENTS OF HYDROCHLORIC ACID AND *p*-TOLUENESULFONIC ACID IN MIXED AQUEOUS SOLUTIONS FROM ELECTROMOTIVE FORCE MEASUREMENTS

BY O. D. BONNER AND LINDA LOU SMITH[1,2]

Department of Chemistry, University of South Carolina, Columbia, South Carolina

Received October 5, 1959

Activity coefficients of hydrochloric acid and *p*-toluenesulfonic acid have been determined at 25° in binary aqueous solutions up to concentrations of 5 molal by electromotive force measurements of the cells Pt, H_2/HCl(m_1), *p*-TSA(m_2)/AgCl(s) Ag. The mole ratios of hydrochloric acid to *p*-toluenesulfonic acid ranged from 4.95 to 0.27. The results show that at constant total molality the activity coefficients of HCl are decreased by the addition of *p*-toluenesulfonic acid, while the activity coefficients of *p*-toluenesulfonic acid are increased by the addition of hydrochloric acid. Both components obey Harned's rule approximately in dilute and in moderately concentrated solutions, but in solutions of very high ionic strength deviations from Harned's rule become quite marked.

The determination of activity coefficients in solutions of mixed electrolytes is of special interest to one of the authors due to the fact that such knowledge is essential for the interpretation of ion-exchange equilibria processes.[3-5] For example, when a sulfonated polystyrene divinylbenzene type resin such as Dowex-50 is immersed in an aqueous electrolyte solution, a number of processes occur in order to establish equilibrium conditions. First, the strongly polar exchange groups and their counterions attract the solvent molecules, and the resin network swells to accommodate this water. Cations and anions from the external solution phase pass into the internal resin phase, and at equilibrium all of the ions except the structurally bound sulfonate anions are present in both phases. These conditions are those necessary for the establishment of a Gibbs–Donnan type equilibrium in which the resin particle acts as its own membrane; and a rigorous application of the Gibbs–Donnan theory requires a knowledge of the activity coefficients of the inbibed electrolyte as well as those of the resinate itself. Boyd and Larson[6] have investigated the Donnan uptake of HCl by the hydrogen form of Dowex-50 as a function of divinylbenzene (DVB) content of the resin and of the concentration of HCl in the external solution. Their results indicate that the activity coefficient of HCl in the concentrated resin phase is lower than that of HCl in its pure aqueous solutions at the same total molality of hydrogen ion as exists in the resin phase and also that the activity coefficient of the hydrogen resinate is lowered by the entry of HCl into the resin. In order to compare their results with those of a system in which it is possible to apply exact thermodynamic methods over a wide range of concentrations, it was decided to investigate mixtures of HCl and *p*-toluenesulfonic acid (*p*-TSA). This is a system which, to a first approximation, represents the internal gel electrolyte phase in that *p*-toluenesulfonic acid is similar in structure to the monomeric units of the ion exchange polymer but which has the advantage of being more flexible due to the solubility of the *p*-TSA.

The activity coefficients of HCl in the aqueous mixtures were determined directly from electromotive force measurements of the cells

$$\text{Pt, } H_2/\text{HCl}(m_1),\ p\text{-TSA}(m_2)/\text{AgCl, Ag}$$

The over-all reaction for this cell is

$$\tfrac{1}{2}H_2 + \text{AgCl} \longrightarrow \text{Ag} + \text{HCl}(m_1)$$

and $(\gamma\pm)_{HCl}$ can be calculated from the Nernst expression

$$E = E^0 - \frac{RT}{F} \ln(m\pm\gamma\pm)^2_H$$

The calculation of values of $\gamma\pm$ *p*-TSA are somewhat more involved but an equation for their calculation may be derived by the use of cross-differentiation.[7] From the fundamental expression

$$d\overline{G} = -\bar{S}\,dT + \bar{V}\,dP + \mu_1 dn_1 + \mu_2 dn_2 + \mu_w dn_w \quad (1)$$

one may obtain the cross-differentiation relation

$$\left(\frac{\partial \ln \mathcal{A}_1}{\partial n_2}\right)_{n_1,\ n_w} = \left(\frac{\partial \ln \mathcal{A}_2}{\partial n_1}\right)_{n_2,\ n_w} \quad (2)$$

or the equivalent expression

(1) These results were developed under a project sponsored by the United States Atomic Energy Commission.

(2) Part of the work described herein was included in a dissertation submitted by Linda Lou Smith to the University of South Carolina in partial fulfillment of the requirements for the degree of Doctor of Philosophy.

(3) O. D. Bonner, W. J. Argersinger and A. W. Davidson, *J. Am. Chem. Soc.*, **74**, 1047 (1952).

(4) O. D. Bonner and F. A. Unietis, *ibid.*, **75**, 511 (1953).

(5) O. D. Bonner and V. F. Holland, *ibid.*, **77**, 5833 (1955).

(6) G. E. Boyd and Q. V. Larson, "The Gibbs-Donnan Model for Ionic and Solvent Equilibria with Organic Ion-Exchange Polymers," presented before Symposium on Complex Ions and Polyelectrolytes, American Chemical Society, Ithaca, New York, June 18–21, 1951.

(7) (a) H. A. C. McKay, *Nature*, **169**, 464 (1952); (b) H. A. C. McKay and J. K. Perring, *Trans. Faraday Soc.*, **49**, 163 (1953).

$$\left(\frac{\partial \log \gamma_1}{\partial n_2}\right)_{n_1,\, n_w} = \left(\frac{\partial \log \gamma_2}{\partial n_1}\right)_{n_2,\, n_w} \quad (3)$$

Introducing the molalities m_1 and m_2 the expression

$$\left(\frac{\partial \log \gamma_1}{\partial m_2}\right)_{m_1} = \left(\frac{\partial \log \gamma_2}{\partial m_1}\right)_{m_2} \quad (4)$$

is obtained. At constant molality m_2

$$d \log \gamma_2 = \left(\frac{\partial \log \gamma_1}{\partial m_2}\right)_{m_1} dm_1 \quad (5)$$

which upon integration holding the molaity m_2 constant gives

$$\log \gamma_2 = \log \gamma_2^0 + \int_0^{m_1} \left(\frac{\partial \log \gamma_1}{\partial m_2}\right)_{m_1} dm_1 \quad (6)$$

where γ_2^0 is the mean activity coefficient of component 2 in its pure solution of the same molality m_2 at which it is present in the mixture.

Experimental

Electrodes.—Silver–silver chloride electrodes were prepared by a procedure similar to that of Shedlovsky and MacInnes.[8] A small piece of silver foil was first electrolyzed in a solution of potassium silver cyanide at 4 mamp. for 24 hours; then, in a dilute hydrochloric acid solution for an hour or longer at 4 to 6 mamp. The electrodes were then rinsed in distilled water and allowed to age in dilute HCl for at least a week before being used. When not in use, the electrodes were stored in dilute HCl.

Hydrogen electrodes were freshly prepared immediately before each period of use. A finely divided deposit of platinum black was obtained by electrolysis of a 5% chloroplatinic acid solution with platinum wire as cathode at a high current density for several minutes. The electrode, still as cathode was next electrolyzed in a dilute sulfuric acid solution to saturate it with hydrogen. Before being used the electrode was rinsed, first with distilled water, then with some of the solution which was being used in the cell.

Description of Cell and Measurements.—The Pt, H_2/HCl(m_1),p−TSA(m_2)/AgCl, Ag cell consisted of two compartments: one containing the silver–silver chloride electrode; the other, the bubbling hydrogen electrode. Deoxygenation of the solutions is essential in order to prevent the hydrogen electrode from becoming poisoned. This was accomplished by allowing H_2 gas, which was first passed through a series of saturators, to bubble through the solution in the cells. The electrodes were then placed in the cells, and the potential was recorded until it became steady. In some of the more concentrated solutions it was necessary to bubble hydrogen through the solutions for as long as 10 hours before inserting the electrodes in order to obtain a constant potential.

Apparatus.—For the electromotive force measurements a Leeds and Northrup galvanometer with a sensitivity of 5×10^{-4} μ amp. per mm. was used in conjunction with a Rubicon potentiometer. All e.m.f. measurements were made in a constant temperature bath maintained at 25 ± 0.05°.

Standardization of Solutions.—The total hydrogen ion concentrations of the mixtures was determined by titration with standard base employing phenolphthalein as indicator. The chloride ion concentration was determined by titrating with silver nitrate, dichlorofluorescein serving as indicator. The concentration of p-toluenesulfonic acid was then obtained by difference.

Discussion

The observed potentials, corrected to a partial pressure of one atmosphere for the hydrogen gas, are given in Table I for the various mixtures. The values of γ_{HCl}, obtained from these primary data, are presented as a function of the total ionic strength of the solution in Table II for different mole ratios of HCl to p-TSA. The activity coefficients of HCl in its pure aqueous solutions were obtained from the tables of Robinson and Stokes.[9] The calculated values of $\gamma_{p\text{-TSA}}$ as a function of concentration for the various ratios is shown in Table III, the activity coefficients of p-toluenesulfonic acid in its pure solutions having been obtained from the data of Bonner, Easterling and Holland.[10]

TABLE I

E.M.F. DATA (CORRECTED TO A PARTIAL PRESSURE OF 1 ATM. FOR H_2 GAS) FOR THE CELLS: Pt, H_2/HCl(m_1), p- TSA(m_2)/AgCl, Ag

$\frac{m_{HCl}}{m_{p\text{-TSA}}}$	μ	E (cor.)
4.938	6.046	0.1648
	5.372	.1740
	4.150	.1937
	2.525	.2166
	1.353	.2306
	0.6786	.2365
	.3108	.2377
	.1513	.2356
	.0738	.2336
	.0645	.2328
	.0099	.2276
	.0049	.2263
2.151	6.078	.1670
	5.022	.1830
	4.043	.1968
	2.947	.2119
	1.988	.2241
	0.9642	.2339
	.4840	.2379
	.2419	.2361
	.1200	.2343
	.0598	.2320
	.0099	.2273
1.021	6.032	.1717
	5.034	.1870
	4.012	.1997
	3.039	.2123
	2.062	.2254
	1.024	.2347
	0.4994	.2372
	.2490	.2374
	.1065	.2348
	.0526	.2326
	.0105	.2279
0.270	6.120	.1788
	5.094	.1916
	4.020	.2050
	2.956	.2183
	1.983	.2276
	1.002	.2350
	0.5016	.2375
	.2518	.2365
	.1019	.2336

From these data it is apparent that the activity coefficient of HCl decreases as the mole per cent. of p-TSA increases at constant molality. This is in contrast to the behavior of the HCl–$HClO_4$ system[11] where the activity coefficient of HCl is

(8) T. Shedlovsky and D. A. MacInnes, *J. Am. Chem. Soc.*, **58**, 1970 (1936).

(9) R. A. Robinson and R. H. Stokes, "Electrolyte Solutions," Butterworth Scientific Publications, London, 1955, pp. 476, 489.

(10) O. D. Bonner, G. D. Easterling, D. L. West and V. F. Holland, *J. Am. Chem. Soc.*, **69**, 2818 (1947).

(11) P. G. Murdock and R. C. Barton, *ibid.*, **55**, 4074 (1933).

TABLE II

ACTIVITY COEFFICIENTS OF HYDROCHLORIC ACID AS A FUNCTION OF COMPOSITION IN AQUEOUS MIXTURES OF *p*-TOLUENESULFONIC ACID AND HYDROCHLORIC ACID

μ	Mole fraction sulfonic acid = $m_2/(m_1 + m_2)$ 0.000	0.168	0.317	0.495	0.787	1.000
5.0	2.38	2.28	2.15	2.00	1.78	1.60
4.5	2.04	1.97	1.88	1.76	1.58	1.42
4.0	1.76	1.70	1.63	1.55	1.40	1.27
3.5	1.52	1.47	1.42	1.36	1.24	1.15
3.0	1.32	1.28	1.24	1.19	1.10	1.04
2.5	1.15	1.11	1.09	1.05	0.991	0.950
2.0	1.01	0.982	0.966	0.937	.906	.879
1.8	0.960	.935	.922	.899	.875	.855
1.6	.916	.895	.885	.865	.847	.832
1.4	.876	.859	.851	.835	.820	.809
1.2	.840	.828	.822	.809	.800	.787
1.0	.809	.801	.796	.787	.780	.772
0.9	.795	.790	.783	.776	.772	.764
.8	.783	.780	.774	.767	.765	.757
.7	.772	.769	.765	.762	.759	.753
.6	.763	.760	.759	.755	.751	.750
.5	.757	.755	.753	.751	.751	.751
.4	.755	.755	.755	.755	.755	.755
.3	.756	.756	.756	.756	.756	.756
.2	.767	.767	.767	.767	.767	.767
.1	.796	.796	.796	.796	.796	.796

TABLE III

ACTIVITY COEFFICIENT OF *p*-TOLUENESULFONIC ACID AS A FUNCTION OF COMPOSITION IN AQUEOUS MIXTURES OF *p*-TOLUENESULFONIC ACID AND HYDROCHLORIC ACID

μ	Mole fraction sulfonic acid = $m_2/(m_1 + m_2)$ 0.000	0.168	0.317	0.495	0.787	1.000
5.0	2.07	1.27	0.981	0.747	0.538	0.448
4.5	1.67	1.17	.929	.725	.528	.437
4.0	1.44	1.07	.875	.705	.512	.430
3.5	1.26	0.990	.820	.678	.501	.425
3.0	1.11	.900	.765	.654	.505	.427
2.5	0.995	.835	.729	.632	.506	.439
2.0	.899	.781	.694	.625	.519	.459
1.8	.871	.769	.685	.618	.526	.469
1.6	.841	.755	.678	.616	.534	.483
1.4	.818	.745	.674	.619	.544	.498
1.2	.798	.735	.671	.624	.557	.515
1.0	.783	.734	.669	.631	.570	.535
0.9	.778	.726	.673	.635	.578	.546
.8	.771	.724	.676	.641	.589	.559
.7	.765	.722	.681	.649	.600	.573
.6	.762	.720	.682	.653	.614	.589
.5	.762	.731	.700	.670	.628	.608
.4	.765	.737	.714	.691	.649	.630
.3	.772	.752	.731	.706	.679	.660
.2	.783	.769	.752	.734	.716	.703
.1	.801	.795	.783	.776	.768	.759

raised by the addition of $HClO_4$. These results are not surprising, however, since at any given concentration in the pure solutions

$$\gamma_{HClO_4} > \gamma_{HCl} > \gamma_{p\text{-TSA}}$$

As might be predicted from this sequence, the activity coefficient of *p*-toluenesulfonic acid is raised by the addition of HCl at constant total molality.

A point of particular interest is that the ionic strength at which the minimum value of γ_{HCl} occurs changes only slightly as *p*-toluenesulfonic acid is added; whereas the ionic strength at which the minimum value of $\gamma_{p\text{-TSA}}$ is observed shifts

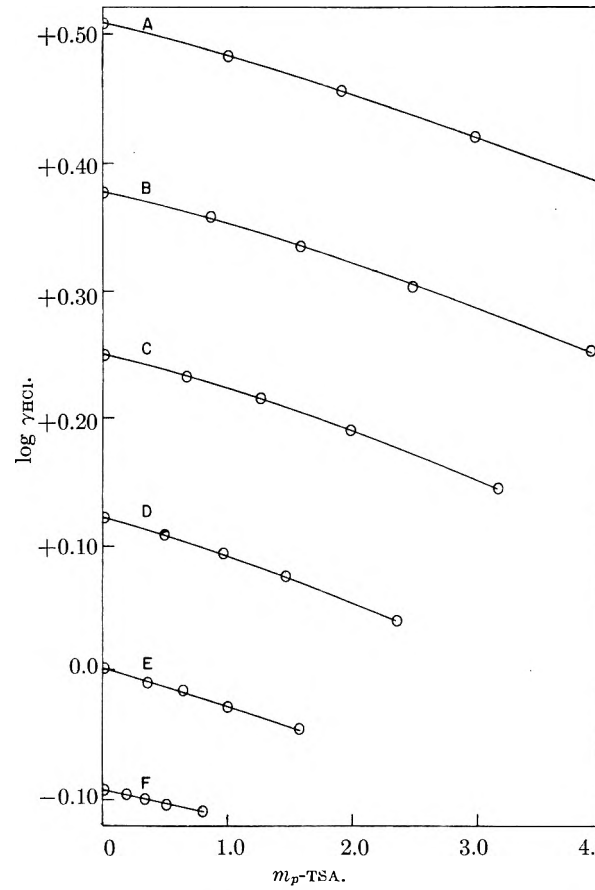

Fig. 1.—Variation of log γ_{HCl} with molality of *p*-TSA: A, μ = 6.0; B, μ = 5.0; C, μ = 4.0; D, μ = 3.0; E, μ = 2.0; F, μ = 1.0.

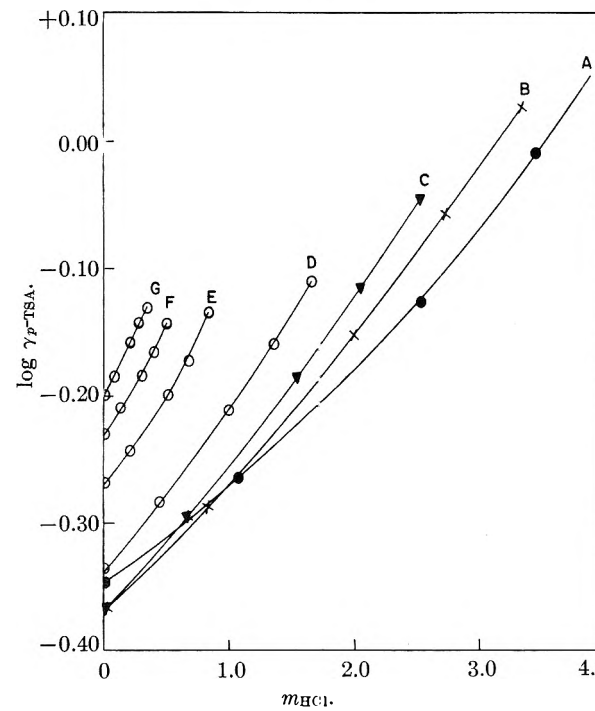

Fig. 2.—Variation of log $\gamma_{p\text{-TSA}}$ with molality of HCl: A, μ = 5.0; B, μ = 4.0; C, μ = 3.0; D, μ = 2.0; E, μ = 1.0; F, μ = 0.6; G, μ = 0.4.

from 3.5 when no HCl is present to approximately 0.6 for a trace of *p*-TSA in HCl. A similar shift in the ionic strength at which the minimum in γ occurs is exhibited by NaCl–HCl and KCl–HCl mixtures.[12] The shift in μ at which the minimum value of γ_{NaCl} is observed is not as drastic because the minimum value of γ_{NaCl} in its pure solutions occurs at an ionic strength of approximately 1.2. For KCl (γ^0_{KCl} has its minimum value at an ionic strength between 2.5 and 3.0) in aqueous mixtures of HCl this shift is greater than that observed for NaCl but less than that for *p*-TSA. Again the ionic strength at which the minimum of γ_{HCl} occurs when a trace of HCl is present in KCl solutions is only slightly different from that for pure HCl.

The applicability of Harned's rule, $\log \gamma_1 = \log \gamma_1^0 - \alpha_{12} m_2$, to this system is illustrated in Fig. 1 and 2. In dilute and in moderately concentrated solutions both components obey Harned's rule approximately, while at very high values of μ, there is a noticeable deviation from this linear relationship. The interaction coefficients, α_{12} and α_{21}, are of opposite sign with α_{12} for HCl being positive whereas α_{21} for *p*-TSA is negative. The crossover of the curves observed in Fig. 2 for large values of μ results from the previously mentioned shift in the ionic strength at which the minimum value of $\gamma_{p\text{-TSA}}$ is observed.

The data for the HCl–*p*-TSA system have been compared with data obtained by Boyd and Larson[6] for 8% DVB Dowex-50. Although a direct comparison is impossible, the results indicate that the activity coefficient of HCl in the ion-exchange resin phase is lower than γ_{HCl} in the mixed HCl–*p*-TSA solutions of the same total hydrogen ion concentration that exists in the resin phase. A difference in behavior should be expected since the resin is in reality a polyelectrolyte. At present no explanation is offered for the fact that the activity coefficients of *p*-toluenesulfonic acid are raised by the addition of HCl, while those of the hydrogen resinate appear to be lowered by the presence of HCl in the resin.

(12) H. S. Harned and B. B. Owen, "The Physical Chemistry of Electrolytic Solutions," Reinhold Publ. Corp., New York, N. Y., 1958, p. 608.

SPECTROPHOTOMETRIC STUDIES OF COMPOUNDS OF THE TYPE R_2SeI_2 IN CARBON TETRACHLORIDE SOLUTION. THE RELATIONSHIP BETWEEN THE ABSORPTION MAXIMA AND THE DISSOCIATION CONSTANTS[1]

BY J. D. McCULLOUGH AND DENISE MULVEY

Contribution from the Department of Chemistry of the University of California, Los Angeles, Calif.

Received October 6, 1959

The dissociation constants of six additional compounds of the type R_2SeI_2 have been determined in carbon tetrachloride solution at 24° by spectrophotometric procedures. The results obtained by use of the Benesi–Hildebrand equation as modified by Keefer and Andrews have been compared with the results obtained by use of the Scott equation. With the exception of some of the *ortho*-substituted diarylselenides, a linear relationship has been found to hold between log *K* for the dissociation and the absorption maximum of the compound expressed in reciprocal centimeters.

The present study is an extension of previous investigations[2-4] in these laboratories on the dissociation constants of compounds of the type R_2SeI_2. The dissociations follow the equation

$$R_2SeI_2 = R_2Se + I_2$$

and the dissociation constants have the form

$$K = [R_2Se][I_2]/[R_2SeI_2]$$

Experimental

Materials.—Di-*p*-ethoxydiphenylselenide was prepared by the method of Alquist and Nelson[5] from phenetole and selenium oxychloride. The resulting dichloride was reduced with aqueous sodium metabisulfite to give the selenide. Di-*o*-chlorodiphenylselenide, di-*o*-tolyselenide and di-(*o*-biphenyl)-selenide were prepared by the method of Leicester and Bergstrom.[6] The unsymmetrical 2-phenyl-4'-methyldiphenylselenide was prepared by the method of Campbell and McCullough[7] and dibenzoselenophene was prepared by the method of McCullough, Campbell and Gould.[8] All six selenides were carefully recrystallized several times from methanol shortly before use. They were thoroughly dried in air at room temperature in the dark and were stored in the dark until used, as some of the selenides discolor after prolonged storage in clear glass containers in the laboratory illumination. Stock solutions of each selenide were prepared in dry carbon tetrachloride as needed.

Iodine (J. T. Baker Reagent) was resublimed and stock solutions in dry carbon tetrachloride were prepared.

Carbon tetrachloride (J. T. Baker Reagent) was dried, distilled through a vacuum jacketed bubble plate column (30 bubble plates) and stored so as to exclude moisture. The initial 10% and final 10% of the distillate were rejected.

Spectrophotometric Measurements.—All spectra were measured on a Cary recording spectrophotometer, Model 11PMS by the procedure described earlier.[9]

Methods of Calculation.—In addition to the method of successive approximations described earlier[9] in which the Keefer and Andrews[10] modification of the Benesi–Hildebrand[11] equation was used, least-squares calculations were

(1) Based on research which was assisted financially by the National Science Foundation under Research Grant NSF-G2354.

(2) J. D. McCullough, *J. Am. Chem. Soc.*, **64**, 2672 (1942).

(3) J. D. McCullough and B. A. Eckerson, *ibid.*, **73**, 2954 (1951).

(4) N. W. Tideswell and J. D. McCullough, *ibid.*, **79**, 1031 (1957).

(5) F. N. Alquist and R. E. Nelson, *ibid.*, **53**, 4033 (1931).

(6) H. M. Leicester and F. W. Bergstrom, *ibid.*, **51**, 3587 (1929).

(7) T. W. Campbell and J. D. McCullough, *ibid.*, **67**, 1965 (1945).

(8) J. D. McCullough, T. W. Campbell and E. S. Gould, *ibid.*, **72**, 5753 (1950).

(9) J. D. McCullough and Denise Mulvey, *ibid.*, **81**, 1291 (1959).

(10) R. M. Keefer and L. J. Andrews, *ibid.*, **74**, 1891 (1952).

(11) H. A. Benesi and J. H. Hildebrand, *ibid.*, **71**, 2703 (1949).

carried out for each compound at each wave length by use of a modification of the equation proposed by Scott.[12]

As modified to suit the present study, the equation of Keefer and Andrews has been written as

$$\frac{SHl}{(S + H - C)A_c} = \frac{1}{(S + H - C)} \times \frac{K}{\epsilon} + \frac{1}{\epsilon} \quad (1)$$

and that of Scott as

$$\frac{SHl}{A_c} = (S + H - C)\frac{1}{\epsilon} + \frac{K}{\epsilon} \quad (2)$$

In these equations, the symbols have the following meanings: S and H are the formal or total concentrations (in moles per liter) of the selenide and iodine, respectively, C is the molar concentration of the compound at equilibrium, A_c is the absorbance of the solution corrected for absorbance due to uncombined I_2 and selenide, l is the optical path length in cm., ϵ is the molar absorptivity (extinction coefficient) of the compound and K the dissociation constant in moles per liter. Equations 1 and 2 result from the combination of the equilibrium equation $K = (S - C)(H - C)/C$ with the absorbance equation $A_c = \epsilon lC$. In the forms thus derived, the equations are not restricted to the condition that $S \gg H$ as is the case with the original forms of the Benesi–Hildebrand and the Scott equations. As pointed out by Scott, the roles of slope and intercept are interchanged in the two equations and the second equation has the theoretical advantage that one extrapolates through regions of decreasing concentration to the intercept. If there were no experimental errors, and if the solutions were ideal, the two equations should give the same result. In practice, however, the two give different results because of the different ways in which they weigh the data.

Results and Discussion

The experimental data are similar to those shown in ref. 9. The final least-squares results obtained by use of equations 1 and 2 are listed separately in Table I and the averaged results are given in Table II with the results from previous work.

TABLE I

MOLAR ABSORPTIVITIES AND DISSOCIATION CONSTANTS FOR SELENIDE–IODINE COMPOUNDS AT 24°. COMPARISON OF RESULTS FROM EQUATIONS 1 AND 2

		Equation 1		Equation 2	
	λ	ε	K	ε	K
Di-*p*-ethoxydiphenyl	360	15,400	0.0130	15,000	0.0125
	370	16,600	.0132	16,200	.0127
	380	16,400	.0133	15,900	.0130
2-Phenyl-4′-methyldiphenyl	350	14,800	.0287	13,200	.0252
	360	16,200	.0287	14,400	.0253
	370	15,600	.0286	13,800	.0252
Di-(*o*-biphenylyl)	350	13,100	.0304	16,200	.0401
	360	14,900	.0308	18,450	.0388
	370	14,500	.0310	18,000	.0390
Di-*o*-tolyl	350	38,200	.214	25,500	.140
	360	41,500	.214	27,700	.142
	370	39,300	.215	26,200	.143
Di-*o*-chlorodiphenyl	340	6,040	.201	8,100	.254
	350	6,920	.189	9,240	.256
	360	6,680	.187	8,950	.252
Dibenzoselenophene	360	18,200	.553	13,400	.488
	370	21,300	.552	15,500	.468
	380	20,900	.553	15,200	.488

In earlier work[3] it was noted (but not reported since only four compounds had been studied) that there was a relationship between the dissociation constants and the wave length of maximum absorption, for the compounds. If one plots log K against the frequency of maximum absorption, the points fall fairly closely to a straight line. In Fig. 1 such a plot is shown for data on eleven R_2SeI_2 compounds measured in these laboratories at temperatures near 25°. Except for some of the compounds with *ortho*-substituents, and dibenzoselenophene (which may also be considered in the broad sense to have *ortho*-substituents) the points lie close to a straight line. The line indicated on the plot is the least-squares line fit to the six compounds without *ortho*-substituents.

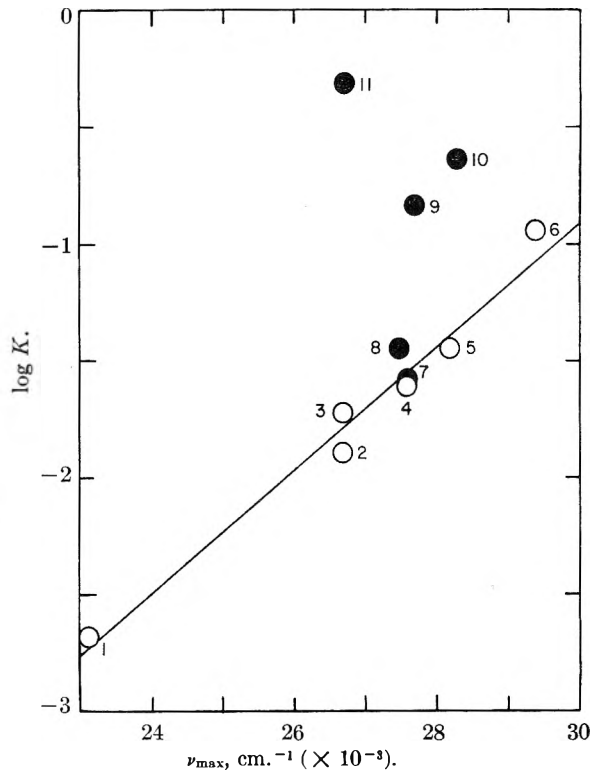

Fig. 1.—Graph showing relationship between log K and the frequency of maximum absorption for organoselenium–iodine compounds without *o*-substituents. The numbers correspond to the numbering of the compounds in Table II. Open circles represent compounds without *o*-substituents, filled circles compounds with *o*-substituents. The "least-squares line" for compounds 1–6 (open circles) is indicated.

Relationships between the ionization potential of the base and the position of the absorption maximum for iodine complexes with aromatic hydrocarbons, olefins, ethers, alkyl halides, alcohols and thioethers have been pointed out by McConnell, Ham and Platt[13] and by Hastings, Franklin, Schiller and Matsen.[14] Merrifield and Phillips[15] have reported a linear relationship between $\Delta F°$ (for formation of the complexes) and the ionization potential of the base for complexes between tetracyanoethylene and various aromatic molecules. Since ΔF^0 is proportional to log K and since the ionization potential of the base is apparently related to the position of the absorption maximum for *iodine* complexes, the relationship found by Merrifield and Phillips is similar to the one reported

(12) R. L. Scott, *Rec. trav. chim.*, **75**, 787 (1956).

(13) H. McConnell, J. S. Ham and J. R. Platt, *J. Chem. Phys.*, **21**, 66 (1953).

(14) S. H. Hastings, J. L. Franklin, J. C. Schiller and F. A. Matsen, *J. Am. Chem. Soc.*, **75**, 2900 (1953).

(15) R. E. Merrifield and W. D. Phillips, *ibid.*, **80**, 2778 (1958).

TABLE II

SUMMARY OF EQUILIBRIUM AND SPECTROGRAPHIC DATA FOR SELENIDE–IODINE COMPOUNDS AT 25°

No.	Selenide	K	log K	λ_{max} (mμ)	ν_{max} (cm.$^{-1}$)	ϵ_{max}	Ref.
1	Dimethyl	0.0021	−2.67	433	23,100	2,860	4
2	Di-*p*-ethoxydiphenyl	.013	−1.89	374	26,700	16,500	
3	Di-*p*-methoxydiphenyl	.019	−1.72	374	26,700	16,500	3
4	Di-*p*-tolyl	.025	−1.60	362	27,600	20,200	3
5	Diphenyl	.036	−1.44	355	28,200	13,300	2
6	Di-*p*-chlorodiphenyl	.12	−0.92	340	29,400	16,900	3
7	2-Phenyl-4′-methyl-diphenyl	.027	−1.57	362	27,600	15,000	
8	Di-(*o*-biphenylyl)	.035	−1.46	364	27,500	18,000	
9	Di-*o*-tolyl	.18	−0.74	361	27,700	30,000	
10	Di-*o*-chlorodiphenyl	.22	−0.66	353	28,300	9,000	
11	Dibenzoseleneophene	.52	−0.28	374	26,700	16,000	

here for the compounds R_2SeI_2. This relationship suggests that the compounds R_2SeI_2 may be charge-transfer complexes and indeed a structural study of 1,4-diselenane·$2I_2$ now in progress in these laboratories shows Se—I–I bonding rather than I–Se–I bonding. A preliminary report of this structural study has been published elsewhere.[16] This result is in sharp contrast to the structures of numerous compounds of the type $R_2(Se,Te)Br_2$ and $R_2(Se,Te)Cl_2$ where X–Se–X and X–Te–X bonding[17] is the rule.

It is noted that those *ortho*-substituted compounds which are not on or near the line in Fig. 1 have higher dissociation constants than indicated by the positions of their absorption maxima. This suggests that steric hindrance by the *ortho* groups may be causing additional instability in the compounds and invites speculation that the position of the absorption maximum may be an indication of the "true dissociation constant." In the cases of the two compounds with *o*-phenyl substituents (whose points lie near the line), the steric effect may be offset by an additional attractive interaction between the *o*-phenyl groups and iodine. Such attractive effects are the basis of the charge-transfer complexes between aromatic hydrocarbons and iodine.

Acknowledgment.—The authors gratefully acknowledge the financial assistance of the National Science Foundation under Research Grant NSF-G2354.

(16) J. D. McCullough, G. Y. Chao and D. E. Zuccaro, *Acta Cryst.*, **12**, 815 (1959).

(17) See G. D. Christofferson, R. A. Sparks and J. D. McCullough, *ibid.*, **11**, 782 (1958), for references to earlier structural studies.

SOLID–VAPOR EQUILIBRIA FOR THE COMPOUNDS Cd_3As_2 AND $CdAs_2$

BY V. J. LYONS AND V. J. SILVESTRI

Research Laboratory, International Business Machines Corporation, Poughkeepsie, New York

Received October 7, 1959

Cd_3As_2 and $CdAs_2$ are shown to thermally dissociate according to the reactions (1) $Cd_3As_2 \rightleftarrows 3Cd + {}^1/_2As_4$ and (2) $CdAs_2 \rightleftarrows {}^1/_3Cd_3As_2 + {}^1/_3As_4$. Dissociation pressures were measured by a dew-point technique and by a direct pressure method employing a quartz Bourdon gauge. The dissociation of Cd_3As_2 in the gas phase was observed through a comparison of the data obtained from the two methods and the identity of the gaseous species was deduced therefrom. The experimental data may be represented by the equation $\log P_{mm} = -6600/T + 9$ ($\Delta H = 106$ kcal./mole). In contrast to Cd_3As_2, thermal dissociation of $CdAs_2$ is readily observed. The compound dissociation pressures measured by the two techniques were in good agreement and the data may be represented by the equation $\log P_{mm} = -7100/T + 11$ ($\Delta H = 11$ kcal./mole).

Introduction

Both $CdAs_2$ and Cd_3As_2 are of particular interest because of their semi-conductor properties. $CdAs_2$, which has an energy gap of 1.1 e.v. at 300°K.,[1] exhibits electrical and optical anisotropy as would be expected from its tetragonal crystal structure ($c/a = 0.586$).[2] Cd_3As_2 exhibits an anomalously high electron mobility of approximately 10,000 cm.^{2}/volt-sec. for material with a carrier concentration of about 2×10^{18}/cc.[3] The reported energy gap of Cd_3As_2 is 0.5 e.v.[4]

Nesmeyanov, *et al.*,[5] have measured the vapor pressure of Cd_3As_2 in the range 238 to 375° employing an effusion technique and assuming the molecular species Cd_3As_2 in the vapor phase. In the present investigation, which was carried out at higher temperatures, the vapor pressure was measured by two methods selected for the purpose of determining the degree of dissociation of Cd_3As_2 in the vapor phase. In the measurement of vapor pressure by the dew-point technique, observation was made of the condensation temperature of a known quantity of Cd_3As_2 vapor in a measured volume. Since Cd_3As_2 can be sublimed and then recondensed from the vapor phase with no apparent dissociation, vapor pressures were calculated from dew-point measurements using the assumption that the compound exists as a monomer in the vapor phase. A comparison of these results with those obtained by direct pressure measurements employing a quartz Bourdon gauge has demonstrated the vapor phase dissociation of the compound. From the ratio of the vapor pressures determined by the two methods, the identity of

(1) W. J. Turner, A. S. Fischler and W. E. Reese, Electrochemical Society Meeting, Columbus, Ohio, Oct. 18–22, 1959, Abstract No. 101.

(2) M. Senko, private communication.

(3) A. S. Fischler, private communication.

(4) T. S. Moss, *Proc. Phys. Soc.*, **A63**, 167 (1950).

(5) A. N. Nesmeyanov, B. Z. Iofa, A. A. Strel'nikov and V. G. Fursov, *J. Phys. Chem. USSR*, **30**, 1250 (1956),

the gaseous species resulting from the dissociation was deduced, and thus the reaction may be represented by the equation

$$Cd_3As_2(s) \rightleftarrows 3Cd(g) + 1/2As_4(g)$$

Both the dew-point method and the total pressure method were also used to study the solid–vapor equilibrium for $CdAs_2$. In preliminary experiments wherein $CdAs_2$ was heated under non-equilibrium conditions such as to sublime the material, the resulting condensate was found by X-ray diffraction powder analysis to be arsenic and Cd_3As_2 thus demonstrating thermal dissociation of the compound. It was also observed that a much greater quantity of arsenic was found in the condensate while most of the Cd_3As_2 remained on the surface of the $CdAs_2$. It was assumed therefore that a reasonably good approximation of the dissociation pressure of $CdAs_2$ could be obtained from dew-point measurements wherein the vapor in equilibrium with the solid compound was considered to be tetrameric arsenic only. Subsequent total pressure measurements carried out in the Bourdon gauge were in good agreement with the dew-point measurements thereby indicating the validity of the assumption.

Experimental

I. Cd_3As_2.—Cd_3As_2 was synthesized by reacting stoichiometric quantities of cadmium and arsenic of 99.999+% purity at 750° in an evacuated sealed quartz tube. The compound was further purified by sublimation in a stream of H_2 at 700°. X-Ray diffraction examination of the sublimed crystals showed a pattern of Cd_3As_2 only and spectrographic analysis of the material revealed the presence of 0.0005% Cu as an impurity. Wet chemical analysis of the sublimate identified the stoichiometry Cd_3As_2.

The vapor pressures were initially determined from dew-point measurements in the range 434 to 695°. For the determination of each experimental point an accurately weighed[6] quantity of Cd_3As_2 was sealed in a quartz tube which was evacuated to a pressure of 1×10^{-5} mm. A thermocouple well was located at one end of each tube. The experiments were carried out in a furnace consisting of nichrome ribbon wound on a quartz tube which was then enclosed by a second quartz tube such that the entire reaction tube was visible. The furnace was long enough to provide a gradient-free temperature zone over the reaction tube. Regulation of the furnace temperature was achieved through a variable transformer operating from a constant voltage supply. The temperature was measured by a Pt–Pt, 10% Rh thermocouple[7] located in the reaction tube thermocouple well.

The procedure for measuring each dew-point was the following. After the furnace temperature was increased until all of the Cd_3As_2 was in the vapor phase, a ten minute period was allowed for equilibration at this temperature (T_E). An air blast was then directed into the thermocouple well and continued until Cd_3As_2 was observed condensing on the cooled well. The air blast was used to overcome possible supersaturation of the vapor and to help ensure that the well remained the coolest part of the reaction tube. The well temperature was then allowed to return to T_E. When T_E was considerably above the dew-point, the condensate would rapidly disappear after turning off the air blast. T_E was then lowered to a new value, equilibrated for 10 minutes, and the procedure was repeated. In this manner the approach of T_E to the dewpoint was observed as a function of the length in time required for condensation and vaporization of the Cd_3As_2. At temperatures within 3° above the dew-point the condensate remained on the well for several hours. In order to increase the accuracy and also reduce the time required for measurement, a modification in the technique was introduced at this point. An infrared lamp was focused on the condensate thereby raising its temperature slightly above T_E. This local heating was continued until most of the condensate had returned to the vapor phase. The remaining condensate was then observed over a period of 0.5 to 1 hour during which time a change in the quantity of the condensate could be noted. This established T_E as being either above or below the dewpoint. T_E was then varied over a narrow temperature range and the procedure was repeated until the dew-point was located within ±1°. The precision attained for each experimental point is shown in Table I. After each measurement, the reaction tube was cut open and the volume was measured by filling with water from a buret. Using the assumption that the compound existed as a monomer in the vapor phase, the vapor pressures were calculated from the equation $PV = nRT$. A plot of the experimental results is shown in Fig. 1.

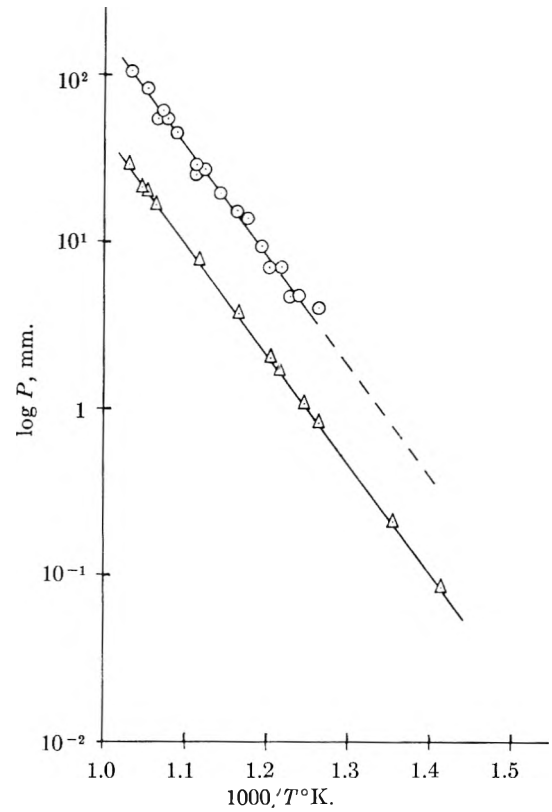

Fig. 1.—Dissociation pressure of Cd_3As_2: (a) circles represent Bourdon gauge measurements; (b) triangles represent dew-point measurements.

In order to determine the degree of association or dissociation of Cd_3As_2 in the vapor, a quartz Bourdon gauge was used to measure the vapor pressure. The apparatus consisted of a Bourdon spoon enclosed in a quartz tube to which a stopcock was sealed. The sample tube was connected to the opening at the lower end of the flexible spoon. A 30 cm. long quartz fiber was attached to the top end of the spoon in order to increase the accuracy of the measurement. The Cd_3As_2 was sealed in a separate evacuated quartz tube which had been baked out at 700°. After loading the sample tube and an iron slug sealed in quartz into the apparatus, both sides of the Bourdon spoon were simultaneously evacuated to a pressure of 1×10^{-5} mm. and outgassed by heating to 700° for 3 hours with continued pumping. The sample tube was then sealed by fusion and the Bourdon gauge enclosure was sealed with the stopcock. During the pressure measurements the tube enclosing the Bourdon spoon was maintained at 800° by a Wheelco controlled Hoskins furnace. The temperature of the sample furnace was controlled through a variac operating from a

(6) Weighings were made using a Cahn Range-Selector Electrobalance. See Table I for individual values.

(7) All thermocouples were calibrated with an N.B.S. standardized Pt–Pt, 10% Rh thermocouple both before and after each experimental series. Thermocouple voltages were read on a Rubicon Potentiometer, Model #2732.

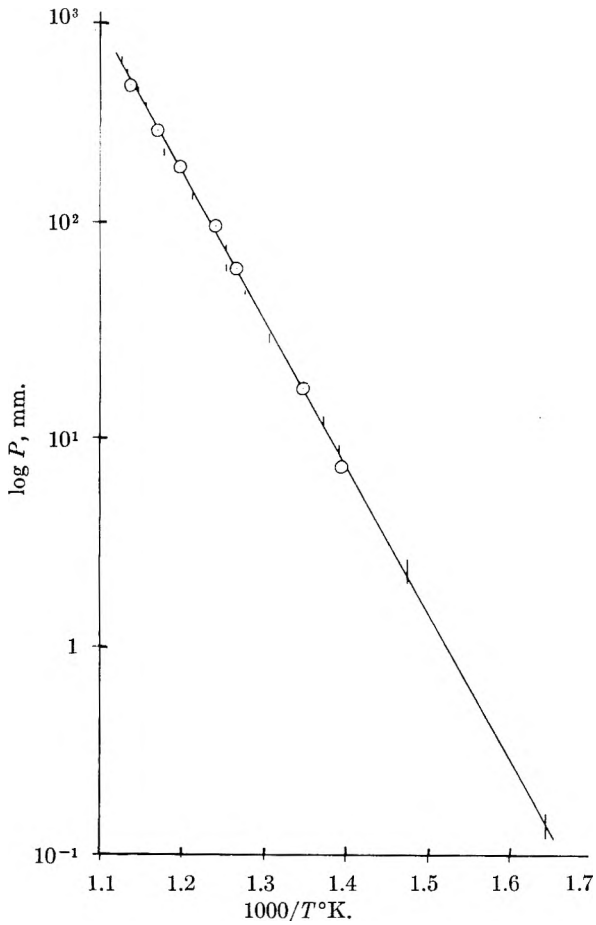

Fig. 2.—Dissociation pressure of $CdAs_2$: (a) vertical lines represent dew-point measurement; (b) circles represent Bourdon gauge measurements.

constant-voltage transformer. The gauge was used as a null-point instrument, *i.e.*, a deflection in the 30 cm. long quartz fiber due to the sample vapor pressure was balanced by an equal pressure of nitrogen admitted to the upper section of the tube. Nitrogen pressures were read on a mercury manometer. Sightings on the quartz fiber were made through a Wild–Heerbrugg cathetometer which has a probable reading error of approximately 0.01 mm. The procedure for making each measurement was as follows.

After establishing the zero-point position of the quartz fiber, the Bourdon spoon was heated to 800° and allowed to equilibrate for one hour. Although the sample had remained at room temperature, there was usually a slight deflection in the quartz fiber during this heating. Separate experiments wherein no sample tube was attached to the gauge also showed a slight drift of the fiber and an equal drift in the quartz enclosure tube during heating. The reason for the apparatus drift was not immediately obvious, but it may have been caused by thermal expansion of the supporting frame during the heating cycle. After equilibration of the upper furnace, the sample furnace was turned on and heated to approximately 500° in steps of 80–100°. Thus, any further apparatus drift could be observed by sightings made both on the fiber and on the quartz tube. Throughout the pressure measurements, sightings on the quartz tube were continued such that any apparatus drift could be observed and corrections could be applied to the fiber zero-point. After each change in the sample temperature, equilibration times of 0.5 to 3.0 hours were allowed. Observations indicated that equilibrium between gas and solid occurred within 0.5 hour. Identical results were obtained in measuring pressures during both the heating and cooling of the sample. Sample temperatures were measured with a Pt–Pt, 10% Rh thermocouple. The results of several series of measurements are plotted as log P *vs.* $10^3/T$ in Fig. 1. Although reasonably good precision was obtained for pressures above 5 mm., the lack of gauge sensitivity at lower pressures prevented precise measurements below this value.

TABLE I

DEW-POINT MEASUREMENTS

A. Cd_3As_2

Wt. of Cd_3As_2, mg.	Tube vol., ml.	Dew-point, °C.	Pressure, mm.
0.067 ± 0.001	74.82 ± 0.05	434.3 ± 0.5	0.081 ± 0.002
.158 ± .001	72.35 ± .05	463.7 ± 1.0	.205 ± .002
.540 ± .001	68.17 ± .05	517.0 ± 0.6	.801 ± .002
.699 ± .001	69.27 ± .05	526.8 ± .7	1.033 ± .002
1.199 ± .005	71.70 ± .05	549.1 ± .8	1.760 ± .008
1.330 ± .005	71.53 ± .05	553.8 ± .9	1.968 ± .008
2.368 ± .005	71.10 ± .05	581.5 ± 1.1	3.643 ± .010
4.619 ± .005	70.09 ± .05	620.3 ± 0.6	7.535 ± .008
9.83 ± .01	67.68 ± .05	666.5 ± .3	17.47 ± .01
12.64 ± .02	77.02 ± .05	673.9 ± .8	19.89 ± .04
13.24 ± .02	79.62 ± .05	675.6 ± .7	20.19 ± .04
15.44 ± .02	68.39 ± .05	695.5 ± 1.0	27.99 ± .05

B. $CdAs_2$

$CdAs_2$ temp., °C.	As condensation, temp., °C.	As pressure,[a] mm.
334.8	318.5–323.2	0.12– 0.15
404.8	389.3–395.9	2.07– 2.61
446.1	432.0–434.3	8.54– 9.17
455.7	444.5–446.7	12.5 – 13.4
474.8	460.7–463.3	20.3 – 21.8
492.6	475.3–477.8	30.7 – 32.9
509.6	493.7–494.4	50.5 – 51.5
524.8	512.1–513.9	81.4 – 85.2
525.2	502.8–505.2	64.2 – 68.3
552.6	535.7–537.1	145.2 –150.1
575.9	556.6–559.1	235.9 –249.6
592.3	580.3–581.5	397.6 –408.0
599.8	587.6–590.5	464.2 –493.3
609.9	597.4–599.3	569.1 –591.7
615.0	603.9–607.1	649.8 –693.3

[a] Arsenic pressures were obtained from R. E. Honig, *R. C. A. Rev.*, 18, 195 (1957).

TABLE II

BOURDON GAUGE MEASUREMENTS

A. Cd_3As_2

Temp., °C.	Pressure, mm.	Temp., °C.	Pressure, mm.
516.9	4.0	619.2	28.7
533.7	4.8	620.1	28.9
536.2	4.7	621.4	26.5
536.2	4.7	642.6	45.8
540.6	7.2	654.6	55.8
549.9	7.2	658.5	55.2
563.3	9.6	659.4	60.8
577.4	13.9	676.6	82.1
584.9	15.5	692.4	104.0
600.1	19.5		

B. $CdAs_2$

444.0	7.4	562.1	204.3
468.9	17.7	581.7	307.0
516.4	67.6	605.7	502.5
533.4	105.4		

II. $CdAs_2$.—Spectrographically pure $CdAs_2$ was synthesized by direct combination of cadmium and arsenic of 99.999+% purity at 630° in a sealed quartz tube under an arsenic pressure of approximately 0.5 atmosphere. Single crystals of the material were obtained by directional freezing in a temperature gradient. X-Ray diffraction powder analysis of the crystals confirmed the presence of $CdAs_2$ only. The technique and apparatus employed in measuring the compound dissociation pressures by the dew-point method were essentially the same as used previously for the compound $ZnAs_2$.[8] About 10 g. of $CdAs_2$, broken into

(8) V. J. Lyons, THIS JOURNAL, **63**, 1142 (1959).

small pieces, was sealed in an evacuated quartz tube. The $CdAs_2$, located at one end of the tube, was then heated to various temperatures while dew-points were observed at the opposite end of the tube in an independently controlled furnace. The use of an infrared lamp in the manner described above was the only difference between the technique used here and that used for $ZnAs_2$. Dew-point measurements were carried out on two samples in the temperature range 334 to 615°. The data, which are presented graphically in Fig. 2, were taken with both increasing and decreasing $CdAs_2$ temperature.

Measurements of the dissociation pressure of $CdAs_2$ were also carried out using the Bourdon gauge. The procedures were the same as those used for Cd_3As_2 except that a lower temperature (400°) was used during the outgassing. The results of the measurements are plotted in Fig. 2. A comparison of the two methods shows excellent agreement.

Discussion

I. Cd_3As_2.—A comparison of the vapor pressure data obtained by the two methods shows that the pressures measured by the Bourdon gauge are greater than those calculated from the dew-point experiments by a factor of about 3.6. Since the dew-points were calculated assuming the existence of monomeric Cd_3As_2 molecules in the vapor phase, the 3.6:1 ratio between the two sets of data indicates the degree of dissociation of Cd_3As_2 in the vapor phase. In order to correct the values of vapor pressure calculated from the dew-points to the values obtained by direct measurement, an average molecular weight of about 129 must be assigned to the gaseous species. Complete dissociation of the compound to monomeric cadmium and tetrameric arsenic would result in an average molecular weight of 135. Therefore, within experimental error, it can be deduced that the compound thermally dissociates according to the reaction

$$Cd_3As_2(s) \rightleftarrows 3Cd(g) + \frac{1}{2}As_4(g) \qquad (1)$$

The assumption of monomeric cadmium and tetrameric arsenic is based on data tabulated by Stull and Sinke.[9] The equilibrium constant for the dissociation represented by equation 1 is

$$K_p = \left(\frac{3.0}{3.5}P\right)^3\left(\frac{0.5}{3.5}P\right)^{1/2} = 0.24P^{3.5} \qquad (2)$$

The vapor pressure data when plotted as log P *vs.* $10^3/T_{0K}$ as in curve 2 of Fig. 1 may be represented by the straight line equation

$$\log P_{mm} = -\frac{6600}{T_{0K}} + 9 \qquad (3)$$

From equations 2 and 3, the heat calculated for the reaction 1 is 106 kcal./mole.

II. $CdAs_2$.—The good agreement between the vapor pressures obtained from the two methods shows that the dissociation pressure of $CdAs_2$ may be considered in terms of the arsenic pressure only. The pressure contribution from the simultaneous dissociation of Cd_3As_2 appears to be negligible. The equilibrium reaction, then, may be written as

$$CdAs_2(s) \rightleftarrows \frac{1}{3}Cd_3As_2(s) + \frac{1}{3}As_4(g) \qquad (4)$$

and the equilibrium constant for the reaction is

$$K_p' = P_{As_4}^{1/3}$$

The experimental data may be represented by the equation

$$\log P_{mm} = -\frac{7100}{T_{0K}} + 11 \qquad (5)$$

From equation 5 the heat calculated for the reaction 4 is 11 kcal./mole of solid $CdAs_2$.

Acknowledgments.—The authors wish to express their thanks to Dr. G. A. Silvey, Dr. T. G. Dunne and Dr. K. Weiser for valuable discussions, and to Mr. C. L. Fisher for constructing the Bourdon gauge.

(9) D. R. Stull and G. C. Sinke, "Thermodynamic Properties of the Elements," Advances in Chemistry Series, No. 8, 1956.

THE HEAT OF FUSION OF THE ALKALI METAL HALIDES

BY A. S. DWORKIN AND M. A. BREDIG

Chemistry Division, Oak Ridge National Laboratory, Oak Ridge, Tennessee[1]

Received October 21, 1959

The heat of fusion of seventeen alkali halides has been measured by means of a copper block drop calorimeter. The salts and their heats of fusion in kcal. mole^{-1} are as follows: LiCl, 4.76; LiBr, 4.22; LiI, 3.50; NaCl, 6.69; NaBr, 6.24; NaI, 5.64; KCl, 6.27; KBr, 6.10; KI, 5.74; RbF, 6.15; RbCl, 5.67; RbBr, 5.57; RbI, 5.27; CsF, 5.19; CsCl, 4.84; CsBr, 5.64; and CsI, 5.64. The heats of fusion are believed to be accurate to at least ± 1–2%. Except for the Li salts and, to some slight extent, the sodium salts, the entropy of fusion is constant when the anion varies, but decreases with increasing atomic number of the cation.

In the course of an investigation of the metal–metal halide systems being pursued in this Laboratory, a knowledge of the heat of fusion of the alkali halides became necessary.[2] Many of the heats of fusion listed in a number of commonly used compilations[3a,b] stem from an earlier U. S. Bureau of Mines compilation.[4] These heats are derived from phase diagrams and at best are averages of widely scattered values; while at their worst are derived from systems now known to be wholly unsuitable for this purpose. As an example, the heat of fusion of LiF as determined calorimetrically at the National Bureau of Stand-

(1) Work performed for the U. S. Atomic Energy Commission at the Oak Ridge National Laboratory, operated by the Union Carbide Corporation, Oak Ridge, Tennessee.

(2) M. A. Bredig and H. R. Bronstein, *J. Phys. Chem.*, **64**, 64 (1960).

(3) (a) Leo Brewer, in L. L. Quill, "Chemistry and Metallurgy of Miscellaneous Materials: Thermodynamics," National Nuclear Energy Series IV-19B, McGraw-Hill Book Co., New York, N. Y., 1950, pp. 196–197. (b) "Selected Values of Chemical Thermodynamic Values," Circular 500, Natl. Bur. Standards (1952).

(4) K. K. Kelley, U. S. Bur. Mines Bulletin 393, 1936.

ards was found to be 6,470 cal.,[5] whereas the value accepted before this measurement was 2,360 cal. We, therefore, have measured calorimetrically the heat of fusion of the halides of Li, Na, K, Rb and Cs for which calorimetric data were unavailable.

The method used entailed the measurement of heat content over a sufficient temperature range above and below the melting point of the salt to allow extrapolation to the melting point. A copper block drop calorimeter was chosen as the simplest to build and operate to obtain the desired accuracy. Although it was not deemed necessary to seek the very fine precision now attainable in high temperature heat content measurements, sufficient care was taken in both the design and operation of the calorimeter to ensure heat of fusion values good to approximately 1%.

Experimental

Apparatus.—The calorimeter is essentially of standard design. A gold-plated copper block of 5 in. diameter and 8 in. long supported by three micarta legs is centered in a 6 by 9 in. brass tank which in turn is submerged in a large constant temperature water-bath. The well in the copper block into which the sample container falls is 7 in. deep, the lower 1.5 in. being tapered. A copper gate at the top of the well in contact with the Cu block can be opened just before the container is dropped from the furnace and then closed immediately afterward to prevent loss of heat by radiation.

The sample is equilibrated in a 3.5 in. bore Marshall tube furnace 16 in. long, having ten external taps for the attachment of shunt resistors to help eliminate the temperature gradient. To further reduce gradients, the furnace tube contains a 3.5 in. diameter nickel block 9 in. long, above and below which are lavite insulators. The nickel block sheathes the Inconel tube in which the sample container is held. The 1.2 in. diameter Inconel tube extends 10 in. into the furnace and a sufficient distance below the furnace to bring it just above a similar tube 5 in. long welded to the brass tank. A gate in the Inconel tube just below the furnace lessens heat losses from the furnace. The whole furnace assembly is mounted on a track so that it can be rolled over the copper block immediately preceding a drop and rolled away immediately afterward.

The Inconel sample containers were tapered to fit the taper in the well in the copper block. This, together with the fact that the container bottoms were slightly larger in diameter than that of the bottom of the well, ensured good thermal contact between the container and the copper block.

The temperature of the water-bath around the calorimeter was maintained constant to better than ±0.001° at approximately 26° by means of a thermistor as the temperature-sensitive element in a bridge circuit employing a Speedomax recorder-controller operating an infrared heat lamp external to the bath. The furnace was controlled by a Chromel–Alumel thermocouple which operated a Leeds and Northrup recorder-controller in conjunction with a Leeds and Northrup "DAT" controller. The actual temperature of the sample was measured with a platinum, 90% platinum–10% rhodium thermocouple by means of a Rubicon precision potentiometer. The temperature of the sample container could be maintained to about ±0.1° with the temperature gradient over the height of the container (about 1¾″) about 0.2°. The temperature rise of the copper block was measured with a calorimetric type platinum-sheathed platinum resistance thermometer by means of a precision Mueller bridge. The thermometer was imbedded three inches deep in the copper block midway between the well and the outer wall of the block. Temperature differences of 0.001° could be measured.

Purification of Materials.—Of the salts used, NaCl, KCl, KBr, KI, CsBr and CsI were Harshaw optical grade single crystals; LiCl, LiBr, LiI, NaBr, NaI, RbF, RbI and CsCl were reagent grade materials; RbCl and RbBr were made from Rb metal; and CsF was made from CsCl. The Harshaw crystals were taken to be pure and dry except for surface moisture which was removed by pumping. The remaining salts were purified by gradual heating under vacuum to just below their melting temperatures, melting under dry argon, and filtering while molten. Special care was taken with the hygroscopic salts of Li and with CsF in that the corresponding halogen acids were introduced during the very slow heating process to prevent hydrolysis. The dry salts were handled in a dry box and then sealed by welding in the Inconel containers under argon. Upon completion of an experiment, the containers were opened and the salts examined for discoloration, basicity and insoluble material. In no case was a basic solution found. In a very few cases, slight discoloration and a trace of insoluble material were noted. Analysis in these cases showed a few hundredths of a per cent. of Fe, Cr and Ni.

Experimental Procedure.—The sample was heated to a known temperature in the furnace, dropped into the copper block, and the temperature rise of the block measured. During the course of the experiment, the sample was allowed to remain in the furnace for varying lengths of time in order to determine an adequate length of time for equilibration with special care being taken for measurements a few degrees above the melting points of the salts. The temperature drift rate of the copper block was measured before and after each drop and extrapolated to an appropriate time during the temperature rise period in order to determine the initial and final temperatures of the copper block.

The heat equivalent of the calorimeter was determined using an N.B.S. sample of synthetic sapphire (Al_2O_3).[6,7] The experimental procedure was the same as that used for the salts except that the temperature rise of the copper block contributed by the empty container was measured and subtracted from the temperature rise of the container filled with Al_2O_3. Approximately 20-g. samples of Al_2O_3 were used. Nine determinations over a temperature range of 400–800° showed the heat equivalent to be 1752 ± 4 cal./degree rise of the copper block.

For each salt, a minimum of four points over a sixty degree temperature range above the melting point and five points over a one hundred degree range below were measured. Data were obtained to within five to ten degrees of the melting point for both the solid and liquid salts. Premelting was encountered in a number of instances which necessitated the longer range of measurements in the solid region since the data obtained in the premelting zone could not be used in the extrapolation. The salts were always melted before the first drop in any series to ensure intimate contact between the salt and container throughout the measurements. The sample size varied from about 0.1 to 0.25 mole depending on the molar volume of the salts.

Results and Discussion

The data were plotted as temperature rise of the copper block due to the heat contributed by container plus salt *versus* temperature from which the drop was made. (Small corrections were applied for differences in the final temperature of the copper block.) Straight lines could best represent the data over the relatively short temperature ranges measured. These lines were extrapolated to the melting points of the salts. The difference between the lines for the solid and liquid at the melting point was taken as the temperature rise of the copper block due to the heat of fusion of the salt (the contribution of the container is cancelled out at this point). The product of this value and the heat equivalent of the calorimeter divided by the number of moles of salt was taken as the molar heat of fusion of the salt.

The scatter of the points about the straight lines

(5) T. B. Douglas and J. L. Dever, *J. Am. Chem. Soc.*, **76**, 4826 (1954).

(6) D. C. Ginnings and R. J. Corruccini, *J. Research Natl. Bur. Standards*, **38**, 593 (1947), RP 1797.

(7) G. T. Furukawa, T. B. Douglas, R. E. McCoskey and D. C. Ginnings, *ibid.*, **57**, 67 (1956), RP 2694.

TABLE I

HEAT AND ENTROPY OF FUSION OF THE ALKALI HALIDES

		ΔH_m (kcal. mole^{-1})			ΔS_m (e.u. mole^{-1})		
	T_m, °K.	This work	Other calorimetric work	Other lit.[3,4]	This work	Other calorimetric work	Other lit.[3,4]
LiF	1121[5]		6.47[5]	2.36		5.77	2.1
LiCl	883[3]	4.76	4.72[8], 4.83[9]	3.20	5.39	5.35, 5.47	3.6
LiBr	823[3]	4.22		2.90	5.13		3.5
LiI	742[14]	3.50		1.42	4.72		2.0
NaF	1268[1]		8.03[12], 7.78[10]	7.00		6.33, 6.14	5.5
NaCl	1073[1]	6.69	6.85[10]	7.22	6.23	6.38	6.7
NaBr	1020[1]	6.24		6.14	6.12		6.0
NaI	933[1]	5.64		5.24	6.04		5.6
KF	1131[15]		6.75[10]	6.50		5.97	5.8
KCl	1043[16]	6.34	6.27[8], 6.10[10]	6.41	6.08	6.01, 5.85	6.2
KBr	1007[16]	6.10		5.00	6.06		4.9
KI	954[16]	5.74		4.10	6.02		4.3
RbF	1068[16]	6.15	5.49[11]	4.13	5.76	5.14	3.9
RbCl	995[17]	5.67		4.40	5.70		4.4
RbBr	965[17]	5.57		3.70	5.77		3.9
RbI	920[17]	5.27		2.99	5.73		3.3
CsF	976[18]	5.19		2.45	5.32		2.6
CsCl	918[3]	4.84	4.97[9]	3.60	5.27	5.40	3.9
CBr	909[3]	5.64		3.00	6.20		3
CsI	899[18]	5.64		2.50	.27		3

which represent the data was of the order of 0.1%. The actual measured temperature rises of the block ranged from about 1.5 to 3.0° while the differences between the lines for the solid and the liquid at the melting points ranged from about 0.4 to 0.8°. On consideration of the use in the heat of fusion calculations of this difference between two measured larger numbers, the precision of the heat equivalent and heat content measurements, and the small uncorrected systematic errors inherent in the method, the heat of fusion values are believed to be accurate to at least ± 1–2%.

Table I lists the heat and entropy of fusion of all of the alkali halides. The values listed in literature compilations[3,4] are included for comparison with the calorimetric values. Calorimetric values obtained by other investigators are given with those reported in this work. The entropy of fusion was calculated merely by dividing the heat of fusion by the absolute temperature at which the salts melt.

A number of the salts measured in the present work may be compared with values found calorimetrically by other investigators. As can be seen in Table I, Douglas'[8] values for LiCl and KCl and Smith's[9] value for LiCl agree very well with our values. Smith's[9] value for CsCl and Kelley's[10] values for NaCl and KCl are somewhat outside our experimental error. However, the latter two values had been based on heat contents reported to only 3%. Smith's[11] value for RbF is considerably lower than ours, which may be due to the rather large scatter of his heat content data in the vicinity of the melting point. Of the calorimetric measurements not repeated in this work, the values for LiF[5] and NaF[12] are derived from heat content measurements reported to a high degree of accuracy, whereas the value for KF[10] is based on heat contents reported to 3%.

As has been predicted previously,[13] among the

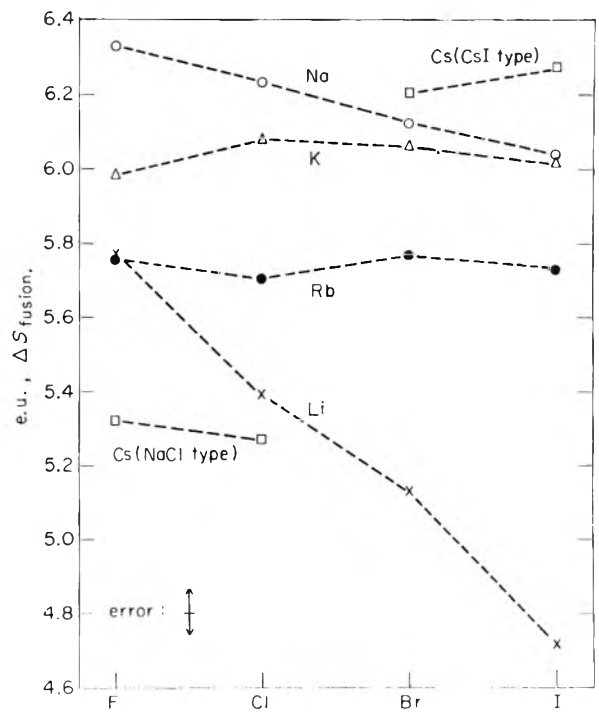

Fig. 1.—Entropy of fusion of the alkali halides.

(8) T. B. Douglas, Natl. Bur. Standards, private communication.
(9) D. F. Smith, Univ. of Alabama, private communication.
(10) K. K. Kelley, U. S. Bur. Mines Bulletin 476, 1949.
(11) C. E. Kaylor, G. E. Walden and D. F. Smith, *J. Am. Chem. Soc.*, **81**, 4172 (1959).
(12) C. J. O'Brien and K. K. Kelley, *ibid.*, **79**, 5616 (1957).
(13) J. W. Johnson, P. A. Agron and M. A. Bredig, *ibid.*, **77**, 2734 (1955).
(14) J. W. Johnson and M. A. Bredig, unpublished data.
(15) J. W. Johnson and M. A. Bredig, THIS JOURNAL, **62**, 604 (1958).
(16) O. Schmitz-Dumont and E. Schmitz, *Z. anorg. Chem.*, **252**, 329 (1944).
(17) I. S. Yaffe and E. R. Van Artsdalen, THIS JOURNAL, **60**, 1125 (1956).

cesium halides the two groups having different crystal structures, CsF–CsCl (NaCl type) and CsBr–CsI (CsI type), are distinguished by different entropies of fusion, approximately 5.3 and 6.2 e.u. mole^{-1}, respectively. The magnitude of the difference as predicted in the above reference was incorrect because the value for the heat of transition of CsCl available at that time was in error. Smith[9] has since measured the heat of transition of CsCl from the CsI structure to the NaCl structure and found it to be 581 cal. mole^{-1} at 742.5° K. This corresponds to an entropy of transition of 0.78 e.u. mole^{-1}, of the same order as the difference in the entropy of fusion of the two groups of cesium halides.

The spread in the entropy of fusion of the alkali halides evident in the older erroneous values is considerably reduced in the present data. Definite trends in the data have now become obvious (Fig. 1). There is a trend in the Li salts for the entropy of fusion to decrease from 5.8 e.u. in LiF to 4.7 e.u. in LiI, while in the other salts, the entropy of fusion remains essentially constant with an increase in *anion* size. However, a residue of the effect noticeable in the Li salts is still apparent in the sodium salts. In another trend, with an increase in the size of the *cation*, the entropy of fusion decreases from that for NaF and NaCl of approximately 6.3 to 5.3 e.u. for CsF and CsCl. The entropy curve for the Li salts appears to be displaced downwards by 1 to 2 e.u. It may be significant that, excepting the Li salts, the anion and cation affect the entropy of fusion in a differing manner. The heats of fusion, on the other hand, show a decrease with an increase of the size of either the cation (except Li) or the anion. CsBr and CsI with their different crystal structure are, of course, excluded from the above considerations. As the entropy of melting is relatively constant for the salts of NaCl type structure (ΔS_m average = 5.75 ± 0.30 e. u. mole^{-1}), it follows that a plot of the heats of fusion bears great resemblance to a plot of the melting points which has been discussed from various points of view.[19a,b]

Acknowledgment.—We wish to acknowledge the assistance of D. E. Lavelle of this Laboratory, who prepared the samples of the anhydrous salts used in this work.

(18) M. A. Bredig, H. R. Bronstein and W. T. Smith, Jr., *J. Am. Chem. Soc.*, **77**, 1454 (1955).

(19) (a) K. Fajans, "Radioelements and Isotopes. Chemical Forces and Optical Properties of Substances," McGraw-Hill Book Co., New York, N. Y., 1931 p. 66; (b) L. Pauling, The Nature of the Chemical Bond, Cornell University Press, Ithaca N. Y., 1939.

NOTES

A REMEASUREMENT OF THE SELF-DIFFUSION COEFFICIENTS OF IODIDE ION IN AQUEOUS SODIUM IODIDE SOLUTIONS

By E. Berne and M. J. Weill

Contribution from the Department of Inorganic Chemistry, Chalmers Institute of Technology, and the Swedish Institute of Silicate Research, Gothenburg, Sweden

Received November 21, 1958

The self-diffusion of iodide ions in the solutions of alkali metal iodides has been investigated by Mills and Kennedy,[1] Friedman and Kennedy,[2] and by Wang and Kennedy.[3] The open-ended capillary method, introduced by Anderson and Saddington[4] and modified by Wang[5] has been used for the measurements in HI, LiI, KI, RbI and CsI. The usual plot D *vs.* $\sqrt{c}$ showed a close similarity of the behavior of I^- in these five iodides: as the concentration of electrolyte increased, D was regularly decreasing from the Nernst limiting value corresponding to infinite dilution.

The self-diffusion of I^- in NaI solutions, at 25°, has not been studied with the same method. Wang and Kennedy have used a free diffusion method, where the diffusion process took place from one capillary into a second identical one, pressed against the first capillary. This technique has not been used any more after this first trial, and other authors have criticized it.

As the results found by Wang and Kennedy were different from those corresponding to the other alkali iodides, and as there is no apparent reason why NaI should behave in a singular way, it seemed of interest to remeasure the self-diffusion coefficients of the iodide ion in sodium iodide solutions, using the open-ended capillary method.

Experimental

We have used a type of diffusion cell whic is different from the one described by Wang, and applied no stirring. Details of the apparatus and manipulations are to be found in a preceding paper.[6]

The radioactive solutions were prepared by adding 5 μl. of a carrier-free ^{131}I solution (specific activity = 5 mc./ml.) provided by the Isotope Division, A.E.R.E., Harwell, England, to 10 ml. of the sodium iodide solutions. The diffusion times were of 4 to 5 days.

Results and Discussion

The self-diffusion coefficients of I^- in aqueous NaI solutions, at 25°, have been measured over the range 10^{-4} to 4 M. The results are listed in Table I, and the plot of D *vs.* $\sqrt{c}$ is represented in Fig. 1, We reproduce also, for comparison purposes, the curve of Wang and Kennedy.

Each value reported in Table I is the average value of 3 to 4 measurements, and the error quoted

(1) R. Mills and J. W. Kennedy, *J. Am. Chem. Soc.*, **75**, 6596 (1953).
(2) A. M. Friedman and J. W. Kennedy, *ibid.*, **77**, 4499 (1955).
(3) J. H. Wang and J. W. Kennedy, *ibid.*, **72**, 2080 (1950).
(4) Ja. Anderson and K. Saddington, *J. Chem. Soc.*, S381 (1949).
(5) J. H. Wang, *J. Am. Chem. Soc.*, **73**, 510 (1951).
(6) E. Berne and M. J. Weill, This Journal, **64**, 258 (1960).

TABLE I

SELF-DIFFUSION COEFFICIENTS OF I^- IN AQUEOUS NaI SOLUTIONS AT 25°

Concn. of NaI soln. (formular wt./l.)	$D \times 10^5$ (cm.²/sec.)
10^{-4}	2.043 ± 0.006
0.04	1.974 ± .015
0.25	1.906 ± .007
0.50	1.842 ± .023
1.00	1.755 ± .013
2.00	1.606 ± .011
3.20	1.442 ± .009
4.00	1.310 ± .009

corresponds to the root mean square deviation. The average tabulated error is ± 0.7%. The accuracy of our method is then better than the one yielded by Wang's method, *ca.* ± 1 to 2% and is of the same order as the accuracy of Mill's method,[7] which used a streamline flow over the mouth of the capillary.

Figure 1 shows a regular decrease in D when the concentration of NaI increases, and the curve has the same regular shape as the curves obtained in other iodides.

It is to be noticed that the value we found in a $10^{-4}M$ solution agrees perfectly with the one predicted by the Nernst limiting equation, *i.e.*, $D^0 = 2.045 \times 10^{-5}$ cm.²/sec.

Our results agree with those of Wang and Kennedy only in a narrow range of concentration, from 0.6 up to 1.4 M. In the lower concentration zone, our results are markedly higher than those of Wang and Kennedy and in the higher concentration zone, they are much lower (17.5% for c = 4 M).

The relative position of these two curves may be compared to the relative position of the curves of Mills and Adamson,[8] and Nielsen, Adamson and Cobble,[9] concerning the self-diffusion coefficients of Na^+ in aqueous NaCl (see Fig. 2). Both works were performed with a diaphragm cell technique. As Mills and Adamson's values have been confirmed later on by a very fine work of Mills,[7] who used a modified open-ended capillary method, we believe their results to be the most reliable.

Furthermore, in the same paper, Nielsen, Adamson and Cobble have measured the self-diffusion coefficients of Na^+ in NaI, and found values which agreed closely with those of Wang and Kennedy.

Together with Mills and Adamson, we could come to the conclusion that both Nielsen, Adamson and Cobble and Wang and Kennedy found incorrect values, for the self-diffusion coefficients of Na^+ in NaI.

According to our present results, and to these remarks, we may conclude that Wang and Kennedy's results were also incorrect for D_{I^-} in NaI.

We have not observed for our results any linear relation between D_{I^-} and c. as found by Mills[7] for D_{Na^+} in aqueous NaCl. Neither have we found a linear relation when the relative viscosity of the solutions is taken into account, as suggested by Mills and Kennedy[1] for the case of unhydrated ions.

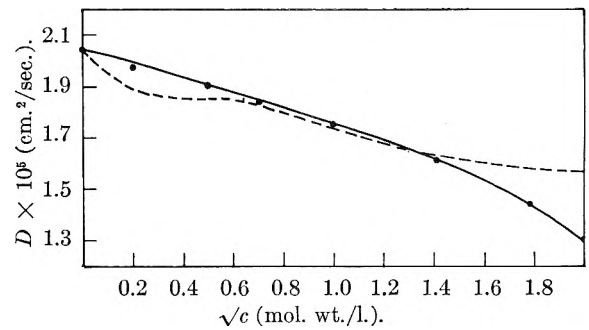

Fig. 1.—Self-diffusion coefficients of I^- in aqueous NaI solutions at 25°: ----, data of Wang and Kennedy; ———, this work.

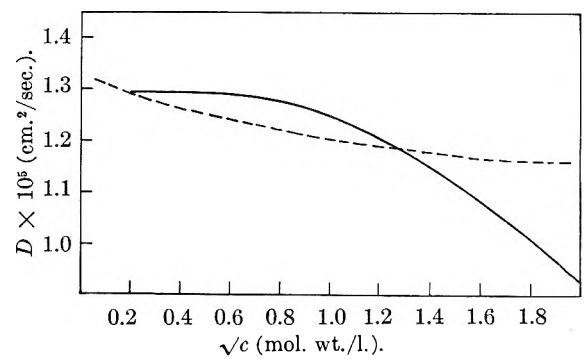

Fig. 2.—Self-diffusion coefficients of Na^+ in aqueous NaCl solutions at 25°: ----, data of Nielsen, Adamson and Cobble; ———, data of Mills and Adamson.

Acknowledgments.—The authors are grateful to Professor C. Brosset for his kind interest in the present work, and M.J.W. wishes to acknowledge financial support from the Swedish Institute for Cultural Relations with Foreign Countries, during part of the work.

(7) R. Mills, *J. Am. Chem. Soc.*, **77**, 6116 (1955).

(8) R. Mills and A. W. Adamson, *ibid.*, **77**, 3454 (1955).

(9) J. M. Nielsen, A. W. Adamson and J. W. Cobble, *ibid.*, **74**, 446 (1952).

SOME RECENT MEASUREMENTS OF DIAMAGNETIC ANISOTROPY IN SINGLE CRYSTALS

BY DERCK A. GORDON[1]

Contribution Number 2394 from the Gates and Crellin Laboratories of Chemistry, California Institute of Technology, Pasadena, California

Received July 17, 1959

Some measurements of diamagnetic anisotropy in single crystals recently have been made in these laboratories in the course of an investigation, described more fully elsewhere,[2] devoted to improving the precision and accuracy of a method of measurement originally developed by Krishnan and coworkers.[3] The method involves suspending a crystal (mass m, gram formula weight W) on a quartz fiber (torsion constant K) in a homogeneous magnetic field (strength H) and twisting the free end of the fiber until the crystal suddenly turns through a large angle. The anisotropy in the plane

(1) Stanford Research Institute, Menlo Park, California.

(2) D. A. Gordon, *Rev. Sci. Instr.*, **29**, 929 (1958).

(3) K. S. Krishnan, *et al.*, in a series of papers in *Phil. Trans. Roy. Soc. London*, between 1933 and 1939, especially **234A**, 265 (1935).

perpendicular to the axis around which the crystal is constrained to rotate is calculated from the relation

$$\Delta\chi = 2KW(\alpha_{max} - \vartheta_{crit})/mH^2 \sin 2\vartheta_{crit}$$

in which α_{max} is the angle through which the free end of the initially untwisted fiber is twisted and ϑ_{crit} is the angle through which the crystal rotates from its initial position of stable equilibrium before suddenly beginning to spin. The value of ϑ_{crit} may be assumed to be $\pi/4$, with negligible error, provided α_{max} is greater than two revolutions; values of α_{max} actually used ranged from 10 to 400 revolutions but were generally in the range 30 to 100 revolutions.

For this work crystals of suitable size and perfection were taken directly from reagent bottles whenever possible or otherwise were obtained by recrystallization. Specimens ranging in mass from 0.3 to 40 mg. and generally of irregular shape were first weighed with a precision of about ±0.002 mg. and then attached to one end of a relatively long and stout glass fiber, the opposite end of which was later attached to the calibrated quartz-fiber suspension system. The mode of suspension thus was such that the axis about which the crystal rotated very nearly coincided with the axis of the glass fiber. Laue X-ray diffraction photographs were used to verify in each case that the desired crystal direction was parallel to the glass fiber within one degree, an accuracy sufficient for this work.

The anisotropy measurements were made at relatively high field strengths (15 to 24 kilogauss) and the anisotropy was determined from the slope of a plot of $(2KW/M)$ $(\alpha_{max} - \pi/4)$ *vs.* the square of the field strength. At each of several field strengths the value of α_{max} was determined for both directions of rotation and with the crystal initially in each of the two stable equilibrium positions, normally obtaining four slightly different results which were plotted separately. The slopes of the corresponding four straight lines were averaged to obtain the accepted anisotropy value; this procedure greatly reduced the effects of ferromagnetic impurities and of a small field inhomogeneity. Data points for a series of field strengths fitted separate straight lines with negligible scatter provided the anisotropy involved was greater than about 1.0 ($\times 10^{-6}$ c.g.s./mole).

Data which have been obtained thus far are given in Table I. The uncertainties attached to the anisotropy values (third column) are either average deviations of measurements on two to four specimens or, when only one specimen was tested, average deviations of values obtained for the different equilibrium positions and directions of rotation. There is an additional uncertainty of ± 1.2% in the absolute value of each anisotropy caused partly by the uncertainty in the value of the moment of inertia of a torsion pendulum used to calibrate the quartz fibers and partly by the uncertainty in the calibration of a search coil used to make field strength measurements.

The measurements on anhydrous potassium hydrogen oxalate were made for comparison with the anisotropy of the oxalic acid molecule reported on the basis of measurements on oxalic acid

TABLE I

MAGNETIC ANISOTROPY DATA

Substance	Anisotropy investigated	Obsd. value ($\times 10^{+6}$ c.g.s./mole)	Other reported values	
KNO_3 (orthorhombic)	$\chi_b-\chi_c$	7.03 ± 0.24	4.82[4]	5.9[5]
	$\chi_a-\chi_c$	6.98 ± .15	4.87	5.7
	$\chi_b-\chi_a$	0.15 ± .02	0.05	0.2
Urea (tetragonal)	$\chi_\parallel-\chi_\perp$[a]	2.45 ± .04	2.57[6]	
Anthracene (monoclinic)	$\chi_1-\chi_2$[b]	138.7 ± .9[c]	136.3[7]	140.3[8]
		$\psi = 10 \pm 1°$	$\psi = 8°$	$\psi = 8°$
KHC_2O_4 (anhyd.) (monoclinic)	$\chi_1-\chi_2$	13.05 ± 0.10		
	$\chi_3-\chi_2$	12.61 ± .13		
	$\chi_1-\chi_3$	0.43 ± .05		
		$\psi = 0 \pm 1°$		
Glycine (monoclinic)	$\chi_2-\chi_3$	4.58 ± 0.07		
	$\chi_1-\chi_2$	1.59 ± .03		
	$\chi_1-\chi_3$	6.17 ± .07		
		$\psi = 46 \pm 2°$		
Monomethylurea (orthorhombic)	$\chi_b-\chi_a$	1.87 ± 0.02		
	$\chi_c-\chi_b$	3.33 ± .05		
	$\chi_c-\chi_a$	5.23 ± .01[c]		
Thiourea (orthorhombic)	$\chi_c-\chi_b$	2.52 ± .02		
	$\chi_c-\chi_a$	2.75 ± .04		
	$\chi_b-\chi_a$	0.23 (calcd.)		

[a] The susceptibility parallel to the tetragonal axis is $\chi_\parallel$. The susceptibility in any direction perpendicular to this axis is $\chi_\perp$. [b] ψ is the angle between the principal axis χ_1 and the *c*-axis, measured in the obtuse angle β; χ_3 is the susceptibility parallel to the monoclinic axis, *b*. [c] Measurements made on a single specimen only.

dihydrate.[9] In both substances the oxalate group is very nearly planar and has three mutually perpendicular approximate mirror planes.[10] The principal magnetic axes of the group are therefore very nearly perpendicular to the mean plane of the group (n) parallel to the projection of the C–C bond onto the mean plane of the group (l) and perpendicular to the first two axes (m). The calculated molecular anisotropy values for the oxalate group, $K_l - K_m$, $K_l - K_n$ and $K_m - K_n$, based on measurements on potassium hydrogen oxalate are +0.5, +13.1 and +12.6, respectively; the corresponding values reported as a result of measurements on oxalic acid dihydrate are −0.4, +9.3 and +9.7.

In addition, potassium chlorate was investigated, using twinned crystals belonging to a fairly common habit[11] in which the crystals twin repeatedly by reflection across a plane, forming myriads of microscopically thin laminae.[12] The separate laminae consist of normal monoclinic potassium chlorate crystals in which the atoms of each chlorate ion form approximately a trigonal pyramid with unique axis normal to the twofold axis, *b*, making an angle of 34°18′ with the normal to (001), the plane of twinning[13]; in each lamina, the plane of the optic axes is normal to *b*. The

(4) K. S. Krishnan, B. C. Guha and S. Banerjee, *Phil. Trans. Roy. Soc. London*, **231A**, 235 (1933).

(5) I. I. Rabi, *Phys. Rev.*, **29**, 174 (1927).

(6) K. Lonsdale, *Proc. Roy. Soc. (London)*, **177A**, 272 (1941).

(7) K. S. Krishnan and S. Banerjee, *Phil. Trans. Roy. Soc. London*, **235A**, 343 (footnote) (1936).

(8) N. Lumbroso-Bader, *Ann. Chem.*, 687 (1956).

(9) K. Lonsdale, *J. Chem. Soc.*, 364 (1938).

(10) S. B. Hendricks, *Z. Krist.*, **91**, 48 (1935).

(11) P. Groth, "Chemische Krystallographie," Vol. 2, W. Engelmann Verlag, Leipzig, 1908, p. 90–92.

(12) Repeated attempts to obtain untwinned crystals by recrystallization were unsuccessful.

(13) W. H. Zachariasen, *Z. Krist.*, **71**, 501 (1929).

specimens were identified as belonging to the laminarly twinned habit on the basis of morphology, convergent-light interference figures and Laue diffraction photographs. The latter revealed that the twinning had introduced apparently perfect orthorhombic symmetry, indicating that both components of the twin were present in nearly equal amounts. Measurement of the anisotropy in the plane normal to the *b*-axes of the separate laminae (*i.e.*, in the plane of the optic axes of the twinned crystals), using two different specimens, gave an average value of 1.09 ± 0.01, the crystals orienting themselves preferentially with the magnetic field normal to the plane of twinning. From this information and the assumptions that the chlorate ions were truly uniaxial and that both components of the twinned specimens were present in equal amounts, it was possible to calculate a tentative value for the anisotropy of the chlorate ion: this value was $K_{\parallel} - K_{\perp} = 1.09/\cos 2(34°18') = +2.99$, or about half the value, $K_{\parallel} - K_{\perp} = +5.9$, calculated by Mookherji[14] from data on monoclinic potassium chlorate obtained by Krishnan.[4]

Acknowledgment.—The author is indebted to the Allied Chemical and Dye Corporation which granted him a fellowship for the year 1955-1956.

(14) A. Mookherji, *Acta Cryst.*, **10**, 25 (1957).

RESTRICTED INTERNAL ROTATION IN PROTONATED AMIDES

By E. Spinner

Department of Medical Chemistry, The Australian National University Canberra, A.C.T. Australia

Received July 31, 1959

The purpose of this note is to resolve the apparent contradiction between infrared spectral results which have shown that protonation in acetamide,[1a] N-ethylacetamide[1b] and urea[1c,a] takes place preferentially at the nitrogen atom,[2] and nuclear magnetic resonance data for some N-methyl-amides in strong acid[3] that have been regarded as evidence for preferential protonation at the oxygen atom.[3]

The n.m.r. spectra do not show the signal of the proton that has added to the basic site; thus there is no *direct* evidence of a hydroxylic or nitrogen-bound proton. O-Protonation was postulated *solely* to explain the splitting of the signal of the N-methyl hydrogen atoms, observed frequently, but not invariably, in protonated N-methyl-amides, the argument being that in a cation $HOCR{=}\overset{+}{N}R'{\cdot}CH_3$ rotation about the CN bond is restricted by virtue of its partial[3a] or complete[3b] double bond character (possibility of *cis/trans* isomerism, etc.), while in ions I and II there is free rotation about the C_{CO}–N bond.

However, this latter assumption is fallacious. Even in acetaldehyde, acetyl fluoride, chloride and cyanide, there are barriers restricting rotation,[4] of 1.08–1.35 kcal./mole, because a CH bond tends to eclipse the C=O bond[5]; for the restricting barrier in trifluoroacetaldehyde[6] the (somewhat doubtful) very high value of 9.8 kcal./mole has been proposed. Furthermore, rotational isomerism in substances of the type $RCO{\cdot}CH_2X$, due to restricted rotation about the C_{CO}–C_{CX} bond, often has been observed.[7] Rotation about the C_{CO}–$\overset{+}{N}$ bond in ions of the type of I and II must be similarly restricted: an $\overset{+}{N}$–C_{Me} or $\overset{+}{N}$–H bond will tend to eclipse the C=O bond. In addition, rotation about the $\overset{+}{N}$–C_{Me} bond is restricted: only conformations with *staggered* C–H and $\overset{+}{N}$–H bonds are stable. The possibilities of rotational isomerism thus arising explain all the splittings of proton magnetic resonance bands observed in protonated amides.

An N-protonated *mono*-N-methyl-amide (I) can exist in a "*trans*" or in a "*gauche*" conformation (*trans* arrangement of the R–C–$\overset{+}{N}$–C or of the R–C–$\overset{+}{N}$–H chain). The N-Me proton signals should be different in the two forms. In the "*trans*" form of I, which should be energetically

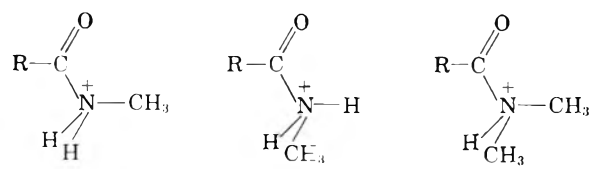

(I) *trans* (I) *gauche* (II) *trans/gauche*

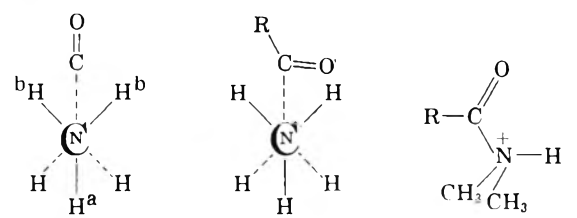

(I) *trans* End-on view (I) *gauche* End-on view (II) *gauche/gauche*

preferred, by analogy with neutral N-methyl-acetamide,[8] the proton marked "a" is different from those marked "b," and two separate n.m.r. signals are to be expected from them, the splitting being due mostly to interaction with the protons

(1) (a) E. Spinner, *Spectrochim. Acta*, 95 (1959); C. G. Cannon, *Mikrochim. Acta*, 562 (1955); M. Davies and L. Hopkins, *Trans. Faraday Soc.*, **53**, 1563 (1957).

(2) The cations of acetamide and urea show a prominent band near 2400 cm.$^{-1}$ which is characteristic of the $^{+}NH_3$ group (R. D. Waldron, *J. Chem. Phys.*, **21**, 734 (1953); C. Sandorfy, in "The Technique of Organic Chemistry" (Editor A. Weissberger), Vol. IX, Interscience Publishers, Inc., New York, N. Y., 1956, p. 515.

(3) (a) G. Fraenkel and C. Niemann, *Proc. Natl. Acad. Sci. U. S. A.*, **44**, 688 (1958); (b) A. Berger, A. Loewenstein and S. Meiboom, *J. Am. Chem. Soc.*, **81**, 62 (1959).

(4) E. B. Wilson, *Proc. Natl. Acad. Sci. U. S. A.*, **43**, 816 (1957); C. C. Lin and R. W. Kilb, *J. Chem. Phys.*, **24**, 631 (1956); P. H. Verdier and E. B. Wilson, *ibid.*, **29**, 340 (1958).

(5) The author attributes this to attraction between the C=O and the CH bonds by intramolecular van der Waals–London and induction forces.

(6) R. E. Dodd, H. L. Roberts and L. Woodward, *J. Chem. Soc.*, 2783 (1957).

(7) S. Mizushima and collaborators, *J. Chem. Phys.*, **20**, 1720 (1952); **21**, 815 (1953); M. L. Josien and R. Calas, *Compt. rend.*, **240**, 1641 (1955); L. J. Bellamy, L. C. Thomas and R. L. Williams, *J. Chem. Soc.*, 3704 (1956); 4294 (1957); R. N. Jones and E. Spinner, *Can. J. Chem.*, **36**, 1020 (1958).

(8) S. Mizushima, *et al.*, *J. Am. Chem. Soc.*, **72**, 3490 (1950).

attached to the $\overset{+}{N}$ atom. When the latter are replaced by deuterons, which appear to interact weakly with protons[3a] (possibly on account of the fast nuclear quadrupole relaxation of deuterons[3b]), most of the splitting should disappear, in agreement with observation (*cf.* the n.m.r. spectra of N-methylacetamide[3a] in H_2SO_4 and D_2SO_4).

An N-protonated N,N-dimethylamide (II) can exist in a "*trans/gauche*" or in a "*gauche/gauche*" conformation; the former should be more stable and more abundant. The proton signal from the "*trans*" N-methyl group should differ from that from the "*gauche*" methyl group, just as the proton signals are different for the *trans* and the *cis* N-Me group in a neutral N,N-dimethylamide. However, the difference between a "*trans*" and a "*gauche*" position (rotation of 120°) is smaller than that between a *trans* and a *cis* position (rotation of 180°); the splitting of the N-Me proton signal might therefore be expected to be smaller in the (N-protonated) cation than in the neutral N,N-dimethylamide; this is, in fact, always the case.[3a]

The three hydrogen atoms in a "*trans*" or "*gauche*" N-methyl group in II (and in a "*gauche*" N-Me group in I) are all different from one another and should all give different proton signals. Such band splitting has, however, not been observed. In protonated N-methylacetamide the splitting of the signal is only observed in special favorable conditions (*e.g.*, in 72% perchloric acid only after addition of dioxane); in protonated N,N-dimethylacetamide it is not observed in 72% perchloric acid.[3a] This shows that sometimes the life time of the isomer may be quite short compared to the time required for the completion of a nuclear magnetic transition (the exact environmental conditions being critical). Such short life times are much more readily explained if the isomerism is attributed to (moderately) restricted rotation about a single bond (like a $C-\overset{+}{N}$ bond in I or II), rather than to (strongly) restricted rotation about a CN bond with a large amount of double bond character, in an amide cation protonated at the oxygen atom.

HIGH TEMPERATURE HEAT CONTENT AND ENTROPIES OF CESIUM CHLORIDE AND CESIUM IODIDE[1]

By C. E. Kaylor,[2] G. E. Walden[2] and Donald F. Smith[2]

Contribution from the Southern Experiment Station, Region V, Bureau of Mines, U. S. Department of the Interior, and the School of Chemistry University of Alabama, University, Alabama

Received August 3, 1959

This paper presents the results of heat content measurements throughout the temperature range 273.15° to 1172°K., with calculated entropies for cesium chloride and cesium iodide. The heat of transition for cesium chloride at 742.5°K. has been measured, and the heats of fusion of cesium chloride and cesium iodide have been measured at their respective melting points.

Data on these compounds, in the range studied, have not been published previously.

Materials

The cesium chloride and the cesium iodide used in this investigation were supplied by the Oak Ridge National Laboratory. The cesium chloride was resublimed in a Vycor sublimation tube. The cesium iodide was of the same purity as the resublimed cesium chloride, and no additional purification was attempted. Impurities, determined spectrographically,[3] were Li, 0.1%; K, less than 0.1%, Na, less than 0.1%; and Ca, less than 0.01%. Total impurity was estimated to be less than 0.2%.

The samples were enclosed in platinum crucibles, the heat contents of which were determined by separate measurements. After filling with sample, the crucibles were evacuated, filled with helium, evacuated to approximately 10 mm. helium pressure and sealed by platinum welding.

Measurements and Results

Heat content measurements were made in a Bunsen ice calorimeter of the type described in detail by Ginnings and Corruccini.[4] The calibration factor for the unit, established electrically, was found to be 270.44 ± 0.66 joule per gram of mercury. Additional calibration tests made on a synthetic sapphire sample, at four different temperatures, yielded enthalpy values that checked accepted values[5] with less than 0.15% deviation.

The experimental procedure used in the calorimetric studies is described.

A sample of approximately 18 g., sealed in the platinum container, was heated to an approximate predetermined temperature in a Marshal furnace designed so that it could be shunted to obtain a region of uniform temperature. The temperature of the furnace was measured with a platinum–platinum 10% rhodium thermocouple previously calibrated against a National Bureau of Standards thermocouple. Once it had been assured that the entire sample and container had reached the test temperature, the container was dropped into the calorimeter, the system was closed and the heat evolved in cooling to 273.15°K. was measured. This procedure was repeated at temperature intervals of approximately 30°K. over the 273.15 to 1172.0°K. range. In each run the previously determined heat content of the container for that temperature was deduced from the total heat evolved.

The experimentally determined heat content values of the samples are listed in Table I. They are expressed in defined calories per mole and the molecular weights are in accord with the 1956–1957 Atomic Weight Report.

Cesium chloride exhibited two phase changes within the temperature range studied. One change was a transition from the alpha to the beta form and the other from solid beta to the liquid at the melting point. The heat of transition was found to be 581 cal. per mole at 742.5°K. and the heat of fusion at the melting point 918°K. was determined as 4964 cal. per mole.

(1) The work upon which this report is based was carried out in cooperation with the University of Alabama.

(2) Bureau of Mines, Tuscaloosa, Ala.

(3) E. E. Creitz, Bureau of Mines, Southern Experiment Station, Tuscaloosa, Ala.

(4) D. C. Ginnings and R. J. Corruccini, *J. Research, Natl. Bur. Standards*, **38**, 583 (1947).

(5) D. C. Ginnings and G. T. Furukawa, *J. Am. Chem. Soc.*, **75**, 522 (1953).

TABLE I

MEASURED HEAT CONTENTS ABOVE 273.15°K. (CAL. MOLE^{-1})

T, °K.	$H_T - H_{273.15}$	T, °K.	$H_T - H_{273.15}$
	CsCl (mol. wt. 168.37)		
385.2	1476(α)	718.7	5873
390.5	1575	728.2	6079
397.7	1660	740.5	6257(α)
407.2	1835	753.7	7193(β)
422.0	1997	761.3	7266
440.5	2174	779.8	7397
442.2	2264	795.0	7529
462.2	2450	825.3	8158
468.8	2551	836.7	8278
472.7	2610	852.9	8539
484.4	2766	880.0	9082
514.8	3152	904.9	9515
532.9	3372		
541.5	3487	Liquid	
568.2	3792		
590.2	4096	923.6	14667
605.2	4197	936.1	14894
624.9	4542	970.2	15272
632.9	4585	1001.6	16009
636.1	4685	1035.6	16742
668.2	5154	1070.2	17364
676.8	5269	1128.5	18386
700.9	5631	1168.0	19050
	CsI (mol. wt. 259.83)		
369.3	1024	670.0	5121
394.7	1419	695.5	5480
397.1	1493	715.9	5790
420.2	1762	741.5	6132
421.5	1786	759.6	6437
443.2	2066	766.1	6678
449.7	2213	796.5	7041
463.2	2351	825.0	7399
470.2	2464	858.9	8021
484.1	2589	870.2	8183
500.7	2886	903.7	8875
504.2	2892		
532.9	3344	Liquid	
542.1	3395	907.7	14910
559.7	3720	918.5	15211
573.0	3858	937.1	15449
595.8	4074	960.2	15589
597.8	4252	1003.3	16362
611.2	4408	1041.4	17104
624.7	4581	1073.7	17674
628.5	4612	1106.2	18139
630.0	4667	1135.3	18830
659.0	4924	1172.2	19416

Cesium iodide had one phase change, that of melting, within the temperature range studied. The heat of fusion was determined as 5979 cal. per mole at the melting point 907°K.

Table II presents smooth heat content and entropy data for the two substances at even 50° intervals in the 400 to 1,200°K. range.

The heat content equations of solid cesium chloride (alpha) and solid cesium iodide were derived to fit the conditions

$$H_T - H_{273.15} = a + bT + cT^2 + dT^{-1} \quad (1)$$

$$C_p = b + 2cT - dT^{-2} \quad (2)$$

TABLE II

HEAT CONTENTS (CAL. MOLE^{-1}) AND ENTROPY INCREMENTS (CAL. DEGREE^{-1} MOLE^{-1}) ABOVE 273.15°K.

	CsCl		CsI	
T, °K.	$H_T - H_{273.15}$	$S_T - S_{273.15}$	$H_T - H_{273.15}$	$S_T - S_{273.15}$
298.15	320	1 11	320	1.09
400	1630	4 92	1560	4.71
450	2280	6 46	2210	6.23
500	2940	7 84	2870	7.61
550	3610	9 06	3530	8.88
600	4270	10 26	4220	10.07
650	4940	11 34	4910	11.18
700	5630	12 35	5620	12.23
742.5	6230(α)	13 18	...	...
742.5	6810(β)	13 97	...	...
750	6920	14 12	6360	13.25
800	7720	15 21	7110	14.22
850	8530	16 12	7880	15.16
900	9360	17 13	8670	16.06
907	...	. .	8770(s)	16.17
907	...	. .	14750(l)	22.77
918	9650(β)	17 57	...	...
918	14610(l)	22 97	...	...
950	14810	23 67	15580	23.64
1000	15710	25 31	16500	24.62
1050	16550	26 80	17380	25.46
1100	17330	28 16	18220	26.24
1150	18050	29 35	19020	26.81
1200	...	. .	19740	27.50

Where $C_p = 12.56$ at 283.15°K. for cesium chloride[6] and $C_p = 12.39$ at 283.15°K. for cesium iodide[7]

$$0 = a + bT + cT^2 + dT^{-1} \text{ at } 273.15°\text{K.} \quad (3)$$

The heat content equation of solid cesium chloride (beta) was derived to fit only condition (1), and the heat content equations of liquid cesium chloride and liquid cesium iodide were derived to fit the condition $H_T - H_{273.15} = a + bT + cT^2$.

The heat content equations presented below were derived by the method of least squares, using the experimental data from Table I. Least square solutions were obtained by means of a Univac electronic computer.[7] Entropy increments were calculated by means of the method suggested by Kelley.[8] Average deviations are indicated by the figures in parentheses.

The heat content data are represented by the equation

CsCl (solid, alpha)

$$H_T - H_{273.15} = -3705 + 12.78T + 6.14 \times 10^{-4}T^2 + 4.56 \times 10^{4}T^{-1}$$

(385.2–740.5°K.; ± 0.5%)

CsCl (solid, beta)

$$H_T - H_{273.15} = 1365 + 0.805T + 8.82 \times 10^{-3}T^2 + 8.91 \times 10^{4}T^{-1}$$

(753.7–904.9°K.; ± 0.5%)

CsCl (liquid)

$$H_T - H_{273.15} = -0.69 + 13.86T + 2.14 \times 10^{-3}T^2$$

CsI (solid) (923.6–1168.0°K.; ± 0.5%)

(6) J. W. Brønsted, *Z. Elektrochem.*, **20**, 554 (1914).

(7) R. W. Smith, Jr., Supervisory Mathematician, Region V, Bureau of Mines, U. S. Department of the Interior, Pittsburgh, Penna.

(8) K. K. K. Kelley, Bulletin 476, Bureau of Mines, U. S. Department of the Interior, Berkeley, California.

$$H_T - H_{273.15} = -1610 + 7.06T + 5.18 \times 10^{-3}T^2 - 1.93 \times 10^{6}T^{-1}$$
(369.3–903.7°K.; ± 0.5%)

CsI (liquid)
$$H_T - H_{273.15} = 10{,}400 - 4.29T + 1.025 \times 10^{-2}T^2$$
(907.7–1172.2°K.; ± 0.5%)

THE REACTIONS OF DIPHENYLMETHYLENE RADICALS IN THE GAS PHASE

By W. Fielding and H. O. Pritchard

Chemistry Department, University of Manchester, Manchester 13, England

Received September 14, 1959

The photolysis of diphenyldiazomethane in rigid media at low temperatures showed that the diphenylmethylene radical reacted very readily with oxygen to form benzophenone and with diphenyldiazomethane to form benzophenone-azine.[1] We have both photolyzed and pyrolyzed diphenyldiazomethane in the gas phase to see what further information could be gained about the reactivity of the diphenylmethylene radical. All the experiments were performed by picking up diphenyldiazomethane in a gas stream at 2 cm. pressure from a reservoir at 20°, carrying it through either a heated tube or a suitably constructed mercury lamp, and trapping out the products in a refrigerated U-tube immediately following the reaction zone; the products were identified by their ultraviolet spectra. From the known extinction coefficient of diphenyldiazomethane, its vapor pressure was found to be about 10^{-5} mm. at 20°, and at the rates of flow employed, a sufficient sample for ultraviolet analysis (*ca.* 10^{-5}–10^{-4} g.) was carried over in about 2 hours. The diphenyldiazomethane is not very stable and goes off at room temperature or in light to the azine and (if air is present) some benzophenone. Our sample was kept refrigerated, *in vacuo* and in the dark when not in use, but a little decomposition did occur; consequently, some benzophenone (which is rather more volatile) always showed up in the spectra, but the azine (which is much less volatile) did not.

Photolysis using high-purity nitrogen gave solely benzophenone. Further purification of the nitrogen over heated copper gave the same result, but if the nitrogen was first bubbled through molten sodium, at 360° it was sufficiently freed of oxygen to suppress the benzophenone formation; under these conditions, benzophenone-azine was formed, as in the low-temperature studies. Pyrolysis at 90° gave identical results. Several other carrier gases were used *i.e.*, wet nitrogen, hydrogen, carbon monoxide, carbon dioxide and propane, but no other reaction of the radical was found either at 90 or 250°. The only new reaction which was found was a reaction with ethylene at 250° (but not at 90°) to give a product which we believe is 1,1-diphenylcyclopropane: the same product was formed from propane containing 0.5% ethylene, but in the presence of traces of oxygen benzophenone was again formed. This places the order of reactivity of the diphenylmethylene radical as

$$O_2 > Ph_2CN_2 >> C_2H_4 >>> H_2,\ CO,\ CO_2,\ H_2O,\ C_3H_8$$

However, it is difficult to make quantitative kinetic measurements when the radical source has only a vapor pressure of 10^{-5} mm., and no further experiments along these lines are projected.

The product of the reaction with ethylene gave an ultraviolet spectrum consisting of seven sharp peaks or shoulders superimposed on that of the benzophenone impurity; the wave lengths were 300, 292, 288, 277, 272, 226 and 220 mμ. 1,1-Diphenylcyclopropane has been reported as having been prepared from 1,1-diphenylethylene, either directly by reaction of diazomethane, or indirectly by reaction with diazoacetic ester followed by saponification and decarboxylation.[2] We failed to obtain any reaction between diphenylethylene and diazomethane, either using the literature conditions, or by irradiation or raising the temperature. Using the second method, we obtained 1,1-diphenylcyclopropane carboxylic acid (m.p. 171°) as stated, but decarboxylation of this with calcium oxide leads to diphenylpropylene and not diphenylcyclopropane (the product reacts instantly with bromine water and has the spectrum of 1,1-diphenylpropylene[3]); milder decarboxylations were tried, but the acid was recovered unchanged. However, both the acid and the ester have a fine structure in the ultraviolet, *e.g.*, the acid gives peaks at 274, 266, 260, 254, 248 and 221 mμ, whereas the 1,1-diphenylpropylene spectrum has virtually no structure; thus, although we have failed to prepare 1,1-diphenylcyclopropane, it seems likely that it is the product of the reaction between ethylene and diphenylmethylene radicals.

Diphenylmethylene is clearly less reactive than methylene, except perhaps in its reaction with oxygen. It does not react with H_2, CO, C_3H_8 as methylene does, even at 250°, and its reaction with ethylene only takes place with difficulty; this reaction shows a positive temperature dependence indicating an energy of activation. It has been suggested[4] that diphenylmethylene, which reacts rapidly with oxygen, must be a triplet molecule, whereas methylene is a singlet because it does not (but see Avramenko and Kolesnikova[5]); however, methylene does show a typically free-radical reaction with hydrogen and we suggest that it is unwise to infer anything about the electronic state of the methylene radical from the fact that its typically radical reactions may in general be rather slower than its non-typical reactions. Some brief experiments on the difluoromethylene radical, which is definitely known to be a singlet,[6] show it to be quite unreactive as expected. The radicals can be produced by a Penning discharge in difluorodichloromethane[7]; a stream of the fluorocarbon

(1) W. B. DeMore, H. O. Pritchard and N. Davidson, *J. Am. Chem. Soc.*, **81**, 5874 (1959).

(2) H. Wieland and O. Probst, *Ann.*, **530**, 274 (1937).

(3) M. Ramart-Lucas and M. J. Hoch, *Bull. soc. chim.*, **2**, 1376 (1935).

(4) R. M. Etter, H. S. Skovronek and P. S. Skell, *J. Am. Chem. Soc.*, **81**, 1008 (1959).

(5) N. N. Semenov, "Some Problems in Chemical Kinetics and Reactivity," Princeton University Press, Princeton, N. J., 1959, p. 157.

(6) P. Venkateswarlu, *Phys. Rev.*, **77**, 608 (1950).

(7) W. B. DeMore, Ph.D. Thesis, California Institute of Technology, 1957.

was mixed downstream from the discharge with the other reactant gas in a heated reaction vessel and the products were subjected to mass-spectral analysis. Under all conditions, small amounts of C_2F_4 were formed and some polymer was deposited outside the reaction vessel, but even at 250°, there was no evidence of any reaction with O_2, H_2, C_3H_8, C_2H_4 or CO. Thus, it is clear that the methylene radical resembles the diphenylmethylene radical much more closely than it does the singlet difluoromethylene.

INFRARED INTENSITIES OF SULFUR DIOXIDE: A RE-DETERMINATION[1]

By D. F. Eggers, Jr., and E. D. Schmid

Department of Chemistry, University of Washington, Seattle, Washington

Received August 31, 1959

An earlier report from this Laboratory[2] listed the infrared intensities for sulfur dioxide, measured in the gas phase. Since that time, similar measurements have been made by others[3,4]; our measurements were about 30 to 40% lower than these, which agreed quite well with each other. A re-examination of our original spectral recordings and calculations disclosed no errors; therefore, we undertook a complete re-measurement of these intensities.

Experimental

The gas was drawn from the same cylinder used in the earlier investigation. A metal cell was used again, but the windows were sealed with an epoxide resin, instead of beeswax–rosin mixture. The possibility of error due to adsorption on the walls of the cell was investigated, and found to be less than the experimental uncertainty of our intensities. Path length of the cell was 4.43 cm. Sample pressures were measured directly with a mercury manometer for the bands ν_1 and ν_2; an oil manometer was used for the band ν_3. Dry nitrogen at 200 p.s.i. served as the pressure-broadening gas. The spectrometer has been described elsewhere[5]; it differs from the instrument used in the earlier investigation in two respects: it has been converted from single-pass to double-pass, and from double-beam to single-beam. Prisms of sodium chloride, potassium bromide and calcium fluoride were used for the bands ν_1, ν_2 and ν_3, respectively. The spectra recorded were replotted as $\ln(T_0/T)$ *vs.* frequency, and the area measured with a polar planimeter. Sample pressures were chosen so that the maximum value of $\ln(T_0/T)$ was in the range from 0.4 to 1.8.

The area determined by a given replotted curve is denoted β, and $B = \beta/pl$, the apparent intensity, where p is the sample pressure in atmospheres and l the length of the cell. Figures 1, 2 and 3 show the apparent band intensities, B as a function of pl, together with a line giving the estimated extrapolation to zero sample pressure.

Results and Discussion

The values of A, the "true" intensity obtained from the extrapolation are listed in Table I, together with the values obtained by other workers.

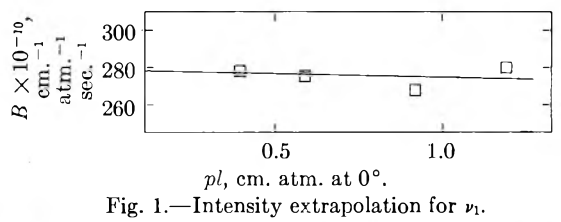

Fig. 1.—Intensity extrapolation for ν_1.

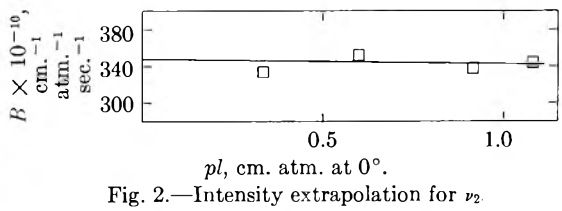

Fig. 2.—Intensity extrapolation for ν_2.

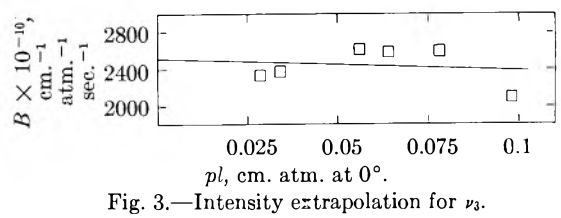

Fig. 3.—Intensity extrapolation for ν_3.

Table I

Intensities of Sulfur Dioxide, C.p.s. Cm.$^{-1}$ Atm.$^{-1}$ $\times 10^{-10}$ at 0°

Band	This research	Mayhood[a]	Morcillo and Herranz[b]
ν_1	278	317 ± 8	350 ± 20
ν_2	348	376 ± 20	360 ± 30
ν_3	2520	2560 ± 70	2640 ± 80

[a] See reference 4. [b] See reference 3.

We estimate the limits of error in our measurements to be about 10%. This is appreciably larger than the scatter of the points for ν_1 and ν_2, but is based upon the uncertainty in reproducing the 100% line, *i.e.*, with no absorbing material in the cell. The over-all agreement of the present measurements with those of the other two groups is quite good, and indicates that the earlier measurements[2] were consistently too low.

The reason for this discrepancy is difficult to determine. The mass-spectrometric analysis of the sulfur dioxide–nitrogen mixture taken from the infrared cell eliminates the possibility of impurities and adsorption. We feel the only answer can be in the instrument employed in the earlier work, patterned after that of Hornig, Hyde and Adcock.[6] Our version of this instrument had an adjustable gain control in the earlier stages of its amplifier, which made it possible to drive the output tube beyond the point where output voltage is a linear function of input voltage The qualitative effect of this is to reduce the signal from the reference beam by a larger fraction than the signal from the sample beam, which will appear as an erroneously small absorption by the sample. However, the earlier paper on sulfur dioxide[2] also reports intensity measurements for acetylene and its various isotopic derivatives which were carried out on the same instrument at about the same time. Our acetylene measurements, as mentioned in the paper,

(1) Supported in part by the National Science Foundation and by the United States Air Force through the Air Research and Development Command under Contract No. AF 18(600)-1522. Reproduction in whole or in part is permitted for any purpose of the United States Government.

(2) D. F. Eggers, Jr., I. C. Hisatsune and L. Van Alten, This Journal, **59**, 1124 (1955).

(3) J. Morcillo and J. Herranz, *Anales real soc. espan. fis. y quim. (Madrid)*, **A52**, 207 (1956).

(4) J. E. Mayhood, *Can. J. Phys.*, **35**, 954 (1957).

(5) L. D. Kaplan and D. F. Eggers, Jr., *J. Chem. Phys.*, **25**, 876 (1956).

(6) D. F. Hornig, G. E. Hyde and W. A. Adcock, *J. Opt. Soc. Am.*, **40**, 497 (1950).

are in rather good agreement with those of other workers. The instrument was drastically modified shortly after the earlier measurements, so that it is not possible to check this suggested source of error.

A more detailed comparison of the results in Table I shows, for ν_2 and ν_3, none of the results differs by more than about 4% from the average of all three groups. This high order of agreement is most pleasing, though the scatter of our points is appreciably larger for ν_3. In ν_1, however, our measurements are 13% lower than the average, while those of Morcillo and Herranz are 11% higher. It is of interest to note the large variation in the ranges of *pl* values investigated. For ν_1, we employed values higher than either of the others; for ν_2, Mayhood worked in a lower range than Morcillo and Herranz or ourselves; for ν_3, Morcillo and Herranz worked in a lower range than Mayhood or ourselves.

The major conclusion of this investigation is that, with proper care, infrared intensities can be measured with reasonable precision. It is most unfortunate that each system involves an absolute measurement, since relative measurements can usually be made with facility and precision.

We must also point out that our earlier paper contained several errors in the calculation of bond moments from intensities, which have been noted and corrected by Mayhood.[4]

THE ELECTRIC MOMENTS OF MOLECULES WITH SYMMETRIC ROTATIONAL BARRIERS

By H. Bradford Thompson

Department of Chemistry, Gustavus Adolphus College, St. Peter, Minnesota

Received August 3, 1959

In his classic note on the electric moments of complex molecules, Eyring gives an equation (1, below) for the free rotation moment.[1,2] The usefulness of this equation is enhanced by the observation that it applies also for internal rotations restricted by p-fold symmetric potential barriers, where p is greater than one. This fact has apparently been known by a number of workers in the field.[3] A proof and demonstration of the generality of this result are presented below.

According to Eyring, the free-rotation moment μ_a is given by

$$\mu_a^2 = \sum_{j=1}^{n} m_j^2 + 2\sum_{j=1}^{n}\sum_{s<j} m_j m_s \prod_{k=j}^{s+1} \cos\theta_k \qquad (1)$$

Here m_j and m_s represent the magnitudes of the separate group or bond moments within the molecule, these moments being n in number. θ_k is the angle between two consecutive bonds in the bond framework or chain between the bonds having moments m_j and m_s. The product is then taken over all the bond angles between these two moments. The signs of m_j and m_s are so taken that $m_j m_s$ is positive if the moments point in the same direction passing along the bond framework.

Following Eyring's development, the moment for any particular rotational conformation is given by

$$\mu^2 = \sum_{j=1}^{n} m_j^2 + 2\sum_{j=1}^{n}\sum_{s<j} (m_j e_{xj})\cdot(A_j \ldots A_s m_s e_{xs}) \qquad (2)$$

where e_{xj} and e_{xs} are unit vectors in the bond directions corresponding to m_j and m_s. $A_j \ldots A_s$ represents a series of transformations which, applied successively to the vector $m_s e_{xs}$, refer this vector successively to rectilinear coördinate systems based on each of the bonds along the chain from m_s to m_j, until finally both $m_j e_{xj}$ and $m_s e_{xs}$ are in the same coördinate system. With coördinates as defined by Eyring

$$A_k = \begin{bmatrix} \cos\theta_k & -\sin\theta_k\cos\phi_k & \sin\theta_k\sin\phi_k \\ \sin\theta_k & \cos\theta_k\cos\phi_k & -\cos\theta_k\sin\phi_k \\ 0 & \sin\phi_k & \cos\phi_k \end{bmatrix} \qquad (3)$$

where ϕ_k is a suitably-defined angle of intramolecular rotation.

The symmetrical-barrier moment is found, essentially, by taking the mean of moments for a number of equally probable conformations, as given by equation 2. This mean must be taken over all combinations of equilibrium positions for all the rotational angles ϕ_k, the angles θ_k remaining constant. We may express the equilibrium values of ϕ_k as ϕ_{ko}, $\phi_{ko} + 2\pi/p$, $\phi_{ko} + 4\pi/p$, ..., $\phi_{ko} - 2\pi/p$ where the k'th rotation has p-fold symmetry. The sum expressing the desired mean will be indeed complicated, but for each term in the double sum of equation 2 the resultant expression will contain, in terms of a given angle ϕ_k, terms of the form

$$B[\cos\phi_{ko} + \cos(\phi_{ko} + 2\pi/p) + \ldots. + \cos(\phi_{ko} - 2\pi/p)] + C[\sin\phi_{ko} + \sin(\phi_{ko} + 2\pi/p) + \ldots.. + \sin(\phi_{ko} - 2\pi/p)] \qquad (4)$$

B and C are here expressions involving m_j, m_s, and the various angles θ and ϕ, but not involving ϕ_k. Each of the expressions in brackets is identically zero for any choice of ϕ_{ko} if p is an integer greater than one. It may now be shown simply that all terms in A_k involving ϕ_k will disappear when the average is taken. Thus for symmetrical barriers, as for free rotation, we can use

$$A_k = \begin{bmatrix} \cos\phi_k & 0 & 0 \\ \sin\phi_k & 0 & 0 \\ 0 & 0 & 0 \end{bmatrix} \qquad (5)$$

The treatment above might appear to apply only to the case where ϕ_k in each conformation is restricted closely to the neighborhood of its equilibrium position. For high temperatures or shallow barriers one must evaluate, in place of the sum in equation 4, an integral of the form

$$I = \int_0^{2\pi} (B'\cos\phi_k + C'\sin\phi_k) e^{-E/RT}\, d\phi_k \qquad (6)$$

However, this integral may be divided into p integrals over intervals $2\pi/p$ in length. Over each interval the exponential function has the same shape, so

(1) H. Eyring, *Phys. Rev.*, **39**, 746 (1932).

(2) C. P. Smyth, "Dielectric Behavior and Structure," McGraw-Hill Book Co., Inc., New York, N. Y., 1955, section VIII-2. The choice of symbols herein is patterned after Smyth.

(3) See for example A. Tobolsky, R. E. Powell and H. Eyring, in "The Chemistry of Large Molecules," R. E. Burk and O. Grummitt, Editors, Interscience Publishers, Inc., New York, N. Y., 1943; footnote to p. 155.

$$I = \int_0^{2\pi/p} \{B'[\cos\phi_k + \cos(\phi_k + 2\pi/p) + \ldots\ldots] + C'[\sin\phi_k + \sin(\phi_k + 2\pi/p) + \ldots\ldots]\} e^{-E'/RT}\, d\phi_k \quad (7)$$

As before, the expressions in brackets are identically zero.

Conclusion.—Equation 1 applies not only to free rotation, but to the more general case of rotational barriers of twofold or higher symmetry. Experimental electric moments deviating from those predicted by this equation thus indicate non-symmetrical barriers or interactions between rotating groups.

THE HEAT OF COMBUSTION OF TETRAMETHYLTETRAZENE AND 1,1-DIMETHYLHYDRAZINE

By Terence M. Donovan, C. Howard Shomate and William R. McBride

Chemistry Division, Research Department, U. S. Naval Ordnance Test Station, China Lake, California

Received September 26, 1959

Interest in 1,1-dimethylhydrazine and related compounds for consideration as propellants for rocket propulsion applications led to the present experimental work for the determination of the heat of combustion of tetramethyltetrazene, the lowest alkyl homolog of the 2-tetrazenes >N—N=N—N<. The redetermination of the heat of combustion of 1,1-dimethylhydrazine was used as check on the experimental technique in view of the fact that a method utilizing Lucite on sealed thin-walled Pyrex bulbs was devised for the present work. The heat of combustion of hydrazine was determined by Hughes, Corruccini and Gilbert[1] and of several methylhydrazines including 1,1-dimethylhydrazine by Aston and co-workers.[2]

Experimental

Materials.—1,1-Dimethylhydrazine (Westvaco-Chlor-Alkali Div., Food Machinery and Chemical Corp.) was dried with barium oxide and purified by fractional distillation. Tetramethyltetrazene was synthesized by the oxidation of 1,1-dimethylhydrazine with potassium bromate in aqueous hydrochloric acid,[3] dried with barium oxide and fractionally distilled under reduced pressure. Purity of the compounds was verified by gas chromatographic techniques and various chemical and physical methods.

Apparatus and Procedure.—The heats of combustion were determined with calorimetric equipment described previously[4,5] except for the following modification. The energy of ignition of the sample was determined by direct experimental measurement.

National Bureau of Standards benzoic acid, sample No. 39f, was used in the determination of the energy equivalent of the calorimeter which was 2,785.03 ± 0.29 cal. deg.$^{-1}$ for the tetramethyltetrazene combustions and 2,783.23 ± 0.93 cal. deg.$^{-1}$ for the 1,1-dimethylhydrazine experiments. The difference is due to minor alterations of the apparatus. All weighings were reduced to vacuum and all heat values are expressed in defined calories (1 cal. = 4.1840 abs. joules).

Small Pyrex ampoules (approximately 0.5 g.) were filled with the liquids on a vacuum manifold by an extension of a technique previously employed for potassium[6] and hydrazine.[7] Ignition was accomplished by two methods. In the first a film of benzoic acid covering the bulb was ignited by fuse paper. The resulting heat concentration broke the bulb. This method of breaking the bulbs proved unreliable so a second procedure was developed. A drop of a concentrated solution of Lucite (polymethyl methacrylate) in acetone was applied to the bulb. The platinum ignition wire was set in this drop. Then the acetone was pumped off in a vacuum desiccator (leaving *ca.* 5 mg. of Lucite). The bulb was supported between the electrodes by the ignition wire (no crucible was used). This method proved very reliable for breaking the bulbs. Aston[2] reported breaking bulbs containing volatile liquids by means of a small pellet of benzoic acid. Long[8] had equally good results using a piece of magnesium turning. However, the presently reported method has the advantages of a more intimate contact between the glass and the auxiliary material and a smaller amount of auxiliary material is used than in previous methods. The mean of three combustions of Lucite under bomb conditions, *i.e.*, 5-mg. samples applied to glass ampoules, gave 6440 cal. g.$^{-1}$ as its heat of combustion.

A 360-ml. Parr double-valve oxygen bomb, to which 1 ml. of water had been added, was flushed for 15 minutes with oxygen at slightly greater than atmosphere pressure and then filled to 30 atmospheres in all combustions. The combustion gases were analyzed spectrographically for carbon monoxide and oxides of nitrogen and any runs with a positive test were discarded.

Corrections were made for the ignition wire and auxiliary material. The observed values for the heat of the bomb process were corrected to obtain values for the energy of the idealized combustion reaction in which all the reactants and products were in their standard states at 25° and no external work was performed. The corrections, which included those for the formation of nitric acid were made in the manner described by Hubbard, Scott and Waddington.[9]

Results and Discussion

The heats of formation of the tetramethyltetrazene and 1,1-dimethylhydrazine were calculated using −68,316 and −94,059.6 (at. wt. C = 12.011) cal. mole^{-1} as the heats of formation of water and carbon dioxide, respectively, and our experimentally determined values of −841.47 ± 0.21 and −473.28 ±0.43 kcal. mole^{-1} as the heats of combustion of tetramethyltetrazene and 1,1-dimethylhydrazine, respectively. These values are listed in Table I.

The N=N bond energy in the atomization of gaseous tetramethyltetrazene was estimated to be 75.9 kcal. mole^{-1} by means of our experimental heat of combustion of tetramethyltetrazene, its heat of vaporization (10.4 kcal. mole^{-1}) calculated from vapor pressure data,[10] and reported bond energy values.[11]

The heat of combustion value for 1,1-dimethylhydrazine compares well with the value of −472.65 ±0.70 kcal. mole^{-1} reported by Aston.[2] Six determinations were made with 1,1-dimethylhydrazine but three were unacceptable because of carbon monoxide in the exhaust gases. The value for

(1) A. M. Hughes, R. J. Corruccini and E. C. Gilbert, *J. Am. Chem. Soc.*, **61**, 2639 (1939).

(2) J. G. Aston, E. J. Rock and S. Isserow, *ibid.*, **74**, 2484 (1952).

(3) W. R. McBride and H. W. Kruse, *ibid.*, **79**, 572 (1957).

(4) M. M. Williams, W. S. McEwan and R. A. Henry, This Journal, **61**, 261 (1957).

(5) W. S. McEwan and M. W. Rigg. *J. Am. Chem. Soc.*, **73**, 4725 (1951).

(6) G. W. Watt and D. M. Sowards, *ibid.*, **76**, 4742 (1954).

(7) G. W. Watt and W. R. McBride, *ibid.*, **77**, 2088 (1955).

(8) L. H. Long and R. G. W. Norrish, *Roy. Soc. (London), Phil. Trans.*, C241, Series A (1949).

(9) W. N. Hubbard, D. N. Scott and G. Waddington, *J. Am. Chem. Soc.*, **58**, 152 (1954).

(10) Unpublished data of A. Adams and W. R. McBride. The following expression was found to hold over the temperature range indicated

$$\log P = -\frac{2271.54}{T} + 8.5620 \quad (25\text{–}50°)$$

(11) S. S. Penner, "Chemistry Problems in Jet Propulsion," Pergamon Press, New York, N. Y., 1957, p. 62.

TABLE I

COMBUSTION DATA

Compound	Sample wt., g. (vacuum)	Total heat evolved (cal.)	Aux. material corrn. (cal.)	Fuze corrn. (cal.)	HNO_3 corrn. (cal.)	$-\Delta H^0c$, kcal./mole	ΔH^0f, kcal./mole
Tetramethyltetrazene	0.85423	6243.79	−31.61	−12.91	−21.82	841.62	
	.90990	6652.32	−31.61	− 9.68	−29.94	841.80	
	.93513	6854.35	−58.80	−10.49	−30.73	840.66	
	.91851	6712.56	−43.85	0	−27.76	841.50	
	.91000	6657.89	−46.43	0	−29.78	841.79	
					Mean =	841.47 ± 0.21	55.34
1,1-Dimethylhydrazine	.94861	7519.04	−24.51	0	−43.52	472.91	
	.81663	6494.53	−36.76		−31.17	474.15	
	.77797	6169.03	−39.98		−24.14	472.79	
					Mean =	473.28 ± 0.43	11.90

tetramethyltetrazene represents the mean of five acceptable determinations. Four were rejected for the above reason.

THERMAL EFFECTS IN MAGNESIUM AND CALCIUM OXIDES

BY C. N. R. RAO AND KENNETH S. PITZER

Department of Chemistry and Lawrence Radiation Laboratory, University of California, Berkeley 4, California

Received October 7, 1959

In connection with our studies on the transitions and thermal anomalies in silver oxide[1,2] we became interested in the thermal behavior of magnesium and calcium oxides. These oxides show large differences in the heat contents of the crystalline and finely divided samples.[3,4] The crystalline samples of the oxides were prepared by the decomposition of the hydroxides at high temperatures while the finely divided samples were prepared by the decomposition at relatively low temperatures. We have now studied, by the technique of differential thermal analysis, the decomposition of $Mg(OH)_2$ and $Ca(OH)_2$ and, in addition, a sample of MgO prepared by the low temperature decomposition of the hydroxide. Since no further work on these oxides is now planned, it seems desirable to report the rather fragmentary results at this time.

The differential thermal analysis apparatus described by Pask and Warner[5] was used. The measurable sensitivity of the apparatus is 0.25 to 0.5 cal. A constant heating rate of 12° per min. was employed in all the runs. The indicated reaction peak temperatures are constant only for a given set of experimental conditions. The samples of $Mg(OH)_2$ and $Ca(OH)_2$ were of reagent grade. A sample of MgO was prepared by the decomposition of the hydroxide around 350° *in vacuo* (at least 95% decomposition took place). Typical differential thermal analysis curves are shown in Fig. 1.

X-Ray diffraction patterns of the samples were taken using a North American Phillips diffractometer fitted with a geiger-counter recording device.

Magnesium hydroxide first showed a very large endothermic reaction peak around 500° due to the decomposition of the hydroxide to the oxide and water vapor, immediately following which was observed a small exothermic reaction peak around 560°. The finely divided MgO prepared by the low temperature decomposition of the hydroxide showed a small endothermic peak around 390° (possibly due to the decomposition of the hydroxide impurity or removal of occluded water) and the exothermic peak around 450°. This seemed to suggest that the exothermic reaction temperature

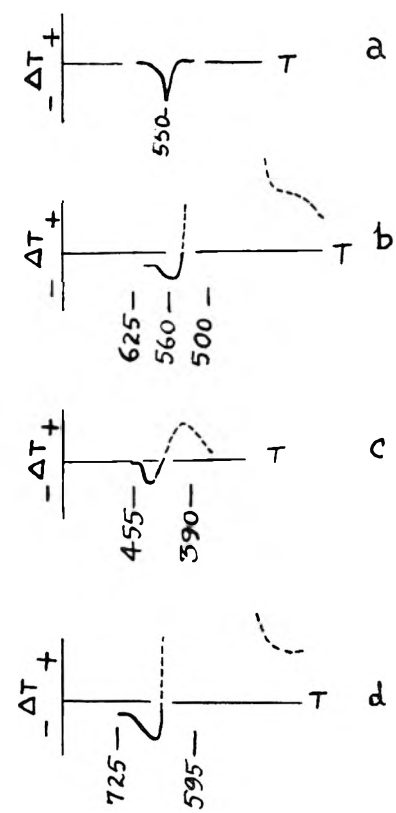

Fig. 1.—Differential thermal analysis curves: (a) alpha-beta inversion peak for quartz corresponding to about 4.5 cal. heat evolution; (b) $Mg(OH)_2$; (c) MgO prepared by the decomposition of $Mg(OH)_2$ at 350° *in vacuo*; (d) $Ca(OH)_2$. The dotted peaks correspond to the decomposition of the hydroxide.

(1) K. S. Pitzer and W. V. Smith, *J. Am. Chem. Soc.*, **59**, 2633 (1937).

(2) K. S. Pitzer, R. E. Gerkin, L. V. Gregor and C. N. R. Rao, "Symposium on Chemical Thermodynamics," International Union of Pure and Applied Chemistry, Wattens, Austria, 1959.

(3) W. F. Giauque, *J. Am. Chem. Soc.*, **71**, 3192 (1949).

(4) K. Kobayashi, *Sci. Repts. Tohoku Univ.*, **34**, 153 (1950).

(5) J. A. Pask and M. F. Warner, *Am. Ceram. Soc. Bull.*, **33**, 168 (1951).

is dependent on the temperature at which the hydroxide is decomposed. The $Ca(OH)_2$ showed the endothermic reaction peak around 600° and the exothermic reaction peak around 670°. In all these cases, when the samples were cooled down to a lower temperature after the completion of the exothermic reaction, the repeat differential thermal curves did not show the exothermic peaks indicating that these exothermic reactions are irreversible.

There was no difference in the crystal structure or the parameter of the oxides before and after the exothermic reaction. However, an MgO sample heated past the exothermic peak showed considerably sharper lines in its X-ray diffraction pattern. Such a decrease in the X-ray line widths may be taken as evidence for the greater crystallinity of the oxide attained after the exothermic reaction.

The heats of these exothermic reactions were estimated by comparing the peak sizes with the peak size for the alpha-beta inversion of quartz (4.3 cal. per g.). The heats thus estimated are of the order of 300 to 400 cal. per mole for MgO and CaO, although curves (b) and (d) in Fig. 1 give some indication of continued heat evolution at higher temperatures.

The most interesting aspect of these results is the sharpness of the heat evolution as contrasted with wide variability in the temperature of its occurrence. Thus the principal effect covers not over a 50° range in temperature in any one case, but it occurs at a temperature over 100° higher for sample (b) than for sample (c). There is every reason to believe that a reduction of surface area[6] occurs when finely divided MgO is heated, but this effect probably continues over a wider temperature range. While reduction in surface undoubtedly contributes to the heat evolution, we suspect that the removal of internal crystal defects is also important.

Exothermic reactions similar to those reported here have been observed in the case of silver oxide[7] and also in hydrates of ferric and chromic oxides.[8]

The authors are indebted to Professor J. A. Pask for the use of his laboratory facilities and to Mrs. M. P. Lewis for her generous assistance. The research was performed under the auspices of the U. S. Atomic Energy Commission.

(6) See R. I. Razouk and R. Sh. Mikhail, THIS JOURNAL, **63**, 1050 (1959); and references there cited.

(7) K. Kobayashi, *Sci. Rep. Tohoku Univ.*, [I] **35**, 173 (1951).

(8) S. K. Bhattacharyya, V. S. Ramachandran and J. C. Ghosh, *Adv. in Catalysis*, **9**, 114 (1957).

THE HEAT OF ISOMERIZATION OF THE *cis* AND *trans* ISOMERS OF 9-METHYLDECAHYDRONAPHTHALENE

BY WILLIAM G. DAUBEN, O. ROHR,

Department of Chemistry, University of California, Berkeley 4, California

ABBAS LABBAUF AND FREDERICK D. ROSSINI

Chemical and Petroleum Research Laboratory, Carnegie Institute of Technology, Pittsburgh 13, Pennsylvania

Received September 16, 1959

The heat of isomerization of *trans*-decahydronaphthalene to *cis*-decahydronaphthalene in the liquid state, measured as the difference in the heats of combustion, was reported in 1941 by Davies and Gilbert[1] to be $\Delta H = 2.1$ kcal./mole at 25°. Using the concept of the non-bonded interactions characteristic of skew butane conformation,[2] Turner[3] evaluated the difference in energy to be 2.4 kcal./mole for the gaseous state, which becomes 2.1 kcal./mole for the liquid state. More recent experimental measurements of the heats of combustion of very pure API Research samples of the *cis* and *trans* forms of decahydronaphthalene in the liquid state, by Speros and Rossini,[4] yield $\Delta H = 2.69 \pm 0.31$ kcal./mole at 25° for the heat of isomerization of the *trans* form to the *cis* form.

Applying the same conformational concepts to the *cis* and *trans* forms of 9-methyldecahydronaphthalene, Turner[3] predicted that the *trans* isomer would be more stable than the *cis* isomer by only 0.8 kcal./mole, this smaller difference in energy being due mainly to the interactions of additional non-bonded atoms. Since the 9-methyldecahydronaphthalene structure is a common structural unit in many natural products, it was important to obtain experimental evidence with regard to the reliability of conformational analysis in this latter type of system.

Samples of the *cis* and *trans* forms of 9-methyldecahydronaphthalene were synthesized at the University of California by methods described earlier,[5] and purified for the calorimetric measurements. The properties of the two samples were as follows: *cis* form, b.p. 93–94° at 20 mm., n_D 1.4788 at 27°; *trans* form, b.p. 91–93° at 20 mm., n_D 1.4749 at 27°. By gas phase chromatographic adsorption, using a 240-foot column containing Tween (giving about 50,000 theoretical plates), each isomer was found to contain 1.8 to 2.0% of the other isomer.[6]

Measurements of the heats of combustion of the two compounds were made in the apparatus[7,8] of the Thermochemical Laboratory at the Carnegie Institute of Technology. Five calorimetric experiments were completed for each compound, using the procedure previously described.[9] The amount of reaction in each experiment was determined from the mass of carbon dioxide produced in the combustion, which was near 2.75 g. in each experiment and measured to 0.1 mg. No evidence

(1) G. F. Davies and E. C. Gilbert, *J. Am. Chem. Soc.*, **63**, 1585 (1941).

(2) For a discussion of the conformational concepts involved, see W. G. Dauben and K. S. Pitzer, "Steric Effects in Organic Chemistry," edited by M. S. Newman, published by John Wiley and Sons, New York, N. Y., 1956, p. 23.

(3) R. B. Turner, *J. Am. Chem. Soc.*, **74**, 2118 (1952).

(4) D. M. Speros and F. D. Rossini, Paper in preparation, Chemical and Petroleum Research Laboratory, Carnegie Institute of Technology, Pittsburgh 13, Pennsylvania.

(5) W. G. Dauben, J. B. Rogan and E. J. Blanz, Jr., *J. Am. Chem. Soc.*, **76**, 6384 (1954).

(6) These analyses were kindly performed by Dr. Roy Teranishi, Western Regional Research Laboratory, U. S. Department of Agriculture, Albany, California.

(7) C. C. Browne and F. D. Rossini, paper in preparation, Chemical and Petroleum Research Laboratory, Carnegie Institute of Technology, Pittsburgh 13, Pennsylvania.

(8) A. Labbauf and F. D. Rossini, paper in preparation, Chemical and Petroleum Research Laboratory, Carnegie Institute of Technology, Pittsburgh 13, Pennsylvania.

(9) W. H. Johnson, E. J. Prosen and F. D. Rossini, *J. Research Natl. Bur. Standards*, **42**, 251 (1949).

TABLE I

RESULTS OF THE COMBUSTION EXPERIMENTS

(See ref. 9 for explanation of the symbols).

No. of expt.	Av. mass of CO_2, g.	$k \times 10^4$, min.$^{-1}$	$K \times 10^4$, ohms	$U \times 10^4$, ohms	ΔR_c, ohms	$\Delta r_i \times 10^4$, ohms	$\Delta r_n \times 10^4$, ohms	Av. value of B, ohms/g. CO_2	Stand. dev. of the mean, ohms/g. CO_2
				9-Methyl-*cis*-decahydronaphthalene					
5	2.86	16.07 to 16.52	7.73 to 12.81	0.13 to 4.17	0.183196 to 0.202214	3.45 to 3.49	0.10 to 0.14	0.069169	±0.000011
				9-Methyl-*trans*-decahydronaphthalene					
5	2.76	16.17 to 16.60	10.59 to 15.03	−0.02 to −3.04	0.187079 to 0.193369	3.39 to 3.55	0.06 to 0.11	0.069111	±0.000009

TABLE II

VALUES[a] OF THE STANDARD HEATS OF COMBUSTION AND FORMATION OF 9-METHYL-*cis*-DECAHYDRONAPHTHALENE AND 9-METHYL-*trans*-DECAHYDRONAPHTHALENE

Compound: Name	Formula	State	B at 30°, ohm/g. CO_2	$-\Delta E_B$ at 30°, kj./mole	$-\Delta E^0$ at 30°, kj./mole	$-\Delta Hc^0$ at 30°, kj./mole	$-\Delta Hc^0$ at 25°, kj./mole	$-\Delta Hc^0$ at 25°, kcal./mole	ΔHf^0 at 25°, kcal./mole
9-Methyl-*cis*-decahydronaphthalene	$C_{11}H_{20}$	Liq.	0.069169 ±0.000022	6930.37 ±1.88	6928.38 ±1.88	6941.00 ±1.88	6943.06 ±1.88	1659.43 ±0.45	−58.31 ±0.47
9-Methyl-*trans*-decahydronaphthalene	$C_{11}H_{20}$	Liq.	0.069111 ±0.000018	6924.56 ±1.72	6922.57 ±1.72	6935.19 ±1.72	6937.24 ±1.72	1658.04 ±0.41	−59.70 ±0.44

[a] The uncertainties in this table are twice the standard deviation.

of incomplete combustion was found in any of the experiments reported. The results are listed in Tables I and II. These data give for the reaction

9-methyl-*trans*-decahydronaphthalene (liquid) = 9-methyl-*cis*-decahydronaphthalene (liquid),

$\Delta H = 1.39 \pm 0.64$ kcal./mole, at 25°

Within the respective limits of uncertainty, this value is in substantial accord with the predicted value[3] arrived at using the concept of non-bonded atoms.

Assuming the values of the change in entropy for the preceding reaction to be the same as found by McCullough, *et al.*,[10] (see also reference[11]) for the corresponding *trans* and *cis* isomers of decahydronaphthalene, namely, 0.02 cal./deg. mole for the liquid state at 25°, with an uncertainty estimated to be near ±0.5 cal./deg. mole, it is to be expected that 9-methyl-*trans*-decahydronaphthalene will be more abundant than the *cis* isomer at equilibrium at 25°.

(10) J. P. McCullough, H. L. Finke, J. F. Messerly, S. S. Todd, T. C. Kincheloe and G. Waddington, *J. Phys. Chem.*, **61**, 1105 (1957).

(11) N. L. Allinger and J. L. Cook, *J. Am. Chem. Soc.*, **81**, 4080 (1959).

ADSORPTION ON POROUS SOLIDS

BY BERT H. CLAMPITT AND DALE E. GERMAN

Physical Sciences Staff, Boeing Airplane Company, Wichita Division, Wichita, Kansas

Received October 10, 1959

The original Brunauer–Emmett–Teller (BET) theory of adsorption[1] was extended by Brunauer–Deming–Deming and Teller (BDDT)[2] to include adsorption by porous solids. The latter theory leads to an equation involving four constants. Two of these, "Vm" and "c," are found in the original BET theory; while the others, "n" and "g," are unique to adsorbents containing capillaries. The BET "c" constant recently was modified[3] to give heats of adsorption in closer accord to calorimetric heat values. It is the purpose of this note to extend the previous treatment to include the BDDT theory. It will be shown that the "g" constant proves to be a unique property of the adsorbate, and can be determined without recourse to adsorption experiments.

Method

It was shown previously[3] that the liquid–vapor surface energy is important even in adsorption on a non-porous surface, since it makes E_L vary with the number of adsorbed layers; indeed it was shown that

$$E_L = \frac{m-1}{m}\Delta H^0 + \frac{1}{m}\Delta H_s \qquad (1)$$

where m is the number of liquid layers, ΔH^0 is the heat of vaporization of bulk liquid, and ΔH_s is the heat of vaporization of the surface layer. ΔH_s may be calculated from surface tension data by means of the equation

$$\Delta H_s = \Delta H^0 - 1.35\left[kT + \gamma\left(\frac{M}{\rho}\right)^{2/3}\right] \qquad (2)$$

where k is the Eotvos constant, γ the surface tension, ρ the density, M the molecular weight, and T the absolute temperature.

The "g" constant in the BDDT theory arises because the last adsorbed layer in a capillary is attracted on both sides, releasing the surface energy of the liquid. This gives rise to an additional ad-

(1) S. Brunauer, P. H. Emmett and E. Teller, *J. Am. Chem. Soc.*, **60**, 309 (1938).

(2) S. Brunauer, L. S. Deming, W. E. Deming and E. Teller, *ibid.*, **62**, 1723 (1940).

(3) B. H. Clampitt and D. E. German, THIS JOURNAL, **62**, 438 (1958).

sorption energy "Q," and "g" is defined as $g = \exp(Q/RT)$.

Consider that the capillary is filled but for one molecular layer; then the total energy of adsorption of $(n - 1)$ layers is according to the BDDT theory

$$E_{\text{total}} = E_1 + (n - 2)E_L \qquad (3)$$

As in the original BET theory, it was assumed that E_L was equal to the heat of liquefaction of bulk liquid; however, equation 1 indicates that E_L is a function of the number of liquid layers present. Combining (1) and (3) gives the total energy of adsorption of $(n - 1)$ layers as

$$E_{\text{total}} = E_1 + (n - 3)\Delta H^0 + \Delta H_s \qquad (4)$$

The addition of the last adsorbed layer makes the entire system approach the conditions of bulk liquid; therefore, all of the layers above the first adsorbed layer *do* have an energy of adsorption equal to that of bulk liquid. The $(n - 1)$ layers now have an energy of adsorption given by equation 3, where E_L is equal to the heat of liquefaction of bulk liquid. Q, therefore, equals the new energy of adsorption of all the lower layers, minus the old energy of adsorption of all the lower layers or

$$Q = [E_1 + (n - 2)\Delta H^0] - [E_1 + (n - 3)\Delta H^0 + \Delta H_s] \qquad (5)$$

or

$$Q = \Delta H^0 - \Delta H_s \qquad (6)$$

Combining equations 2 and 6 gives

$$Q = 1.35\left[kT + \gamma\left(\frac{M}{\rho}\right)^{2/3}\right] \qquad (7)$$

where Q is expressed in calories and γ is expressed in ergs/cm.^{2}. By means of equation 7 "Q," and therefore "g," may be determined independently of adsorption experiments.

The BDDT paper also indicated that if $C >> 1$, then in the neighborhood of saturation pressure, the equation (8) is approximately correct.

$$V = Vm\left\{\frac{n}{2} - \frac{n(n-1)(n-2)}{12}\left[\frac{c^2}{(nc^2 - c^2 + 2c)g}\right]\right\} \qquad (8)$$

In the BDDT paper "g" was unknown and therefore this formula was difficult to use to evaluate "n." As "g" is now implicitly known, and as $(nc^2 - c^2 + 2c)g \simeq c^2g(n - 1)$, equation 8 reduces to the simple quadratic

$$n^2 - (6g + 2)n + \frac{12V(1)g}{Vm} = 0 \qquad (9)$$

where $V(1)$ represents the amount of vapor adsorbed at saturation pressure. Provided $C >> 1$ (*i.e.*, at least 10) this equation serves very well for determining "n." This is true for the great majority of adsorbent–adsorbate systems.

Results and Discussion

The BDDT theory generally has been recognized as a logical extension of the BET theory to porous solids; however, the equation is rather complex and the evaluation of the constants "n" and "g" by successive approximations makes its use extremely difficult. If "g" is implicitly known, then only one arbitrary constant remains and it may be rather easily evaluated. Indeed the order of magnitude of "n" can be determined from equation 9.

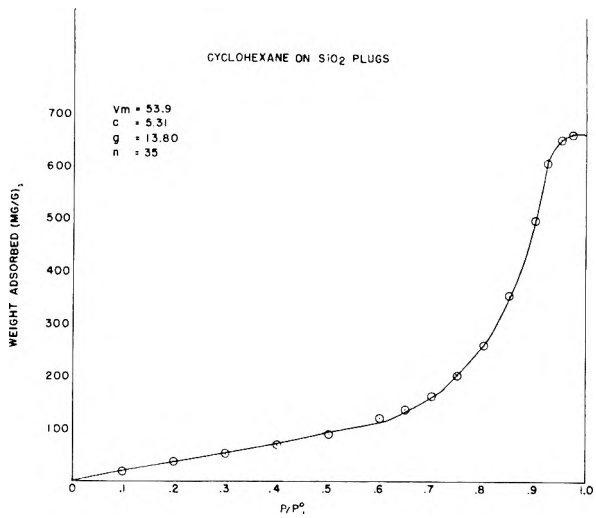

Fig. 1.—Best fit of experimental curve.

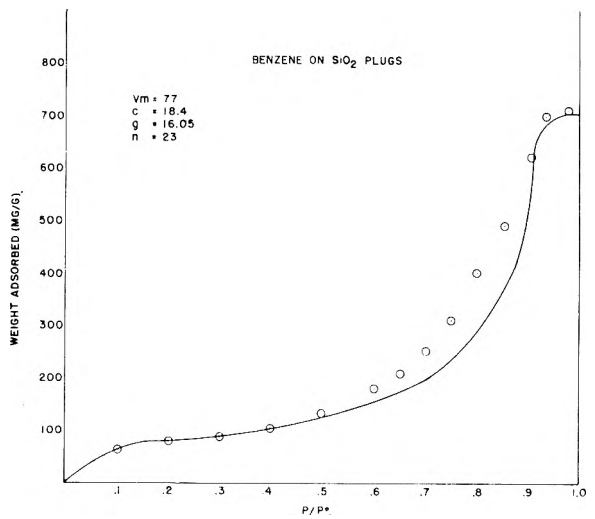

Fig. 2.—Poorest fit of experimental curves.

The data of Lambert and Clark[4] for the adsorption of benzene on ferric oxide gel were used originally to test the BDDT theory. The constants "g" and "n" were determined by trial and error to give the best fit of the experimental data. Equations 7 and 9, however, lead to the same numerical results with considerably less effort.

The BDDT equation was used to fit the data of several other workers with the results shown in Table I. In each case the value of "g" was determined from equation 7 and the approximate value of "n" from equation 9. The exact value of "n" was determined as the best fit of the experimental curve as determined on an IBM 610 computer. In all cases where $C > 10$, the two values of "n" agree within 4%.

The agreement between the theory and the experimental curves is shown in Figs. 1 and 2. In these figures the solid lines represent the experimentally determined adsorption isotherm while the points are calculated from the BDDT equation. Figure 1 probably represents the best fit of the experimental curve; while Fig. 2 shows the poorest

(4) B. Lambert and A. M. Clark, *Proc. Roy. Soc.* (*London*), **A122**, 497 (1929).

TABLE I

DATA FIT TO THE BDDT EQUATION

Adsorbent	Adsorbate	T (°K.)	Vm	C	g	n	Ref.
Ferric oxide gel	Benzene	323	0.081	27.0	13.07	6	4
Silica plug	Benzene	299	77.0	18.35	16.05	23	5
Silica plug	Cyclohexane	299	53.9	5.31	13.8	35	5
Silica plug	*n*-Hexane	299	54.6	10.75	14.0	25	5
Silica–alumina gel	Nitrogen	78	76.07	79.7	8.58	11.5	6
Catalysis -660	Nitrogen	78	98.8	65.0	8.58	7	7
Catalysis -680	Nitrogen	78	88.5	57.0	8.58	7	7
Catalysis -970	Nitrogen	78	43.5	65.0	8.58	7	7

agreement. In the other cases the agreement was intermediate between the results shown in Fig. 1 and 2. It should also be pointed out that variation of "*g*" from the calculated value did not improve the fit of the experimental curve. On the whole, it is felt that the theory adequately represents the experimental adsorption isotherm.

In order to calculate adsorption isotherms at different temperatures, the BDDT paper assumes Q to be independent of temperature. Examination of equation 7 reveals this to be a necessary consequence of this equation. This interesting fact also means that Q can be evaluated at any temperature, where surface tension and density data are available, and the results will be applicable at the adsorption temperature.

(5) J. J. Van Voorhis, R. G. Craig and F. E. Bartell, THIS JOURNAL, **61**, 1513 (1957).

(6) W. D. Harkins and G. Jura, *J. Am. Chem. Soc.*, **66**, 1366 (1944).

(7) H. E. Ries, *Advances in Catalysis*, **4**, 87 (1952).

CHEMICAL KINETICS OF THE ZIRCONIUM–HYDROFLUORIC ACID REACTION[1]

BY W. J. JAMES, W. G. CUSTEAD AND M. E. STRAUMANIS

Departments of Chemical and Metallurgical Engineering, School of Mines and Metallurgy, University of Missouri, Rolla, Missouri

Received October 24, 1959

Many reports have been published on the resistance of zirconium and its alloys to chemical attack, particularly in more recent years with respect to corrosion in water and steam at elevated temperatures. Published material pertaining to the corrosion of zirconium in hydrofluoric acid has been more limited. However, interest in the aqueous processing of zirconium–uranium reactor fuels has stimulated more research into the zirconium hydrofluoric acid reaction and is reflected in the recent literature.[2-5]

In particular Smith and Hill[3] using radioactive Zr^{95} as a tracer measured the rates of dissolution in HF–HCl mixtures up to approximately 0.5 N. They found the reaction to be first order with respect to un-ionized HF, independent of oxygen concentration in the vapors above the acid and independent of small additions of NO_3^-, Cl^-, ClO_4^-, F^-, HF_2^- and K^+ to the acid. From their value of the activation energy they concluded the slow step to be one of diffusion of molecular HF through an effective boundary layer.

The purpose of this study was (1) to extend the dissolution studies above 0.5 N HF using pressure measurements of evolved hydrogen for rate determinations, (2) to study the effect of temperature on rate, (3) to investigate the effect of noble salt additions to the acid, and (4) to explain the mechanism of dissolution.

Experimental

Material and Apparatus.—A low-hafnium content zirconium was used with an average analysis: O, 0.11%; N, 0.005%; Fe, 0.04%; Hf, 0.01% b.w. After rolling, the zirconium was given a stress relief by an annealing treatment *in vacuo* for 30 minutes at 700°.

The apparatus operated on the principle of measuring a differential pressure between a selected standard atmosphere and the resulting pressure of the gaseous product formed in the unplasticized polyvinyl chloride reactor vessel. Use of a differential pressure between the reaction vessel and a ballast vessel of the same volume containing the same liquid reactant eliminated the necessity of corrections for changes in atmospheric pressure and temperature during a run and for vapor pressure effects of the liquid reactant. Furthermore, it permitted the study of reactions at pressures up to the operating pressure limit of the reactor (165 p.s.i.a.) and down to the equilibrium vapor pressure of the liquid reactant.

Zirconium samples were mounted in unplasticized polyvinyl chloride in a metallographic mounting press at 6000 p.s.i. and 130°. The polished sample was attached to the stirrer so as to expose approximately 1 cm.^{2} of surface area. Due to the relatively large volumes of liquid used (500 ml.), changes in temperature of the bulk solution did not exceed more than one degree up to 1.0 N and two degrees to 3 N.

The Rates.—Since the velocity of the liquid across the sample surface influences the rate of dissolution, the effect of stirrer speed was studied on samples in 0.25 N HF at 30°. The rate of hydrogen evolution was found to be directly proportional to the stirrer speed, $r = 0.7s - 200$ where r is in units of mm.^{3} cm.$^{-2}$ min.$^{-1}$ and s is the stirrer speed in r.p.m. In this study a stirrer speed of 90 r.p.m. was arbitrarily selected in order to approximate the measured rates observed in a previous study at lower concentrations.[4]

The differential pressures recorded on the chart were converted into mm.^{3} of H_2 evolved. The rates were calculated using the expression

$$r = \frac{1000\ \Delta V}{A\ \Delta t} \qquad \text{(I)}$$

where r = rate in mm.^{3} cm.$^{-2}$ min.$^{-1}$, V = cc. of H_2 at STP evolved in Δt minutes, A = area of the sample in cm.^{2}, or

$$r = \frac{2.035 \Delta V}{A\ \Delta t} \qquad \text{(II)}$$

where r is now in units of mg. of Zr cm.$^{-2}$ min.$^{-1}$.

The reaction rates were observed for an acid concentration range of 0.1 to 3.0 N at a temperature of 30° in aqueous HF. At concentrations above 3.0 N the reaction was so rapid that accurate measurements could not be made. The rate equation for the dissolution of zirconium in these concentrations was assumed to be

$$\frac{d[Zr]}{dt} = k[HF]^n \qquad \text{(III)}$$

A plot of log rate *versus* log acid concentration (stoichiometric) is shown in Fig. 1. In concentrations up to approximately 0.5 N the reaction obeys a first-order rate law. The deviation from linearity at higher concentrations would appear to indicate that either the order of the reaction is changing or that the rate is not proportional to HF only at these higher concentrations. Rates also were observed in the same concentration range in mixtures of HF and 1 N HCl to control the equilibrium concentrations of fluoride complexes.

The rate of hydrogen evolution in the HF–HCl mixtures

(1) This work supported by the U. S. Atomic Energy Commission.

(2) J. C. Baumrucker, Dissolution of Zirconium in Hydrofluoric Acid, ANL-5020 (March 31, 1950).

(3) T. Smith and G. R. Hill, *J. Electrochem. Soc.*, **105**, 117 (1958).

(4) M. E. Straumanis, W. J. James and A. S. Neiman, *Corrosion*, **15**, 286t (1959).

(5) E. M. Vander Wall and E. M. Whitner, *Ind. Eng. Chem.*, **51**, 51 (1959).

was higher but similar in shape to that of pure HF, Fig. 1. Thus, the effect of added HCl apparently was to shift the equilibrium further in the direction of un-ionized HF thereby increasing the rate of hydrogen evolution.

Influence of Temperature on Rate.—The equipment was similar to that used by Straumanis, *et al.*[4] The experiments were made at seven concentrations of acid from 0.01 to 0.25 *N*. Duplicate runs were made at 30, 40, 50 and 60° in each of the seven concentrations. The temperature was controlled to within ±0.2°. A stirring speed of 200 r.p.m. was maintained throughout all runs.

From plots of initial rate *versus* HF concentrations at each temperature, specific reaction rate constants were calculated. From a graph of log k *versus* $1/T$ an activation energy of 3.8 kcal./mole was obtained.

The increase in rate above $0.5N$ suggested the possibility of higher temperatures at the liquid–metal interface than in the bulk solution. Accordingly the change in temperature ($\Delta T'$) was investigated by attaching an iron-constantan thermocouple to the back of a mounted zirconium specimen immersed in various concentrations of HF stirred at 200 r.p.m. (Fig. 2).

Effect of Noble Salt Additions.—Gold chloride, platinum chloride and silver nitrate additions were made after sufficient time had elapsed to allow the rates to become constant in pure acid. A rate increase was observed in the first ten minutes following addition after which there was a rather rapid and continuous drop for the remainder of the runs. All samples were covered with loose deposits identified by X-ray analysis as the respective reconstituted noble metals. For equivalent amounts of added salts the platinum was most effective in passivating the metal surface (93%) with silver next (18%) and gold (16%).

A plot of rate *versus* time is shown for a platinum chloride addition (Fig. 3).

Discussion and Conclusions

At 30.0° and a concentration of 0.25 *N* HF the value of k expressed in g(Zr) cm.$^{-2}$ min.$^{-1}$ (mole HF)$^{-1}$ liter is $4.3 \pm 0.4 \times 10^{-3}$.

On the basis of an activation energy of 3.8 kcal./mole (Smith and Hill, 3.34)[3] (Baumrucker, 4.2)[2] (Vander Wall and Whitner, 6.6)[5] and the fact that the rate increases at high HF concentrations (excluding the slow step as one of adsorption) it is likely that the slow step is diffusion of molecular HF to the metal surface. The high value of activation energy obtained by Vander Wall and Whitner was observed in HF–HNO_3 solutions. The high concentration of HNO_3, a strongly oxidizing acid, would favor the formation of oxide layers which in turn would further hinder the diffusion of HF molecules resulting in lower rates and a higher activation energy. In our studies we have also observed that the addition of oxidizing agents such as $CrO_4^=$ and MnO_4^- reduces the rate of reaction considerably.

Up to approximately 0.5 *N* HF the reaction is first order with respect to $(HF)_{un}$. In concentrations of HF or HF–HCl mixtures up to approximately 0.4 *N*, a black film, ZrH_2, is present on the metal surface.[4,6] In the vicinity of 0.4 *N* the hydride is quite soluble in HF and this may in part account for the increased rate since the HF need no longer diffuse through the porous hydride. In addition, Fig. 2 suggests that a temperature gradient exists in the boundary layer which could account further for some of the observed increase in the rate. However, the temperature coefficient is far too small to account for all of the increase.

It is interesting to consider the reactions which might occur in the sample surface. Even high purity zirconium is covered with a thin tenacious oxide layer. Thus, the reaction probably begins

(6) W. J. James and M. E. Straumanis, *J. Electrochem. Soc.*, **106**, 631 (1959).

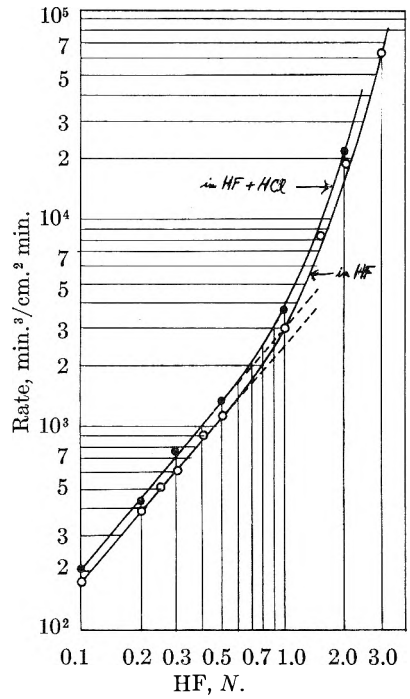

Fig. 1.—Plot of hydrogen evolution rate *versus* HF concentration for zirconium dissolving in HF at 30°.

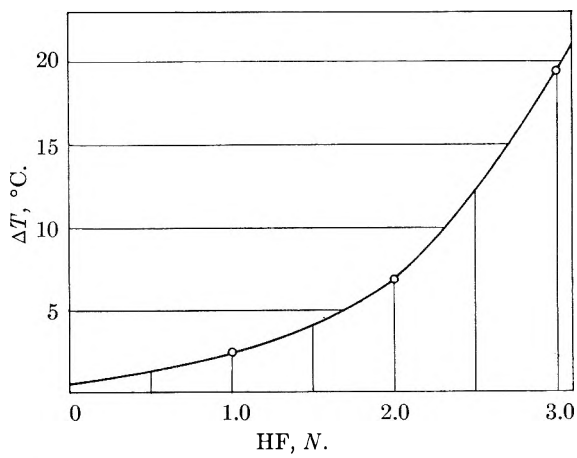

Fig. 2.—Difference in temperature between bulk solution and metal–liquid interface as a function of HF concentration for zirconium dissolving in HF.

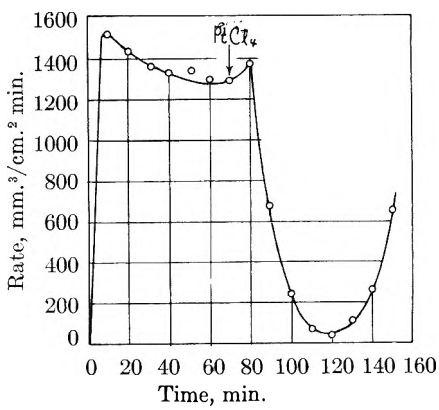

Fig. 3.—Rate of hydrogen evolution *versus* time upon adding $PtCl_4$ at the 70th minute to Zr dissolving in HF.

by the attack of HF on the oxide layer with subsequent formation of the hydride layer up to 0.4 *N* HF. Once the oxide layer is removed or traversed by HF the reaction of zirconium can take place by direct chemical attack of un-ionized HF.

The increase in rate of Zr dissolving in HF-HCl mixtures can be attributed to a shift in equilibrium to un-ionized HF, increase in conductivity of the solution and an increase in the solubility of the reaction products.

The small initial rate increases observed with noble metal salt additions are difficult to explain. They may be attributed to increased cathodic areas in local cells (as postulated in electrochemical dissolution). The subsequent decrease of reaction rate is then due mainly to passivation of the surface by the plating of noble metal and in part due to the increasing anodic current. Vander Wall and Whitner[5] added silver nitrate and reported no effect. However, it should be noted that the addition was made in the presence of strongly oxidizing nitric acid, thus preventing the reduction of Ag^+.

It should be emphasized that this study is not just typical of the particular sample used since almost identical results were obtained with zirconium samples containing 3% hafnium. Studies now in progress on hafnium, titanium, and solid solutions ZrO_x, TiO_x, are resulting in activation energies of the same magnitude lending further support to the idea that these reactions are not controlled by a chemical activation step.

DETERMINATION OF ΔF^0_{298}, ΔH^0_{298} AND ΔS^0_{298} FROM EQUILIBRIUM DATA AT VARIOUS TEMPERATURES

By John L. Margrave

Department of Chemistry, University of Wisconsin, Madison, Wisconsin

Received September 21, 1959

The usefulness of the free energy function for treatment of equilibrium data to yield ΔH^0_{298} has been widely demonstrated.[1] In some cases, one is prevented from developing reliable thermodynamic data at 298°K. by the lack of low temperature heat capacities and adequate entropies. There are, however, often available heat capacity data above 298°K. where measurements are somewhat easier. These data are normally utilized for calculation of thermodynamic properties at a desired temperature by empirical heat capacity equations and ΔC_p.[2]

(1) (a) Various papers in the literature, especially high temperature vapor pressure measurements; (b) J. L. Margrave, *J. Chem. Ed.*, **32**, 520 (1955).

(2) G. N. Lewis and M. Randall, "Thermodynamics and the Free Energy of Chemical Substances," McGraw-Hill Book Co., New York, N. Y., 1923, pp. 102–105 and 173–175.

A more convenient method is outlined here which makes maximum utilization of available equilibrium data on systems for which $(H^0_{298} - H^0_0)$ and S^0_{298} are not known but high temperature heat contents have been measured and tabulated as $(H^0_T - H^0_{298})$ and $(S^0_T - S^0_{298})$.[3]

Consider the free energy function

$$\left(\frac{F^0_T - H^0_{298}}{T}\right) = -S^0_T + \left(\frac{H^0_T - H^0_{298}}{T}\right) \quad (1)$$

$$= -(S^0_T - S^0_{298}) - S_{298} + \left(\frac{H^0_T - H^0_{298}}{T}\right) \quad (2)$$

For a chemical reaction, the change of free energy function is

$$\Delta\left(\frac{F^0_T - H^0_{298}}{T}\right) = \frac{\Delta F^0_T}{T} - \frac{\Delta H^0_{298}}{T} =$$

$$-\Delta(S^0_T - S^0_{298}) - \Delta S^0_{298} + \Delta\left(\frac{H^0_T - H^0_{298}}{T}\right) \quad (3)$$

$$\frac{\Delta F^0_T}{T} + \Delta(S^0_T - S^0_{298}) - \Delta\left(\frac{H^0_T - H^0_{298}}{T}\right) = \frac{\Delta H^0_{298}}{T} - S^0_{298} \quad (4)$$

One may define a function φ =

$$-\Delta(S^0_T - S^0_{298}) + \left(\frac{H^0_T - H^0_{298}}{T}\right) \quad (5)$$

$$= -\int_{298}^{T} \frac{C^0_p dT}{T} + \frac{1}{T}\int_{298}^{T} C^0_p dT \quad (6)$$

Thus

$$\Phi = \frac{\Delta F^0_T}{T} - \Delta\varphi = -R \ln K - \Delta\varphi = \frac{\Delta H^0_{298}}{T} - \Delta S^0_{298} \quad (7)$$

and, when Φ is plotted *versus* $1/T$, the curve should be a straight line of slope ΔH^0_{298} and intercept at $1/T = 0$ equal to ΔS^0_{298}. At $T = 298$°K. $\Phi = \Delta F^0_{298}$, and this value can be used to check ΔH^0_{298} and ΔS^0_{298}. Analytically, one may obtain independent values of ΔH^0_{298} and ΔS^0_{298} from every pair of equilibrium measurements.

This treatment yields a highly reliable ΔH^0_{298} definitely better than can be obtained by ignoring available heat capacity data above 298°K. or by simply extrapolating a log K_T *vs.* $1/T$ plot back to 298°K. The approach should find application in high temperature calculations, and might also be useful for converting solution equilibrium data at temperatures other than 298°K. to the standard reference temperature. When necessary, values of $\Delta\varphi$ should be somewhat easier to estimate than $\Delta\left(\frac{F^0_T - H^0_{298}}{T}\right)$ since C^0_p is a nearly linear function at 298°K. and above for many substances.

(3) For example, see K. K. Kelley, U. S. Bureau of Mines, Bulletin 476, 1949.

PHYSICAL PROPERTIES OF CHEMICAL COMPOUNDS—II

Number 22 in

Advances in Chemistry Series

This is a continuation of R. R. Dreisbach's compilation of physical properties of organic compounds (Advances 15). The present volume includes accurate data on 476 acyclic compounds not hitherto published. It also includes parameters which can be used for interpolating and extrapolating the determined data for practically all of the compounds listed.

Cloth bound—486 pages plus index—$6.50

order from:

Special Issues Sales
American Chemical Society
1155 16th Street, N. W.
Washington, D. C.

Engineers and Scientists
STRETCH YOUR IMAGINATION

... at Beckman Instruments, last refuge of the Non-Organization Man. Here's a company that is concerned with the man, his mind and his original contributions.

Commercial, industrial and military projects tickle the fancy of unconstrained intellects at these Beckman Divisions:

Beckman / *Scientific and Process Systems Division*
Helipot Division

Don't get crushed in the Organization Mill ... look into these imagination stretching positions ...

ENGINEERS/SCIENTISTS ...

at all levels in the fields of precision electronic components and analytical instrumentation for engineers and scientists with degrees in engineering or physical science. Some of our specific needs include project engineers and senior electronic engineers. We also have openings for exceptional recent graduates.

And you can stretch your legs in Orange County, too, where you and your family will enjoy Southern California living at its barbecuing best.

Overcome your own organizational inertia ... phone, wire or write Mr. T. P. Williams for all the parameters.

Beckman Instruments, Inc. Fullerton, Calif. Telephone TRojan 1-4848; from Los Angeles OWen 7-1771 ©B.I.I. 1960.

OZONE CHEMISTRY AND TECHNOLOGY

Number 21 in
Advances in Chemistry Series

Coverage of 60 papers presented at the International Ozone Conference directing interest towards the current contributions concerning ozone as it affects science and technology. At one time primarily an important reagent of the organic chemist, ozone now has the interests of meteorologist, photochemists, organic and analytical chemists and plant physiologists.

Cloth bound—466 pages—$7.00

order from:

Special Issues Sales
American Chemical Society
1155 Sixteenth Street, N. W.
Washington, D. C.

NEW VARIAN

100kcEPR

SPECTROMETER

(Electron Paramagnetic Resonance)

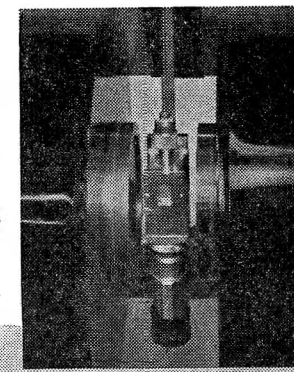

SAMPLE CAVITY OF THE NEW 100 KC EPR SPECTROMETER, SHOWING RADIATION SLOTS AND VARIABLE TEMPERATURE INSERT.

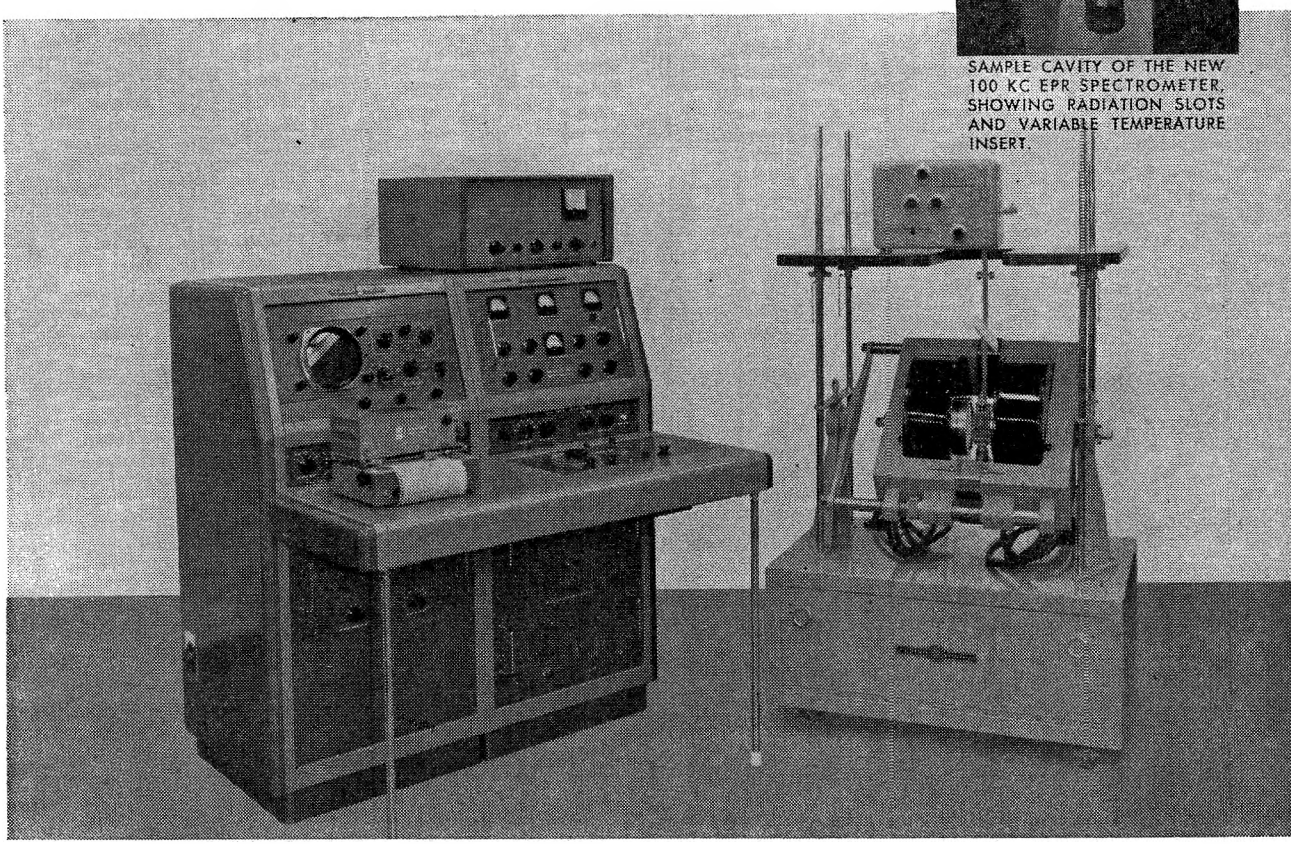

VARIAN 100-KC EPR SPECTROMETER WITH STANDARD SIX-INCH MAGNET.

A RECENT ADVANCE IN INSTRUMENTATION ACHIEVES THE FINEST IN SENSITIVITY AND VERSATILITY

HIGH SENSITIVITY — *At a response time of one second, the limiting sensitivity of the instrument is* $2 \times 10^{11} \Delta H$ *unpaired electron spins, where* ΔH *is the signal line width in gauss.* This high sensitivity has been achieved through the use of 100 kc magnetic field modulation together with a special frequency stabilization system.

SAMPLE TEMPERATURE CONTROL — The sample temperature can be controlled to within 1°C anywhere in the range −196°C to +300°C by means of a quartz Dewar insert system utilizing gas flow.

Write the Instrument Division for literature which fully explains the 100 kc EPR Spectrometer and its application to basic and applied research in physics, chemistry, biology and medical research.

SAMPLE IRRADIATION — A slotted window on the cavity permits the sample to be irradiated during EPR observation with U-V or visible light, with no adverse effect on the microwave properties of the cavity.

RAPID RESPONSE — For studying rapid reactions, the instrument is capable of response times as short as 100 microseconds.

OSCILLOSCOPE PRESENTATION — For quick observation, an oscilloscope presentation covering 75 gauss of the spectrum is available at a sensitivity of $10^{18} \Delta H$ unpaired electron spins.

VARIAN associates

PALO ALTO 52, CALIFORNIA

KLYSTRONS, WAVE TUBES, GAS SWITCHING TUBES, MAGNETRONS, HIGH VACUUM EQUIPMENT, LINEAR ACCELERATORS, MICROWAVE SYSTEM COMPONENTS, NMR & EPR SPECTROMETERS, MAGNETS, MAGNETOMETERS, STALOS, POWER AMPLIFIERS, GRAPHIC RECORDERS, RESEARCH AND DEVELOPMENT SERVICES